THE ROLE OF SPATIAL SCALES AND HABITAT HETEROGENEITY IN PATTERNS AND DRIVERS OF DEEP-SEA BENTHIC BIODIVERSITY AND ECOSYSTEM FUNCTIONING

by

© Alessia Caterina Ciraolo

A Thesis submitted to the School of Graduate Studies

in partial fulfillment of the requirements for the degree of

Doctor of Philosophy

Department of Ocean Science

Memorial University of Newfoundland

August 30th, 2023

St. John's Newfoundland and Labrador

Abstract

Deep-sea environments support ecosystem functioning and services, however, the challenge in accessing deep-sea sediments limits intensive investigations of interactions between diversity, functioning, and spatial heterogeneity. The influence of spatial heterogeneity strongly depends on the scale of study, adding to the challenge. Nonetheless, understanding the potential role of spatial heterogeneity can inform efforts to protect and conserve deep-sea environments.

In field experiments, I examined potential effects of different scales of spatial heterogeneity - habitat heterogeneity (large scale, 100s of km), a natural water column oxygen gradient (medium scale, tens of km), and organic matter addition (small scale, cm to m) - on deep-sea benthic ecosystem function and biodiversity. I found that large-scale habitat heterogeneity affects benthic macro- and microbial community assemblages, as well as functional and taxonomic infaunal diversity but with no obvious effect on benthic nutrient fluxes. Whereas quantity and quality of organic matter best explained variation in microbial community composition, interaction of several environmental factors acting over a large spatial scale complicated understanding of variation in infaunal communities. At a medium spatial scale (hypoxia), the quantity and quality of food shaped infaunal community variation where filter-feeder polychaetes dominated surface sediments. Bioturbation features decreased spatially with decreasing O_2 levels and response to the O_2 gradient varied with scale. The smaller video camera field of view suggested significantly lower megafaunal density and diversity during the period of reduced oxygen concentrations, but not in sediment trace diversity and density. In contrast, the larger field imaged with rotary sonar documented biological pit distribution, a significantly greater proportion of reworked seafloor area, and increases in pit size with increased oxygen levels. Furthermore, North Pacific infaunal composition could not explain variation in nutrient fluxes (mostly influxes) in relation to hypoxia.

In contrast to microbial community composition that explained variation in benthic nutrient flux and organic matter degradation among three Atlantic continental slope habitats. At small scales, phytodetrital deposition did not affect oxygen consumption and short-term nutrient cycling. However, adding labeled phytodetritus demonstrated that polychaetes in particular influence rapid carbon uptake and C cycling, irrespective of bottom-water oxygen concentrations.

Acknowledgments

This endeavor would have not been possible without the help and support of many scientists, colleagues, friends, and family members, who deserve a few lines in this thesis.

Firstly, words cannot express my gratitude to my professor, Dr. Paul V. R. Snelgrove, for his continuous support of my Ph.D. study and related research, and for his invaluable patience, motivation, feedback, and immense knowledge. His guidance, no matter what time and where he was, helped me to build and develop my scientific side. I also deeply thank him for always encouraging me to take part in cruises, meetings, symposiums, and conferences which helped me to improve my communication skills, to be more confident with my thesis topic, and to build my network. He also deserves a big thanks for his very precious guidance in the writing process of this thesis, for making my Ph.D. experience always constructive and exciting, and for placing his trust in my abilities. Everything mentioned above also influenced somehow my continuous and gradual personal growth, and therefore I will always be deeply grateful for having the opportunity to have Dr. Snelgrove as my supervisor.

I would also like to give a special thanks to all my committee members, Dr. Suzanne Dufour and Dr. Amanda Bates for their detailed inputs on each chapter of my thesis. I also appreciated the opportunity given by Dr. Suzanne Dufour in approaching molecular microbial lab experience.

I thank the Exploration Vessel Nautilus' crew for my first cruise opportunity at the North-East Pacific Seamounts in 2018. It helped me to understand better what field-work means and how to improve my field-work skills for future sampling experiences. In addition, I thank Dr. Kim Juniper for the cruise opportunity with Ocean Networks Canada at the Clayoquot continental slope in 2019, for welcoming me and helping me on my second research cruise on board the Canadian Coast Guard John P. Tully vessel, and his valuable input during all experiments. I also thank

Vanessa Reid for her help in putting the multicore together during our samplings, and for her constant support during the challenging and long nights of experiments. A special thanks to Dr. Clare Woulds and Dr. Andrew K. Sweetman for advice on the oxystat system and the use of labelled algae without which part of my pulse-chase experiments would have not been possible. It was a great experience despite all the challenges we encountered. I thank the Chief Scientist Dr. M. Nizinski, Dr. Anna Metaxas, and crewmembers of the NOAA ship Henry B. Bigelow for sampling opportunities in 2019. Accordingly, I also thank my supervisor, Dr. Paul Snelgrove for the Bigelow 2019 cruise which at that time almost overlapped with the Tully 2019 cruise. Without his kind help in collecting samples for me, I would have not been able to develop two of the chapters of my thesis. Thank you to all the other scientists who took part in the cruises, with whom it was great to work.

I also deeply acknowledge valuable inputs from Douglas Schillinger who very kindly helped in developing ideas and providing data through MATLAB software for the acoustic chapter. I thank Dr. Fabio De Leo who provided new ideas for the acoustic chapter and also did his best to avoid overlap between other ongoing research in the same sampling area. I also thank Dr. Jacopo Aguzzi for providing technical suggestions, and Azeez Sarafadeen, for help with the video analysis. Moreover, I thank Dr. Christopher K. Algar for his significant contribution to Chapter 5.

I thank all of the Fisheries and Oceans Canada (DFO) team who took part in our sampling trips for their collaboration. I also thank Vanessa Reid for her help with field material and purchases, and all people who helped and assisted with different aspects of lab work. Jeanette Wells (Memorial University) helped with lipids analysis; Dr. Barbara de Moura Neves (Fisheries and Oceans Canada (DFO)) assisted with chlorophyll analysis, Dr. Owen Brown (Natural Resources Canada) helped with grain size analysis; Dr. Gary Maillet, Ms. Gina Doyle (DFO) and

Maria Ignacia Diaz Wells (Memorial University) helped with benthic nutrient analysis; Dr. Joanne Potter Wells (Memorial University) helped with isotope analysis; and Dr. Andrew Comeau (Dalhousie University, Halifax) helped with microbial analysis. I also thank JoAnn Greening (Ocean Science Center (OCS)) for her patience during my fieldwork preparation. A kind thank you goes also to the workshop people from the OSC who provided support and help with building pieces for my experiments until the last minute available before flying to join the ship.

I am also grateful of being part of a wonderful team with so many inspiring people and researchers. I thank Dr. Paul Snelgrove for putting this delightful lab together. I also want to thank my lab mates, Emilie Geissinger, Marta Miatta, Benjamin King, Neus Campanyà-Llovet, Ty Colvin, Mary Clinton, Amy McAllister, and Becky Evans for always being there for either a laugh or a more scientific and/or technical conversation. I want to especially thank my desk-mates Emilie Geissinger and Marta Miatta with whom I started and finished my journey. Both of their overall direction helped me a lot in building my own pathway in this wonderful Ph.D. and personal experience!

Thanks also to the associations that provided funding for making true the thesis accomplishment and allowed me to travel and present at national and international conferences. I therefore want to thank the NSERC Canadian Healthy Oceans Network and its Partners: Department of Fisheries and Oceans Canada and INREST (representing the Port of Sept-Îles and City of Sept-Îles), the School of Graduate Studies at Memorial University, and Ocean Networks Canada, who supported part of the travel funding for one of the workshops and conferences I gratefully attended.

Many thanks to my roommates, especially Mirelle Caouette and Samantha Crowley, and my group of funny friends who have become my Canadian family. They were always there to support

me, listen to me, and encourage me to keep working hard, even during the emotional lows. Without their support and funny moments together, I would not have loved this experience as much as I do!

I also want to thank my Italian friends, Valeria, Toti, Vera, Jejola, Ali, e Carbone e Attina' families who contributed to this experience through their lovely words and encouragement over time.

Vorrei anche ringraziare I miei amici italiani, Valeria, Toti, Vera, Jejola, Ali, e le famiglie Carbone e Attina'per aver contribuito a questa esperienza attraverso le loro costanti parole d'amore e incoragiamenti.

Last but not least, I am deeply grateful to all my family, my Dad, my Mum, and my amazing brother Biagio. I am aware of the challenges they have passed through with me being so far, but even so they have ALWAYS shown their immense love. They have always encouraged me to work hard in order to always grow as person and as a marine biologist. I thank my mum and dad for teaching me how to be a good person and a good worker, to never give up even when situations may become challenging, and to always be grateful for the experiences beyond words and for the wonderful people I had the honor to meet in this endeavor. I also want to reserve a special thank to my brother who has ALWAYS supported my choice in becoming a marine biologist and who has always been on my side when hard decisions were coming through, and for ALWAYS being there for me no matter the time and place we were. Their presence in this journey made me accomplish this unbelievable experience of my life!

Gli ultimi ma no meno importanti – vorrei profondamente ringraziare la mia famiglia, papa', mamma, e il mio fantastico fratello Biagio. Nonostante le difficolta' che hanno attraversato con me cosi lontana, mi hanno SEMPRE supportata e incoraggiata a lavorare duro per diventare una

persona e una biologa mairna migliore, cosi come mi hanno sempre dimostrato il loro immenso amore. Ringrazio mamma e papa' per avermi insegnato ad essere una brava persona e un bravo lavoratore, a non mollare mai nemmeno in situazioni difficili, e per essere sempre grata delle persone indiscrivibili che ho avuto l'onore di incontrare durante questo viaggio. Un ringraziamento speciale va a mio fratello che ha da sempre supportato la mia scelta di diventare biologa marina, che e' sempre stato accanto a me anche durante decisioni difficili, e per essere sempre li per me incondizionatamente. La loro presenza mi ha decisamente permesso di realizzare questa indiscrivibile esperienza!

List of Contents

List of tables

List of figures

List of Supplementary table

List of Supplementary figures

List of common nomenclature and abbreviations

ANOVA	Analysis of variance
ARC	Aquatic Research Cluster
B	Biodiffusors
BEF	Benthic Ecosystem Functioning
BM	Subsurface deposit-feeder
BWO_2	Bottom-water oxygen concentration
C	Carnivorous
CCGS	Canadian Coast Guard
CD	Carnivore, discretely motile
Chl*a*	Chlorophyll-*a*
CHN	Carbon, Hydrogen, Nitrogen
CHONe	Canadian Healthy Oceans Network
CM	Carnivore, motile
CN	Carbon nitrogen ratio
CT	Corsair Tributary Canyon
CTD	Conductivity-Temperature-Depth
D	Surface deposit-feeders
DC	Downward conveyors
DFO	Fisheries and Oceans Canada
DOM	Dissolved organic matter
E	Epifauna
ENP	Eastern North Pacific
ES	Expected number of species
ESP	Eastern South Pacific
FB	Feeding behaviour
FD	Functional diversity
FDT	Filter-feeder, discretely mobile
FEve	Functional evenness
FMBS	Free movement in burrow system
FMSM	Free movement in sediment system
FO_2	Flux of oxygen consumption
FOV	Field of View
Frich	Functional Richness
FT	Live in fixed tubes
GLM	General linear model
HDPE	High-density polyethylene
HM	Herbivore, mobile
ID	Internal diameter

IFREMER	Institut Français de Recherche pour l'Exploitation de la Mer
IP	Instrument Platform
J	Shannon index
KHM	Kinlan-Heezen Inter-canyon
LM	Limited movement
MUN	Memorial University of Newfoundland
NE	Northeast
NEC1	Northeast Channel 1
NEC2	Northeast Channel 2
NEPTUNE	North East Pacific Undersea Networked Experiments
NH_4^+	Ammonia
nMDS	Non-metric Multidimensional Scaling
NO_2^-	Nitrite
NO_3^-	Nitrate
NOAA	National Oceanic and Atmospheric Administration
NSERC	Natural Sciences and Research Council of Canada
NW	Northwest
O	Omnivorous
O_2	Oxygen
OD	Outside diameter
OM	Organic matter
OMZ	Oxygen Minimum Zone
ONC	Ocean Network Canada
P-value	p-value
P	Parasite
PAP	Porcupine Abyssal Plain
PCR	Polymerase chain reaction
PERMANOVA	Permutational multivariate analysis of variance
PERMIDISP	Homogeneity of Multivariate Dispersion
Phaeo	Phaeopigments
PM	Powell-Munson Inter-canyon
PO_4^{3-}	Phosphate
POC	Particulate organic carbon
POM	Particulate organic matter
PON	Particulate organic nitrogen
PSS	Particle Sizing Software
PSU	Practical Salinity Unit
P-W	Pairwise Wilcoxon test
R^2	R square

RDA	Redundancy analysis
RNA	Ribonucleic acid
ROPOS	Remotely Operated Platform for Ocean Science
ROV	Remotely Operated Vehicle
R_{VPDB}	Vienna Pee Dee Belemnite
S	Surficial modifiers
SB	Subsurface deposit-feeder
SBE	Sea-bird Electronics
SD	Surface deposit feeders, discretely motile
SIMPER	Similarity percentages
$Si(OH)_4+$	Silicate
SDM	Surface deposit-feeders, motile
SM	Slow movement
spp.	Species plural
SS	Surface deposit-feeder, sessile
SWI	Sediment-water interface
THSD	Tukey HSD test
TLC-FID	Thin-layer chromatography-flame ionization detector system
TOC	Total organic carbon
TOM	Total organic matter
UC	Upward conveyors
Venus	Victoria Experimental Network Under the Sea
VIF	Variance inflation factor

Co-authorship statement

The research detailed in this thesis was designed and conceptualized by Alessia Caterina Ciraolo in collaboration with Dr. Paul V. R. Snelgrove. All data were collected and analyzed by Alessia C. Ciraolo; Douglas Schillinger provided assistance on sonar data analysis (Chapter 3); and Dr. Christopher K. Algar provided analytical advice and editorial assistance on Chapter 5. Dr. Paul Snelgrove provided assistance with sampling and with delineating the content and structure of Chapters 1-6. Dr. Fabio De Leo assisted in data access for Chapter 3 and provided detailed feedback on the subsequent analysis and manuscript. Dr. Andrew K. Sweetman and Dr. Marta M. Cecchetto provided valuable input to the experimental design of Chapter 2, which is currently being prepared for submission to an international journal with authors Ciraolo, Snelgrove, Sweetman and Cecchetto. Chapters 4 and 5 have been published in *Deep-Sea Research* as Ciraolo and Snelgrove (2023), and Ciraolo, Snelgrove and Algar (2023). Chapter 3 is in review with *Deep-Sea Research* as Ciraolo, Snelgrove, Schillinger and De Leo (2023).

Chapter 1. - Introduction

To protect the ocean and the biosphere, and at the same time satisfy human needs, human society must enhance its knowledge of ocean environments to conserve and sustain the ecosystems that provide function and services. The many ecosystem processes mediated by marine organisms influence multiple ecosystem functions (e.g., nutrient cycling, carbon sequestration) (Danovaro et al., 2001; Danovaro et al., 2008a; Snelgrove et al., 2014) that support different ecosystem services (provision of food, buffering against acidification, and carbon sequestration) and yield benefits to human populations (Snelgrove et al., 2014) (**Fig. 1.1**). Here, we define ecosystem services as the benefits that people obtain from ecosystems (Armstrong et al., 2012), and functions as the interactions that occur between abiotic and biotic elements of the ecosystem. The combination of individual functions falls into the definition of ecosystem functioning (Reiss et al., 2009).

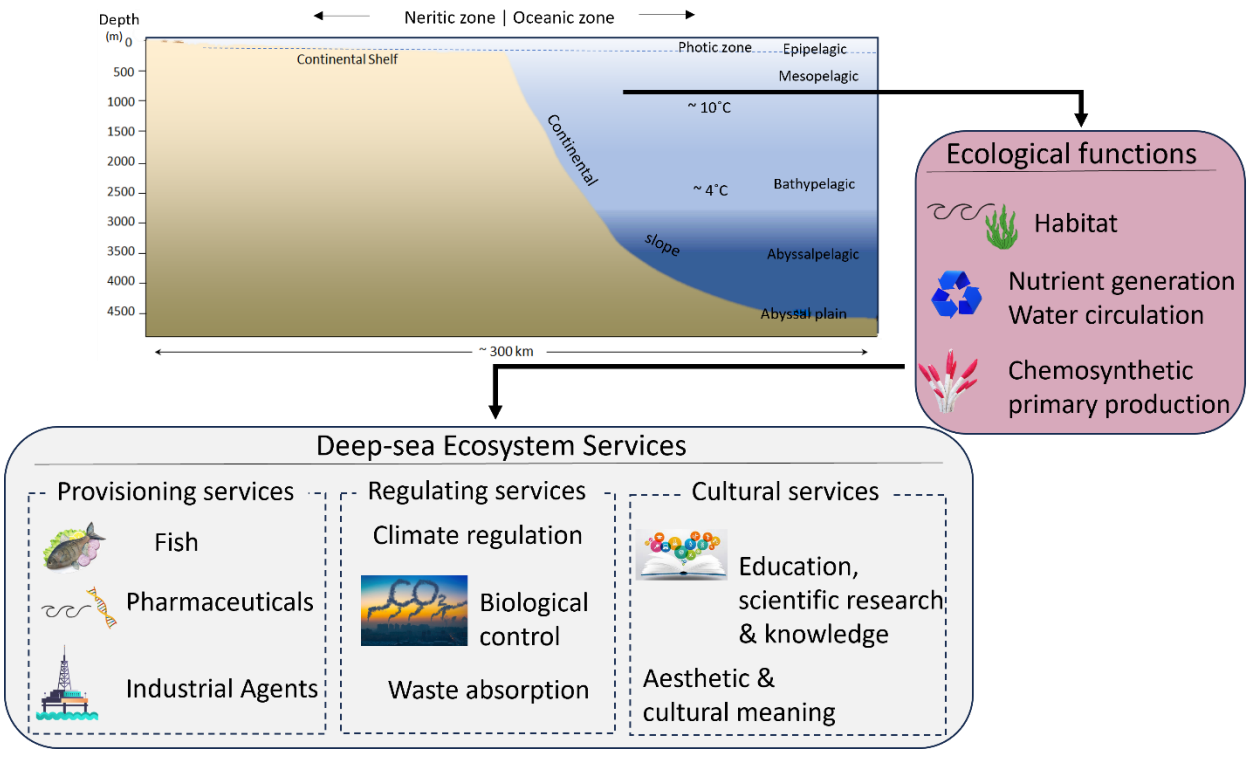

Fig. 1.1. Deep-sea environments support important ecosystem functions and services

The ecosystem is composed of different biotic and abiotic elements whose complexity, along with external disturbances (e.g., food supply; biogenic structure such as burrows and sediment mounds, etc.) may increase spatial heterogeneity. Heterogeneity, defined as the multiscale spatial and temporal patterning of organisms and the environment in which they live (Charton and Ruzafa, 1999) (**Fig. 1.2**), can modify the outcomes of ecological processes (Wiens, 1976; Levin, 1992; Oksanen et al., 1992), thus influencing how species coexist in space and time (Downing, 1986), and their organization in trophic webs (Polis and Strong, 1996).

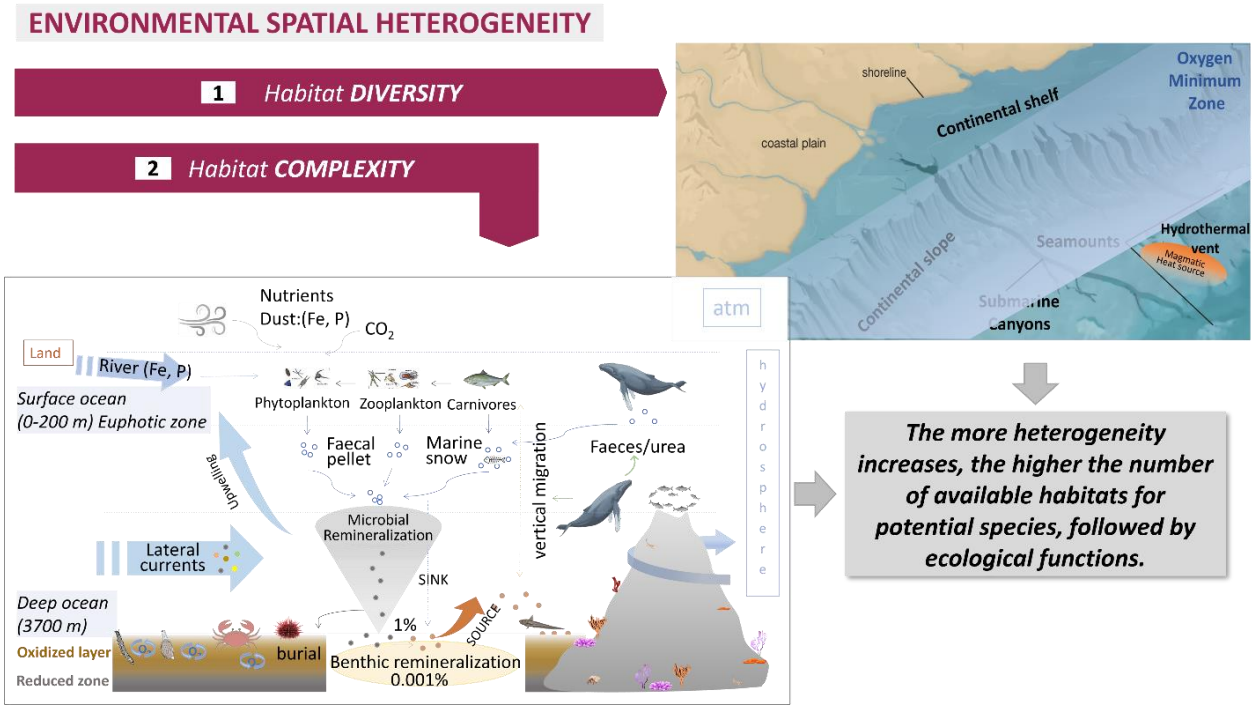

Fig. 1.2. Spatial heterogeneity definition (habitat diversity + complexity), and the consequences of higher heterogeneity on species diversity and ecosystem functioning.

Biotic and abiotic factors, as well as their interactions, tend to vary less in relatively homogeneous habitats, emphasizing the importance of such heterogeneity in conservation and management of species and habitats. Although the deep sea is not a homogeneous environment, the spatial heterogeneity within it may not be obvious, and interactions between species,

functioning, and spatial heterogeneity remain poorly understood. Biogenic and environmental sources influence temporal and spatial variation in the deep-sea, as exemplified by resuspension of sediment, low oxygen, pulse of organic matter, and the activities of animals on the bottom (Grassle, 1989). The degree of spatial heterogeneity (whether low or high) in one or more abiotic conditions along with body size may allow species to thrive only in some areas, thus producing patchy distributions (Azovsky, 2000; Leibold et al., 2004). Spatial heterogeneity can also be identified as different habitats with associated animals and their functions. However, the role of spatial heterogeneity at different spatial scales remains elusive (**Fig. 1.3**). Understanding spatial variation in habitats is the critical factor that helps to enhance knowledge on the role of specific habitats in ecosystem function, defining the consequence of the functional species, and changes in habitat spatial distributions.

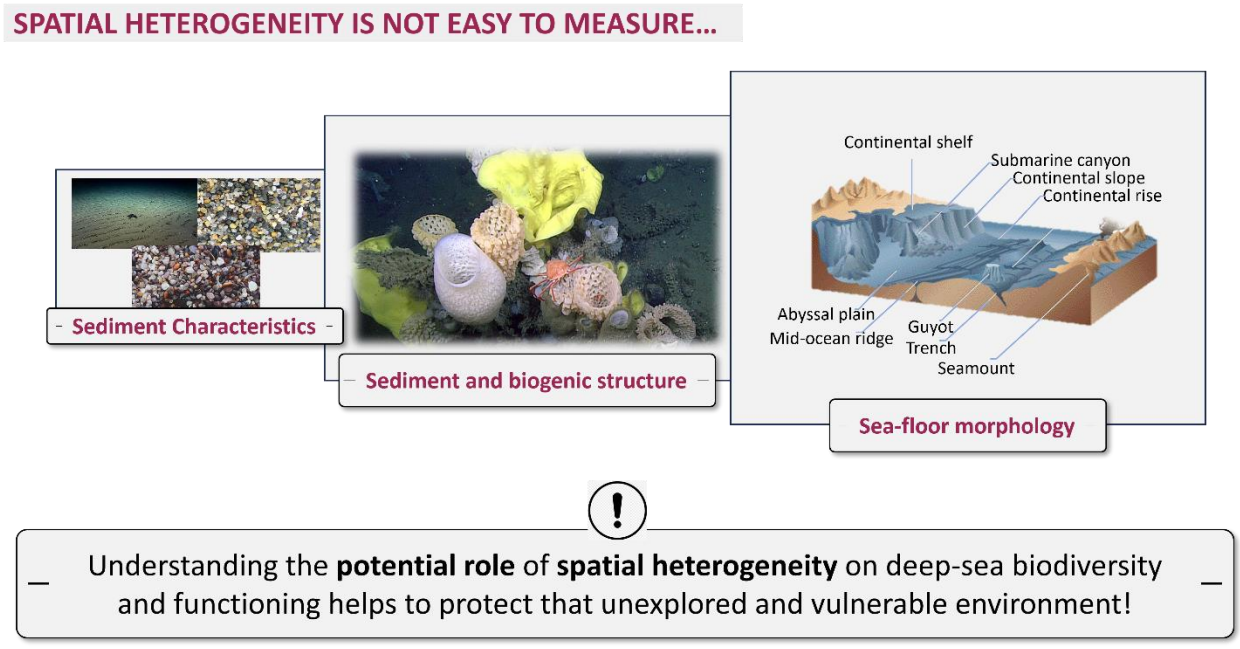

Fig. 1.3. Spatial heterogeneity measurement depends on the spatial scale examined varying from small scales (e.g., sediment characteristics) to large scales (e.g., sea-floor morphology).

Benthic ecosystem drivers of heterogeneity, depending on scale and habitat type, may include both chronic and acute sources. Low oxygen concentrations associated within oxygen minimum zones illustrate both chronic and acute disturbance in that some locations experience consistently low oxygen concentrations whereas others may experience intermittent hypoxia. Disturbances, directly and indirectly, can cause ecosystem shifts, changing resource levels and producing habitat gaps that new species can subsequently colonize (Sousa 1980). Despite numerous studies on various types of disturbance, few have considered simultaneous disturbance effects, and fewer still have considered different scales. The effect of multiple anthropogenic and natural stressors on an ecological component depends strongly on the context in which interactions occur, and may vary with place, time, and species (Menge and Sutherland, 1987). Alteration of habitat heterogeneity through disturbance can also alter the effects that population sources have on the region. Whole ecosystems can shift to an alternate state characterized by different species and species interactions following significant altering of biophysical conditions. The altered ecosystem may respond differently to a stressor (e.g., OMZs, fishing activity etc.) than the previous ecosystem or may follow any number of recovery trajectories (Murry and Farrell, 2014).

The association of marine benthic communities with spatial heterogeneity varies across scales. Identifying which spatial scale bears more importance in regulating community characteristics is crucial. Understanding biodiversity, environment, and ecosystem services under different spatial scales helps to inform efforts to protect them through management and policy decisions. However, this approach has received relatively little attention in deep-sea scientific literature. Previous studies evidenced deep-sea structure and dynamics on regional and relatively large-scales (10-100 km) (Levin et al., 2001a), with others on small-scale (micro-scale) habitat variability (Snelgrove and Smith, 2002; Ingels and Vanreusel, 2013) that for instance, showed how many species are

associated with particular substrate types (e.g., rocks versus sediments, fine versus coarse sediment) which can vary across local to regional scales (e.g., Levin et al. 2001b). Furthermore, broad environmental differences, such as bottom currents, influence heterogeneity even within substrate types on a temporal scale. For example, Thistle et al. (1991) showed the effect of a benthic storm that occurred in 1983 at 4820 m on the Nova Scotia Rise on the sediment and infauna living in it. They observed no differences in isopod abundance between the 0-1 cm and then 1-2 cm sediment samples each one collected, instead of observing isopods only in the 1-2 cm layer for example, from 1982 and 1983, inferring a sediment and infauna resuspension event as a consequence of the benthic storm.

In my thesis, I specifically examine variation in deep-sea ecosystem functions by highlighting patterns of marine assemblage heterogeneity induced by a variety of environmental drivers. These drivers include habitat variability (large scale, 100s of km, Chapters 4 and 5), temporal variability (months, Chapter 3), a natural oxygen gradient (medium-scale, 10s to 100 km, Chapters 2 and 3), and the addition of organic matter as a simulation of organic matter flux from the surface to the deep-sea floor (small-scale, cm to m, Chapter 2) (**Fig.1.4**). This research aimed to understand, explore, and combine macrofaunal community dynamics and ecosystem functioning (carbon cycling, and nutrient cycling) in the North-East Pacific Ocean oxygen minimum zone, and in Northwest Atlantic Ocean contrasting habitats.

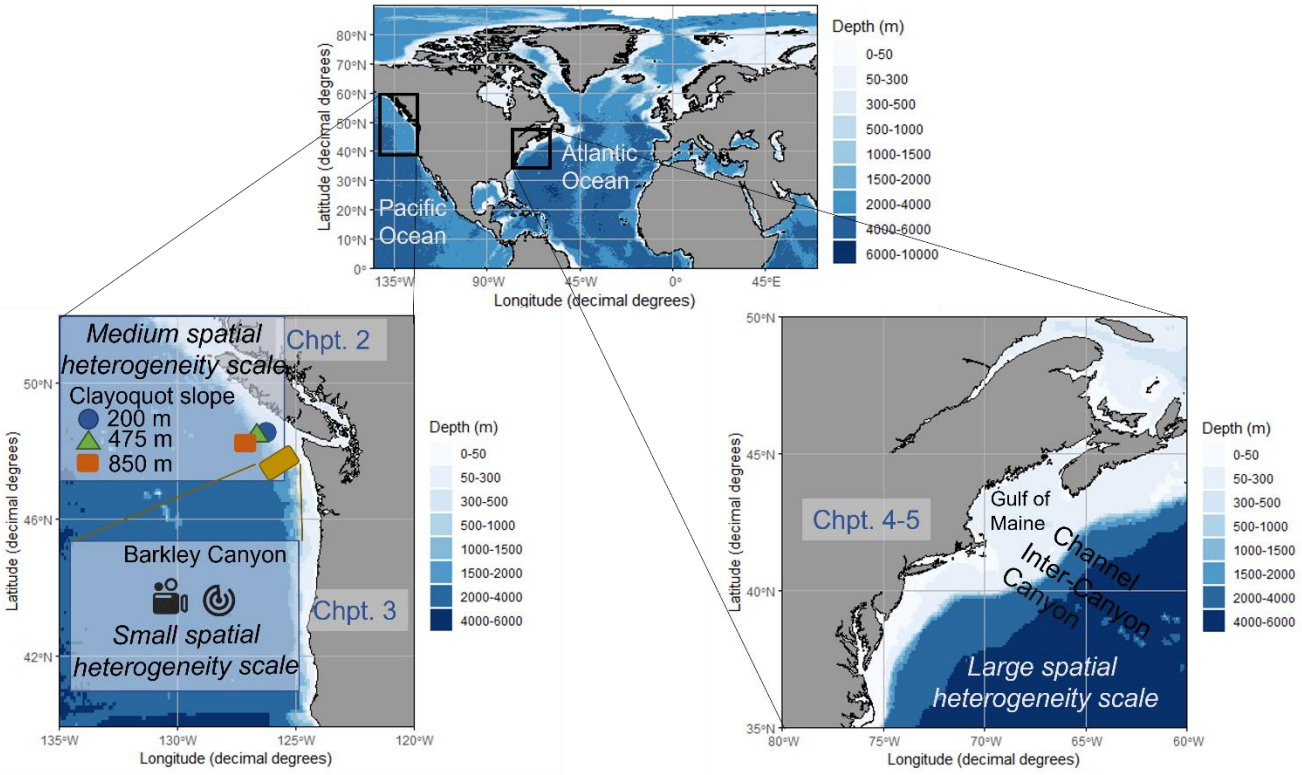

Fig. 1.4. The top center picture refers to a map of the world's ocean from which I extrapolated the two main study sites of the thesis, Pacific Ocean (left bottom figure), and Atlantic Ocean (right bottom figure). At each study site, I explored the effect of the OMZ and contrasting habitats at different spatial scale on deep-sea benthic ecosystems. From the Northeast Pacific Ocean, I evaluated the potential small (Barkley Canyon) and medium (Clayoquot slope) scale impacts of the OMZ on macro-and megafauna, nutrient and carbon fluxes, and reworked sediment and trace pattern. In the Atlantic Ocean, I explored the effect of a large spatial scale (contrasting habitats) on microbes and macroinfauna, and OM remineralization in terms of nutrient cycling.

1.1 Deep-sea features and its role as source and sink of nutrients

The deep-sea is a unique and in some ways extreme marine environment, with no sunlight (Gage and Tyler, 1991; Smith and Demopoulos, 2003), typically cold temperatures (1- 4˚C), and low food flux. In general, low physical energy, including sluggish currents (~ 0.25 knots) (Smith

and Demopoulos, 2003), and very slow sediment accumulation rates (0.1 – 10 cm per thousand years) characterize the deep-sea floor. The deep-sea floor and overlying waters below 200 m depth also form the largest biome on Earth, which remains poorly explored. From an ecosystem functioning perspective, the deep sea drives the nutrient regeneration and global biogeochemical cycles required to sustain primary and secondary production in the global ocean (Danovaro et al., 2008b).

1.1.1 Benthic-pelagic coupling

Despite the massive depth spanned by the deep sea, it strongly links to the surface of the ocean. Most deep-sea biota ultimately derive their energy from an attenuated 'rain' of detritus from surface waters (typically 1 – 10 $g \cdot C_{org} \cdot m^{-2} \cdot yr^{-1}$). This rain arrives in the forms of either sinking phytoplankton or marine snow, in addition to larger organic particles such as fish, whale carcasses, or kelp, transporting carbon and nutrients (ammonium, nitrate, nitrite, silicate, phosphate) that vary in quantity and quality both spatially and temporally (Glover and Smith, 2003; Mayor et al., 2012). The heterogeneity of food supply (seasonal/spatial) drives heterogeneity in community composition and benthic-pelagic coupling. Benthic biota spanning microbes, meiofauna, macrofauna, and even megafauna ultimately benefit from and remineralize this particulate material. Any organic carbon (or other nutrients) that escapes mineralization may become buried in the sediment for periods as long as millennia (Lampitt et al., 2008). Historically, some 300 $Tg \cdot C \cdot y^{-1}$ has undergone burial globally, but increasing natural and anthropogenic disturbance could increase or decrease this value, with unknown effects on global C cycling (Jahnke, 1996).

The heterogeneity of seafloor habitats influences nutrient cycling, noting that some habitats such as hydrothermal vents and cold seeps produce autochthonic organic matter through chemolithoautotrophic primary production (Nakagawa and Takai, 2008). Carbon and sulfur

element cycles, which are mediated by chemosynthetic bacteria, occur in these biological communities. The products of these reactions promote the generation of carbonate and sulfide minerals which contribute to fluid flow modification (Pancost et al., 2000).

The carbon and nutrient fluxes are based on a physical–biological process that occur both on the surface, in the water column, and on/ in the seabed. Therefore, to identify and verify such key driving forces, it is necessary to know the primary productivity, the depth of the mixed layer, grazing efficiency, as well as the physical conditions of the water column accompanying a given vertical flux scenario at a specific spatial and temporal scale.

1.2 Biological and environmental factors linked to benthic ecosystem functions

1.2.1 Deep-sea benthic macrofauna

Diverse macrofauna (polychaete annelids, crustaceans, mollusks, and other phyla), referring to organisms retained on a 300 μm sieve (Snelgrove, 1998), dominate the biomass within the sediments that cover much of the deep-sea floor (Snelgrove, 1998). No simple pattern or single mechanism clearly explains sedimentary macrofaunal diversity, with some evidence for peak diversity on the upper continental slope (~2000-3000 m depth) (Rex, 1983) and increasing with latitude (Rex et al., 1993). However, further studies suggest more complicated patterns that might depend on sampling method and performance, and on environmental factors such as patchy organic matter (Snelgrove et al., 1992, 1996).

Macrofauna potentially impact both carbon and nutrient cycling, as well as how sinking organic matter could provide a conduit of material for multiple trophic levels. By mixing sediments and modifying sediment biogeochemistry and nutrient fluxes, macrofauna directly impact organic matter, oxygen, and associated nutrients (Welsh, 2003; Belley and Snelgrove, 2016a). Macrofauna include selective and non-selective suspension feeders that remove particles from the water

column and improve water column quality (Ostroumov, 2005). Deposit feeders that ingest sediment particles and organic material associated with these particles increase sediment oxygenation (Rhoads, 1974), vertical movement of sediment particles (Whitlatch and Obrebski, 1980), and alter sediment stability (Rhoads and Young, 1970). The complex link between benthic organisms and organic matter involves complex feedback in which the organisms help to determine the fate of the organic matter but at the same time, the quantity and quality of organic matter regulate the benthic organism community.

1.2.2 Bacteria

The flux of materials carried through the water column and then incorporated within the sediment influences the deep-sea sediment-water interface (SWI) that represents the area between the water column and sediment. This detrital or particulate organic matter forms the nutritional basis for most deep-sea life. Bacteria can respond rapidly to the arrival of organic matter, remineralizing the material (Lochte and Turley, 1988; Gooday and Turley, 1990), producing enzymes that break it down into smaller fractions (Turley, 2000), which they can incorporate to fuel their metabolism. Bacteria are responsible for at least 13-30% of the total biological consumption of organic carbon in deep-sea sediments (Rowe and Deming, 1985) through their high respiration and low growth efficiency. This process dominates the biogeochemistry of the SWI and, therefore, the rate and nature of preservation of organic matter in sediments which also links with macrofaunal presence/absence and their burrowing and irrigation activities.

1.2.3 Functional traits and environmental factors

Researchers have recently begun to use functional traits of organisms to evaluate ecosystem functions because species traits link to environmental conditions (e.g., Miatta et al., 2021). Functional traits refer to the individual behaviour, morphological, phenological, and physiological

traits that impact individual fitness indirectly, and ecosystem functioning; they do not require additional information from the environment or at any other organizational level (Violle et al., 2007). The combination of different functional traits, or changes in them, can influence processes at higher organization levels and can be used to evaluate environmental change (Violle et al., 2007; Bremner, 2008). The lack of a standardized method to quantify functional traits has led to studies using species richness as a surrogate (Díaz and Cabido, 2001). However, species richness can either over- or underestimate functional traits, for example with competition or anthropogenic and natural disturbances (Díaz and Cabido, 2001; Bremner, 2008). Beyond these biological factors, the quantity and quality of organic matter (Mayor et al., 2012), temperature, and pressure (Yayanos, 1986) influence biogeochemical processes in the deep sea.

The quantity and quality of organic matter strongly influence the type and amount of biological energy available in a given environment. Discrete pulses of diatoms and zooplankton fecal pellets can dominate the annual flux of organic matter to the deep seabed (Witte et al., 2003; Sweetman and Witte 2008; Woulds et al., 2009; Jeffrey et al., 2013; Sweetman et al., 2019). Sedimented organic substrates differ in quality, with breakdown of diatoms occurring at a rate > 300% faster than fecal pellets, thereby influencing the rates and pathways of organic carbon cycling (Mayor et al., 2012). The quality of available organic matter therefore influences rates of organic matter remineralization and ecosystem functioning.

Quantification of organic matter remineralization is often performed by measuring oxygen and nutrient flux rates at the sediment-water interface (Giller et al, 2004). Some studies use in-*situ* benthic chambers deployed on the seafloor (Archer and Devol, 1992; Devol and Christensen, 1993; Berelson et al., 1996; 2003; 2013) whereas others use *ex-situ* sediment core incubations (Rowe and Phoel, 1992; Belley and Snelgrove, 2016a; Belley et al., 2016 b), which provide oxygen uptake

estimates from sediments collected at depths < 1000 m (Glud et al., 1994). Several studies (Danovaro et al., 2008b; Belley et al., 2016b) have identified temperature as a key environmental variable for deep-sea functioning; temperature also influences microbial composition (Arndt et al., 2013), as well as degradation and transformation of slow sinking particles (Beaulieu, 2002). In turn, multiple abiotic factors (O_2, depth, T, sediment reworking etc.) may influence biotic processes including colonization and competition for food. However, the multifunctional nature of natural environments creates a significant challenge in finding suitable measures to quantify whole ecosystem functioning because the concept incorporates many different processes and includes physical, chemical, and biological phenomena (Snelgrove et al., 2014).

1.2.4 Technological developments

The logistical challenges of deep-sea sampling add to the critical need for efficient integration of ongoing technological developments into a strategic framework for deep-sea monitoring (Danovaro et al., 2020). Building on the first semi-quantitative data on deep-sea diversity collected using anchor dredges and sleds (Sanders and Hessler, 1969), box corers added new insights on deep-sea diversity (Grassle and Maciolek, 1992). Thenceforth, broader application of submersibles, video imagery, remotely operated vehicles (ROVs), and current sophisticated cabled observatories, have facilitated quantitative sampling of different habitats (Danovaro et al., 2014). For example, sonar technology enabled detection of shape and depth of deep-sea seamounts, oceanic crust, and trenches (Danovaro et al., 2014). Moreover, submarine technology has enabled the discovery of many new habitats following expansion of deep-sea exploration in the 1970s (Williams et al., 1979). ROVs, another type of submersible, allow remote observation of deep-sea environments through the incorporated camera (e.g., Vigo et al., 2023) and, for ROVs equipped with mechanical manipulators, to conduct simultaneously both manipulative experiments and

collection of physical samples (Miatta and Snelgrove, 2018, 2022; Ciraolo and Snelgrove, 2023). However, although the new technologies involve high costs, they also help to overcome risks associated with human-occupied vehicles (HOV). While filling some gaps, increasingly innovative tools have enabled new deep-sea ecology discoveries and raised new scientific questions. This evolution of sampling capacity underscores the need for more studies and the integration of multiple sampling tools and data forms. Therefore, I try to implement this aspect into my thesis by using rotary sonar and video images and pulse-chase experiments followed by isotopic analysis.

In parallel to rapid advances in marine instrumentation, scientists and engineers are working together across oceanographic disciplines to build technology and to interpret and analyze data. Increasing our knowledge and capacity to predict ocean change and its interactions with the land and atmosphere requires this type of collaboration.

1.3 Natural gradient and habitat heterogeneity areas

1.3.1 Barkley Canyon in the Northeast Pacific Ocean

The Northeast Pacific study focuses on the continental slope (400-2000 m depth) off the coast of Vancouver Island, British Columbia, Canada, a dynamic ocean region with complex circulation and geomorphology, an oxygen minimum zone (~ 200 -1,200 m depth), and changing physical, chemical, and biological conditions. Ocean Networks Canada assesses some of these changes (from a daily to yearly temporal scale) by supporting a regional cabled array. A recent study (De Leo et al., 2017) showed that the oxygen minimum zone (OMZ) impinges on this area's continental margin, with a core between 600 and 1200 m depth.

One of the best-studied canyons of British Columbia's slope, the Barkley Canyon, extends from the continental margin (~200 m) to the deep oceans (~2000 m), and cuts across the core of the OMZ at ~ 900m depth, where dissolved oxygen can reach as low as 0.16 $ml \cdot l^{-1}$ (Domke et al.,

2017). The Barkley Canyon upper slope (~400 m), experiences a higher and more variable oxygen concentration, ranging from 0.79 $ml \cdot l^{-1}$ to 1.94 $ml \cdot l^{-1}$. Barkley canyon resembles other submarine canyons in providing a "keystone structure" (Vetter et al., 2010) that encompasses heterogeneous habitats (e.g., different grain sizes, deep-water corals), specific abiotic characteristics, and acts as conduits of organic matter from the land to the deep sea (Jahnke, 1990) supporting high abundances, biomass, and biodiversity of benthic communities and associated food webs (De Leo et al., 2010; Campanyà-Llovet et al., 2018). Barkley Canyon, like other canyons, also acts as nursery sites (Sardà and Cartes, 1994; Hoff, 2010; Fernandez-Arcaya et al., 2013) and refuges for marine life from adjacent habitats (Yoklavich et al., 2000; De Leo et al., 2010; Vetter et al., 2010; Morris et al., 2013). Barkley Canyon displays a low diversity and abundance of megafauna within the OMZ compared to the upper slope. For instances, the OMZ restricted pennatulids, and the OMZ boundaries host ophiuroids (Domke et al., 2017). Moreover, the geomorphology of the sea floor affects the distribution of taxa across the canyon, with Porifera mainly found along the walls and Echinoidea within the canyon axis. Furthermore, Barkley Canyon Upper slope hosts sea pink urchin *Strongylocentrotus fragilis* with high urchin density corresponding to high oxygen (Command et al., 2022). However, the pink sea urchin might also forage in deeper water during weak upwelling and migrates to shallower habitats during low oxygen conditions (Command et al., 2022).

1.3.1.1 Oxygen Minimum Zone (OMZ – natural gradient)

Persistent low oxygen occurs in mid-water oxygen minimum zones, defined as regions with oxygen concentrations < 0.5 $ml \cdot l^{-1}$ (or ~7.5% saturation; 22 M), called also "extreme hypoxia" (Levin et al., 2003). The consensus definition for hypoxia is oxygen levels below 1.4 $ml \cdot l^{-1}$ (Tyson and Pearson, 1991). These features, also sometimes called oxygen minimum layers or oxygen-

deficient zones, occur at water depths ranging from shelf to upper bathyal zones (10–1300 m) (Wyrtki, 1962). OMZs generally form where strong upwelling leads to high surface productivity whose export and decomposition leads to depleted oxygen within the water column. Indeed, Diaz and Rosenberg (2008) summarized how increases in primary production and consequent worldwide coastal eutrophication fueled by riverine runoff of fertilizers and the burning of fossil fuels has increased the formation of dead zones in coastal waters. However, oxygen minimum zone formation also requires reduced circulation, long residence times (the absence of oxygen exchange), and a source of oxygen-depleted waters (Sarmiento et al., 1988) given a lack of exchange by circulation, vertical and horizontal diffusion, and water ascending from below(Wyrtki, 1962).

The largest OMZs occur at bathyal depths in the eastern Pacific Ocean, where older intermediate-depth waters exhibit lower oxygen concentrations than other water masses (Wyrtki, 1966, Paulmier and Ruiz-Pino, 2009). They also occur in the Arabian Sea, in the Bay of Bengal, and off southwest Africa (Kamykowski and Zentara, 1990). OMZs intercept a wide area of the sea floor. Helly and Levin (2004) used seafloor topographic data and US National Oceanographic Data Center oxygen data to estimate that bottom water with 0.5 $ml \cdot l^{-1}$ O_2 overlays over 1.148.000 km^2 of seafloor.

Deep-water hypoxia also occurs in some comparatively shallow basins, for example in Baja California, in the southern California borderland, in Saanich Inlet, and in some fjords (Diaz and Rosenberg, 1995; Zaikova et al., 2010; Hamersley et al., 2011). All OMZs exhibit a similar general oxygen profile but with regional variation in thickness and depth of oxygen levels (Levin et al., 2003). Typically, a steep drop in oxygen from the surface to the upper boundary of the OMZ characterizes a vertical profile of dissolved oxygen concentration through an OMZ. Below this

layer, an exponential decrease in oxygen consumption with depth leads to a zone of continuous low oxygen (Wyrtki, 1962). The lower OMZ boundary increases more gradually with water depth. The circulation and oxygen content of the ocean region strongly influence the thickness of the OMZ. OMZ thickness of > 1000 m off Mexico and in the Arabian Sea (Wishner et al., 1990; Fuenzalida et al., 2009) contrasts the 400 m thick OMZ off Chile (Fuenzalida et al., 2009). Greater OMZ thickness in the North Pacific results from older water masses with lower oxygen content than in the South Pacific (Wyrtki, 1966). Along continental margins, minimum oxygen concentrations typically occur between 200 m and 700 m where alter the spatial heterogeneity of the area where it impinges, the original benthic population, and the effects that these population have on the region (Murry and Farrell, 2014).

OMZs often support bacterial denitrification that utilizes nitrate ions for oxidation of organic matter, reducing nitrate to molecular nitrogen with nitrite as an intermediate (Codispoti and Christiansen, 1989). Nitrification, the oxidation of nitrate and ammonium, also occurs in these waters (Ward et al., 1989). Biochemical oxygen consumption creates oxygen minima, in which circulation affects OMZ distribution and position within the water column (Wyrtki, 1962).

In contrast to relatively well-studied oxygen-related patterns in shallow water (Diaz and Rosenberg, 2009), only a few detailed investigations have considered macrobenthic diversity, nutrient cycling, and carbon uptake along deep-water oxygen gradients. Moreover, in contrast to the most studied site, in Barkley canyon from the Northeast Pacific area, thanks to the development of the ONC observatory and associated maintenance cruises, interesting results have been conducted in terms of seasonal variations in bentho-pelagic coupling in the region and on the distribution of fauna along the OMZ. I, therefore, explored the contribution of the infaunal community to organic matter remineralization, and for initial carbon uptake in this region.

Moreover, I propose a new methodological approach to quantify bioturbation activity, specifically addressing how the OMZ affects bioturbation using video and sonar images simultaneously.

1.3.2 Northwest Atlantic Ocean (habitat heterogeneity)

The Gulf of Maine is a continental shelf sea on the east coast of North America, located between Cape Cod, MA, and Nova Scotia, Canada. This enclosed body of water overlays three Basins (Wilkinson, Georges, and Jordan – moving from West to East), Georges Bank, and the Northeast Channel. The three basins all exceed 250 m depth but are isolated from each other below 200 m (Townsend, 1991). Moreover, nutrient cycling dominated by the seasonal cycle of primary production characterizes the Gulf of Maine. High nutrient concentrations in the surface water during winter mixing led to abundant phytoplankton in the spring that forms the bulk of organic matter sinking to deeper depths. The Gulf's shape and physical features produce a characteristic internal circulation (Townsend, 1991; Christensen et al., 1996), in which water flowing along the Northeast Channel brings deep, cold, and rich nutrient water, first to Georges Basin, then to Jordan Basin, and then to the Wilkinson Basin. The latter basin has lower inorganic nitrogen concentrations than the eastern side, but higher phosphate and silicate concentrations (Christensen et al., 1996). Wilkinson Basin receives much less of the nutrient-rich slope waters and has high rates of sedimentary (within the first 20 cm of the sediment) denitrification and nitrogen loss (0.8-1.21 pgat N cm^2 s^{-1}, Christensen et al., 1996). However, surface sea water temperature within the typical internal circulation of the Gulf of Maine has increased noting the summertime average of ~13°C in the early 1990s that has not fallen below 15°C in summertime since 2007. For the last 10 years between 2011 – 2021, the average warming rate increased by nearly 15% to 0.63°C per decade (by the "Gulf of Maine Research Institute" (https://www.gmri.org/stories/gulf-of-maine-warming-update-summer-2021), while using satellite measurements compiled by NOAA's

National Centers for Environmental Information). The increasing temperature due to climate change and the shift of water masses (increasing in surface temperature and consequently strong differences in density between the surface- and deep-water masses) is reshaping ecosystems in ways that affect resources and ecosystem services at different spatial and temporal scale. For example, on a temporal scale, Balch et al. (2022) showed a decrease in surface primary production correlated to decreases in chlorophyll and particulate organic carbon and increase in temperature in a time series between 1998 and 2018.

On a relatively smaller scale, the Gulf of Maine is shaped by canyons, inter-canyons, and channels typified by an average temperature of ~15˚C, ~35 ppm salinity. The inherent topographic complexity, and the lack of in-depth studies on their local benthic communities, motivated us to study spatial patterns of macrofaunal community patterns, sedimentary characteristics, and nutrient fluxes by comparing the three habitats. Moreover, this study also provides an examination on benthic microbial communities among the three different habitats, given the lack of studies on it based on our knowledge.

1.4 Thesis format

This thesis investigates the effects of heterogeneity at different scales on deep-sea benthic ecosystems of the Pacific and Atlantic Oceans in order to improve understanding of the linkage between environmental and biological factors that influence benthic ecosystem functioning (BEF). Specifically, I extrapolated and identified four different spatial heterogeneity scales classified from a large to a small heterogeneity scale (**Fig. 1.5**).

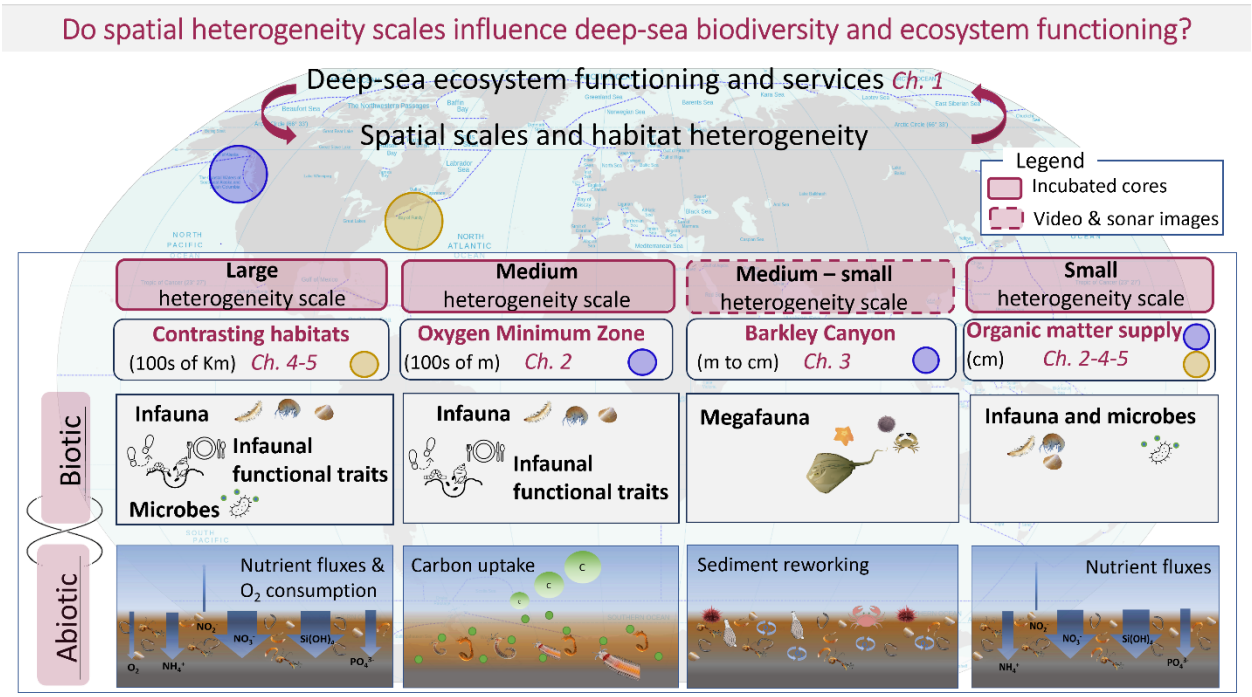

Fig. 1.5. Thesis summary. The gray box on top shows the main research question, followed by the main topics explored in each chapter. The blue circle refers to the Pacific Ocean and yellow to the Atlantic Ocean study sites. The red boxes illustrate the four heterogeneity scales followed by the corresponding subject chapters, respectively, along with abiotic and biotic factors evaluated in each scale and/or chapter.

This introductory chapter (Chapter 1) provides a general description of the importance of ecosystem function, how function connects to biological and environmental factors, and how spatial habitat heterogeneity affects biota and functioning. In Chapter 2, I explore the response of Pacific Ocean infaunal communities to the natural oxygen gradient in bottom-water, and the role of infauna in carbon cycling under otherwise similar environmental conditions. Chapter 3 follows on by considering macrofaunal community response to the OMZ, and the associated effects of reworked sediment. I also consider how complementary technological novelties can fill gaps in deep-sea benthic ecosystem knowledge. In Chapters 4 and 5, I study infaunal and microbial

community distribution and diversity, and associated nutrient fluxes in contrasting habitats of the western coast of the Atlantic Ocean, the Gulf of Maine. I also explore potential environmental and biological drivers that contribute to variation in infauna, microbes, and organic matter remineralization among contrasting habitats of the Gulf of Maine. Finally, Chapter 6 combines the results from the entire thesis to support an overall conclusion. Accordingly, spatial heterogeneity at different scales largely defines biodiversity patterns and contributes to ecosystem functioning. While we observe interesting biological responses in terms of mega, macro-, and microfauna, as well as abiotic drivers (e.g., quantity and quality of OM) at each study of the thesis, we could not find clear drivers of nutrient patterns. The last unclarity might be linked to the complexity of the environment where multiple abiotic factors such as temperature, salinity, bottom water oxygen concentration overlap each other leading to a difficult interpretation of our results at any spatial scale. Moreover, we were able to evaluate the major role of infauna in carbon cycling at a relatively small scale which may play a substantive role in C flow through the benthic food web as well as in organic matter remineralization and nutrient regeneration. Furthermore, we also highlight a technical aspect that might help to improve future studies. We show how video and sonar images can return independent, but complementary at the same time, results of reworked sediment at a small scale. While video images may show megafauna communities patterns (biological aspect), the sonar images can illustrate the presence/absence, and diversity of pits referring to biological features left on the sediment by organisms (physical aspect).

1.5 References

Archer, D., and Devol, A. 1992. Benthic oxygen fluxes on the Washington shelf and slope: A comparison of in situ microelectrode and chamber flux measurements. Limnol. Oceanogr., 37 (3), 614-629.

Armstrong, C. W., Foley, N. S., Tinch, R., and van den Hove, S. 2012. Services from the deep: Steps towards valuation of deep-sea goods and services. Ecosyst. Serv., 2, 2-13.

Arndt, S., Jørgensen, B. B., LaRowe, D. E., Middelburg, J. J., Pancost, R. D., et al. 2013. Quantifying the degradation of organic matter in marine sediments: a review and synthesis. Earth-Sci. Rev., 123, 53-86.

Azovsky, A. I. 2000. Concept of scale in marine ecology: linking the words or the worlds?. Web ecology, 1 (1), 28-34.

Balch, W. M., Drapeau, D. T., Bowler, B. C., Record, N. R., Bates, N. R., et al. 2022. Changing hydrographic, biogeochemical, and acidification properties in the Gulf of Maine as measured by the Gulf of Maine North Atlantic Time Series, GNATS, between 1998 and 2018. J. Geophys. Res. Biogeosci, 127 (6), e2022JG006790.

Beaulieu, S. E. 2002. Accumulation and fate of phytodetritus on the sea floor. Oceanogr. Mar. Biol., Volume 40, 179-217.

Belley, R., and Snelgrove, P. V. R. 2016a. Relative contributions of biodiversity and environment to benthic ecosystem functioning. Front. Mar. Sci., 3, 242.

Belley, R., Snelgrove, P.V. R., Archambault, P., Juniper, S. K. 2016b. Environmental drivers of benthic flux variation and ecosystem functioning in Salish Sea and Northeast Pacific sediments. PLoS One, 11 (3), e0151110.

Berelson, W. M., McManus, J., Coale, K. H., Johnson, K. S., Kilgore, et al. 1996. Biogenic matter diagenesis on the sea floor: A comparison between two continental margin transects. J. Mar. Res., 54 (4), 731-762.

Berelson, W., McManus, J., Coale, K., Johnson, K., Burdige, D., et al. 2003. A time series of benthic flux measurements from Monterey Bay, CA. Cont. Shelf Res., 23 (5), 457-481.

Berelson, W. M., McManus, J., Severmann, S., Reimers, C. E. 2013. Benthic flux of oxygen and nutrients across Oregon/California shelf sediments. Cont. Shelf Res., 55, 66-75.

Bremner, J. 2008. Species' traits and ecological functioning in marine conservation and management. J. Exp. Mar. Biol. Ecol., 366 (1-2), 37-47.

Campanyà-Llovet, N., Snelgrove, P. V. R., De Leo, F. C. 2018. Food quantity and quality in Barkley Canyon (NE Pacific) and its influence on macroinfaunal community structure. Prog. Oceanogr., 169, 106-119.

Charton, J. A. G., and Ruzafa, Á. P. 1999. Ecological heterogeneity and the evaluation of the effects of marine reserves. Fisheries research, 42 (1-2), 1-20.

Christensen, J. P., Townsend, D. W., Montoya, J. P. 1996. Water column nutrients and sedimentary denitrification in the Gulf of Maine. Cont. Shelf Res., 16 (4), 489-515.

Ciraolo, A. C., Snelgrove, P. V. R. 2023. Contrasting benthic ecological functions in deep-sea canyon and non-canyon habitats: Macrofaunal diversity and nutrient cycling. Deep Sea Res. Part I: Oceanogr. Res., 197, 104073.

Ciraolo, A. C., Snelgrove, P. V. R., Algar, C. K. 2023. Habitat heterogeneity effects on microbial communities of the Gulf of Maine. Deep Sea Res. Part I Oceanogr. Res., 197, 104074.

Command, R. J., De Leo, F. C., Robert, K. 2022. Temporal dynamics of the deep-sea pink urchin *Strongylocentrotus fragilis* on the Northeast Pacific continental margin. Deep Sea Res. Part I Oceanogr. Res. Pap, 103958.

Codispoti, L.A., Christiansen, J.P. 1989. Nitrification, denitrification and nitrous oxide cycling in the eastern tropical South Pacific Ocean. Marine Chemistry 16: 277-300.

Danovaro, R., Dell'Anno, A., Fabiano, M., Pusceddu, A., Tselepides, A. 2001. Deep-sea ecosystem response to climate changes: the eastern Mediterranean case study. Trends in Ecology and Evolution. 16(9), 505-510.

Danovaro, R., Dell'Anno, A., Corinaldesi, C., Magagnini, M., Noble, R., et al. 2008a. Major viral impact on the functioning of benthic deep-sea ecosystems. Nature, 454 (7208), 1084-1087.

Danovaro, R., Gambi, C., Dell'Anno, A., Corinaldesi, C., Fraschetti, S., et al. 2008b. Exponential decline of deep-sea ecosystem functioning linked to benthic biodiversity loss. Current Biology. 18 (1), 1-8.

Danovaro, R., Snelgrove, P. V., Tyler, P. 2014. Challenging the paradigms of deep-sea ecology. Trends in ecology and evolution, 29 (8), 465-475.

Danovaro R., Aguzzi, J, Fanelli E., Billett D., Carugati L., et al. 2020. Ecological indicators for an integrated global deep-ocean strategy. Nature Ecol. Evol. 4:181-192.

De Leo, F. C., Gauthier, M., Nephin, J., Mihaly, S., Juniper, S. K. 2017. Bottom trawling and oxygen minimum zone influences on continental slope benthic community structure off Vancouver Island (NE Pacific). Deep Sea Res. Part II Top. Stud. Oceanogr., 137, 404-419.

De Leo F.C., Smith C.R., Rowden A.A., Bowden D.A., Clark M.R. 2010 Submarine canyons: hotspots of benthic biomass and productivity in the deep sea. Proc Biol Sci. 22;277 (1695):2783-92. doi: 10.1098/rspb.2010.0462.

Devol, A. H., and Christensen, J. P. 1993. Benthic fluxes and nitrogen cycling in sediments of the continental margin of the eastern North Pacific. J. Mar. Res., 51 (2), 345-372.

Díaz, S., and Cabido, M. R. 2001. Vive la différence: Plant functional diversity matters to ecosystem processes. doi: https://doi. org/10.1016. S0169-5347 (01), 02283-2.

Diaz, R. J., and Rosenberg, R. 2008. Spreading dead zones and consequences for marine ecosystems. Science, 321(5891), 926-929.

Domke, L., Lacharité, M., Metaxas, A., and Matabos, M. 2017. Influence of an oxygen minimum zone and macroalgal enrichment on benthic megafaunal community composition in a NE Pacific submarine canyon. Mar. Ecol., 38(6), e12481.

Fernandez-Arcaya, U., Rotllant, G., Ramirez-Llodra, E., Recasens, L., Aguzzi, J., et al. 2013. Reproductive biology and recruitment of the deep-sea fish community from the NW Mediterranean continental margin. Progr. Ocean., 118, 222-234.

Fuenzalida, R., Schneider, W., Garcés-Vargas, J., Bravo, L., and Lange, C. 2009. Vertical and horizontal extension of the oxygen minimum zone in the eastern South Pacific Ocean. Deep Sea Res. Part II Top. Stud. Oceanogr., 56 (16), 992-1003.

Gage, J. D., and Tyler, P. A. 1991. Deep-sea biology: a natural history of organisms at the deep-sea floor. Cambridge University Press.

Giller, P. S., Hillebrand, H., Berninger, U. G., Gessner, M. O., Hawkins, S., et al. 2004. Biodiversity effects on ecosystem functioning: emerging issues and their experimental test in aquatic environments. Oikos 104, 423–436.

Glover, A. G., Smith, C. R. 2003. The deep-sea floor ecosystem: current status and prospects of anthropogenic change by the year 2025. Environ Conserv., 30 (3), 219-241.

Glud, R. N., Gundersen, J. K., Jørgensen, B. B., Revsbech, N. P., Schulz, H. D. 1994. Diffusive and total oxygen uptake of deep-sea sediments in the eastern South Atlantic Ocean: in situ and laboratory measurements. Deep Sea Res. Part I Oceanogr. Res. Pap., 41 (11-12), 1767-1788.

Gooday, A. J., and Turley, C. M. 1990. Responses by benthic organisms to inputs of organic material to the ocean floor: a review. Philosophical Transactions of the Royal Society of London. Series A, Mathematical and Physical Sciences, 331 (1616), 119-138.

Grassle, J. F. 1989. Species diversity in deep-sea communities. Trends Ecol. Evol., 4 (1), 12-15.

Grassle, J. F., Maciolek, N. J. 1992. Deep-sea species richness: regional and local diversity estimates from quantitative bottom samples. Am. Nat., 139 (2), 313-341.

Hamersley, M. R., Turk, K. A., Leinweber, A., Gruber, N., Zehr, J. P., et al. 2011. Nitrogen fixation within the water column associated with two hypoxic basins in the Southern California Bight. Aquat. Microb. Ecol., 63 (2), 193-205.

Hoff, G. R. 2010. Identification of skate nursery habitat in the eastern Bering Sea. Mar. Ecol. Prog. Ser., 403, 243-254.

Helly, J. J., and Levin, L. A. 2004. Global distribution of naturally occurring marine hypoxia on continental margins. Deep Sea Res. Part I Oceanogr. Res. Pap., 51 (9), 1159-1168.

Ingels, J., and Vanreusel, A., 2013. The importance of different spatial scales in determining structural and functional characteristics of deep-sea infauna communities. Biogeosciences, 10(7), 4547-4563.

Jahnke, R. A. 1990. Early diagenesis and recycling of biogenic debris at the seafloor, Santa Monica Basin, California. J. Mar. Res., 48 (2), 413-436.

Jahnke, R. A. 1996. The global ocean flux of particulate organic carbon: Areal distribution and magnitude. Global Biogeochem Cycles. 10 (1), 71-88.

Kamykowski, D., and Zentara, S. J. 1990. Hypoxia in the world ocean as recorded in the historical data set. Deep Sea Research Part A. Oceanographic Research Papers, 37 (12), 1861-1874.

Lampitt, R. S., Achterberg, E. P., Anderson, T. R., Hughes, J. A., Iglesias-Rodriguez, M. D., et al. 2008. Ocean fertilization: a potential means of geoengineering. Philos. Trans. Royal Soc. A. 366 (1882), 3919-3945.

Leibold, M. A., Mouquet, M. H. M. N. Amarasekare, P ,Chase, J. M, Hoopes, M. F. et al. 2004. The metacommunity concept: a framework for multi-scale community ecology. Ecol. Lett. 7:601–613.

Levin, S. A. 1992. The problem of pattern and scale in ecology: the Robert H. MacArthur award lecture. Ecology, 73 (6), 1943-1967.

Levin, L. A., Boesch, D. F., Covich, A., Dahm, C., Erseus, C., et al. 2001a. The function of marine critical transition zones and the importance of sediment biodiversity. Ecosystems, 4, 430–45.

Levin, L. A.. Etter, R. J, Rex, M. A., Gooday, A. J., Smith, C. R. 2001b. Environmental influences on regional deep-sea species diversity. Annu Rev Ecol Evol Syst. 32:51–93

Levin, L. A., Rathburn, A. E., Gutiérrez, D., Muñoz, P., and Shankle, A. 2003. Bioturbation by symbiont-bearing annelids in near-anoxic sediments: implications for biofacies models and paleo-oxygen assessments. Palaeogeogr. Palaeoclimatol. Palaeoecol., 199 (1-2), 129-140.

Lochte, K., and Turley, C. M. 1988. Bacteria and cyanobacteria associated with phytodetritus in the deep sea. Nature, 333 (6168), 67-69.

Mayor, D. J., Thornton, B., Hay, S., Zuur, A. F., Nicol, et al. 2012. Resource quality affects carbon cycling in deep-sea sediments. The ISME journal. 6 (9), 1740-1748.

Miatta, M., and Snelgrove, P. V. R. 2018. Biological and environmental drivers of deep-sea benthic ecosystem functioning in Canada's Laurentian Channel Area of Interest (AOI). *PeerJ PrePrints*.

Miatta M., Bates, A. E. Snelgrove, P. V. R., 2021. Incorporating biological traits into marine protected area strategies. Ann. Rev. Mar. Sci. 13:421–43. DOI: 10.1146/annurev-marine-032320-094121.

Miatta, M., and Snelgrove, P. V. R. 2022. Sea pens as indicators of macrofaunal communities in deep-sea sediments: Evidence from the Laurentian Channel Marine Protected Area. Deep Sea Res. Part I: Oceanogr. Res., 182, 103702.

Morris, K. J., Tyler, P. A., Masson, D. G., Huvenne, V. I., Rogers, A. D. 2013. Distribution of cold-water corals in the Whittard Canyon, NE Atlantic Ocean. Deep Sea Res. Part II Top. Stud. Oceanogr., 92, 136-144.

Murry, B. A., Farrell, J. M. 2014. Resistance of the size structure of the fish community to ecological perturbations in a large river ecosystem. Freshw. Biol., 59 (1), 155-167.

Nakagawa, S., and Takai, K. 2008. Deep-sea vent chemoautotrophs: diversity, biochemistry and ecological significance. FEMS Microbiol. Ecol. 65 (1), 1-14.

Oksanen, T., Oksanen, L., Gyllenberg, M. 1992. Exploitation ecosystems in heterogeneous habitat complexes II: impact of small-scale heterogeneity on predator-prey dynamics. Evol. Ecol., 6 (5), 383-398.

Ostroumov, S. A. 2005. Suspension-feeders as factors influencing water quality in aquatic ecosystems. In The comparative roles of suspension-feeders in ecosystems. JEES. Springer, Dordrecht. 147-164.

Pancost, R. D., Sinninghe Damsté, J. S., de Lint, S., van der Maarel, M. J., Gottschal, J. C., et al. 2000. Biomarker evidence for widespread anaerobic methane oxidation in Mediterranean sediments by a consortium of methanogenic archaea and bacteria. Appl. Environ. Microbiol, 66 (3), 1126-1132.

Paulmier, A., and Ruiz-Pino, D. 2009. Oxygen minimum zones (OMZs) in the modern ocean. Progr. Oceanogr., 80 (3-4), 113-128.

Pfannkuche, O., Boetius, A., Lochte, K., Lundgreen, U., Thiel, H. 1999. Responses of deep-sea benthos to sedimentation patterns in the North-East Atlantic in 1992. Deep Sea Res. Part I Oceanogr. Res. Pap., 46 (4), 573-596.

Polis, G. A., and Strong, D. R. 1996. Food web complexity and community dynamics. Am. Nat., 147 (5), 813-846.

Reiss, J., Bridle, J. R., Montoya, J. M., Woodward, G. 2009. Emerging horizons in biodiversity and ecosystem functioning research. Trends in Ecol and Evol. 24 (9), 505-514.

Rex, M. A. 1983. Geographic patterns of species diversity in the deep-sea benthos. The sea. 453-472.

Rex, M. A., Stuart, C. T., Hessler, R. R., Allen, J. A., Sanders, H. L., et al.. 1993. Global-scale latitudinal patterns of species diversity in the deep-sea benthos. Nature. 365 (6447), 636-639.

Rhoads, D. C., and Young D. K. 1970. The influence of deposit-feeding organisms on sediment stability and community structure. J. mar. Res., 28, 150-178.

Rhoads, D.C. 1974. Organism-sediment relations on the muddy sea floor. Oceanogr. Mar. Biol. Ann. Rev. 12, 263-300.

Rowe, G. T., and Deming, J. W. 1985. The role of bacteria in the turnover of organic carbon in deep-sea sediments. J. Mar. Res., 43 (4), 925-950.

Rowe, G. T., and Phoel, W. C. 1992. Nutrient regeneration and oxygen demand in Bering Sea continental shelf sediments. Cont. Shelf Res., 12 (4), 439-449.

Sanders, H. L., Hessler, R. R. 1969. Ecology of the Deep-Sea Benthos: More detailed recent sampling has altered our concepts about the animals living on the deep-ocean floor. Science. 163(3874), 1419-1424.

Sardà, F., and Cartes, J. E. 1994. Spatio-temporal variations in megabenthos abundance in three different habitats of the Catalan deep-sea (Western Mediterranean). Mar. Biol., 120 (2), 211-219.

Sarmiento, J. L., Herbert, T. D. Toggweiler, J. R. 1988. Causes of anoxia in the world ocean. Global Biogeochem. Cycles. 2, 115–128.

Schmidt, J. L., Deming, J. W., Jumars, P. A., Keil, R. G. 1998. Constancy of bacterial abundance in surficial marine sediments. Limnol. Oceanogr., 43 (5), 976-982.

Smith, C. R., and Demopoulos, A. W. 2003. The deep Pacific Ocean floor. Ecosystems (N. Y., Print). 179-218.

Snelgrove, P. V. R., Grassle, J. F., Petrecca, R. F. 1992. The role of food patches in maintaining high deep-sea diversity: Field experiments with hydrodynamically unbiased colonization trays. Limnol. Oceanogr. 37(7), 1543-1550.

Snelgrove, P. V. R., Grassle, J. F., Petrecca, R. F. 1996. Experimental evidence for aging food patches as a factor contributing to high deep-sea macrofaunal diversity. Limnol. Oceanogr. 41(4), 605-614.

Snelgrove, P. V. R. 1998. The biodiversity of macrofaunal organisms in marine sediments. Biodivers. Conserv, **7,** 1123–1132.

Snelgrove, P. V. R., Thrush, S. F., Wall, D. H., Norkko, A. 2014. Real world biodiversity–ecosystem functioning: a seafloor perspective. Trends Ecol. Evol., 29 (7), 398-405.

Snelgrove, P. V. R. and Smith, C. R. 2002. A riot of species in an environmental calm: The paradox of the species-rich deep-sea floor. Oceanog. Mar. Biol., 40, edited by: Gibson, R. N., Barnes, M., and Atkinson, R. J. A., Taylor and Francis Ltd, London, 311–342.

Sousa, W. P. 1980. The responses of a community to disturbance: the importance of successional age and species' life histories. Oecologia, 45, 72-81.

Sweetman, A. K., and Witte, U. 2008. Response of an abyssal macrofaunal community to a phytodetrital pulse. Mar. Ecol. Prog. Ser., *355*, 73-84.

Sweetman, A. K., Smith, C. R., Shulse, C. N., Maillot, B., Lindh, M., et al. J. 2019. Key role of bacteria in the short-term cycling of carbon at the abyssal seafloor in a low particulate organic carbon flux region of the eastern Pacific Ocean. Limnol. Oceanogr., 64 (2), 694-713.

Thistle, D., Ertman, S. C., Fauchald, K. 1991. The fauna of the HEBBLE site: patterns in standing stock and sediment-dynamic effects. Marine Geology, 99(3-4), 413-422.

Townsend, D. W. 1991. Influences of oceanographic processes on the biological productivity of the Gulf of Maine. Aquat. Sci., 5 (3), 211-230.

Turley, C. 2000. Bacteria in the cold deep-sea benthic boundary layer and sediment-water interface of the NE Atlantic. FEMS Microbiol. Ecol., 33 (2), 89-99.

Tyson, R. V., and Pearson, T. H. 1991. Modern and ancient continental shelf anoxia: an overview. Geol. Soc. Spec. Publ., 58 (1), 1-24.

Vigo, M., Navarro, J., Aguzzi, J., Bahamón, N., García, J. A., et al. 2023. ROV-based monitoring of passive ecological recovery in a deep-sea no-take fishery reserve. Sci. Total Environ., 883, 163339.

Violle, C., Navas, M. L., Vile, D., Kazakou, E., Fortunel, C.,et al. 2007. Let the concept of trait be functional. Oikos. 116(5), 882-892.

Vetter, E. W., Smith, C. R., and De Leo, F. C. 2010. Hawaiian hotspots: enhanced megafaunal abundance and diversity in submarine canyons on the oceanic islands of Hawaii. Mar. Ecol., 31(1), 183-199.

Ward, B. B., Glover, H. E., Lipschultz, F. 1989. Chemoautotrophic activity and nitrification in the oxygen minimum zone off Peru. Deep Sea Res. Part I Oceanogr. Res. Pap., 36 (7), 1031-1051.

Welsh, D. T. 2003. It's a dirty job but someone has to do it: the role of marine benthic macrofauna in organic matter turnover and nutrient recycling to the water column. Chem and Ecol. 19 (5), 321-342.

Whitlatch, R. B., Obrebski, S. 1980. Feeding selectivity and coexistence in two deposit-feeding gastropods. Mar. Biol., 58 (3), 219-225.

Wiens, J. A. 1976. Population responses to patchy environments. Annu Rev Ecol Evol Syst, 81-120.

Williams, D. L., Green, K., van Andel, T. H., von Herzen, R. P., Dymond, J. R., et al. 1979. The hydrothermal mounds of the Galapagos Rift: Observations with DSRV Alvin and detailed heat flow studies. J. Geophys. 84 (B13), 7467-7484.

Wishner K, Levin L, Gowing M, Mullineaux L. 1990. Involvement of the oxygen minimum in benthic zonation on a deep-sea mount. Nature. 346:57-59.

Witte, U., Wenzhöfer, F., Sommer, S., Boetius, A., Heinz, P., et al. 2003. In situ experimental evidence of the fate of a phytodetritus pulse at the abyssal sea floor. Nature, 424 (6950), 763-766.

Woulds, C., Andersson, J. H., Cowie, G. L., Middelburg, J. J., Levin, L. A. 2009. The short-term fate of organic carbon in marine sediments: comparing the Pakistan margin to other regions. Deep Sea Res. Part II Top. Stud. Oceanogr., 56 (6-7), 393-402.

Wyrtki, K. 1962. The oxygen minima in relation to ocean circulation. Deep-Sea Research 9, 11–23.

Wyrtki, K. 1966. Oceanography of the eastern Pacific Ocean. Oceanography and Mar. Biol.: an Annual Review. 4, 33–68.

Wyrtki, K. 1973. Physical oceanography of the Indian Ocean. J. Indian Ocean Reg., B. Zeitzschel (ed.). Berlin: Springer, 18–36.

Yayanos, A. A. 1986. Evolutional and ecological implications of the properties of deep-sea barophilic bacteria. Proc. Natl. Acad. Sci. U.S.A., 83 (24), 9542-9546.

Yoklavich, M. M., Greene, H. G., Cailliet, G. M., Sullivan, D. E., Lea, R. N., et al. 2000. Habitat associations of deep-water rockfishes in a submarine canyon: an example of a natural refuge. Fish. Bull., 98 (3), 625-625.

Zaikova, E., Walsh, D. A., Stilwell, C. P., Mohn, W. W., Tortell, P. D., et al. 2010. Microbial community dynamics in a seasonally anoxic fjord: Saanich Inlet, British Columbia. Environ. Microbiol., 12 (1), 172-191.

Chapter 2. - The roles of benthic diversity and environmental factors in nutrient and macrofaunal dynamics within the oxygen minimum zone of the British Columbia continental slope

2.1 Abstract

Oxygen minimum zones (OMZs), also known as oceanic "dead zones," are widespread oceanographic features currently expanding because of global warming. OMZs offer a unique opportunity to explore ecosystem functioning along an oxygen concentration gradient. Therefore, in this study, I focused on the OMZ of the Northeast Pacific continental slope (600-1200 m depth) off Vancouver Island, Canada.. Using a multicorer we collected sediment cores from 3 sites (200-, 475-, 850-m depth) with contrasting oxygen concentrations in near-bottom waters (~77, 40, 10 $\mu mol \cdot l^{-1}$, respectively) and performed shipboard incubations to examine organic matter remineralization and nutrient flux rates. In parallel, we performed pulse-chase tracer incubations in cores collected from two hypoxic sites, in which we added isotopically labelled algae (*Phaeodactylum* sp.) to examine macrofaunal community response to fresh phytodetrital input in terms of carbon uptake and benthic nutrient fluxes. Our results suggest a stronger influence of quantity and quality of organic matter, rather than the two collinear bottom-water oxygen concentration and depth on macrofaunal community structure. We also observed no clear relationship between macrofauna community composition and nutrient fluxes. Furthermore, our study suggests an important role for phytoplankton-based food for infaunal organisms living under different oxygen conditions, with stronger response in the shallowest oxygenated site at 475 m. Higher C uptake rate (~0.05 $mg \cdot C \cdot m^{-2} \cdot d^{-1}$), and net nutrient influxes at the 475 m site contrasted lower rates at the 850 m hypoxic site. Here, only one flabelligerid and one cirratulid, followed by amphipods, cumaceans, unidentified crustaceans, and bivalves primarily in the upper 2 cm of

sediment, ingested the organic matter. These results demonstrate no obvious influence of a gradient of decreasing oxygen on the abundances of seafloor macrofauna, rates of nutrient regeneration, or the role of infauna in organic matter remineralization. However, the quality and quantity of organic matter effects may obscure any effects of oxygen conditions.

Graphical Abstract

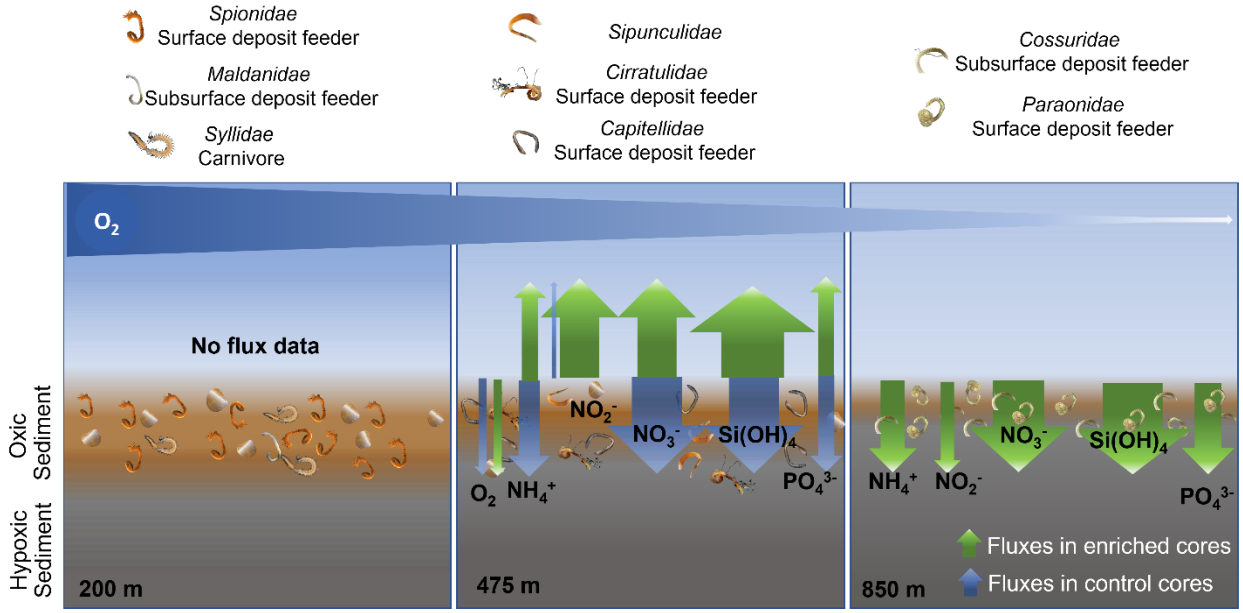

2.2 Introduction

Despite clear recognition of the central role that oxygen (O_2) and food availability play in benthic community composition in shallow environments (e.g., Pearson and Rosenberg, 1978; Diaz and Rosenberg, 2009), less information exists on how these factors interact with other variables in influencing distributions and processes related to benthic fauna in the deep sea (Levin and Gage, 1998). Studying oxygen minimum zones (OMZs) provides an important step in filling this gap because natural O_2 gradients in OMZs provide an opportunity to understand the magnitude of environmental drivers such as depth and temperature in the deep sea, and broader OMZ effects on ocean environments. OMZ continental margin sediments host low macrofaunal biodiversity, but support benthic sulfur-oxidizing bacteria, nitrogen-cycling bacteria, and metazoans adapted to oxygen-deficient conditions (e.g., Gallardo, 1977; Levin, 2003; Risgaard-Petersen et al., 2006). OMZs strongly affect nitrogen cycling, resulting in approximately 30-50% of nitrogen loss from the world's oceans (Codispoti et al., 2001) as microbes use either NO_3^- or NO_2^- as electron acceptors in support of denitrification (NO_3^- / NO_2^- conversion to N_2O or N_2), and anaerobic ammonium nitrification (NH_4^+ conversion to N_2), for example by anammox (Kalvelage et al., 2011; Kraft et al., 2022). OMZs can also stimulate the release of nitrous oxide (N_2O), a potent greenhouse gas that also contributes to stratospheric ozone depletion (Jameson et al., 2021).

Most previous studies on OMZs have focused on microbes (Levin et al., 1991; Lam and Kuypers, 2011; Wright et al., 2012) because of their critical role in organic matter (OM) remineralization. However, larger organisms such as macrobenthos also contribute to sedimentary biogeochemical processes (Meysman et al., 2006) through bioturbation and sediment oxygenation, simultaneously contributing to secondary productivity (Snelgrove, 1998), ecosystem services such as calcite dissolution that helps buffer pH changes, and even geomorphology (Murray et al., 2002).

Macrobenthos therefore provides an opportunity to explore the relationship between biodiversity and ecosystem functioning (Snelgrove, 1999).

Benthic macrofauna also provide an indicator of environmental change through changes in species composition or in biological and/or ecological traits such as motility trophic-mode, and habitat (e.g., Lam-Gordillo et al., 2022). Traits may help in inferring how organisms respond to their environment and their effects on ecosystem processes (Violle et al., 2014; Miatta et al., 2021), but few studies have applied functional diversity approaches to deep-sea environment (including OMZs), limiting our understanding of the role of species in mediating ecosystem functioning. Most OMZ studies utilizing a common set of diversity indices (species richness, expected number of species, and Shannon – Wiener indices), abundance and taxonomic species composition (Arntz et al., 1991; Diaz and Rosenberg, 1995; Gooday et al., 2009; Zettler et al., 2009), and macrofaunal functional diversity (e.g., Belley and Snelgrove, 2016) have focused on coastal waters. In contrast, among the few deep-sea studies, Pacheco et al. (2011) and Sivadas et al. (2020) showed decreasing macrofaunal diversity with increasing depth and decreasing O_2 concentration in deep hypoxic waters off northern Chile, and in the Arabian Sea, but they also reported the dominance of functional traits such as small size, short-lived burrowers, and discretely mobile infauna. Despite the potential applicability of functional diversity approaches in understanding marine ecosystem functioning, little effort has focused on their use in understanding the marine benthic system of the NE Pacific Ocean.

OMZs also provide a natural laboratory in which to study how environmental factors such as O_2 and organic matter availability affect how benthic communities process organic matter (Snelgrove et al., 2014). Most deep-sea ecosystems depend on organic matter, including phyto/phaeopigments, carbohydrates, lipids, and proteins, from episodic arrival of allochthonous

primary production (Dodds and Cole, 2007; Smith et al., 2008; Treude et al., 2009) for their primary food source. The quantity and quality of particles that reach deep-sea environments provide a good indicator of the trophic state of sediments, and vary greatly depending on seasonality, geography and regional productivity, and vertical distributions of organisms within the water column that both produce particulate organic carbon (POC) and mediate its transformation (Alldredge and Silver, 1988; Francois et al., 2002; Henson et al., 2012; Riley et al., 2012). Multiple studies demonstrate a strong link between the flux of POC and the composition of benthic communities and their functions, such as sediment community respiration (Moodley et al., 2005; Yool et al., 2017; Sweetman et al., 2019), and bioturbation depth and intensity (Watling et al., 2013). OM deposition influences bioturbation rates of larger benthos, which influence O_2 and OM transport within the sediment, and presumably accelerates microbial degradation rates (Turley et al., 1995, Diaz and Rosenberg, 2008). Previous studies show greater flux of OM to the seafloor in OMZs compared to flux rates in normoxic waters (Fenchel and Finlay, 1995; Bianchi et al., 2000; Levin et al., 2009) likely relating to reduced remineralisation of sinking organic matter in the hypoxic water column. Reduced remineralization in OMZ is caused by low abundances of infaunal species that would normally mix sediments through their feedingand movement, and higher presence of anaerobic microbes characterized by slower metabolisms compared to the aerobic ones (Jessen et al., 2017).

Benthic POC cycling provides an important ecosystem function in the deep sea because it influences the amount of carbon (C) sequestered into seafloor sediments as well as the efflux of essential macronutrients (NH_4^+, NO_2^-, NO_3^-, PO_4^{3-}, $Si(OH)_4^+$) and dissolved gases (e.g., O_2) across the sediment-water interface (Fowler and Knauer, 1986; Dunlop et al., 2016). Nutrient exchange provides an indicator of the rate of biogenic matter recycling and a measure of the alteration that

takes place between the time when material settles onto the seafloor and potentially permanent burial within the sediment (Berelson et al., 1990). The release of nutrients to the water column above the seafloor can eventually support primary production in surface waters (Aller, 2014). Factors such as depth also affect these co-dependent processes given that the amount of labile OM decreases with increasing depth (Romanelli et al., 2023).

To quantify benthic ecosystem functions and to understand species' diets in contrasting deep-sea ecosystems, researchers have developed techniques to elucidate food-web structure. Conventional analysis using gut contents has proven successful for megafauna (Lauerman et al., 1997), but this approach has limited utility for small-sized biota, such as macro- and meiofauna. Recent studies have therefore used isotopically labeled phytodetritus to trace the fate and quantification of C-flow through the food web, in conjunction with geochemical data (nutrients, oxygen, etc.) (Aberle and Witte, 2003; Woulds et al., 2007; Sweetman and Witte, 2008; Sweetman et al., 2009; Jeffreys et al.; 2013; Sweetman et al., 2014, 2016, 2019, Cecchetto et al. 2023), and in tandem with pulse-chase approach (Levin et al., 1999; Middelburg et al., 2000; Witte et al., 2003). Based on the concept that the natural isotopic signatures of an organism reflect the isotopic composition of its food source (Fry and Sherr, 1989) and the assumption "you are what you eat", isotopic analysis helps to elucidate trophic positions and what food resources support organisms (Peterson, 1999).

In pulse-chase experiments, researchers deposit isotope-labeled OM (e.g., ^{13}C labeled algae) over a defined patch on the seafloor, and then sample the patch to quantify uptake rates of the label by specific sediment-dwelling organisms and transformation into abiotic components such as dissolved inorganic carbon. Inconsistent results in studies of this type point to the need for further research on the role of fauna in sedimentary OM cycling, as well as disentangling the role of the

different factors that contribute to variation. For example, studies that focused on a single coastal or deep-sea site, or an offshore transect with covarying O_2, OM availability, and temperature (e.g., Moodley et al., 2002; Witte et al., 2003) demonstrate that foraminifera and bacteria take up significant proportions of the added label (Sweetman et al., 2019; Cecchetto et al., 2023). Thus, these taxa likely account for a major portion of OM remineralization in deep-sea sediments, but other variables such as water temperature that influences microbial and benthic metabolisms, the insufficient addition of carbon compared to background carbon fluxes (Moodley et al., 2005) may limit interpretation and generalization. In contrast, other studies suggest that macrofauna carry out the majority of faunal OM uptake over short-time scales (Blair et al., 1996; Witte et al., 2003), and expedite transport of fresh OM into the sediment (e.g., Levin et al., 1997) through "hoeing" of organic matter.

Noting previous applications of this approach in the abyssal NE Pacific (Druffel and Smith, 1998; Sweetman and Witte, 2008) and abyssal NE Atlantic (Aberle and Witte, 2003), we adopted a similar strategy in assessing the diversity and carbon-cycling role of macrofaunal communities on the continental slope of British Columbia, Canada. Along the Pacific Canadian continental shelf, the lowest near-bottom oxygen concentrations (0.7 ml $\cdot$ l^{-1}) in the Juan de Fuca eddy region occur in bottom waters at mid-shelf environments. This hypoxia links to summer upwelling that can transport oxygen-poor bottom waters to mid-shelf environments (Crawford and Pena, 2013). This upwelling, in combination with the relatively slow California undercurrent, acts in tandem with organic matter remineralization to further reduce water column oxygen concentrations. Indeed, O_2 concentrations is typically 2.0 ml $\cdot$ l^{-1} and declined at a rate of 0.02 ml $\cdot$ l^{-1} $\cdot$ y^{-1} from 1981 to 2011 (Crawford and Pena, 2013). Specifically, we aimed to investigate the short-term response of the deep-sea Pacific macrofaunal community to a simulated labeled phytodetritus

pulse akin to a seasonal food-pulse (albeit supplied in a single pulse delivery) under continental slope hypoxia, and thus how different O_2 conditions influence organic matter consumption rates and nutrient fluxes in benthic habitats.

In this study, we use ^{13}C labeled algal detritus as a tracer to address the role of specific benthic macrofauna in the short-term processing of OM in soft-sediment slope habitats. We sampled sites within the OMZ of the NE Pacific Ocean along a steep gradient in bottom-water O_2 concentration, depth, and OM availability, with corresponding faunal changes. A related study assessed microbial activities within this OMZ (Jameson et al., 2021). Given the importance of O_2 availability within sediments, and the co-dependency of O_2 and depth, we hypothesized that step changes occur in infaunal composition, and in organic matter remineralization. The latter may slow down with decreasing O_2 levels in the water column and result in reduced carbon uptake by macrofauna across specific O_2 thresholds, higher O_2 consumption rates, and lower benthic nutrient fluxes. We therefore examined total C uptake by macrofauna, sediment community O_2 consumption, and benthic nutrient fluxes.

2.3 Materials and Methods

The oxygen minimum zone in the Northeast Pacific Ocean, located in the Eastern North Pacific (ENP) and Eastern South Pacific (ESP), represents one of the largest such environments in the world (Kamykowski and Zentara, 1990) and has expanded in recent years with increasing ocean temperature (**Fig. 2.1**). Our study focuses on the Clayoquot continental slope near Vancouver Island.

Sampling took place in the fall of 2019 from September 29th to October 4th, onboard the Canadian Coast Guard Ship (CCGS) '*John P. Tully*'. We used an Oktopus multicorer with six separate core tubes (acrylic, 52 cm length, 9.9 cm OD, 9.7 cm ID) to sample each of three stations

where we deployed the multicorer three times. Poor weather condition limited us to only two deployments at the deepest station (850 m depth). **Supplementary table 2.1** provides further details on the experimental design and core allocations at each site.

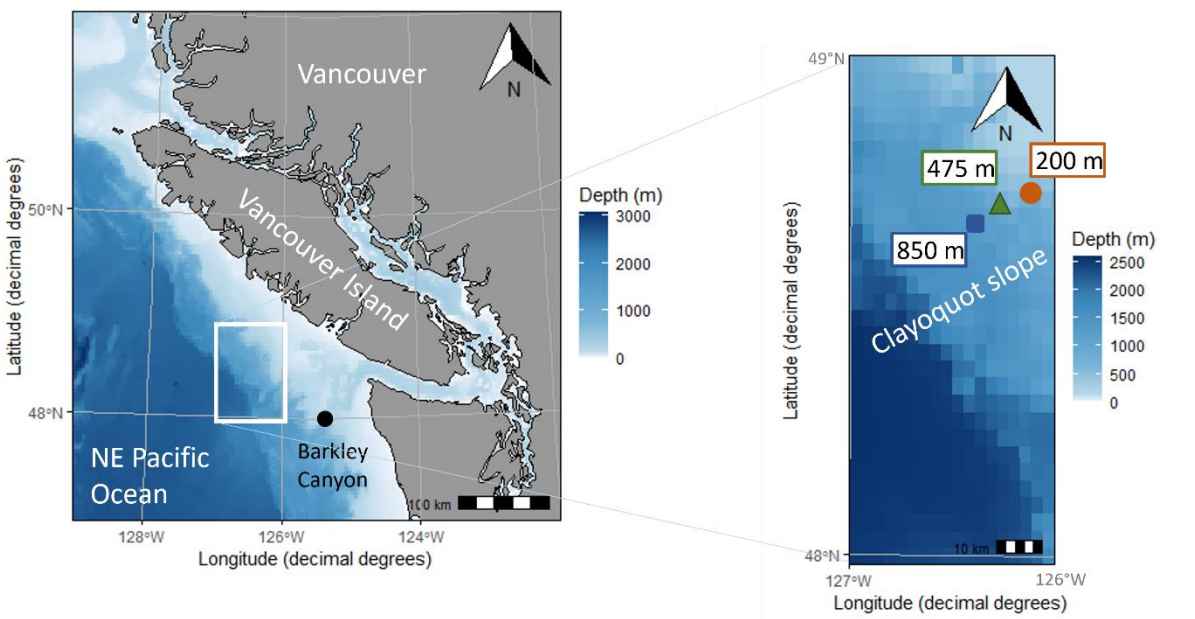

Fig. 2.1. Map of stations sampled on the Clayoquot slope near Vancouver Island in September/October 2019. Label symbols: 1) Colors: blue = normoxic site [O_2 = ~ 77 µmol · l^{-1}] at 200 m; green = reduced oxygen site [O_2 = ~ 40 µmol ·l^{-1}] at 475 m; red = hypoxic site [O_2 = ~ 10 µmol · l^{-1}] at 850 m.

We selected stations based on a transect that spanned an oxygen (and associated depth) gradient. Before deploying the multicorer we measured bottom water column characteristics, including *in-situ* oxygen concentrations, using a Conductivity-Temperature-Depth (CTD) profiler (SBE 43, Sea-Bird Electronics). Through this process, we identified and sampled the oxygenated habitat closest to the upper OMZ layer at 200 m depth ([O_2] ~ 77 µmol · l^{-1}), and then two low oxygen locations at 475 m and 850 m characterized by oxygen concentrations of ~ 40 and ~ 10 µmol · l^{-1}, respectively.

From each deployment, we dedicated three cores to macrofaunal experiments and three to a complementary study of microbial processes (Jameson et al., 2021). We allocated one of the three cores from each deployment to each of three treatments (incubated enriched cores, incubated non-enriched cores, non-incubated cores) to achieve replication and remove pseudo-replication. We dedicated two cores at the normoxic site, and one core from the last deployment at the two low-oxygen sites to quantify OM, lipids, Chl*a* and grain size composition; they were therefore unavailable for incubations.

2.3.1 General description of the incubation set-up

We conducted on-board core incubations for ~24 h in a dark cold room held at *in-situ* temperature (5-7 °C) for each station to simulate deep-sea conditions, acknowledging potential effects of pressure on species' behavior and physiology. Because our study focused on macrofauna we aimed for core penetration of ~15-20 cm to ensure we captured the upper 10 cm of sediments but left sufficient space for bottom water above the sediment. Immediately after the multicorer was back on deck, we transferred each core to the onboard wet lab, fitted the cores with incubation caps to seal them (described below), and moved them to a cold room where we left them for 4-6 h to allow any resuspended sediment particles in the overlying water to settle back to the sediment surface. At the onset of the incubations, which started after the settlement period, we collected water samples for future nutrient analysis, removing two replicate water samples at the beginning, middle (12 h later), and end of each incubation and replacing the water we removed with bottom water collected with a Niskin bottle rosette. Nutrient samples were stored in 50 ml pre-acid-washed plastic falcon tubes in a dark freezer (-80 ^{o} C). We determined oxygen consumption and nutrient fluxes from the slope of the linear regression of nutrient or oxygen concentrations versus time of incubations after correcting for the solute concentration in the replacement water (**Supplementary**

Fig. 2.1). We then sectioned individual cores into three sediment depth layers (0-2, 2-5, 5-10 cm) for preservation in 10% formalin and later transferred the samples to 70% ethanol prior to processing for identification of macrofauna. At the 475 and 850 m sites only, we added an additional component given our interest in short-term carbon flow through sediment-dwelling macrofauna. At the beginning of the incubation, and before collecting water samples, we added isotope labeled *Phaedocatylum* sp to each of the incubated sediment cores, ensuring through visual observation that the algae settled onto the sediment. Cores from 200 m site were dedicated to a different experiment in collaboration with another researcher involved in a related project.

2.3.2 Cultivation of labeled algae

We used an axenic culture of the diatom *Phaeodactylum* sp. obtained from the Scottish Association for Marine Science to produce an isotopically labeled food source for our phytodetritus-addition experiments. We chose this species as a suitable food source because it belongs to a widely distributed diatom genus that occurs throughout the Pacific Ocean (Martino et al., 2007), and sinks to the seafloor in phytodetrital aggregates. Algae were cultured in artificial seawater and F/2 culture medium replacing 25% of the $NaHCO_3$ with 25% $NaH^{13}CO_3$. The algae were grown for 4-5 weeks at 16 °C under a 12 h light dark cycle. Algae were harvested by centrifugation (408 rpm x 3 min), rinsed 5 times with unlabeled artificial seawater to remove labelled inorganic C, frozen, and freeze-dried. The algal biomass had a mean molar C:N ratio of 8.9 ± 1 (SD), a mean organic C content of 8% and a mean ^{13}C content of 22.04 ± 0.1 atom% (SD).

2.3.3 Oxystat System description

Given concerns about reducing oxygen concentrations of hypoxic samples to anoxic conditions, our incubations used a closed and oxygen impermeable system (Schwartz et al., 2007) to monitor oxygen concentrations in the water (see **Fig. 2.2 A), B), C)**).

The water reservoir, a 13.25 L, high-density polyethylene (HDPE) tank, contained bottom water collected from 5 to 10 m above the seafloor with 2.5 L Niskin bottles. The HDPE lid fitted to the container had nine oxygen-impermeable ports sealed with black barb fittings and plugs. We connected the cores to the ports through 5/8-inch Masterflex Precision Pump Tubing (Cole-Parmer, Montreal, CAN). In order to stabilize oxygen concentrations in the water reservoir at concentrations appropriate to the conditions at depth for each simulation, we bubbled either N_2 or medical-grade compressed air through 0.75 inch Tygon tubing. Acrylic caps sealed the bottom and top of sediment cores hermetically using two silicon o-rings, and two gas-tight sampling ports connected the core to the water reservoir; the second port enabled the collection of water samples during incubations. A magnetic stirrer on the inside of the upper lid maintained constant and gentle water movement as it mixed the water above the sediment. We also used a non-intrusive Fibox Polymer Optical Fiber (PreSens, Regensburg, DE) probe and pre-fitted sensor optode spots to monitor oxygen concentrations in the water reservoir every 2-4 h.

The peristaltic pump enabled continuous water circulation between the water reservoir and the sediment cores at a flow rate of ~50 ml $\cdot$ min^{-1} and a flow rate capacity range between 0.006-760 ml $\cdot$ min^{-1}. We chose this specific strategy based on flow velocity (V) calculated from published data (Belley et al., 2016).

$V = [(FO_2 * Ac)/\Delta O_2]$ (Morse et al., 1999)

FO_2 = Flux of oxygen consumption mmol $m^{-2} \cdot h^{-1}$

Ac = area of sediment within the sediment core

ΔO_2 = difference in oxygen concentration between the ambient and sediment core water

2.3.4 Normoxic processes at the 200 m station

For the 200 m site, on September 29, 2019, we set up a control "normoxic" system (described below, **Fig. 2.2**) and three extra cores. We included them in further macrobenthic analysis, but could not include them in nutrient fluxes analysis because they were dedicated to a parallel experiment (Jameson et al., 2021). We also dedicated two non-incubated cores to organic matter analysis.

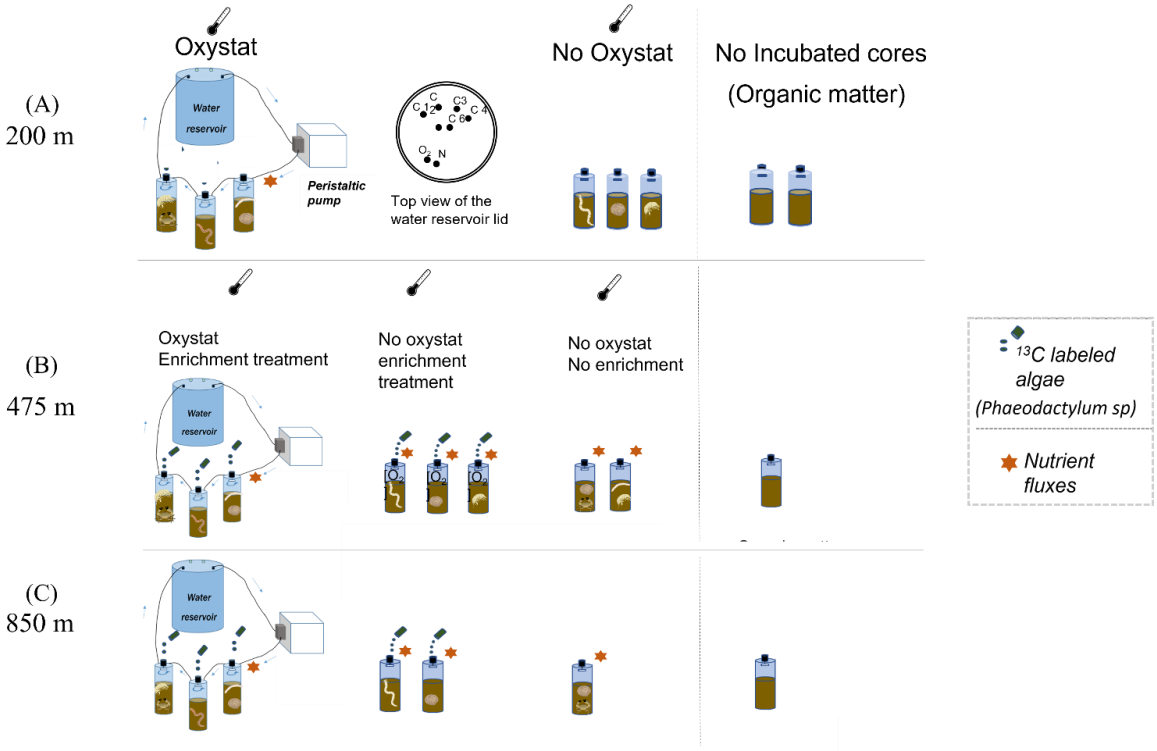

Fig. 2.2. Experimental setup for the normoxic 200 m site (A) and the two low-oxygen sites (475 m (B); 850 m (C)). Oxystat system scheme: The water reservoir, peristaltic pump, incubated cores, and tubing comprise the oxystat system. The water reservoir contained water collected with a Niskin bottle rosette from the water column 200-; 475-; 850 m site, respectively. Sediment cores were incubated at ~5 °C. Orange stars indicate the collection of water samples for nutrient analysis. Green dots refer to the addition of phytodetritus to incubated sediment cores. [O_2] indicates measurements of oxygen consumption. The figure also shows the lid of the water reservoir: C1 to

C6 black dots represent the ports to which the cores were connected. Three, three, and two incubated cores per site, respectively were not connected to the Oxystat system, and two, one, and one core, respectively, were not incubated and dedicated to OM analysis. The numbers of cores, the schematic of macrofaunal analysis, and the water sample numbers represent the actual number of cores used.

We collected bottom seawater from the 200 m site overnight and immediately stored it in the ship's cold room at *in-situ* temperature and oxygen conditions of ~5 °C and ~77 $\mu mol \cdot l^{-1}$, respectively, until we began the simulation experiment the following day. The morning after we collected sediment cores, we filled the water reservoir with bottom water and began the 24-h incubation. We collected replicate nutrient samples from the closest core to the reservoir only, based on the direction of water circulation because the system was sensitive to any disturbance, noting that the interconnected cores precluded true experimental replicates. Moreover, the water – but not the sediment - of the resting three cores was sacrificed for a parallel experiment which precluded adding replicates to the nutrient samples. During taxonomic identification we observed 3 or fewer macrofaunal individuals within any of the 5-10 sediment layers from the 200 m station.

2.3.5 Simulation at the shallower hypoxic site (475 m depth)

On October 1st, 2019, we sampled the 475 m station on the Clayoquot slope, a low-oxygen environment (~ 40 $\mu mol \cdot l^{-1}$) and set up incubations as described in sub-section 2.1. However, for this experiment, we added an additional component. To evaluate biotic responses to seasonal food pulses in this habitat, we carried out an *ex-situ* pulse-chase experiment by adding ^{13}C labelled phytodetritus to six of our cores (two from each multicorer drop), leaving the remaining two cores as experimental "controls". For this experiment, we connected three of the six enriched cores to the Oxystat system, and we added 0.2 g labeled *Phaeodactylum* sp., equivalent to 2.41 $g \cdot C \cdot m^{-2}$

(0.02 g · C · m^{-2} · d) to each of the six incubated sediment cores, excluding the two control cores (**Fig. 2.2 B**, **Supplement table 2.1**). We also measured macrofaunal community structure (e.g., diversity, abundance, composition) and oxygen consumption from these same cores to evaluate the effects of hypoxia on benthic ecosystem structure and functioning. Moreover, we evaluated the polychaete feeding behaviour at the family level (surface deposit-feeder; subsurface deposit-feeder; filter-feeder; carnivore; herbivore) based on published information (Jumars et al., 2015) given their dominance within the infaunal community and potential role in carbon uptake in this study. We incubated and processed cores as described in sub-section 2.1. Macrofauna were totally absent from the 5-10 cm sediment layer at this low-oxygen site.

2.3.6 Simulation at the deeper hypoxia site (850 m)

The oxygen concentration at our third site (850 m depth) was ~10 µmol · l^{-1}. We were only able to dedicate six rather than nine cores to the incubations because of unfavorable weather conditions that limited us to two multicorer deployments (**Fig. 2.2 C**), thus leaving just one unenriched incubated control. Moreover, we dedicated one extra non-incubated core to OM (**Supplementary table 2.1**).

For this experiment, we processed our cores similarly to those at the 475 m site (Section 2.5). However, in contrast to the 475 m site, we added 0.1 g labeled algae, equivalent to 1.60 g · C ·m^2 (0.01 g · C · m^{-2} · d^{-1}) to each five incubated sediment cores to evaluate short-term C flow through sediment-dwelling macrofauna at the 850 m site.

Note that we did not add the same amount of algae at the two deep sites because multiple factors influence the organic carbon flux that actually reaches the sea floor. We therefore calculated vertical carbon flux at our study sites based on Suess' (1980) equation that allowed us

to predict organic carbon flux at any depth below the base of the euphotic zone in relation to mean net primary production rate at the surface and depth-dependent carbon consumption.

2.3.7 Laboratory analysis

2.3.7.1 Macrofaunal analysis and taxonomic identification

In the laboratory, we carefully removed all macrofaunal organisms from the sediment samples and, depending on taxon, identified them to species, family, or order under a binocular dissection microscope. We determined abundance (N) for each taxon and calculated taxonomic richness (S) as the number of taxa present in each sediment core. We also determined diversity indices including Simpson's index (Simp), Pielou's evenness (J'), Rarefaction (ES[] and Shannon-Wiener (H') for each sediment core in R (R Core Team 2016), using the R package "vegan" (Oksanen et al., 2013).

2.3.7.2 Biological traits and functional diversity

We selected three biological traits (mobility, sediment reworking functional type, and feeding type) and 17 levels from published sources, based on their presumed influence on benthic fluxes (**Table 2.1**) (Queirós et al., 2013; WoRMS Editorial Board, 2015). Using a "fuzzy coding" approach, we allowed more than one functional trait for a given taxon and scored them from 0 to 1, where 0 reflected no affinity for the given trait, and 1 denoted exclusive affinity. When a taxon shared more than one trait that varied with environment, we scored each trait as 0.5 for two traits, and 0.3 for three traits. For example, the family Flabelligeridae exhibits surface deposit feeding and filter feeding behaviour. We used trait category scores for each taxon and taxa abundance matrices to obtain functional diversity (FD) indices using the "FD" package (Laliberte et al., 2014) in R. We excluded one core from the 475 m site because it included fewer species than the function required. We then computed the following multidimensional FD indices for subsequent analyses:

functional richness (FRich), functional evenness (FEve), functional divergence (FDiv) (Villéger et al., 2008).

Table 2.1. Biological traits and modalities used in trait analysis.

Trait	Level
Movement	live in fixed tubes (FT)
	limited movement (LM)
	slow movement (SM)
	free movement in sediment matrix (FMSM)
	free movement in burrow system (FMBS)
Reworking types	epifauna (E)
	surficial modifiers (S)
	upward conveyors (UC)
	downward conveyors (DC)
	biodiffusors (B)
	regenerators (R)
Feeding type	carnivorous (predator or passive suspension) (C)
	surface deposit feeder (D)
	filter/Suspension feeder (F)
	omnivorous (scavenger) (O)
	parasite (P)
	subsurface deposit feeder (SB)

2.3.7.3 ^{13}C enriched macrofauna

We measured isotopic ratios of macrofauna on an EA, Carlo Erba NA1500 analyzer attached to a ThermoFinnigan DeltaV plus isotope-ratio mass spectrometer (IRMS), using separate picking utensils for isotopically unlabeled organisms (collected from control incubated cores) and labeled organisms (collected from enriched incubated cores) to avoid cross-contamination with stable isotopes. The spectrometric analysis used a formalin-ethanol preservation method. We treated non-calcified and calcified organisms separately because inorganic C in the form of carbonates can interfere with the measurement of organic ^{13}C in sediments. Single organisms were washed with cool, filtered seawater to remove attached organic debris, transferred into tin (Sn) capsules

(Pressed Standard Weight 8 x 5 mm pack of 250), and dried in an oven at 60 °C overnight until the sample was dry. We decalcified calcareous shelled organisms in double boated silver (Ag) caps following methods described in Sweetman et al. (2009). After drying, we sealed each Ag capsule in a tin cup to avoid leakage sometimes associated with silver cups. Prior to IRMS measurements, we weighed organisms on a microbalance (Mettler Toledo) to determine biomass for each sample (~1 mg). To obtain sufficient biomass for isotope measurements, we sometimes had to combine individual organisms from a given taxon.

Post-experiment samples of enriched and control infauna were processed by the Core Research Equipment and Instrument Training Network – The Earth Resources Research and Analysis Facility (CREAIT – TERRA) Facility at Memorial University completed isotopic analysis. We calculated the carbon isotope ratios ($^{12}C/^{13}C$) from the measured C-contents of the sample against a VPDB-standard (Boutton, 1991), and express the carbon isotope ratios in delta notation ($\delta^{13}C$) as relative difference between sample and standard: $\delta^{13}C$ [‰] = $[((R_{sample})/(R_{standard})) - 1] \times 1000$, where $R_{standard}$ is the ^{13}C:^{12}C of the reference material for C. The international reference material for C is Vienna Pee Dee Belemnite (R_{vpdb} = 0.0112372). We calculated uptake of ^{13}C (expressed as $\Delta\delta^{13}C$ (‰) in macrofaunal organisms as excess (above control ^{13}C values) expressed as the specific uptake: ($\Delta\delta^{13}C = \delta^{13}C_{\text{ sample}} - \delta^{13}C_{\text{ control}}$), where $\delta^{13}C_{\text{ "sample"}}$ refers to organisms collected from enriched cores, and $\delta^{13}C_{\text{ "control"}}$ to organisms collected from unenriched/control cores. Uptake of ^{13}C was then calculated as the product excess of atom% ^{13}C (samples - control) and C content expressed as a unit weight: ^{13}C uptake (unit wt C) = (atom% $^{13}C_{\text{ samples}}$ – atom% $^{13}C_{\text{ control}}$) x (unit wt C of organism). This value was then adjusted to account for ^{13}C algal labelling, yielding total C uptake: C uptake (unit wt C) = ^{13}C incorporation/22.04 atom %. C-uptake was then normalized to 24 h to yield total C-turnover.

2.3.7.4 Laboratory analysis of sediment organic matter

We collected sediments for analysis of organic matter and grain size from the upper 0-2 cm of the core at each site dedicated to sediment analysis, homogenizing the sediment and then placing it in Whirl-Pak bags prior to storage in the dark at -20 °C until analyzed. We stored samples for lipid analysis in pre-combusted aluminium tin foil at -80 °C. We measured OM to summarize practical proxies of OM quantity and quality. Therefore, we used total organic carbon (TOC) to describe food quantity. To characterize organic matter quality, we used chlorophyll *a* (Chl*a*), phaeopigments (Phaeo), and the chlorophyll *a*: phaeopigment ratio (Chl-*a*: Phaeo) as indicators of short-term OM freshness and quality (Guitton et al., 2015); algae and photosynthetic pigments degrade faster than lipids and provide a measure of freshness of OM over time scales of days to weeks. We also used total lipid concentrations as an indicator of intermediate-term (weeks to months) OM lability/ quality (Mayer et al., 1995) because lipids degrade at slower rates compared to pigments. Finally, we used the carbon:nitrogen (C:N) ratio as an indicator of long-term (months - years) OM quality, with lower C:N indicating fresher and higher quality OM because of more rapid use of nitrogen than carbon (Guitton et al., 2015).

2.3.7.4.1 CHN analysis

Total organic carbon and total nitrogen (TN) were determined by drying a sediment subsample of 1-5 g (wet weight) at 60 °C for 24 h, grinding it to a fine powder, and then weighing and acidifying (with pure HCl fumes) for 24 h to eliminate inorganic carbon. Samples were dried again at 60 °C for 24 h prior to CHN analysis. We then weighed an aliquot of dried decarbonated sediments (15 mg) and folded it tightly into a tin capsule. A Carlo Erba NA1500 Series II elemental analyser (EA) determined the sediment concentration of TOC and TN in sediments, expressed as carbon/ nitrogen percent weight.

2.3.7.4.2 Phytopigment content

We measured chlorophyll *a* and phaeopigments spectrophotometrically (Cary 300 BIO) (Danovaro, 2009), noting that spectrophotometric assays are generally used for pigments in sediments with concentrations > 0.5 Chl*a* $\mu g \cdot g^{-1}$. For each sample, we placed 2 g of frozen sediment in a transparent falcon tube wrapped with aluminium foil to block out light. We extracted pigments from the sediment in 90% acetone, vortexed the solution for 30 s, and then placed the samples in an ultrasound bath in ice at 50-100 W for 3 min, with a 30 s interval between each min of sonication prior to overnight storage at 4 °C in the dark. The following day we centrifuged them for 10 min at 800 x g (3800 rpm) and analyzed the supernatant to measure absorbance at wavelengths of 750 nm and 665 nm (against a blank of 90% acetone). At the same wavelengths, we determined phaeopigments by acidifying the acetone extract with 200 µL of 0.1 N HCl added directly in the cuvette. We dried the remaining sediment at 60 °C for 24 h prior to weighing.

2.3.7.4.3 Lipid content

We extracted frozen lipid samples according to Parrish, (1999), a method that required repeating specific steps three times. We used a combination of chloroform: methanol: water (4:2:1.5) in order to create an upper inorganic and a lower organic layer. We were interested in removing and then analysing the bottom organic layer that contained lipids and therefore sonicated the sample for 4 min in an ice bath followed by two min of centrifuging. Without disturbing the top aqueous layer, we used a double pipetting technique that required 2 lipid-cleaned Pasteur pipettes, a long 1-ml pipette inside a short 1-ml pipette. We then added chloroform back to the extraction test tube. As a final step, we transferred all the organic layer into a lipid-cleaned vial, concentrating samples under a flow of nitrogen gas.

Lipid class composition was determined at the Aquatic Research Cluster (ARC) at the Ocean

Science Center of Memorial University, using an Iatroscan Mark VI TLC-FID (thin-layer chromatography-flame ionization detector system; Mitsubishi Kagaku Iatron, Inc., Tokyo, Japan), silica coated Chromarods, and a three-step development method (Parrish, 1987). The lipid extracts were applied to the Chromarods and focused into a narrow band using 100% acetone. The first development system was hexane: diethyl ether: formic acid (99.95:1:00.05). The rods were developed for 25 min, removed from the system for 5 min, and then replaced for 20 min. The second development in hexane: diethyl ether: formic acid (79:20:1) lasted for 40 min. The final development system required two steps, the first involving immersion in 100% acetone for two 15-min periods, followed by two 10-min periods in chloroform:methanol:chloroform-extracted water (5:4:1). Before each solvent system run, we dried the rods in a constant humidity chamber. After each development system, we scanned the rods in the Iatroscan and collected data using Peak Simple software (ver 3.67, SRI Inc). Chromarods calibration used standards from Sigma Chemicals (Sigma Chemicals, St. Louis, Mo., USA).

2.3.7.4.4 Grain size

Sediment samples were analyzed at the Bedford Institute of Oceanography, Marine Environmental Geoscience, Nova Scotia, using a Beckman Coulter LS 230 Laser Diffraction analyzer set at a 0.4 – 2000 μm range. Samples were subjected to 35% hydrogen peroxide digestion over several days to remove organic particles, then centrifuged and freeze dried. After freeze drying, we immediately capped and weighed the vials. Grain size analysis then proceeded on individual samples by first removing the cap and then disaggregating the sample using a metal spatula before pouring the contents over a 2 mm sieve. The >2 mm material was then weighed at ¼ phi intervals and values recorded. The <2 mm fraction was either used in its entirety or microsplit for analysis in the Beckman Coulter LS13-320 laser diffraction analyzer. Samples were

then disaggregated completely in an ultrasound bath before laser diffraction analysis. Samples were analyzed for 60 s and graphed based on size, noting that we also analyzed a control standard daily. Laser files were logged and processed using Femto Particle Sizing Software (PSS) version 5.6. Laser diffraction data was then merged with the gravel fraction to normalize the distribution. PSS uses Folk and Ward graphic statistical parameters using phi midpoints and a geometric mean. Sediments at each station were classified following the sediment classification scheme based on percentages of sand, silt, and clay (Wentworth, 1929).

2.3.8 Data analysis

2.3.8.1 Infaunal structure and nutrient fluxes analysis

We initially investigated infaunal densities as well as diversity indices (species richness (S), Shannon - Wiener index (H' log10), Simpson's diversity index (Simp), Pielou's evenness (J'), and expected number of species (ES[50] i.e., the expected number of taxa in a hypothetical random sample combining the data from the entire 10 cm core at the 200 m site) per core (enriched + control), in order to compare community structure among sites differing in bottom water oxygen concentrations. All analyses below were conducted in the software package R. We examined normality of the residuals (Q-Q plot) and homogeneity of variances (residual vs fitted plot and Levene's test) prior to performing a one-way ANOVA with bottom water oxygen concentrations as fixed factors. In instances where assumptions were not met, we either log or square-root transformed data. When data transformation did not work (e.g., species richness), we performed a Kruskal-Wallis test, followed by a Dunn post-hoc test. For expected number of species ES[50], data were not linear, and we therefore performed a polynomial regression, followed by post-hoc Tukey's tests once we had detected significant differences among sites. Depth (200-, 475-, 850 m) and bottom water oxygen concentrations (~77, 40, 10 $\mu mol \cdot l^{-1}$) were closely related; we therefore

used only oxygen concentration as an explanatory variable but acknowledge that other depth-related environmental variables may have contributed to observed patterns.

We used multivariate statistics to identify differences in benthic community composition among the three different oxygen concentrations (~77, 40, 10 $\mu mol \cdot l^{-1}$) and combining enriched and control cores. Because faunal data sets often include a large number of zeros (no individuals of a given species), we chose Bray-Curtis as an appropriate similarity measure. We present results based on non-transformed data. After verifying homogeneity of multivariate dispersion using the PERMDISP routine (Anderson et al., 2008) we tested for significant differences among oxygen concentrations with PERMANOVA, performed with 9999 random permutations using the function 'adonis' from the package 'vegan'; this function is directly based on McArdle and Anderson, (2001) and performs a sequential test of terms in pair-wise adonis. We also used the similarity percentage procedure (SIMPER) to evaluate which taxa contributed most to community dissimilarities among different oxygen concentrations, which we then plotted with nMDS vectors.

To understand better which environmental variables best explained benthic community variation among depths, we performed a redundancy analysis (RDA - using the "rda" function) with type II scaling that focuses on the explanatory variables rather than response variables. We included both enriched and control cores for infaunal community. We transformed our data with a Hellinger transformation prior to the RDA, and environmental variables were standardized, using the "decostand" function in R. We further analyzed multi-collinearity of the predictor variables from the full models with a variance inflation factor (VIF) test using the "vif" function from the "car" package (Fox and Weisberg, 2011). All predictor variables from the selected best model had a VIF < 10 (Zuur et al., 2009). We also calculated the significance (%) of each predictor variable for both benthic community and benthic flux variation with the "vartest" function (Borcard et al.,

2018). Because we expected a different response from organisms in the surface sediment layers compared to the deeper sediment layers (2-5 cm) within contrasting bottom-water oxygen concentrations, we ran separate statistical analyses comparing depth layers for each site. The low numbers or absence of macrofaunal individuals in the 5-10 cm sediment layer precluded analysis. We performed a one-way ANOVA test with sediment layer as fixed factor. We also examined data normality visually with Q-Q plots but noting the unreliability of visual inspection alone, we also ran a Shapiro-Wilk's test ($p > 0.05$). Levene's tests evaluated homogeneity.

For the 475 m site only, we ran a t-test separately for each nutrient, with treatment as factor (two levels), noting the absence of a specific treatment comparison for the 200 m site and the absence of control replicates at the 850 m site. We then visualized the general trend for each of the nutrient fluxes at each site, averaging cores for a given treatment.

PERMANOVA analysis established no significant differences between enriched and control cores, we therefore also examined the relationships between our response variables and explanatory and biological variables using two separate RDAs with type II scaling. One of the RDAs used the biodiversity indices (J', S, H', Simpson) and Functional indices (FRich, FEve, FDiv) as the explanatory variables.

2.3.8.2 Isotopic analysis

We also analyzed isotope data for the 475 m and 850 m sites where we had added labeled algae. We analyzed this data using a linear regression model (lm()) to assess whether macrofaunal taxa or individual sediment layers differed in total C uptake. In instances where assumptions were not met, we either log or square-root transformed data. When data transformation did not work (475 m), we performed a Kruskal-Wallis test. We only detected and excluded outlier values from analysis and graphs at the 475 m site. Analysis of differences in C uptake between sediment layers

focused on the 475 m site only because the few individuals detected in deeper layers were combined with those from the 0-2 cm at the 850 m site. Normality tests indicated the need for either logarithmic or square root transformation of the data. Insufficient degrees of freedom precluded analyzing the dependency of sediment layers by testing C uptake through a generalized mixed-effect model with a sediment layer factor nested within a core factor. We therefore compared C uptake among different enriched cores to determine the influence of cores, if any, on C uptake variance. This analysis showed no significant differences; we therefore ran a linear regression model with C uptake as a response variable and sediment layers (level: 0-2; 2-5) as categorical variables. We used a dummy code (using ones and zeros) to use categorical predictor variables in regression, avoiding treating these variables as continuous. Given that polychaetes play a particularly important role in sediments because of their feeding behavior, we evaluated whether different feeding behaviors resulted in differences in total C uptake, and we therefore compared total C uptake among the different feeding behaviour that we identified following the polychaete feeding guilds described by Jumars et al. (2015), for the 475 m site, noting the need for a log transformation.

2.4 Results

2.4.1 Macrofaunal assemblages

We identified a total of 1171 individuals of macrofauna representing 63 different families. Macrofaunal density (ind · m^{-2}) averaged over all cores sampled at each site differed significantly between the 200 m and 475 m sites, and between the 200 m and 850 m sites, with highest overall densities in the 200 m normoxic site (**Fig. 2.3 A**). Macrofaunal density also differed significantly between sediment layers (0-2, 2-5 cm) within each of the study sites (**Supplementary table 2.2**). In comparing the 0-2 cm sediment layers from all sites, the highest densities occurred in the

normoxic site (7272 ind · m^{-2}), a pattern also seen when comparing the 2-5 cm layer (normoxic site densities of 2432 ind · m^{-2}) (**Fig. 2.3 B**). Surface deposit-feeders numerically dominated polychaete assemblages at all sites, with subsurface deposit-feeders playing a smaller role, and generally rare herbivores, which were absent from the 850 m site (**Fig. 2.3 C**).

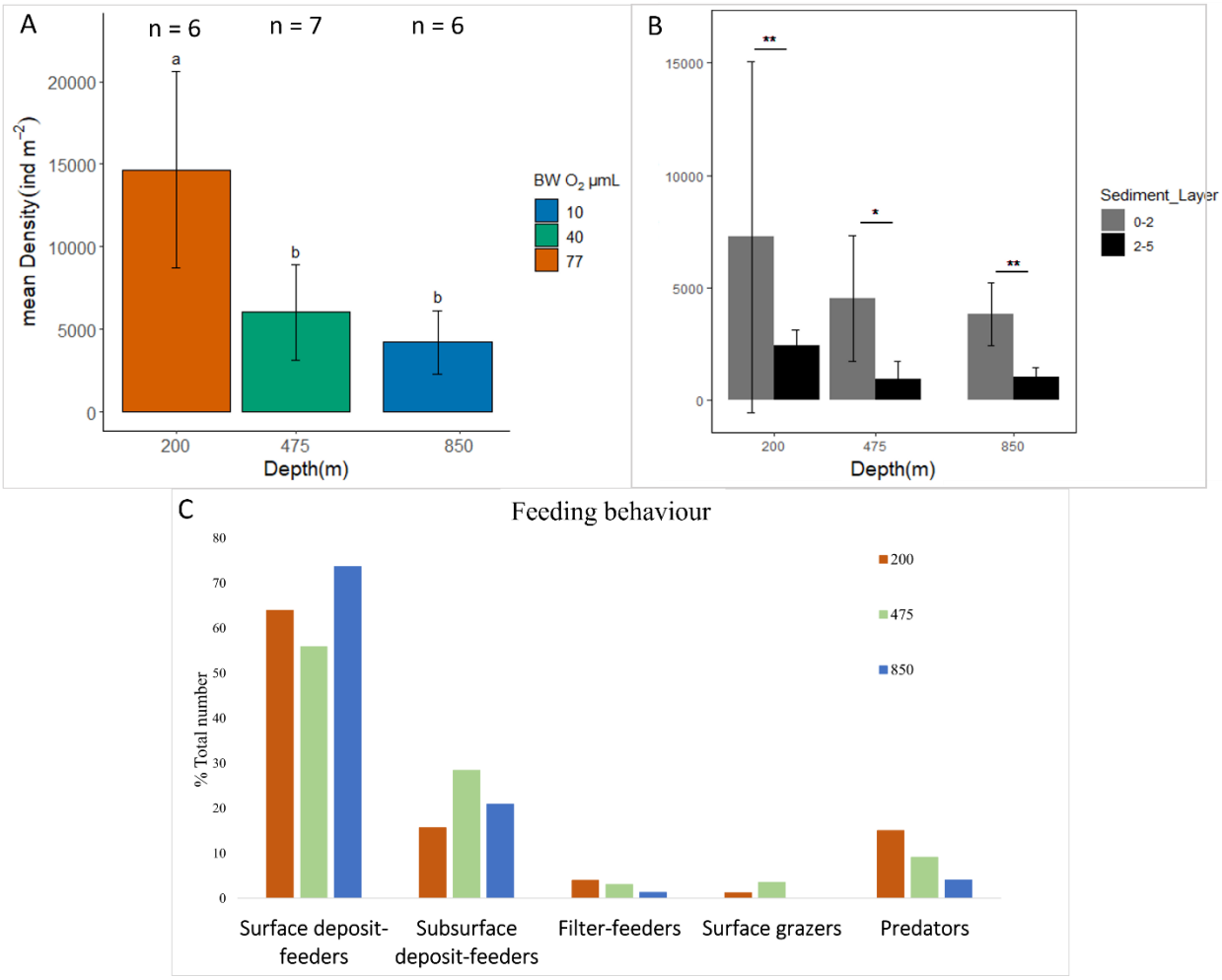

Fig. 2.3. A) Mean macrofaunal density (ind · m^{-2}) at each sampling site (200-, 475-, and 850 m sites) on the Clayoquot slope. "n = 6; 7; 6" above each box refers to the number of cores used to calculate the average density at each site grouping cores of a given treatment. Error bars denote standard deviations. B) Summary of ANOVA results comparing mean macrofaunal density (ind · m^{-2}) across sediment layers (0-2, 2-5 cm) within each sampling site. 200 m (n = 6, 0-2 cm; n = 6,

2-5 cm); 475 m (n = 7, 0-2 cm; n = 7, 2-5 cm); 850 m (n = 6, 0-2 cm; n = 6, 2-5 cm). We grouped all cores of a given treatment. Error bars represent standard deviations. Asterisks indicate significant differences among sediment depths within each site (* = $p \leq 0.05$; ** = $p \leq 0.01$). C) Feeding-type composition of polychaete assemblages from three sites (200-; 475-; 850 m) showing percentage of individuals in relation to the whole assemblage within the different feeding behavior categories. Data were collected from the upper 0-5 cm of sediment.

Our analyses also identified significant differences among sites in species richness (chi-squared = 10.4; df = 2; p = 0.004), with the 200 and 850 m sites differing significantly (Dunn Test p value = 0.003). The expected number of species (ES[50] F = 122.1; df = 2; p < 2e-16) differed significantly between the 200 m and 475 m sites (p <1e-10), the 200 m and 850 m sites (p <1e-10), and the 475 m and 850 m sites (p <1e-10). Other biodiversity indices did not differ significantly between sites. Species richness decreased progressively with decreasing bottom-water oxygen concentration and increasing depth, from 23 ± 3 taxa at 200 m (O_2 ~77 µmol · l^{-1}) to 10 ± 5 taxa at 850 m (O_2 ~10 µmol · l^{-1}). Similarly, expected number of species ES[50] decreased from 13.7 at 200 m to 4.0 at 475 m, increasing slightly to 5.5 at 850 m (**Fig. 2.4 A), B); Table 2.2**).

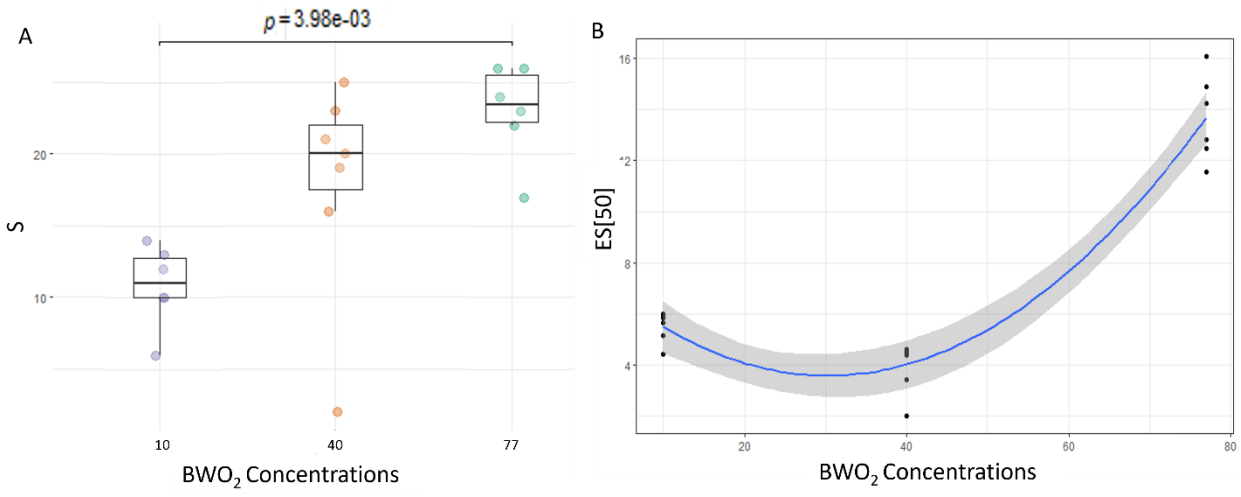

Fig. 2.4. Relationship between sampling bottom water O_2 concentrations and A) species richness (S), and B) expected number of species (ES[50]), as identified by the non-parametric Kruskal-Wallis test, and polynomial regression, respectively. Panel A: p = p value from the post-hoc Dunn test; each dot corresponds to one core per site; long bar above the plots indicates significant differences between 200 m and 850 m S. Error bars are the 95% confidence interval, the bottom and top of the box are the 25th and 75th percentiles, the line inside the box is the 50th percentile (median), and circles located outside the whiskers of the box plot indicate outliers. Panel B: grey shaded area around the regression line indicates 95% confidence interval.

Table 2.2. Density and diversity variables for macrofaunal (> 300 μm) communities within shelf and slope sediments (± standard deviation). Species richness (S), Simpson's diversity index, Shannon-Wiener index (H'), Pielou's evenness (J'), and expected number of species (ES[50]). Bold values indicate significant differences among sites in species richness and expected species richness.

SITE (M)	NUMBER OF CORES	DENSITY (IND · M^{-2})	S	H'	SIMPSON	J'	ES[]
200	6	14657 ± 5942	**23** ± 3	3 ± 0.2	1 ± 1	1 ± 0.1	**14** ± 2
475	7	6036 ± 2883	18 ± 8	2 ± 1	1 ± 0.2	1 ± 0.1	**4** ± 1
850	6	4222 ± 1928	**11** ± 3	2 ± 0.3	1 ± 0.1	1 ± 0.1	**6** ± 1

PERMANOVA indicated significant differences in benthic community taxonomic composition among sampling sites (F = 3.69; p = 0.001). Pair-wise tests revealed that the communities at the three sites all differed significantly from each other ($p < 0.05$), and sites also clearly separated in ordination space (**Fig. 2.5 A**). Polychaete taxa primarily contributed to between-site community differences (**Fig. 2.5 B**). The average dissimilarity of polychaete families between sites varied between 73% (between the 200 m and 475 m sites) and 80% (between the

200 m and 850 m sites) (**Supplementary table 2.3 a, b, c**).

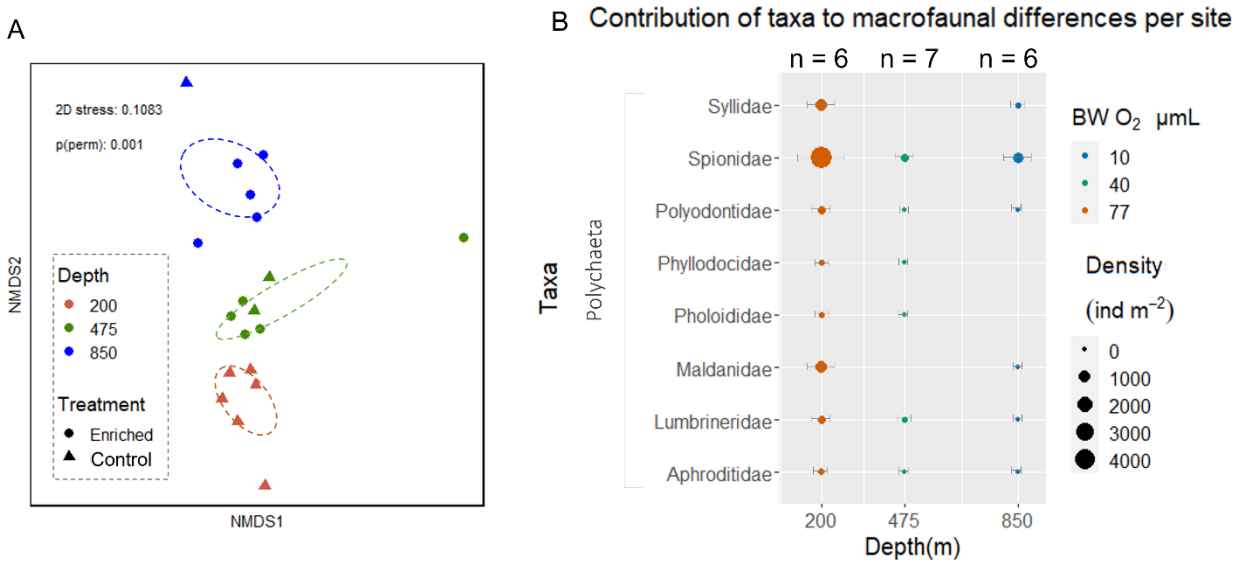

Fig. 2.5. A) nMDS of infaunal communities from sites differing in bottom-water oxygen concentration, with the resemblance matrix based on Bray-Curtis similarity. Control core n = 6 at 200 m-; enriched n = 5, control n = 2 at 475 m-; enriched n = 4, control n = 1 at 850 m site). Dashed ellipses indicate 95% confidence interval. Non-overlapping ellipses indicate significant differences in infaunal community composition between sites. Stress equal to or below 0.1 is considered fair, whereas values equal to or below 0.05 indicate good fit. B) Polychaetes based on density (ind · m^{-2}) that contributed to the differences between the normoxic and the two low-oxygenated sites from all cores at each site (200, 475, 850 m). "n = 6; 7; 6" above each dot column refer to the number of cores (enriched + control) used to calculate the average density of each taxon at each site.

2.4.2 Environmental drivers of infaunal community structure

The best model that emerged from redundancy analysis of benthic community structure and environmental variables explained 20% of the variation (R^2 = 0.20, Adj. R^2 = 0.10, p = 0.001***)

(**Fig. 2.6**). However, the VIF function showed various multi-collinearities between our explanatory variables (C:N; %TOC; Chl*a*; Phaeo; Chl*a*Phaeo; Lipid; Depth; %Gravel; % Sand; %Mud; %Silt; %Clay; Salinity; Temperature; Bottom water O_2) except for C:N and %TOC which were not collinear. Therefore, we only included C:N and %TOC in our final RDA model. Our analysis showed that the first (p = 0.001) and second axis (p = 0.02) of the redundancy model accounted for 75.1% and 25% of the explained variation, respectively. In addition, C:N and %TOC contributed similarly to explained variation of 7.4% and 7.2%, respectively, and both contributed to RDA2 variation. Specifically, the benthic communities structure of the two low oxygenated sites are highly correlated to %TOC, while the infaunal community structure of the normoxic site to C:N.

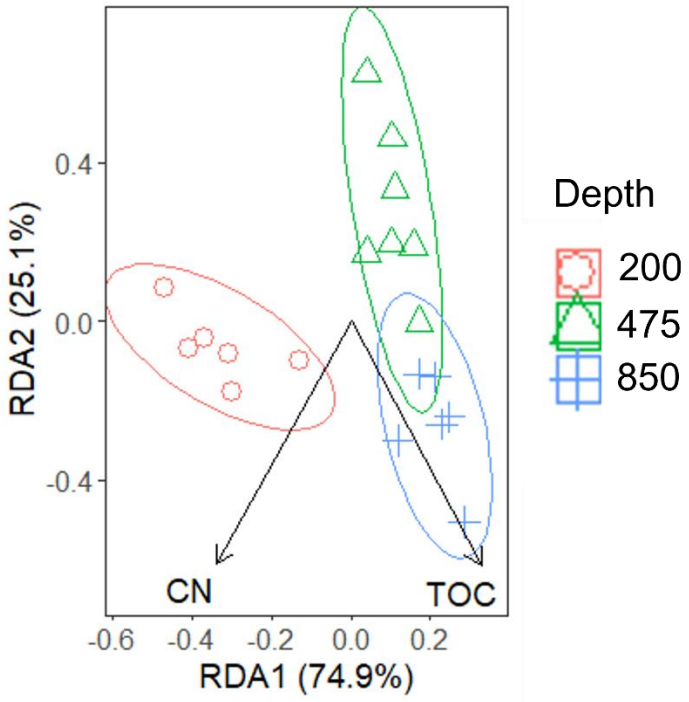

Fig. 2.6. Redundancy analysis (RDA) model plot (scaling 2) of environmental variables best explaining variation in infaunal community structure measured at our sampling sites (200-,. 475 - , and 850 m site) from the Clayoquot slope. Each point represents an individual core. C:N =

Carbon: Nitrogen ratio; %TOC = % of total organic carbon. Longer arrows correspond to variables that strongly drive variation in community matrix. Arrows pointing in opposite directions indicate a negative relationship with a given variable. Arrows pointing in the same direction denote a positive relationship. Ellipses indicate 95% confidence interval.

Low replication may have affected our results. However, sediment grain size comparisons showed no obvious differences between normoxic and hypoxic sites (**Table 2.3**). We observed no clear relationship between %TOC and fine grain size (%Clay) from the upper 0-2 cm (adj R^2 = 0.94, p = 0.11) among sites. However, the more organic-rich sediments (%TOC at the 850 m site) also had the finest average grain size (%Clay). Moreover, the highest Chl*a* and phaeopigments at the deepest site, contrasted the highest lipid and phospholipid values at the 475 m site. Intermediate OM values characterized the normoxic site.

Table 2.3. A) Site, water depth, grain size (% Gravel, % Sand, % Mud, % Silt, % Clay, Mean Sortable Silt (µm); B) sediment OM (Chl*a*, Phaeo, Chl*a*: Phaeo, Lipid, Phospholipid, %TOC, %N, C:N,) within the upper 0-2 cm fraction. Results from the 200 m site represent the average of two cores. We only evaluated one core at the 475 and 850 m sites.

A) Site	***Water Depth (m)***	***% Gravel***	***% Sand***	***% Mud***	***% Silt***	***% Clay***	***% Sortable Silt (>10um<63um)***	***Mean Sortable Silt(um)***
200 m	200	19	57	24	17	7	13	26
475 m	475	0	78	22	14	8	10	25
850 m	850	0	15	85	55	30	35	22

B) Site	***Chla*** **(µg g^{-1})**	***Phaeo*** **(µg g^{-1})**	***Chla/ Phaeo***	***Lipid*** **(µg g^{-1})**	***Phosph*** **(µg g^{-1})**	***% TOC***	***% N***	***C:N***
200 m	1.1±0.7	44±9.8	0.02±0.01	110±0.01	60±0	0.9±0.1	0.1±0.03	8.5±2.1
475 m	1.1	40	0.02	433	52	0.7	0.3	3.5
850 m	3.2	106	0.03	224	37.	2.4	0.4	6.5

2.4.3 Benthic nutrient fluxes at the hypoxic 475 m site after 24 h

Our results suggest higher nutrient influxes rather than effluxes at the 475 m site (**Fig. 2.7**), noting that our experimental setup did not allow for replicate measurements at the 200 and 850 m sites. The values for the 475 m site represent averages from just two cores.

After 24 h of incubation, at the 475 m site, ammonium influxes varied over time, averaging – 513 ± 793 µmol · m^{-2} · d^{-1}, and stable effluxes of nitrite, averaging 0.1 ± 0.4 µmol · m^{-2} · d^{-1}. Nitrate effluxes decreased over time until reaching an average influx value of – 4603 ± 1891 µmol · m^{-2} · d^{-1}.

After 24 h incubations, we observed net silicate influxes at the 475 m site with silicate flux rates varying over time but, averaged – 3140 ± 2946 µmol · m^{-2} · d^{-1}. In comparison, we observed phosphate influxes over time averaging – 188 ± 34.2 µmol · m^{-2} · d^{-1} .

In summary, we observed net influx into sediments for all nutrients except for a weak efflux of nitrite (**Fig. 2.7**).

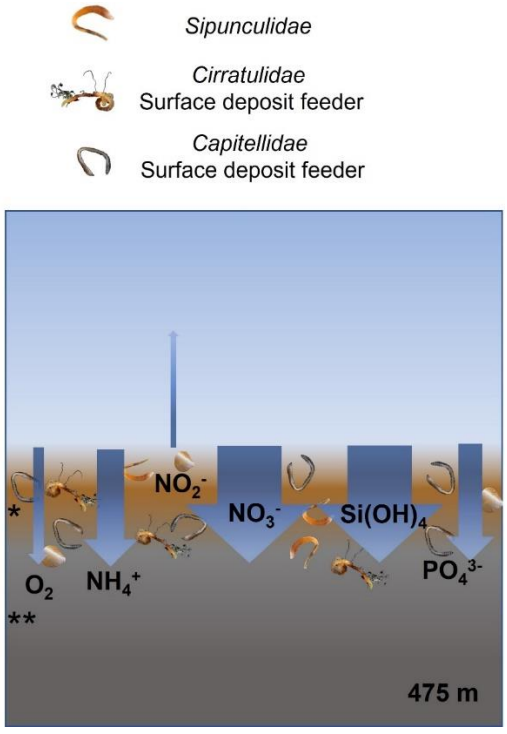

Fig. 2.7. Summary illustration of net benthic nutrient fluxes from control cores only at the 475 m site (n = 2). Brown sediment and a single asterisk indicate inferred oxygenated sediment layer, while dark sediment and double asterisks indicate inferred low oxygenated sediment layer. Nutrient fluxes shown as blue arrows indicate OM remineralization, with positive values from control cores at 475 m site indicating efflux (out of the sediment) and negative values indicating influx (into sediment). Specifically, arrows show averages of ammonium (NH_4^+), nitrate (NO_3^-), nitrite (NO_2^-), silicate ($Si(OH)_4^+$, and phosphate (PO_4^{3-}) flux, respectively. Illustrations at top of Fig. indicate the dominant species at each site. O_2 = oxygen concentration in the water column.

2.4.4 Benthic nutrient fluxes comparisons between algal additions and unenriched cores at the low oxygen 475 and 850 m sites

Comparison of individual nutrients fluxes (μmol · m^{-2} · d^{-1}) and oxygen consumption (mmol · m^{-2} · d^{-1}) at the 475 m site, showed no significant differences between treatments based on our t-test.

At the 475 m site, we observed similar rates of oxygen consumption by sediment biota in enriched and unenriched cores (t-test, p = 0.9) (**Fig. 2.8 A**). We also observed net silicate effluxes in enriched cores (averaging 21972 μmol · m^{-2} · d^{-1}) versus silicate influxes in unenriched control cores (average of -3140 μmol · m^{-2} · d^{-1}) though this was not significant (t-test, p = 0.3) (**Fig. 2.8 A**). Net effluxes of all three nitrogen forms in enriched cores contrasted influxes in unenriched control cores, except for nitrite. Specifically, ammonium efflux averaged 249 ± 387 μmol · m^{-2} · d^{-1} in enriched cores compared to –514 ± 732 μmol · m^{-2} · d^{-1} in unenriched cores (t-test, p = 0.5) (**Fig. 2.8 A**). Nitrite efflux averaged 2801 ± 2858 μmol · m^{-2} · d^{-1} in enriched cores compared to 0.1 ± 0.4 μmol · m^{-2} · d^{-1} in unenriched cores (t-test, p = 0.4) (**Fig. 2.8 A**). Nitrate efflux averaged 124.7 ± 6061 μmol · m^{-2} · d^{-1} in enriched cores compared to an average influx of -4603 ± 1891

µmol · m^{-2} · d^{-1} in unenriched cores (t-test, p = 0.5) (**Fig. 2.8 A**). Phosphate effluxes averaged 398 ± 822 µmol · m^{-2} · d^{-1} in enriched cores over 24 h, contrasting net influx of -188 ± 34 µmol · m^{-2} · d^{-1} in unenriched cores (t-test, p = 0.5) (**Fig. 2.8 A**).

At the 850 m site, we observed similar patterns of influx for enriched and unenriched cores for all nutrients. After adding OM, silicate flux averaged -46661 ± 7036 µmol · m^{-2} · d^{-1} compared to -42407 µmol · m^{-2} · d^{-1} in the one control core (**Fig. 2.8 B**). Ammonium influx averaged –751 ± 327µmol · m^{-2} · d^{-1} in enriched cores and –1242 µmol · m^{-2} · d^{-1} in the unenriched control core (**Fig. 2.8 B**). Nitrite influx averaged -90 ± 88 µmol · m^{-2} · d^{-1} in enriched cores and –176 µmol · m^{-2} · d^{-1} in the unenriched control core (**Fig.2. 8 B**). Moreover, average nitrate influx of -29370 ± 1767 µmol · m^{-2} · d^{-1} in enriched cores was slightly lower than the –33429 µmol · m^{-2} · d^{-1} influx in unenriched core (**Fig. 2.8 B**). At the end of the incubation, we observed similar phosphate influxes in enriched cores (-2658 ± 18.4 µmol · m^{-2} · d^{-1}) and the unenriched core (-2777 µmol · m^{-2} · d^{-1}) (**Fig. 2.8 B**).

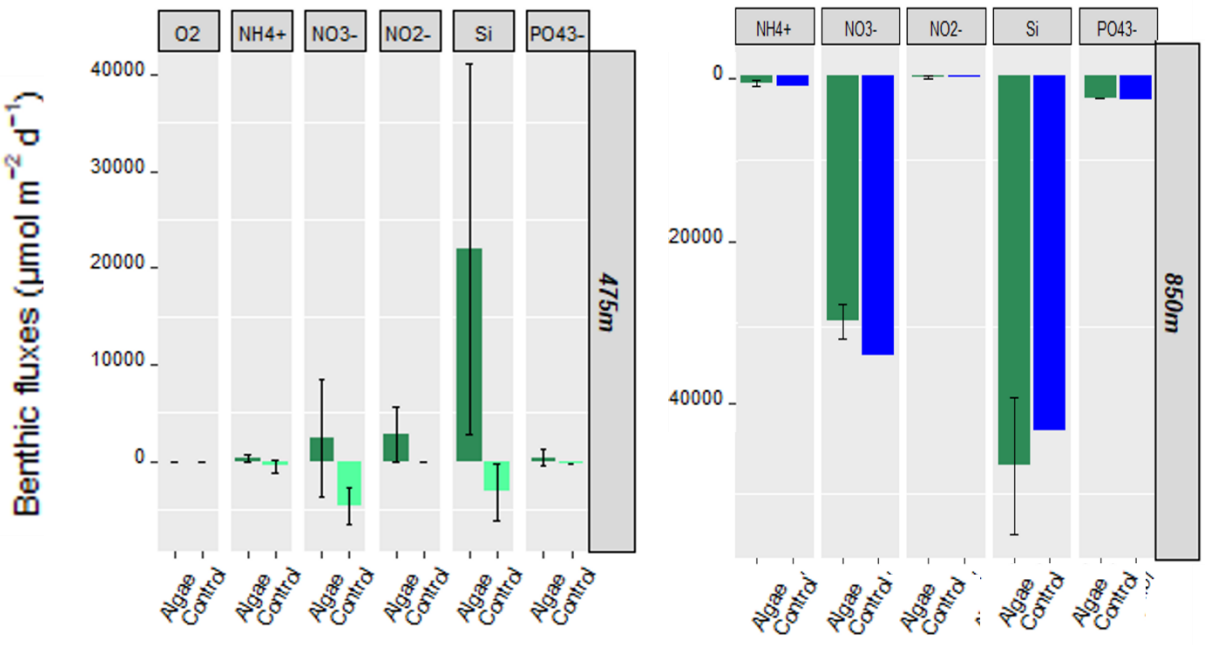

Fig. 2.8. Benthic fluxes (± SE) of oxygen, ammonium, nitrate, nitrite, silicate, and phosphate in enriched and unenriched control cores at the two low oxygen sites, (A) 475 m (enriched n = 4; unenriched control n = 2) and (B) 850 m (enriched n = 3; unenriched control n = 1). "n = " refers to the number of cores used for the analysis. The 0 point along the y axis indicates the sediment-water interface where flux values above the point represent sediment release and those below the lines represent sediment uptake.

2.4.5 Environmental and biological drivers of nutrient fluxes

We performed two distinct RDAs. One RDA included environmental variables and benthic nutrient fluxes (from both enriched and non enriched incubated cores) among the three sampling sites, whereas the second included biological variables (biodiversity and functional indices) and benthic nutrient variables among the three sampling sites. However, because the significance of both models was > 5% ($p = 0.27$; $p = 0.77$), we did not examine contributions of RDA axes and explanatory variables.

2.4.6 Isotopic signatures

We report on natural (background) isotope results only from control samples (macrofaunal organisms) collected from unenriched cores from the hypoxic 475 m site because values for the 850 m site fell below instrument detection levels.

Background isotopic signatures of macrofaunal organisms from unenriched sediments all yielded negative values of varying magnitudes (**Fig. 2.9**; **Supplementary table 2.4**). The mean $\delta^{13}C$ signature for polychaetes of -19.4 ± 1‰ encompassed the lowest measured background $\delta^{13}C$ signatures in scalibregmid ($\delta^{13}C$ = -20.8‰) and terebellid ($\delta^{13}C$ = -20.9‰) polychaetes, with all other polychaetes ranging between -20.2‰ (Sabellidae) and -17.3‰ (Onuphidae). Crustacean background signatures varied from -21.9‰ to -17.6‰. In our trace enrichment experiment, we

considered signals heavier than -17.2‰ for non-calcified macrofauna, and -17.6‰ for calcified macrofauna as evidence for ^{13}C uptake from the added algae.

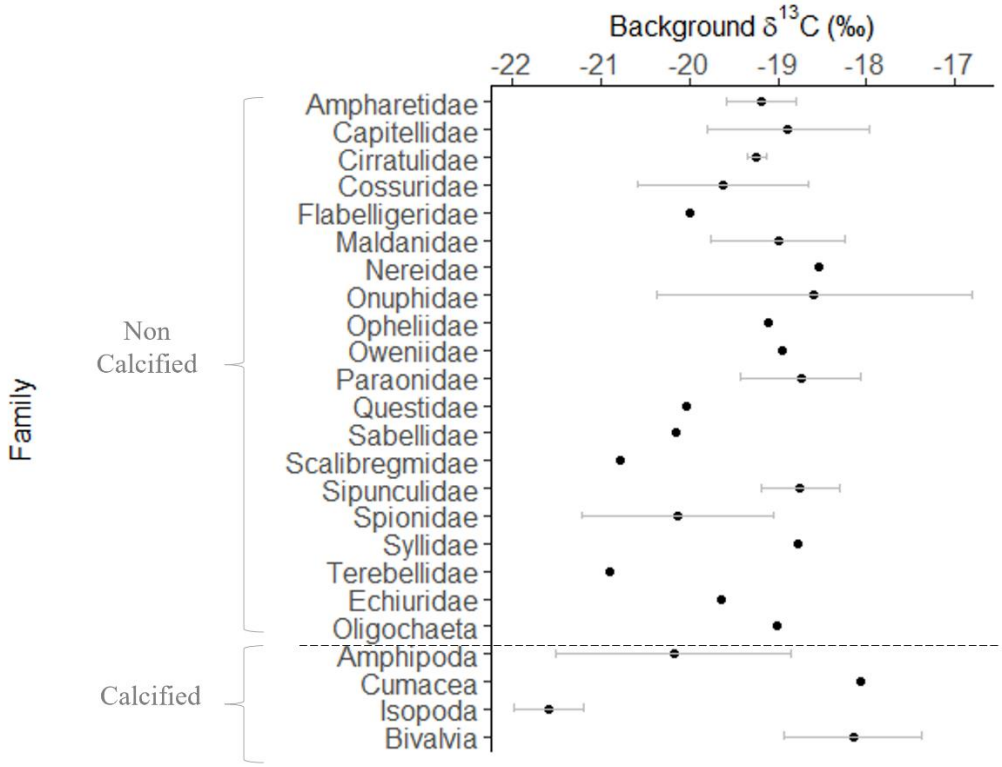

Fig. 2.9. Background $\delta^{13}C$ signatures for non-calcified and calcified macrofaunal taxa at the 475 m. Each black dot indicates the average of $\delta^{13}C$ calculated by one or two samples. Error bars represent standard deviations.

2.4.7 Macrofaunal response to algal enrichment

In our short-term experiments, among all analyzed samples, 29.7% (66 individuals) and 15.3% (28 individuals) showed $\delta^{13}C$ signature heavier than our baseline of -17.2‰, at 475 and 850 m, respectively. To investigate downward transport of organic material in sediments, we also examined isotopic signatures greater than our threshold value (-17.2‰) of macrofauna within different sediment layers.

Regarding specific ^{13}C-uptake ($\Delta\delta^{13}C$) at the 475 m reduced oxygen site specifically, we observed that polychaete families and a single oligochaete from the upper 0-2 cm of the sediment layers showed higher responses to the algae than other taxa, whereas amphipods showed the highest response at the 850 m hypoxic site. Specifically, we found a $\Delta\delta^{13}C$ of 0.005‰ for surface-feeding spionids polychaetes (0-2 cm sediment layer), and for an oligochaete (2-5 cm sediment layer) at the 475 m site. We also observed 0.003‰ and 0.002‰ specific ^{13}C-uptake from a carnivorous dorvilleid polychaete (2-5 cm sediment layer) and surface deposit-feeding ampharetid polychaetes respectively. In contrast, amphipods at the 850 m hypoxia site showed a 0.0009‰ $\Delta\delta^{13}C$ signature. However, differences in the degree of ^{13}C enrichment varied greatly even among individual polychaetes, especially at the 475 m shallower hypoxic site.

Closer inspection of the total carbon uptake rate, applied at the two hypoxic sites separately, revealed no significant differences between taxonomic groups (Kruskal-Wallis test, $p = 0.17$, and lm(), $p = 0.58$ for the 475 and 850 m sites respectively – **Fig. 2.10 A** and **Fig.2. 10 C**). Polychaetes at the 475 m site were responsible for the highest Carbon uptake turnover of macrofaunal taxa during all incubation times, with a mean isotopic rate of 0.02 mg · C · m^{-2} · d^{-1}. In contrast, polychaetes, crustaceans, and bivalves showed similar uptake rates (0.003, 0.002, 0.002 mg · C · m^{-2} · d^{-1}, respectively) at the 850 m site.

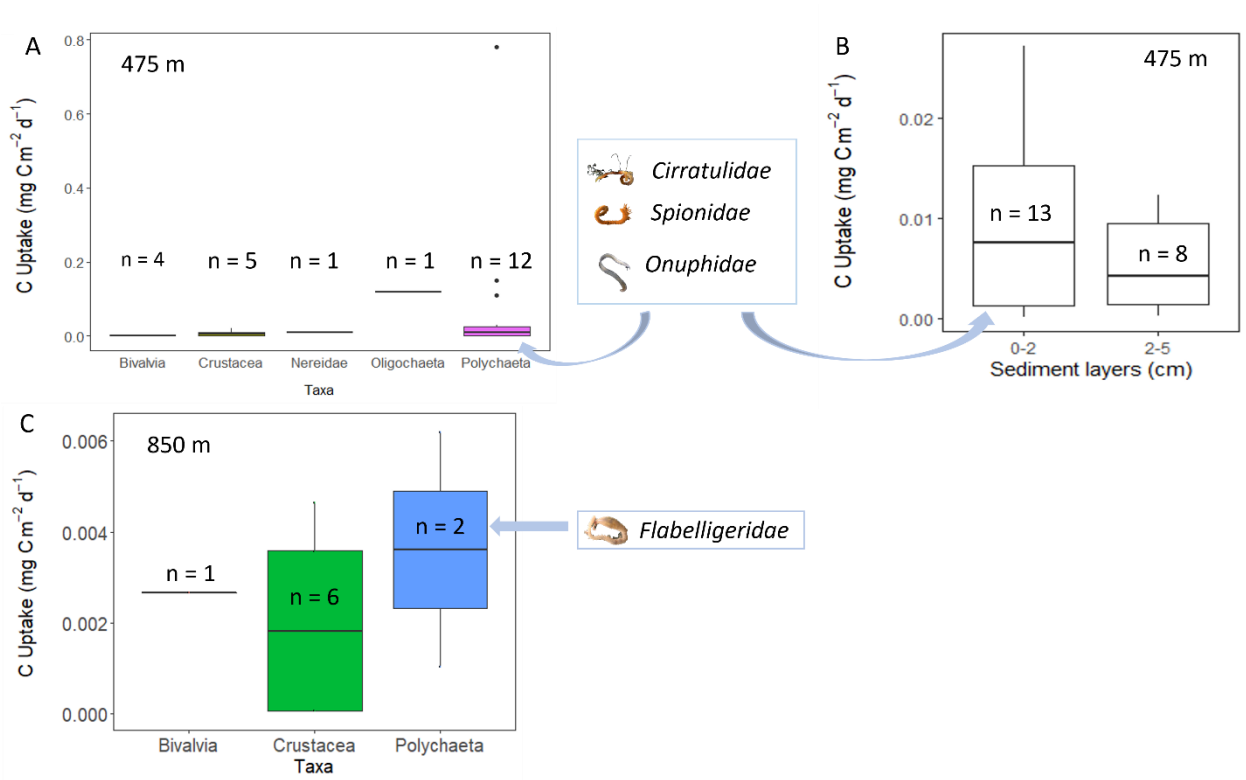

Fig. 2. 10. Average total carbon uptake rate from infaunal organisms (0-5 cm) at 475 m site within taxa (log transformation of C uptake) (A), and sediment layers (B), and within taxa (0-5 cm) at 850 m site (C). Error bars indicate standard deviation. n indicate the number of samples. Each sample may contain more than one individual of the specific taxa (See **Supplementary table 2.5** for more details). "Cirratulidae, Spionidae, Onuphidae" and "Flabelligeridae" refer to the polychaete families that contributed the most to carbon uptake turnover at the 475 and 850 m sites from the top two sediment layers of the sediment, respectively. I did not create a "sediment layers" box plot for the 850 m site given the low number of individuals in the 2-5 cm layer.

Cirratulid polychaetes yielded the highest carbon uptake rate for macrofauna during incubations at the 475 m shallow hypoxic site. Specifically, 4 cirratulids combined from the top two layers of the sediment yielded a C uptake rate of 0.78 mg · C · m^{-2} · d^{-1} followed by 2 onuphid individuals (from the 0-2 cm) combined yielded a C uptake rate of 0.14 mg · C · m^{-2} · d^{-1}. We also

observed 4 combined spionid polychaetes (from the 0-2 cm) which yielded a C uptake rate of 0.11 mg · C · m^{-2} · d^{-1} (**Supplementary table 2.5**) and an oligochaete from the 2-5 cm of the sediment that yielded a C uptake of 0.11 mg · C · m^{-2} · d^{-1}. In contrast, we observed the highest C uptake rate at the 875 m hypoxic site in flabelligerid polychaetes (C uptake rate = 0.006 mg · C · m^{-2} · d^{-1}) from the 0-2 cm sediment layers (**Fig. 2.10 C**, **Supplementary table 2.5**). We also observed no significant differences in carbon uptake rate between sediment layers (lm() p = 0.98 at the 475 m site – **Fig. 2.10 B**), or in comparing total carbon turnover by individual polychaetes with different feeding behaviors at the 475 m sites (lm() p= 0.84). We obtained only two polychaetes from the 850 m site.

In general, 65.2% of macrofaunal individuals measured from the sediment surface layer (0-2 cm) at the 475 m site had taken up the label C, among which 37.9% were polychaetes, 21.2% were crustaceans, and 6.1% were bivalves. In contrast, at the lowest hypoxic 850 m site, 39.3% of macrofaunal individuals took up labeled carbon in the upper two cm of sediment, among which 3.6% were polychaetes, 28.6% were crustaceans, and 7.1% were bivalves. Only 22.7% of individuals in the 2-5 cm layer took up the labeled carbon at the reduced oxygen 475 m site, where we observed no crustaceans.

2.5 Discussion

Our results suggest a combined effect of quantity (%TOC) and quality (C: N) of OM on infaunal community composition and C-cycling activity. Infaunal abundance decreased from the normoxic to the hypoxic site where surface filter-feeder polychaetes consistently dominated. Polychaete families such as Capitellidae, Paraonidae, and Spionidae dominated the two sites with reduced oxygen. Relatively abundant OM (low C: N) shaped benthic communities of both low-oxygenated sites, despite lower OM quantity (low %TOC) at the 475 m site compared to the 850

m site. Low OM quality and quantity shaped the normoxic site infaunal community. In contrast, we did not observe significant relationships either with biological or environmental variables and OM remineralization as quantified through nutrient fluxes at our sampling sites, leading us to infer that other factors might influence OM remineralization.

Our results also showed that the quantity of algae supply and the duration of sample exposure to labeled algae may shape OM remineralization. Indeed, nutrient effluxes occurred after enrichment at the 475m site, in contrast to the 850 m site where we observed stronger nutrient influxes after algal addition. Our study also indicated differences in benthic community response to phytoplankton pulses. More diverse and abundant communities at the 475 m site resulted in greater C-uptake and moved more C to deeper sediment layers than macrofauna from the upper sediment layers of the 850 m site. Finally, we conclude that independent of bottom-water oxygen concentration, OM quantity and quality affect infaunal communities; the latter might affect deep-sea carbon cycling, but factors that influence OM remineralization will require further studies.

2.5.1 The macrofaunal community at the three study sites on the Clayoquot slope

The univariate analysis on macrofaunal density showed a significant decrease in macrofaunal density with increasing depth, as also reported by numerous studies (e.g., Flach and Heip, 1996; Cosson et al., 1997), and with decreasing bottom-water oxygen concentration. However, it is difficult to untangle the effects of bottom-water oxygen, depth, temperature and other factors such as organic matter supply on macrofaunal community density. In deep-sea environments, organic material is mainly supplied from the overlying water column in the form of phytoplankton agglomerates, fecal pellets, and carcasses. However, part of this material can be consumed by metazoans, and part is remineralized by microbes (Glud et al., 2008). As Levin (2003) noted, there is no clear relationship between bottom-water oxygen concentration and absolute faunal density

when OMZ macrofauna are compared globally. For example, Levin (2003) reported macrofaunal densities of ~ 1854 ind·m^{-2} in the sandy sediments of the Peru margins (750 m, 0.08 ml·l^{-1} O_2) versus ~ 21380 ind·m^{-2} in the central sandy sediment margins of Chile (200 m, 0.13 ml·l^{-1} O_2). In our study we reported ~ 14657 ind·m^{-2} in the sandy sediment of the shallow normoxic site (200 m, 0.7 ml·l^{-1} O_2), ~ 6026 ind·m^{-2} in the sandy sediment of the shallowest hypoxic site (475 m, 0.4 ml·l^{-1} O_2), and ~ 4222 ind·m^{-2} in the muddy sediment of the deepest hypoxic site (850 m, 0.1 ml·l^{-1} O_2). The large standard errors in our macrofaunal density estimates suggest high spatial heterogeneity, as reported by Sweetman and Witte (2008) for the sedimentary infauna at Station M (34˚50'N, 123˚00'W, ca 4100 m water depth) in the NE Pacific. However, the small number of replicates, and the small sampling area of the individual subcores on the multicorer in ours and other studies likely contributed to this high variability.

Despite variations in depth and oxygen concentrations, polychaetes consistently dominated the macrofauna at all sampling sites, followed by Crustacea and Bivalvia. This pattern aligns with previous reports (e.g., Schaff and Levin, 1994) and contrasts others (e.g., Sweetman and Witte, 2008), noting that the latter included abundant nematodes, a group we excluded, followed by Crustacea and Polychaeta that contributed to 23% and only 8% of their total abundance, respectively. Among metazoans, uncalcified forms dominate OMZ habitats (Levin et al., 1997), where oxygen levels fall below 0.3 ml · l^{-1} (Levin et al., 2003) and low pH conditions result in weakly calcified or a complete absence of calcified invertebrates. Not surprisingly, we found few bivalves in our low O_2 environments, potentially reflecting low calcium concentrations as well as carbonate dissolution.

Within the Polychaeta, the dominant taxon in our two low bottom-water oxygen concentrations, the dominant feeding mode at all sites was surface filter-feeding, although we

hypothesized a change of feeding behavior given how decreasing O_2 concentrations impact OM cycling. However, a previous study that focused on an OMZ on the Pakistan margin also showed the dominance of surface deposit-feeders (Hughes et al., 2009), while sediment reworkers dominated the Arabian Sea OMZ (Gooday et al., 2009). This contrast in feeding behavior dominance among different OMZ environments might reflect habitat heterogeneity within the OMZ which is strongly influenced by the bottom-water oxygen gradient, sediment characteristics, and organic matter content that, in turn, influence macrofaunal assemblages (Gooday et al., 2009). Grain size and sedimentary OM content may influence polychaete feeding behaviours, but limited number of cores in my study did not enable further comparisons with previous studies. Moreover, the elevated abundances of surface and subsurface deposit feeders in the surficial sediment layer (0-2 cm) compared to deeper sediment layers, combined with reduced oxygen availability, and limited bioturbation, could potentially explain the persistence of labile OM in deeper sediment layers (2-10 cm) in all of our sampling sites.

At the normoxic site, spionids dominated the polychaetes, and amphipods, and isopods dominated the Crustacea, whereas capitellid and paraonid polychaetes dominated the reduced oxygen and hypoxic sites, respectively. Capitellidae and Paraonidae characterize OMZs as reported in the Southern Arabian Sea continental margin (Jaleel et al., 2014; Joydas and Damodaran, 2014). However, spionids and cossurids also characterized our most hypoxic sites but were less abundant than the spionids from the normoxic site. Effectively, Spionidae and Cossuridae exemplify hypoxia tolerance (Levin, 2003; Wright et al., 2012). Physiologically, marine invertebrates have hypoxia sensing systems that regulate their behavioral responses to different O_2 concentrations. For example, the hypoxia-sensing system that contributes to the expansion of the niche of *Capitella* sp. into hypoxic environments helps this polychaete respond

before hypoxia reaches lethal levels (Ogino and Toyohara, 2019). In contrast, cossurid polychaetes have developed an enlarged respiratory surface area (branchiae) to cope with reduced O_2 availability (Lamont and Gage, 2000).

2.5.2 Environmental drivers of macrofaunal community structure

Only two (%TOC and C: N) of the environmental variables included in our study helped to explain community structure of the three sampling sites. However, our results require careful interpretation given the limited number of cores dedicated to OM analysis. Specifically, low quality, long-term, and persistent OM accumulation suggested by the highest values of %TOC and C: N observed in our study, characterized the hypoxic sediment at 850 m. In addition to the %TOC and C: N values, we also infer further factors that may contribute to the low-quality OM and limited fresh OM input of this site. Factors may include degradation of the more labile fraction such as pigments and lipids, high phaeopigments indicative of accumulation of chlorophyll degradation products associated with phytoplankton mortality (Danovaro, 2009), and low proportions of phospholipids as labile molecules essential to cell membrane structures and indicative of (recent) living organisms (bacteria, phytoplankton or zooplankton) (Parrish, 2009). In contrast, apparently fresher and better-quality OM influenced the benthic community at the reduced oxygen 475 m site, and low quality and less OM quantity characterized the normoxic site.

Organic matter as a key driver of infaunal communities therefore aligns with Levin et al. (1991; 2009) who concluded that OM supply and quality play an important role in structuring benthic communities able to cope with permanently low oxygen concentration. In contrast, Jessen et al. (2017) concluded that lack of fauna in the hypoxic-oxic zone led to burial of fresh chlorophyll pigments and accumulation of TOC in the hypoxic shallow site (~150 m) in the Black Sea (e.g., Chl*a* $\mu g \cdot gdw^{-1}$ = 41 ± 9 at 207 m depth). Nevertheless, although OM structured our infaunal

communities, our low replication limited our capacity to describe this relationship. Focusing on the low-oxygenated Crimean shelf below 120 m depth, Jessen et al. (2017) observed preservation of organic matter for time scales of decades explained by decreased faunal abundance and a lower bioturbation rate that favors anaerobic microbial communities and processes.

2.5.3 Hypoxia effect on benthic nutrient fluxes

The RDA revealed no variables (including bottom-water dissolved oxygen concentrations) driving nutrient fluxes among our sampling sites, however, we observed increasing nutrient influxes with decreasing oxygen concentrations. We infer that bottom-water oxygen concentrations likely contributed to nutrient flux differences among the three study sites, especially in hypoxic conditions where the sediment acts as an N and P-sink through denitrification and sorption of phosphate (Woulds et al., 2009). Moreover, bottom water oxygen concentration likely outweighs the effects of OM supply on nutrient fluxes at the hypoxic site, given net influxes of each nutrient to sediments at 850 m.

Minimal oxygen consumption in both algal enriched and unenriched cores at the reduced oxygen 475 m site likely reflects an environment where both aerobic and anaerobic metabolism occur (Zakem et al., 2020). Because we did not replicate sampling across depth, we could not fully establish which environmental factors contributed most to oxygen flux. However, we suggest that as oxygen concentration declines, the viable biological community generally shifts to smaller metazoans and microorganisms that can efficiently utilize oxygen at the lowest (nanomolar or lower) concentrations (Wright et al., 2012). Moreover, infaunal organisms able to survive in low oxygen conditions may contribute to oxygen consumption through respiration and bioirrigation (Jorgensen et al., 2021). Nonetheless, past studies point to the magnitude of POC fluxes (Seiter et al., 2005), the presence/absence of in- and epifaunal organisms, temperature (Hammond et al.,

1985), and bottom water oxygen concentration (Berelson et al., 1987) as critical factors that affect oxygen consumption. In addition, the similar low oxygen consumption values we observed from both enriched and control cores could reflect the similar amount of C we introduced to enriched cores compared to the C already present in the background/control sediment.

In addition to the critical role of oxygen for living organisms, N also plays a central role in living organisms, noting its role as a core component of amino acids, the building blocks of proteins and nucleic acids. Nitrogenous compounds can also provide an alternative O_2 electron acceptor for microbes in the absence of oxygen, with a reduction in potential energy gained in decomposition, followed by manganese oxides, iron oxides, and sulfate (Glud, 2008). However, O_2 depletion may cause an overall imbalance in N flux. The low oxygen sites acted mostly as a N sink, aside from modest nitrite release at the 475 m site. In our study, we infer that within oxic bottom environments (despite availability of only one core) biota can nitrify NH_4^+ produced from remineralization of particulate organic nitrogen in sediments, or that NH_4^+ diffused into the oxic sediment-water layer (Choquel et al., 2021). Subsequently, with decreased O_2 availability (our 475 and 850 m sites) nitrification cannot proceed and anaerobic denitrification may convert nitrate produced in the water and sediment to N gas (Choquel et al., 2021).

The algal additions to cores from reduced oxygen sediments produced different functional responses. Although the 475 m site showed modest NO_3^- and NO_2^- effluxes indicative of N regeneration, net N influxes at the hypoxic 850 m site potentially indicates anaerobic benthic activity within the sediment. Specifically, we assume that benthic communities consumed the little O_2 available in the 850 m sediment which led to anaerobic metabolism that reflects vertical redox zonation where electron acceptors are depleted in the order outlined above. Moreover, reduced infaunal activity supports this process, as observed in our 850 m site; limited bioturbation activity

reduces sediment mixing. Furthermore, we may have added too little algae in our experiment to elicit a stronger response at the 850 m site.

The role of sediments in silicate and phosphate cycling also differed among sites with different oxygen concentrations. Overall, normoxic sediments release silica, an important element for a range of marine biota. Around 80–90 % of deposited silica flux recycles back into the water column as silicic acid, resulting in permanent burial of only a minor fraction (>5%) of newly synthesized biogenic silica (BSi) (DeMaster, 2019). Acknowledging the largely unknown dependence of BSi preservation on oxygen levels, we suggest that influxes of silica under hypoxia (475 and 850 m) may relate to either bioirrigation or the presence of aluminium (Al[III]) in the sediment. First, biogenic silica preservation may occur with diminished bioirrigation because low O_2 penetration into the sediment preserves the organic coating on diatom frustules, slowing down dissolution (Dale et al., 2021). Alternatively, silica reacts with Al(III), forming aluminium-silicate minerals (clay) (Van Cappellen and Qui, 1997). However, thermodynamics inhibits dissolution in silicate moved deeper into sediment layers enriched with Al(III), for example by bioturbation (Ragueneau et al., 2001), thereby increasing silicate preservation in the sediment. Moreover, our findings align with observations from the Pakistan margin OMZ, where Dale et al. (2021) reported moderate BSi burial. In contrast, the elevated silicate effluxes observed in algal-enriched cores at the 475 m site may reflect added phytoplankton that did not reach the sediment and/or a resuspension effect. Katz et al. (2016) hypothesized that bioturbation by bottom-feeding fishes in nearby coastal Saanich Inlet enhanced silica resuspension with subsequent burial loss in the adjacent hypoxic basin.

At our 475 site, and for both treatments (enriched and unenriched), uptake of phosphate, an important element that serves as energy carrier for all living organisms, suggests phosphorus

sequestration and release in unenriched and enriched, respectively. When organic material reaches the seafloor, PO_4^{3-} remineralization or burial may occur (Lovley and Phillips, 1986). In the absence of burial through sedimentation, burial occurs when specific elements in sediments combine with mineralized phosphorous (Lovley and Phillips, 1986). In oxic conditions, PO_4^{3-} reacts with ferric iron and manganese (Ingall and Jahnke, 1994), whereas in low oxygen conditions it reacts with calcium (Kraal et al., 2012).

2.5.4 Biological and environmental drivers of benthic nutrient fluxes

The biological and environmental variables in our study did not yield predictive models explaining variation in benthic nutrient fluxes. In contrast, Belley and Snelgrove, (2016) identified bottom temperature as the primary environmental driver of benthic flux variation and OM remineralization of the Northeast Pacific Ocean continental slope. Our study clearly differed from that of Belley and Snelgrove, (2016), despite focusing on the same general oceanic region. Temporal variability may have played a role, considering their study was conducted in May 2011 (earlier in the year than our 2019 sampling) and in September 2013. Furthermore, starting in the winter of 2013–2014, until the end of 2015, a large patch of anomalously warm water - dubbed "the Blob" - formed in the Northeastern Pacific (Cavole et al., 2016; Tseng et al., 2017) which produced devastating marine ecological impacts. Previous studies showed reduced of phytoplankton biomass as a result of enhanced vertical stratification caused by anomalous surface warming which, combined with the deep nutricline in this region, led to decreased nutrient fluxes to the euphotic zone, with a consequent decrease in total phytoplankton biomass (Cavole et al., 2016). Consequently, changes to the phytoplankton community propagate through the food web. Unfortunately, the extent to which the benthic environment on the continental margin was affected by these events remains understudied. However, we infer that the "Blob's" consequences, such as

a combined decrease in phytoplankton biomass, enhanced vertical stratification that was already present because of the OMZ, and decreased infaunal community abundance - that we also observed - may control benthic flux variation at our sampling sites. Moreover, additional factors not measured in our study, such as sediment resuspension (Katz et al., 2016; Niemistö et al., 2018), bio-irrigation (Archer and Devol, 1992), and bacterial activity (Jørgensen and Boetius, 2007; Fuerst and Sagulenko, 2011; Hoffman et al., 2020), can contribute to benthic flux variation.

2.5.5 Carbon flow through sediments at reduced oxygen sites

The ^{13}C-signatures in our enrichment experiments demonstrate rapid (24 h), though modest, uptake of the labelled algae by macrofauna for each incubation interval at both the 475 m and 850 m sites. Specifically, two macrobenthic taxa (polychaetes and one large oligochaete) of five tested taxa showed relatively high C-uptake, in contrast to the deepest hypoxic site, where all sampled taxa ingested C at a similar rate. We suggest that the rapid response reflects strong macrofaunal utilization of fresh, high-quality food, acknowledging that macrofauna might consume meiofaunal prey that ingested the C label (Aberle and Witte, 2003). The rapid uptake in our experiment contrasts with most previous studies, including both *in-situ* (Aberle and Witte, 2003; Sweetman and Witte, 2008) and on-board (Woulds et al., 2007) incubations over periods of several days assessing the transfer of labeled material through the sedimentary community over sufficient time to yield a macrobenthic response. Woulds et al. (2009) showed that Pakistan margin macrofauna responded differently to different OMZ site conditions, specifically the absence of macrofauna and consequent absence of metazoan C-uptake at the OMZ core (300 m depth, dissolved oxygen level <5 µmol/L), but the presence of abundant and active metazoan macrofaunal communities at the OMZ lower boundary (940 m depth, dissolved oxygen level 6-7 µmol/L) dominated C processing.

The background ^{13}C-isotopic signatures of the macrofaunal community in the Clayoquot slope closely resembled those measured at abyssal depths at Station M, ca. 4100 m depth, California (Sweetman and Witte, 2008) and at the BENGAL station (ca. 4850 m) in the Porcupine Abyssal Plain (PAP) (Aberle and Witte, 2003). Although our upper continental slope sampling focused on shallower depths than these earlier studies, we found similar $\delta^{13}C$ signatures in polychaetes (ranging between -17.3 to -20.2‰) and crustaceans (-17.8 to - 21.9‰) to those reported for Station M (polychaetes ranged between –15.8 and –27.8‰; crustaceans ranged between -15.8 and -21.4‰) but strong differences with the PAP signatures (-15 to -38.9‰; -17.9 to -29.6‰, respectively). Station M and our polychaetes and crustaceans exhibited heavier signatures than those at PAP, suggesting more recent ingestion of fresh C in our study. Timing of sampling may also have contributed to this difference, given that our sampling and that of Sweetman and Witte, (2008) in October occurred ~ 3 to 4 months after the peak POM pulse and around the same time as the autumn particulate OM pulse event. In contrast, Aberle and Witte, (2003) sampled in May/June, before the spring phytodetritus pulse. Furthermore, Iken et al. (2001) measured background $\delta^{13}C$ signatures in polychaetes and crustaceans at PAP immediately after the peak POM pulse and found heavier $\delta^{13}C$ signatures, indicating fresh C-uptake by macrofauna.

Despite low faunal abundances, $\delta^{13}C$-isotopic signatures varied among polychaete families, emphasizing the different roles that polychaetes played in reworking the algae introduced to cores from the low oxygen sites. This result also demonstrated strong variability in selective ingestion, different degrees of assimilation, potential competition for food, and possible differences in the specific feeding modes of different species. For example, among the polychaetes, a light label characterized a carnivorous dorvilleid polychaete from the 475 m site, as was also observed for surface-feeding spionids and cirratulids at 850 m site, in contrast to surface deposit feeding

flabelligerids at the most deoxygenated site. This result confirms previous reports (Levin et al., 1999; Aberle and Witte, 2003) of efficient ingestion of ^{13}C-labeled algae by surface-feeding spionids and cirratulids that actively select fresh algal detritus. Although capable of switching feeding modes depending on environmental conditions (Taghon et al., 1980), spionids and cirratulids are predominantly surface deposit feeders that can select particles based on size and organic content (increasing grain size with decreasing organic content (Sanders, 1958). Moreover, they discriminate particles according to their tentaculate morphology, favoring smaller particles that are easier to ingest than larger particles (Jumars et al., 1982; Taghon, 1982). These discretely motile polychaetes can move around as adults but not while actively feeding (Jumars et al., 2015). The high tracer uptake by spionids in our experiment suggests they play a key functional role in reworking freshly deposited material on the Clayoquot slope. Moreover, our results show the relevance of other feeding behavior in consuming algae although with a less prominent role than surface feeders. For example, Dorvillaidae, not surprisingly prominent members of oxygen minimum zone (Levin, 2003) given their unusual tolerance of sulfides (Levin et al., 2013), usually feed on algal, animal, and bacterial material, with all species likely feeding as facultative carnivores. Dorvilleids graze bacterial mats, and indeed their diets are rich in chemosynthetic bacteria. Limitations in identifying specimens to species level led us to classify our unidentified Dorvilleids as carnivores, and infer that Dorvilleids in our study did not directly feed on algae. Simultaneously, we do not exclude the possibility that some dorvilleids were subsurface filter feeding (Fauchald and Jumars, 1979).

In summary, sub-surface deposit feeders living in hypoxic conditions may outcompete other feeding modes in obtaining fresh phytodetritus. However, the different feeding behaviours may permit coexistence of different species at the same site. Especially at the 475 m, sub-surface

deposit feeders might explain similar C-uptake turnover by macrofauna between the surface and subsurface sediment horizons, because mixing by sedimentary infauna may move food resources into deeper, less oxygenated sediment layers. Moreover, although we added less labelled material to cores from 850 m, crustaceans and polychaetes, primarily from the upper 2 cm, both contributed equally to C recycling at 850 m. These findings, along with those of Aberle and Witte, (2003), Sweetman and Witte, (2008), and Witte et al. (2003), underscore the importance of the upper (0-2 cm) sediment layer and support the assumption that macrofauna living in surface sediments can access freshly deposited material and available O_2, especially in OMZs. Consequently, deeper-dwelling organisms have more limited access to food material unless the biota moves the material deeper, either for storage or to gain an advantage over competitors (Jumars et al., 1990).

2.5.6 Experiment limitations

Our results illustrate the challenge of simulating a deep-sea environment, noting both the low number of collected cores and the extremely low uptake of labelled C by macrofauna at 850 m depth. Only 1.6 $g \cdot C \cdot m^{-2}\ y^{-1}$ reaches the seafloor at this depth, presumably resulting in low total carbon uptake by infaunal organisms. Acknowledging limitations in fully assessing pressure change effects on carbon uptake, we cannot exclude the potential effects of mortality or reduced activity in our results, especially at 850 m. Once our incubations ended, direct preservation of our sediment samples in 10% formalin further precluded quantification of any effects of pressure change (e.g., Mevenkamp et al. 2017). Concerns over confinement artifacts led us to limit incubations to 24 h, and artificially elevated concentrations of labelled phytodetritus could also produce a stronger response by macrobenthic organisms. Improvements in approaches such as benthic landers and *in-situ* sensors have helped to address the challenge of accessibility and high costs and risks of deep-sea sampling (e.g., Sweetman and Witte 2008, Sweetman et al. 2019), but

additional challenges remain. However, further improvements in sensors and remote sampling will enhance baseline surveys, impact assessments, and subsequent monitoring surveys that can fill many remaining knowledge gaps on deep-sea ecosystems such as C cycling and C sequestration, which represent key ecosystem functions and services in the deep sea (Thurber et al., 2014).

2.6 Conclusions

In conclusion, our study describes some of the benthic ecosystem functions of polychaetes, crustaceans, and bivalves that dominate macrofaunal communities in an ecologically significant, but poorly-studied region of the Northeast Pacific Ocean where strong oxygen gradient environments (collinear with depth) exert substantive influence on spatially heterogeneous seafloor communities. We show clear changes in macrofaunal community composition between normoxic, and hypoxic sites shaped by the quantity and quality of organic matter, as well as reduced nutrient regeneration. We also observed uptake of C indicative of active infauna that may play a substantive role in C flow through the benthic food web as well as in OM remineralization and nutrient regeneration.

Our results underscore the need for long-term, time-series pulse-chase experiments with sufficient replication to quantify and understand drivers of spatial variations in deep-sea macrofaunal C cycling.

2.7 Acknowledgements

This research was sponsored by the Natural Sciences and Engineering Council of Canada through the NSERC Canadian Healthy Oceans Network (CHONe), and its Partners: Department of Fisheries and Oceans Canada and INREST (representing the Port of Sept-Îles and City of Sept-Îles). AC also thanks the School of Graduate Studies at Memorial University for additional financial support. We thank Chief Scientist Dr. K. Juniper and crewmembers of the *CCGS John*

P. Tully for ship logistics and sampling opportunities. We also thank Vanessa Reid (Memorial University) and Brett Jameson (University of Victoria) for assisting with sample collection and core incubations. We also thank Jeanette Wells (Memorial University) who helped with lipid analysis, Dr. Barbara Neves (Fisheries and Oceans Canada (DFO)) for assistance with chlorophyll analysis, Dr. Owen Brown (Natural Resources Canada) for help with grain size analysis, Maria Ignacia Diaz (Memorial University) for help with benthic nutrient analysis, and Dr. Joanne Potter Research (Memorial University) who helped with isotope analysis. We also thank Dr. Clare Woulds (University of Leeds) for advice on the oxystat system. Drs. Amanda Bates and Suzanne Dufour, and three examiners of the Ph.D. thesis provided helpful comments on an earlier draft of this manuscript.

2.8 Author contributions

Alessia Ciraolo conducted the literature review, the empirical analysis, and wrote the manuscript. Paul Snelgrove helped to formulate the ideas, the content of the manuscript, and to formulate the structure of the manuscript. Marta Cecchetto and Andrew Sweetman provided labeled algae for the pulse-chase experiments. Paul Snelgrove, Marta Cecchetto, and Andrew Sweetman provided editorial guidance.

2.9 Supplementary tables and figures

Supplementary table 2.1. Coring strategy at each site/depth (200-, 475-, 850 m). "Total cores" refers to the total number of cores collected at each site. "Incubated" indicates the number of incubated cores (from the "total") that were both linked to the Oxystat system and were not. Subsequent four columns refer to the number of incubated cores processes for taxonomy (enriched and control; connected or not to the Oxystat), nutrients analysis, oxygen consumption, and enrichment. Finally, "No Incubated" refers to the number of non-incubated cores dedicated to the

organic matter analysis.

		Incubated		Analysis from Incubated cores				No Incubated
Depth (m)	Total cores	Oxystat system	NO Oxystat system	Taxonomic Identification	Nutrient fluxes	O_2 consumption	Enrichment (*Phaeodactylum sp,* g)	OM
200	8*	6	0	6	1	0	0	2
475	9	3	5	7**	6	3	6 (0.02 g)	1
850	7	3	3	6	4	0	5 (0.01 g)	1

*One core was dedicated to a parallel experiment.

** One of the recovered cores was inadequate for sediment analysis.

Supplementary table 2.2. Summary of each ANOVA analysis of macrofaunal density between 0-2 and 2-5 cm of the sediment within each single sampling site with sediment layer as factor [levels: 0-2, 2-5 cm]. Asterisks indicate significant differences in macrofaunal density among sediment depths within each site (* = $p \leq 0.05$; ** = $p \leq 0.01$).

Site/Depth	*Variable*	*Df*	*F value*	*P value*
200	macrofaunal density	1	18.09	0.002**
475	macrofaunal density	1	6.26	0.03*
850	macrofaunal density	1	22.27	0.001**

Supplementary table 2.3 a), b), c). Results of similarity percentage analyses (SIMPER) showing the contribution (%) of different taxa to dissimilarity across sites with different bottom-water oxygen concentrations [~ 77, 40, 10 µmol · l^{-1}]. Av Density (ind · m^{-2}) = Species contribution to average between-group dissimilarity; % Cum = cumulative contribution based on item average. Taxa shown in the table were mostly chosen based on permutation p-values.

a) 77_40: Average dissimilarity: 73%			
Taxa	**Av Density (ind m^{-2})**	**% Cum**	**P**
Spionidae	0.002	0.28	0.002**
Polyodontidae	0.012	0.73	0.002**
Lumbrineridae	0.010	0.79	0.007**
Aphroditidae	0.007	0.87	0.013*
Phyllodocidae	0.004	0.95	0.020*
Sigalionidae	0.002	0.96	0.023*
b) 77-10: Average dissimilarity: 80%			
Taxa	**Av Density (ind m^{-2})**	**% Cum**	**P**
Spionidae	0.20	0.26	0.002**
Maldanidae	0.04	0.32	0.001***
Syllidae	0.03	0.47	0.006**
Polyodontidae	0.014	0.74	0.001***
Lumbrineridae	0.01	0.77	0.001***
Aphroditidae	0.007	0.85	0.004**
Eunicidae	0.005	0.91	0.047*
Phyllodocidae	0.004	0.95	0.011*
Sigalionidae	0.002	0.97	0.008**
Tanaidacea larvae	0.001	0.98	0.022*
Arabellidae	0.001	0.98	0.019*
Pisionidae	0.001	0.99	0.018*
c) 40-10: Average dissimilarity:730%			
Taxa	**Av Density (ind m^{-2})**	**% Cum**	**P**
Paraonidae	0.08	0.11	0.001***
Capitellidae	0.06	0.20	0.044*
Cossuridae	0.04	0.40	0.005**
Sipunculidae	0.03	0.50	0.001***
Ampharetidae	0.02	0.58	0.014*
Cumacea	0.01	0.65	0.041*
Dorvilleidae	0.01	0.76	0.027*
Onuphidae	0.01	0.80	0.022*
Gastropoda	0.01	0.86	0.012*
Ophelidae	0.01	0.92	0.019*

Supplementary table 2.4. $\delta^{13}C$ from non-calcified and calcified background samples collected at the 475 m site. “Core” refers to the core where the sample comes from. “Taxon” = polychaeta families, Oligochaeta, Echiura, Crustacea, and Bivalvia. “Mean $d^{13}C$VPDB/‰ of all analyses” mean of $\delta^{13}C$ measured from each sample. “average” indicates the average of $\delta^{13}C$ from

the same family (when possible). “SD” refers to the standard deviation. “Abundance” indicated the number of organisms in each sample. “Sed Layer” represents the sediment layers from which the sample was collected.

Core	Taxon	Mean d^{13}CVPDB/‰ of all analyses	Average	SD	Abundance	Sed Layer
13	Ampharetidae	-18.91	-19.19	0.39	5	0-2
35	Ampharetidae	-19.46			4	0-2
13	Capitellidae	-18.24	-18.89	0.91	5	0-5
35	Capitellidae	-19.53			1	2-5
13	Cirratulidae	-19.32	-19.24	0.11	3	0-5
35	Cirratulidae	-19.16			5	0-5
13	Cossuridae	-18.94	-19.62	0.96	6	0-2
35	Cossuridae	-20.3			1	2-5
13	Echiura	-19.64			1	0-2
13	Flabelligeridae	-19.99			2	0-2
13	Maldanidae	-19.53	-19.00	0.75	1	2-5
35	Maldanidae	-18.47			2	0-2
13	Nereidae	-18.54			2	0-2
35	Oligochaeta	-19.01			1	0-2
13	Onuphidae	-17.33	-18.59	1.78	1	2-5
35	Onuphidae	-19.85			1	0-2
35	Opheliidae	-19.1			1	2-5
13	Oweniidae	-18.95			3	0-2
13	Paraonidae	-19.23	-18.75	0.69	2	2-5
35	Paraonidae	-18.26			3	0-5
35	Questidae	-20.03			1	0-2
13	Sabellidae	-20.16			3	0-2
35	Scalibregmidae	-20.79			1	0-2
13	Sipunculidae	-19.06	-18.75	0.44	4	0-2
35	Sipunculidae	-18.44			3	0-2
13	Spionidae	-20.89	-20.13	1.08	3	0-2
35	Spionidae	-19.36			2	0-5
13	Syllidae	-18.77			1	0-2
13	Terebellidae	-20.9			1	0-2
35	Amphipoda	-21.12	-20.18	1.33	4	0-2
13	Amphipoda	-19.24			2	0-2
13	Cumacea	-18.07			1	0-2
35	Isopoda	-21.87	-21.59	0.40	1	0-5
13	Isopoda	-21.31			3	0-2
35	Bivalvia	-18.71	-18.16	0.78	6	0-2
13	Bivalvia	-17.6			6	0-2

Supplementary table 2.5. ^{13}C Isotopic signatures, specific ^{13}C Isotope signatures, and carbon uptake rate for infaunal organisms and their feeding behaviours at each core collected from the two sampling sites (475 m and 850 m) and their vertical position within the sediment column (0-5 cm). Taxa: P = Polychaeta, N = Nereidae, O = Oligochaeta, C = Crustacea, B = Bivalvia. n = number of individuals per sample. FB = Feeding behaviour: SS – Surface deposit-feeder, sessile; SM – Surface deposit-feeders, motile; SD – Surface deposit - feeders, discretely motile; CD – Carnivore, discretely motile; BM – Subsurface deposit-feeder, motile; FDT – Filter-feeder, discretely motile; CM = Carnivore, motile; HM – Herbivore, motile. Sediment layers (cm). N = number of organisms per sub-samples; $\Delta\delta\ ^{13}C$ refers to specific ^{13}C-uptake; $\Delta\delta C$ indicates Carbon uptake rate ($mg \cdot C \cdot m^{-2} \cdot d^{-1}$).

Core	$\delta\ ^{13}C$ ‰	Taxa		FB	N	Sediment layer	$\Delta\delta\ ^{13}C$ ‰	$\Delta\delta C$
20	159.64	Ampharetidae	P	SST	2	0-2	0.002	0.02
20	89.55	Cirratulidae*	P	SMT	4	0-2	0.001	0.78
20	-16.52	Magelonidae	P	SDT	1	0-2	8.9E-06	0.0001
26	0.86	Onuphidae*	P	CDJ	2	0-2	0.0002	0.15
20	32.34	Orbinidae	P	BMX	3	0-2	0.001	0.01
26	87.87	Oweniidae	P	BMX	3	0-2	0.001	0.01
26	415.18	Spionidae*	P	FDT	4	0-2	5E-05	0.11
22	-7.28	Syllidae	P	CMJ	3	0-2	4.7E-05	0.03
26	-11.69	Syllidae	P	CMJ	3	0-2	6.2E-05	0.02
20	-16.67	Cossuridae	P	BMX	3	0-5	7.3E-06	0.0001
26	-14.95	Cirratulidae	P	SMT	1	2-5	2.6E-05	0.0002
37	225.24	Dorvillaidae	P	CMJ	1	2-5	0.003	0.01
37	61.00	Nereidae	N	HMJ	2	2-5	0.001	0.01
37	419.13	Oligochaeta*	O	.	1	2-5	0.005	0.12
37	2.81	Paraonidae	P	SMX	1	2-5	0.0002	0.01
37	-12.81	Spionidae	P	FDT	4	2-5	5E-05	0.002
37	-13.02	Syllidae	C	CMJ	3	2-5	4.7E-05	0.005
20	44.22	Amphipoda	C	.	2	0-2	0.001	0.02
26	48.35	Amphipoda	B	.	1	0-2	0.001	0.01
22	-15.99	Bivalvia	C		3	0-2	1.5E-05	0.0003
26	-13.08	Bivalvia	C		1	0-2	4.7E-05	0.001
20	-16.51	Crustacea	C		2	0-2	9E-06	0.0001
22	-9.38	Cumacea	B		2	0-2	8.7E-05	0.01

20	-9.11	Tanaidacea	C	.	7	0-2	9E-05	0.002
20	-12.68	Ostracoda			5	0-5	5.1E-05	0.0003
37	-5.08	Bivalvia			1	2-5	0.0001	0.004
37	-17.06	Polyplacophora	B	.	1	2-5	3E-06	0.0008
B31	-15.70	Flabelligeridae	P	SDT	1	0-2	1.8E-05	0.01
42	-16.36	Cirratulidae	P	SMT	12	0-5	1.1E-05	0.001
27	-8.90	Amphipoda	C		3	0-2	9.3E-05	0.004
B31	-16.05	Bivalvia	B		2	0-2	1.4E-05	0.003
42	-15.48	Crustacea	C		1	0-2	2E-05	0.00004
27	-17.23	Cumacea	C		2	0-2	1.1E-06	0.00005
B31	-12.06	Cumacea	C		1	0-2	5.8E-05	0.005
42	-17.22	Cumacea	C		1	0-2	1.2E-06	0.0009
42	-14.59	Amphipoda	C		5	0-5	3E-05	0.004

***Samples identified as outliers.**

Fig.s

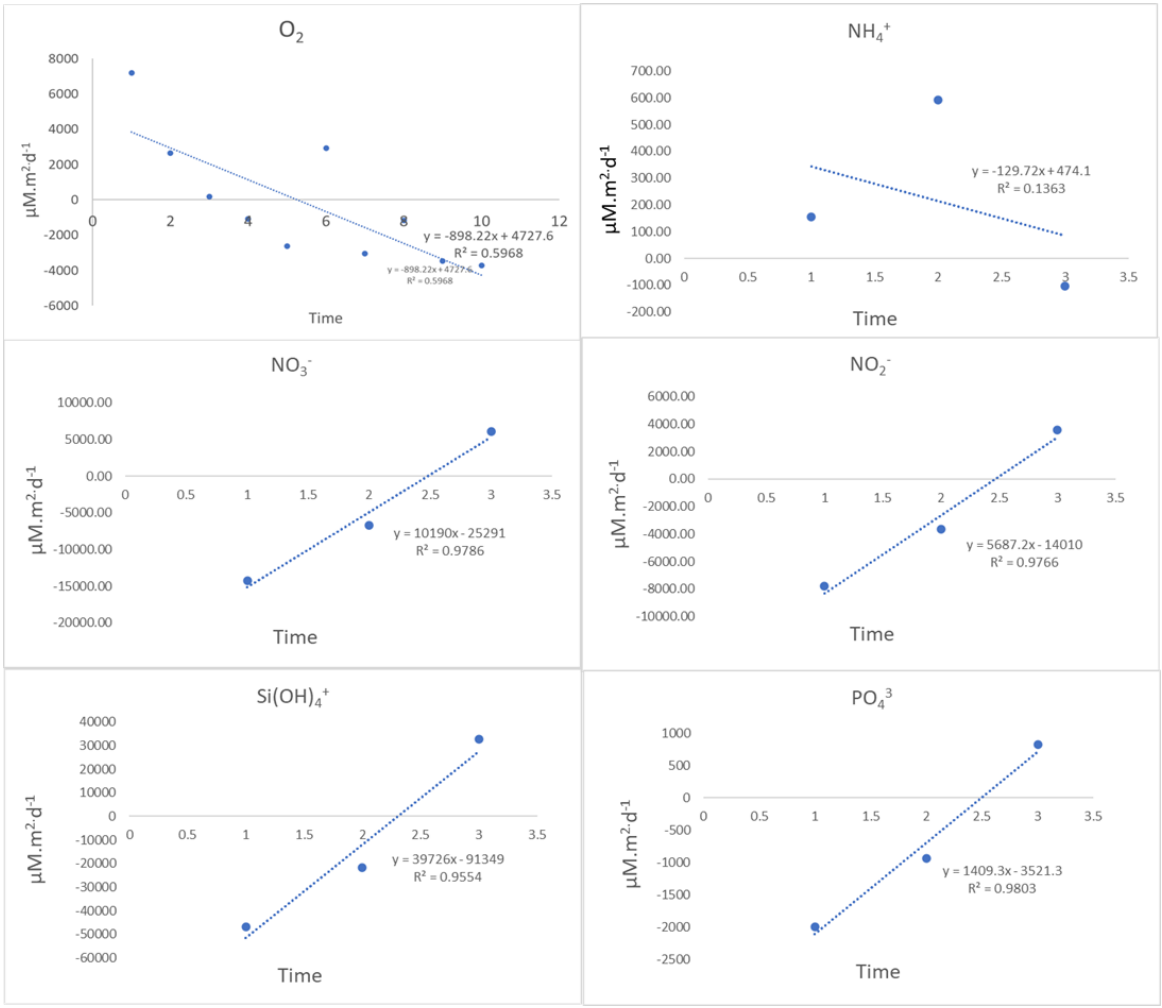

Supplementary Fig. 2.1. Typical changes in concentration of oxygen, ammonium, silicate, nitrate, phosphate, and nitrite. Data is from enriched incubation #25 collected at 475 m.

2.10 References

Aberle, N., Witte, U. 2003. Deep-sea macrofauna exposed to a simulated sedimentation event in the abyssal NE Atlantic: in-situ pulse-chase experiments using ^{13}C-labelled phytodetritus. Mar. Ecol. Prog. Ser., 251, 37 -47. https://doi.org/10.3354/meps251037.

Alldredge, A. L., Silver, M. W. 1988. Characteristics, dynamics and significance of marine snow. Prog. Oceanogr., 20 (1), 41–82. https://doi.org/10.1016/0079-6611(88)90053-5.

Aller R. C. 2014. Sedimentary diagenesis, depositional environments, and benthic fluxes. H. D. H. K. Turekian (Ed.), Treatise on Geochemistry (2nd ed.), Elsevier, Oxford (2014), 8, 293-334.

Anderson, M., Gorley, R., Clarke, K. P. 2008. for PRIMER: guide to software and statistical methods. Primer-e, Plymouth, UK, 32.

Archer, D., Devol, A. 1992. Benthic oxygen fluxes on the Washington shelf and slope: A comparison of *in-situ* microelectrode and chamber flux measurements. Limnol. Oceanogr., 37 (3), 614 - 629. https://doi.org/10.4319/lo.1992.37.3.0614.

Arntz, W. E., Tarazona, J., Gallardo, V. A., Flores, L. A., Salzwedel, H. 1991. Benthos communities in oxygen deficient shelf and upper slope areas of the Peruvian and Chilean Pacific coast, and changes caused by El Nino. Geol. Soc. Spec. Publ., London, 58 (1), 131-154.

Belley, R., Snelgrove, P. V. R. 2016. Relative contributions of biodiversity and environment to benthic ecosystem functioning. Front. Mar. Sci, 3, 242.

Berelson, W. M., Hammond, D. E., O'neill, D., Xu, X. M., Chin, C., Zukin, J. 1990. Benthic fluxes and pore water studies from sediments of the central equatorial north Pacific: Nutrient diagenesis. Geochim. Cosmochim. Acta., 54 (11), 3001–3012. https://doi.org/10.1016/0016-

7037(90)90117-4.

Berelson, W. M., Hammond, D. E., Smith, K. L., Jahnke, R. A., Devol, A. H., et al., 1987. In-*situ* benthic flux measurement devices-bottom lander technology. Mar. Technol. Soc. J., 21 (2), 26-32.

Bianchi, T. S., Johansson, B., Elmgren, R. 2000. Breakdown of phytoplankton pigments in Baltic sediments: effects of anoxia and loss of deposit-feeding macrofauna. J. Exp. Mar. Biol. Ecol., 251 (2), 161–183.

Blair, N. E., Levin, L. A., DeMaster, D. J., Plaia, G. 1996. The short-term fate of fresh algal carbon in continental slope sediments. Limnol Oceanogr., 41 (6), 1208–1219. https://doi.org/10.4319/lo.1996.41.6.1208.

Borcard, D., Gillet F., Legendre P., 2018. Numerical Ecology with R, Springer, New York.

Boutton, T. W. 1991. Stable Carbon Isotope Ratios of Natural Materials: I. Sample Preparation and Mass Spectrometric Analysis. Carbon Isotope Techniques, 155 - 171. https://doi.org/10.1016/b978-0-12-179730-0.50015-1.

Cavole, L. M., Demko, A. M., Diner, R. E., Giddings, A., Koester, I., et al., 2016. Biological impacts of the 2013–2015 warm-water anomaly in the Northeast Pacific: winners, losers, and the future. Oceanogr, 29 (2), 273-285.

Cecchetto, M. M., Moser, A., Smith, C. R., van Oevelen, D., Sweetman, A. K. 2023. Abyssal seafloor response to fresh phytodetrital input in three areas of particular environmental interest (APEIs) in the western clarion-clipperton zone (CCZ). Deep Sea Res. Part I Oceanogr. Res. Pap., 103970.

Choquel, C., Geslin, E., Metzger, E., Filipsson, H. L., Risgaard-Petersen, N., et al., 2021. Denitrification by benthic foraminifera and their contribution to N-loss from a fjord environment. Biogeosciences, 18 (1), 327–341. https://doi.org/10.5194/bg-18,327-2021.

Codispoti, L.A., Brandes, J.A., Christensen, J.P., Devol, A.H., Naqvi, S.W.A., et al. 2001. The oceanic fixed nitrogen and nitrous oxide budgets: Moving targets as we enter the anthropocene? Sci. Mar. 65, 85–105.

Cosson, N., Sibuet, M., Galeron, J. 1997. Community structure and spatial heterogeneity of the deep-sea macrofauna at three contrasting stations in the tropical northeast Atlantic. Deep Sea Res. Part II Top. Stud. Oceanogr., 44 (2), 247–269. https://doi.org/10.1016/s0967-0637(96)00110-0.

Crawford, W. R., Peña, M. A. 2013. Declining oxygen on the British Columbia continental shelf. Atmos-Ocean, 51 (1), 88–103.

Dale, A. W., Paul, K. M., Clemens, D., Scholz, F., Schroller-Lomnitz, U., et al. 2021. Recycling and burial of biogenic silica in an open margin oxygen minimum zone. Global biogeochem cycles, 35 (2), e2020GB006583.

Danovaro, R. 2009. Methods for the study of deep-sea sediments, their functioning and biodiversity. CRC press., 45-51.

DeMaster, D. J. 2019. The global marine silica budget: Sources and sinks.

Diaz, R. J., Rosenberg, R. 1995. Marine benthic hypoxia: a review of its ecological effects and the behavioural responses of benthic macrofauna. Oceanogr. Mar. Biol., 33 (245), 03.

Diaz, R. J., Rosenberg, R. 2008. Spreading dead zones and consequences for marine ecosystems. Science, 321 (5891), 926-929.

Dodds, W. K., Cole, J. J. 2007. Expanding the concept of trophic state in aquatic ecosystems: It's not just the autotrophs. Aquat. Sci., 69 (4), 427–439. https://doi.org/10.1007/s00027-007-0922-1.

Druffel, E. M., Smith, K. L. 1998. Long time-series monitoring of an abyssal site in the NE Pacific. Deep-Sea Res. II: Top. Stud. Oceanogr., 45 (4-5).

Dunlop, K. M., van Oevelen, D., Ruhl, H. A., Huffard, C. L., Kuhnz, et al., 2016. Carbon cycling

in the deep eastern North Pacific benthic food web: Investigating the effect of organic carbon input. Limn. Oceanogr., 61 (6), 1956-1968.

Fauchald, K., Jumars, P. A. 1979. The diet of worms: a study of polychaete feeding guilds. Oceanogr. Mar. Biol.

Fenchel, T., Finlay, B. J. 1995. Ecology and Evolution in Anoxic Worlds. Oxford University, NY, Press on Demand.

Flach, E., Heip, C. 1996. Vertical distribution of macrozoobenthos within the sediment on the continental slope of the Goban Spur area (NE Atlantic). Mar. Ecol. Prog. Ser., 141, 55–66. https://doi.org/10.3354/meps141055.

Fowler, S. W., Knauer, G. A. 1986. Role of large particles in the transport of elements and organic compounds through the oceanic water column." Oceanogr., 16 (3), 147–94.

Fox J, Weisberg S. 2011. An {R} companion to applied regression, 2 Edition.

Francois, R., Honjo, S., Krishfield, R., Manganini, S. 2002. Factors controlling the flux of organic carbon to the bathypelagic zone of the ocean. Global Biogeochem Cy., 16 (4), 34–31. https://doi.org/10.1029/2001gb001722.

Fry, B., Sherr, E. B. 1989. $\delta^{13}C$ Measurements as indicators of carbon flow in marine and freshwater ecosystems. Isotopes Environ Health Stud. Springer, New York, NY, 196–229. https://doi.org/10.1007/978-1-4612-3498-2_12.

Fuerst, J. A., Sagulenko, E. 2011. Beyond the bacterium: planctomycetes challenge our concepts of microbial structure and function. Nat. Rev. Microbiol., 9 (6), 403-413.

Gallardo, V. A. 1977. Large benthic microbial communities in sulphide biota under Peru–Chile subsurface countercurrent. Nature, 268 (5618), 331-332.

Glud, R. N. 2008. Oxygen dynamics of marine sediments. Mar. Biol. Res., 4 (4), 243–289.

https://doi.org/10.1080/17451000801888726.

Gooday, A. J., Levin, L. A., da Silva, A. A., Bett, B. J., Cowie, G. L., et al. 2009. Faunal responses to oxygen gradients on the Pakistan margin: a comparison of foraminiferans, macrofauna and megafauna. Deep Sea Res. Part II Top. Stud. Oceanogr., 56 (6-7), 488-502.

Guitton, M. L., Le Guitton, M., Soetaert, K., Sinninghe Damsté, J. S., Middelburg, J. J. 2015. Biogeochemical consequences of vertical and lateral transport of particulate organic matter in the southern North Sea: A multiproxy approach. Estuar. Coast. Shelf Sci., 165, 117–127. https://doi.org/10.1016/j.ecss.2015.09.010.

Hammond, D. E., Fuller, C., Harmon, D., Hartman, B., Korosec, M., et al. 1985. Benthic fluxes in San Francisco Bay. Temporal Dynamics of an Estuary: San Francisco Bay. Springer, Dordrecht., 69–90. https://doi.org/10.1007/978-94-009-5528-8_5.

Henson, S. A., Sanders, R., Madsen, E. 2012. Global patterns in efficiency of particulate organic carbon export and transfer to the deep ocean. Global Biogeochem Cy., 26, 1. https://doi.org/10.1029/2011gb004099.

Hoffmann, K., Bienhold, C., Buttigieg, P. L., Knittel, K., Laso-Pérez, R., et al. 2020. Diversity and metabolism of *Woeseiales* bacteria, global members of marine sediment communities. The ISME journal, 14 (4), 1042-1056.

Hughes, D. J., Lamont, P. A., Levin, L. A., Packer, M., Feeley, K., et al. 2009. Macrofaunal communities and sediment structure across the Pakistan Margin oxygen minimum zone, north-east Arabian Sea. Deep Sea Res. Part II Top. Stud. Oceanogr., 56 (6-7), 434-448.

Iken, K., Brey, T., Wand, U., Voigt, J., Junghans, P. 2001. Food web structure of the benthic community at the Porcupine Abyssal Plain (NE Atlantic): a stable isotope analysis. Prog. Oceanogr., 50 (1-4), 383–405. https://doi.org/10.1016/s0079-6611(01)000623.

Ingall, E., Jahnke, R. 1994. Evidence for enhanced phosphorus regeneration from marine sediments overlain by oxygen depleted waters. Geochim. Cosmochim. Acta., 58 (11). 2571–2575. https://doi.org/10.1016/0016-7037(94)90033-7.

Jaleel, K. U. A., Abdul Jaleel, K. U., Anil Kumar, P. R., Nousher Khan, K., Correya, N. S., et al. 2014. Polychaete community structure in the South Eastern Arabian Sea continental margin (200–1000m). Deep Sea Res. Part I Oceanogr. Res. Pap., 93, 60–71. https://doi.org/10.1016/j.dsr.2014.07.006.

Jameson, B. D., Berg, P., Grundle, D. S., Stevens, C. J., Juniper, S. K. 2021. Continental margin sediments underlying the NE Pacific oxygen minimum zone are a source of nitrous oxide to the water column. Limnol. Oceanogr., 6 (2), 68–76. https://doi.org/10.1002/lol2.10174.

Jeffreys, R. M., Burke, C., Jamieson, A. J., Narayanaswamy, B. E., Ruhl, et al. 2013. Feeding preferences of abyssal macrofauna inferred from *in-situ* pulse chase experiments. PloS one,8 (11), e80510.

Jessen, G. L., Lichtschlag, A., Ramette, A., Pantoja, S., Rossel, P. E., et al. 2017. Hypoxia causes preservation of labile organic matter and changes seafloor microbial community composition (Black Sea). Science advances, 3 (2), e1601897.

Jørgensen, B. B., Boetius, A. 2007. Feast and famine—microbial life in the deep-sea bed. Nat. Rev. Microbiol., 5 (10), 770-781.

Jørgensen, Wenzhöfer, F., Egger, M,. et al., 2021. Sediment oxygen consumption: Role in the global marine carbon cycle. Earth-Sci. Rev., 228, 103987.

Joydas, T. V., Damodaran, R. 2014. Infaunal macrobenthos of the oxygen minimum zone on the Indian western continental shelf. Mar. Ecol. Prog. Ser., 35 (1) ,22–35. https://doi.org/10.1111/maec.12052.

Jumars P. A, Mayer L. M, Deming J. W, Baross J. A, Wheatcroft R. A. 1990. Deep-sea deposit feeding strategies suggested by environmental and feeding constraints. Philos Trans R Soc A., 331,85–101.

Jumars, P. A., Dorgan, K. M., Lindsay, S. M. 2015. Diet of worms emended: an update of polychaete feeding guilds. Ann Rev Mar Sci, 7, 497-520.

Jumars, P.A., Self, R.F.L., Nowell, A.R.M. 1982 Mechanics of particle selection by tentaculate deposit-feeders. J. Exp. Mar. Biol. 64, 47–70.

Kalvelage, T., Jensen, M. M., Contreras, S., Revsbech, N. P., Lam, P., et al. 2011. Oxygen sensitivity of anammox and coupled N-cycle processes in oxygen minimum zones. PloS one, 6 (12), e29299.

Kamykowski, D., Zentara, S. J. 1990. Hypoxia in the world ocean as recorded in the historical data set. Deep Sea Res. Part I Oceanogr. Res. Pap., 37 (12), 1861–1874. https://doi.org/10.1016/0198-0149(90)90082-7.

Katz, T., Yahel, G., Tunnicliffe, V., Herut, B., Whitney, F., et al. 2016. The silica cycle in a Northeast Pacific fjord; the role of biological resuspension. Prog. Oceanogr., 147, 10-21.

Kraal, P., Slomp, C. P., Reed, D. C., Reichart, G. J., Poulton, S. W. 2012. Sedimentary phosphorus and iron cycling in and below the oxygen minimum zone of the northern Arabian Sea. Biogeosciences., 9 (7), 2603–2624. https://doi.org/10.5194/bg-9-2603-2012.

Kraft, B., Jehmlich, N., Larsen, M., Bristow, L. A., Könneke, M., et al. 2022. Oxygen and nitrogen production by an ammonia-oxidizing archaeon. Science, 375 (6576), 97-100.

Laliberté, E., Legendre, P., Shipley, B., Laliberté, M. E. 2014. Package 'FD'. Measuring functional diversity from multiple traits, and other tools for functional ecology, 1-0.

Lam, P., Kuypers, M. M. 2011. Microbial nitrogen cycling processes in oxygen minimum zones.

Ann Rev Mar Sci, 3, 317–45. 10.1146/annurev-marine-120709-142814.

Lam-Gordillo, O., Mosley, L. M., Simpson, S. L., Welsh, D. T., Dittmann, S. 2022. Loss of benthic macrofauna functional traits correlates with changes in sediment biogeochemistry along an extreme salinity gradient in the Coorong lagoon, Australia. Mar. Pollut. Bull., 174, 113202.

Lamont, P. A., Gage, J. D. 2000. Morphological responses of macrobenthic polychaetes to low oxygen on the Oman continental slope, NW Arabian Sea. In Deep Sea Res. Part II Top. Stud. Oceanogr., 47 (1-2), 9–24. https://doi.org/10.1016/s0967-0645(99)00102-2.

Lauerman, L. M. L., Smoak, J. M., Shaw, T. J., Moore, W. S., Smith, K. L. 1997. ^{234}Th and ^{21}Pb evidence for rapid ingestion of settling particles by mobile epibenthic megafauna in the abyssal NE Pacific. Limnol. Oceanogr., 42 (3), 589–595. https://doi.org/10.4319/lo.1997.42.3.0589.

Levin, L. A. 2003. Oxygen minimum zone benthos: Adaptation and community response to hypoxia. In R. J. A. A. R. N. Gibson (Ed.), Oceanogr. Marine Biol. Annu. Rev, 41, 1-45.

Levin, L. A., Blair, N. E., Martin, C. M., DeMaster, D. J., Plaia, G., et al. 1999. Macrofaunal processing of phytodetritus at two sites on the Carolina margin:*in-situ* experiments using ^{13}C-labeled diatoms. Mar. Ecol. Prog. Ser., 182, 37–54. https://doi.org/10.3354/meps182037.

Levin, L. A., Gage, J. D. 1998. Relationships between oxygen, organic matter and the diversity of bathyal macrofauna. Deep Sea Res. Part II Top. Stud. Oceanogr, 45 (1-3), 129-163.

Levin, L. A., Gage, J., Lamont, P., Cammidge, L., Martin, C., et al. 1997. Infaunal community structure in a low-oxygen, organic rich habitat on the Oman continental slope, NW Arabian Sea. The responses of marine organisms to their environments: Proceedings of the 30th European Marine Biology Symposium, University of Southampton, Southampton, UK. 223-230.

Levin, L. A., Huggett, C. L., Wishner, K. F. 1991. Control of deep-sea benthic community structure by oxygen and organic-matter gradients in the eastern Pacific Ocean. J. Mar. Res. 49 (4),

763-800.

Levin, L. A., Whitcraft, C. R., Mendoza, G. F., Gonzalez, J. P., Cowie, G. 2009. Oxygen and organic matter thresholds for benthic faunal activity on the Pakistan margin oxygen minimum zone (700–1100 m). Deep Sea Res. Part II Top. Stud. Oceanogr. 56 (6-7), 449-471.

Levin, L. A., Ziebis, W., Mendoza, G. F., Bertics, V. J., Washington, T., et al. 2013. Ecological release and niche partitioning under stress: lessons from dorvilleid polychaetes in sulfidic sediments at methane seeps. Deep Sea Res Part II: Top. Stud. Oceanogr, 92, 214-233.

Lovley, D. R., Phillips, E. J. 1986. Organic matter mineralization with reduction of ferric iron in anaerobic sediments. Appl. Environ. Microbiol., 51 (4), 683-689.

Martino, A. D., De Martino, A., Meichenin, A., Shi, J., Pan, K., et al. 2007. Genetic and phenotypic characterization of *Phaeodactylum tricornutum* (Bacillariophyceae) accessions1. J. Phycol., 43 (5), 992–1009. https://doi.org/10.1111/j.1529-8817.2007.00384.x.

Mayer, L. M., Schick, L. L., Sawyer, T., Plante, C. J., Jumars, P. A., et al. 1995. Bioavailable amino acids in sediments: a biomimetic, kinetics-based approach. Limnol. Oceanogr., 40 (3), 511-520.

McArdle, B. H., Anderson, M. J. 2001. Fitting multivariate models to community data: a comment on distance-based redundancy analysis. Ecol., 82 (1), 290-297.

Mevenkamp, L., Stratmann, T., Guilini, K., Moodley, L., van Oevelen, D., et al. 2017. Impaired short-term functioning of a benthic community from a deep Norwegian Fjord following deposition of mine tailings and sediments. Front. Mar. Sci., 4, 169.

Meysman, F. J., Middelburg, J. J., Heip, C. H. 2006. Bioturbation: a fresh look at Darwin's last idea. Trends Ecol. Evol., 21 (12), 688-695.

Miatta M., Bates, A.E. Snelgrove, P.V.R. 2021. Incorporating biological traits into marine

protected area strategies. Ann. Rev. Mar. Sci., 13, 421–43.

Middelburg, J. J., Barranguet, C., Boschker, H. T. S., Herman, P. M. J., Moens, T., et al. 2000. The fate of intertidal microphytobenthos carbon: An *in-situ* ^{13}C-labeling study.Limnol. Oceanogr., 45 (6), 1224–1234. https://doi.org/10.4319/lo.2000.45.6.1224.

Moodley, L., Middelburg, J. J., S. Boschker, H. T., Duineveld, G. C. A., Pel, R., et al. 2002. Bacteria and foraminifera: key players in a short-term deep-sea benthic response to phytodetritus. Mar. Ecol. Prog. Ser., 236, 23–29

Moodley, L., Middelburg, J. J., Soetaert, K., Boschker, H. T. S., Herman, P. M. J., and Heip, C. H. R. 2005. Similar rapid response to phytodetritus deposition in shallow and deep-sea sediments. J. Mar. Res., 63 (2), 457-469.

Morse, J. W., Boland, G., Rowe, G. T. 1999. A gilled benthic chamber for extended measurement of sediment-water fluxes. Mar. Chem, 66 (3-4), 225-230.

Murray, J. M. H., Meadows, A., Meadows, P. S. 2002. Biogeomorphological implications of microscale interactions between sediment geotechnics and marine benthos: a review. Geomorphology, 47 (1), 15–30. https://doi.org/10.1016/s0169-555x(02)00138-1.

Niemistö, J., Kononets, M., Ekeroth, N., Tallberg, P., Tengberg, A., et al. 2018. Benthic fluxes of oxygen and inorganic nutrients in the archipelago of Gulf of Finland, Baltic Sea–Effects of sediment resuspension measured in situ. J. Sea Res., 135, 95-106.

Ogino, T., Toyohara, H. 2019. Identification of possible hypoxia sensor for behavioral responses in a marine annelid, *Capitella teleta*. Biology Open., 8 (3), bio037630 https://doi.org/10.1242/bio.037630.

Oksanen J., Blanchet, F. G., Kindt, R., Legendre, P et al. 2013 vegan: community ecology package. R package version 2.0-10. http://CRAN.Rproject.org/package=vegan.

Pacheco, A. S., González, M. T., Bremner, J., Oliva, M., Heilmayer, O., et al. 2011. Functional diversity of marine macrobenthic communities from sublittoral soft-sediment habitats off northern Chile. Helgol. Mar. Res., 65 (3), 413-424.

Parrish, C. C. 1987. Separation of aquatic lipid classes by chromarod thin-layer chromatography with measurement by iatroscan flame ionization detection. Can. J. Fish. Aquat. Sci Aquat. Sci., 44 (4), 722–731. https://doi.org/10.1139/f87-087.

Parrish, C. C. 1999. Determination of Total Lipid, Lipid Classes, and Fatty Acids in Aquatic Samples. Arts, M.T., Wainman, B. C. (eds) Lipids in Freshwater Ecosystems. Springer, New York, NY., 4-20. https://doi.org/10.1007/978-1-4612-0547-0_2.

Parrish, C. C. 2009. Essential fatty acids in aquatic food webs. Lipids in Aquatic Ecosystems. Springer, New York, NY. 309–326. https://doi.org/10.1007/978-0-387-89366-2_13.

Pearson, T. H., Rosenberg, R. 1978. Macrobenthic succession in elation to organic enrichment and pollution of the marine environment. Oceanogr Mar Biol Annu Rev 16, 229-311.

Peterson, B. J. 1999. Stable isotopes as tracers of organic matter input and transfer in benthic food webs: A review. Acta Oecol, 20 (4), 479-487.

Queirós, A. M., Birchenough, S. N., Bremner, J., Godbold, J. A., Parker, R. E., et al. 2013. A bioturbation classification of European marine infaunal invertebrates. Ecol. Evol., 3 (11), 3958-3985.

R Core Team. 2016. R: A Language and Environment for Statistical Computing. Vienna, Austria. Retrieved from https://www.R-project.org/.

Ragueneau, O., Gallinari, M., Corrin, L., Grandel, S., Hall, P., et al. 2001. The benthic silica cycle in the Northeast Atlantic: annual mass balance, seasonality, and importance of non-steady-state processes for the early diagenesis of biogenic opal in deep-sea sediments. Prog. Oceanogr.,50 (1-

4), 171-200.

Riley, J. S., Sanders, R., Marsay, C., Le Moigne, F. A. C., Achterberg, E. P., et al. 2012. The relative contribution of fast and slow sinking particles to ocean carbon export. Global Biogeochem Cy., 26 (1). https://doi.org/10.1029/2011gb004085.

Risgaard-Petersen, N., Langezaal, A. M., Ingvardsen, S., Schmid, M. C., Jetten, M. S., et al. 2006. Evidence for complete denitrification in a benthic foraminifer. Nature, 443 (7107), 93-96.

Romanelli, E., Sweet, J., Giering, S. L. C., Siegel, D. A., and Passow, U. 2023. The importance of transparent exopolymer particles over ballast in determining both sinking and suspension of small particles during late summer in the Northeast Pacific Ocean. Elementa, 11(1).

Sanders, H.L. 1958. Benthic studies in Buzzards Bay. I. Animal–sediment relationships. Limn. Oceanog. 3, 245–258.

Schaff, T. R., Levin, L. A. 1994. Spatial heterogeneity of benthos associated with biogenic structures on the North Carolina continental slope. Deep Sea Res. Part II Top. Stud. Oceanogr., 41 (4-6), 901–918.https://doi.org/10.1016/0967-0645(94)900531.

Schwartz, M., Smith, J., Woulds, C., Cowie, G. 2007. Laboratory incubations with regulated oxygen concentrations used to measure benthic biogeochemical fluxes in parallel with autonomous lander studies. Limnol. Oceanogr: Methods, In revision, 29.

Seiter, K., Hensen, C., Zabel, M. 2005. Benthic carbon mineralization on a global scale. Global Biogeochem Cy.,19 (1). https://doi.org/10.1029/2004gb002225.

Sivadas, S. K., Singh, D. P., Saraswat, R. 2020. Functional and taxonomic (α and β) diversity patterns of macrobenthic communities along a depth gradient (19–2639 m): a case study from the southern Indian continental margin. Deep Sea Res. Part I Oceanogr. Res., 159, 103250.

Smith, C., Deleo, F., Bernardino, A., Sweetman, A., Arbizu, P. 2008. Abyssal food limitation,

ecosystem structure and climate change. Trends Ecol. Evol. 23 (9), 518–528. https://doi.org/10.1016/j.tree.2008.05.002.

Snelgrove, P. V. R. 1998. The biodiversity of macrofaunal organisms in marine sediments. Biod. Conserv., 7, 1123-1132.

Snelgrove, P. V. R. 1999. Getting to the bottom of marine biodiversity: sedimentary habitats: ocean bottoms are the most widespread habitat on earth and support high biodiversity and key ecosystem services. Bio Science, 49 (2), 129-138.

Snelgrove, P. V. R., Thrush, S. F., Wall, D. H., Norkko, A. 2014. Real world biodiversity–ecosystem functioning: a seafloor perspective. Trends Ecol. Evol., 29 (7), 398-405.

Suess, E. 1980. Particulate organic carbon flux in the oceans—surface productivity and oxygen utilization. Nature, 288, 260-263.

Sweetman, A. K., Chelsky, A., Pitt, K. A., Andrade, H., van Oevelen, D., et al. 2016. Jellyfish decomposition at the seafloor rapidly alters biogeochemical cycling and carbon flow through benthic food-webs. Limnology and Oceanography, 61(4), 1449-1461.

Sweetman, A. K., Norling, K., Gunderstad, C., Haugland, B. T., Dale, T. 2014. Benthic ecosystem functioning beneath fish farms in different hydrodynamic environments. Limnol. Oceanogr. 59 (4), 1139–1151. https://doi.org/10.4319/lo.2014.59.4.1139.

Sweetman, A. K., Smith, C. R., Shulse, C. N., Maillot, B., Lindh, M., et al. 2019. Key role of bacteria in the short-term cycling of carbon at the abyssal seafloor in a low particulate organic carbon flux region of the eastern Pacific Ocean. Limnol. Oceanogr., 64 (2) 694–713. https://doi.org/10.1002/lno.11069.

Sweetman, A. K., Sommer, S., Pfannkuche, O., Witte, U. 2009. Retarded response by macrofauna-size foraminifera to phytodetritus in a deep norwegian fjord. J. Foraminifer. Res., 39

(1) 15–22. https://doi.org/10.2113/gsjfr.39.1.15.

Sweetman, A. K., Witte, U. 2008. Response of an abyssal macrofaunal community to a phytodetrital pulse. Mar. Ecol. Prog. Ser., 355, 73–84. https://doi.org/10.3354/meps07240.

Taghon, G.L. 1982 Optimal foraging by deposit-feeding invertebrates: roles of particle size and organic coating. Oecologia. 52, 295–304.

Taghon, G. L., Nowell, A. R. M., Jumars, P. A. 1980. Induction of suspension feeding in spionid polychaetes by high particulate fluxes. Science, 210 (4469), 562–564. https://doi.org/10.1126/science.210.4469.562.

Thurber, A. R., Sweetman, A. K., Narayanaswamy, B. E., Jones, D. O., Ingels, J., Hansman, R. L., 2014. Ecosystem function and services provided by the deep sea. Biogeosciences, 11(14), 3941-3963.

Treude, T., Smith, C. R., Wenzhöfer, F., Carney, E., Bernardino, A. F., et al.. 2009. Biogeochemistry of a deep-sea whale fall: sulfate reduction, sulfide efflux and methanogenesis. Mar. Ecol. Prog. Ser., 382, 1–21. https://doi.org/10.3354/meps07972.

Tseng, Y. H., Ding, R., and Huang, X. M. 2017. The warm Blob in the northeast Pacific—the bridge leading to the 2015/16 El Niño. Environ. Res. Lett., 12(5), 054019.

Turley, C. M., Lochte, K., Lampitt, R. S. 1995. Transformations of biogenic particles during sedimentation in the northeastern Atlantic. Philos. Trans. R. Soc. Series B: Biol Sci, 348 (1324), 179-189.

Van Cappellen, P., Qiu, L. 1997. Biogenic silica dissolution in sediments of the Southern Ocean. II. Kinetics. Deep Sea Res. Part II Top. Stud. Oceanogr., 44 (5), 1129-1149.

Villéger, S. Mason, N. W., Mouillot, D. 2008. New multidimensional functional diversity indices for a multifaceted framework in functional ecology. Ecol. 89, 2290–2301.

Violle, C., Reich, P. B., Pacala, S. W., Enquist BJ, Kattge J. 2014. The emergence and promise of functional biogeography. Proc. Natl. Acad. Sci. U.S.A. 111 (38), 13690-13696.

Watling, L., Guinotte, J., Clark, M.R., Smith, C.R. 2013. A proposed biogeography of the deep ocean floor. Prog. Oceanogr., 111, 91–112. https://doi.org/10.1016/j.pocean.2012.11.003.

Wentworth, C. K. 1929. Method of computing mechanical composition types in sediments. Geol. Soc. Am. Bull., 40 (4), 771-790.

Witte, U., Wenzhöfer, F., Sommer, S., Boetius, A., Heinz, P., et al. 2003. *In-situ* experimental evidence of the fate of a phytodetritus pulse at the abyssal sea floor. Nature, 424 (6950), 763–766.

WoRMS Editorial Board, 2015. World Register of Marine Species. http://www.marinespecies.org.

Woulds, C., Andersson, J. H., Cowie, G. L., Middelburg, J. J., Levin, L. A. 2009. The short-term fate of organic carbon in marine sediments: comparing the Pakistan margin to other regions. Deep Sea Res. Part II Top. Stud. Oceanogr. 56 (6-7), 393-402.

Woulds, C., Cowie, G. L., Levin, L. A., Andersson, J. H., Middelburg, J. J., et al. 2007. Oxygen as a control on sea floor biological communities and their roles in sedimentary carbon cycling. Limnol. Oceanogr., 52 (4), 1698–1709. https://doi.org/10.4319/lo.2007.52.4.1698.

Wright, J. J., Konwar, K. M., Hallam, S. J. 2012. Microbial ecology of expanding oxygen minimum zones. Nat. Rev. Microbiol. 10 (6), 381-394.

Yool, A., Martin, A. P., Anderson, T. R., Bett, B. J., Jones, D. O. B., et al. 2017. Big in the benthos: Future change of seafloor community biomass in a global, body size-resolved model. Glob Chang Biol., 23 (9) 3554–3566. https://doi.org/10.1111/gcb.13680.

Zakem, E. J., Mahadevan, A., Lauderdale, J. M., Follows, M. J. 2020. Stable aerobic and anaerobic coexistence in anoxic marine zones. The ISME journal, 14 (1), 288-301.

Zettler, M. L., Bochert, R., Pollehne, F. 2009. Macrozoobenthos diversity in an oxygen minimum zone off northern Namibia. Mar Biol 156, 1949–1961.

Zuur, A. F., Ieno, E. N., Walker, N. J., Saveliev, A. A., Smith, G. M. 2009. Mixed effects models and extensions in ecology with R. Springer, New York, NY, USA.

Chapter 3. - Inferring benthic megafaunal sediment reworking activity in relation to bottom water oxygen in Barkley Canyon, NE Pacific from video and acoustic imaging analysis[3]

[3]A version of this chapter is in review with *Deep-Sea Res. Part I Oceanogr. Res* as: Ciraolo, Snelgrove, Douglass, De Leo, (2023) "Inferring benthic megafaunal sediment reworking activity in relation to bottom water oxygen in Barkley Canyon, NE Pacific from video and acoustic imaging analysis".

3.1 Abstract

Sediment reworking activity influences benthic functioning expressed as nutrient fluxes and carbon cycling. Multiple studies have addressed sediment reworking based on observations from individual instrument types (e.g., video camera, side-scan sonar, multibeam), but none have considered reworking based on two or more complementary instruments. We therefore aimed to analyze deep-sea megafaunal and reworked sediment by combining and comparing observations from non-invasive instruments, an underwater video camera and a rotary sonar. Specifically, we examined sediment traces and the benthic megafaunal communities in relation to different bottom-water oxygen levels and at two different spatial scales of analysis. We analyzed videos and sonar images recorded concurrently in May and September 2013 at a node of Ocean Networks Canada's NEPTUNE cabled observatory, located at 396 m depth in Barkley Canyon Upper Slope, NE Pacific Ocean. The camera images (~ 0.5 m^2) documented significantly lower megafaunal density and diversity during the period of reduced oxygen concentrations. Although we did not observe significant differences in sediment trace diversity and density between the two study periods, we focused on how the relief traces generated by unidentified gastropods (likely the family Solariellidae) influenced sediment mixing, noting higher density in low oxygen (May, 1.87 count m^{-2}) than high oxygen (September, 1.17 count m^{-2}) conditions. Sonar images (~1268 m^2), which

lacked sufficient resolution to allow identification of benthic organisms, documented distribution of biological pits, a significantly greater proportion of bioturbated seafloor area, and increases in pit size with increased oxygen levels. Circular regions of low backscatter, identified as “pits” in previous work and originating from biological activity, dominated sonar images at this location and persisted through the two study periods. Some sonar field of view subsections showed a significant increase in circularity of pit shapes in relation to oxygen concentration, likely explained by increased reworked sediment with increasing oxygen concentration. We conclude that, except for relief burrows, higher reworked sediment area coincided with the highest oxygen concentration, which aligns with previously established reduced metabolic activity by benthos adapted to oxygen minimum zones. Furthermore, we emphasize the complementarity of the two imaging techniques (video and sonar) in understanding deep-sea benthic ecosystem dynamics, as well as the importance of considering multiple spatial scales when investigating proxies of bioturbation activity.

3.2 Introduction

The cost and logistical challenges of deep-sea research (Smith et al., 2022) have motivated researchers to develop novel tools to enable remote and *in-situ* time-series data collection. In recent decades, cabled ocean observatories have offered a greater array of tools to study short and long-term Earth-ocean processes (Vardaro et al., 2013; De Leo et al., 2018). For example, Canada's VENUS (Victoria Experimental Network Under the Sea) and NEPTUNE (North-East Pacific Undersea Networked Experiments) observatories, collectively known as Ocean Networks Canada (which also includes observatories in the Arctic and Atlantic Oceans), have collected data remotely from the coast to the deep-sea of the Northeast Pacific Ocean for over a decade (Barnes et al., 2007). These observatories link numerous and diverse sets of sensors through cables, connectors, and instrument platforms (Barnes et al., 2007).

Previous studies on spatial heterogeneity of deep-sea biodiversity, nutrient cycling, and the roles of phytodetritus, scavengers, and carcass falls have utilized remotely operated vehicles (e.g., Campanyà - Llovet et al., 2017; Miatta and Snelgrove, 2021), benthic landers (e.g., Witte et al., 2003; Sweetman et al., 2008) and cabled observatories (Thomsen et al., 2017; De Leo et al., 2018). Of these tools, cabled observatories offer the best opportunity for continuous time series and even real-time observation of processes such as bioturbation, referring to the mixing of sediment particles by biological activity (Kristensen et al., 2012) that leads to biogenic transport of pore water and changes in physical and chemical properties of sediment (Shull 2009). Bioturbation, directly and indirectly, affects nutrient fluxes, oxygen penetration depth, dispersion of contaminants, and particularly the process of organic matter mineralization near the sediment-water interface (Kristensen, 2000; Furukawa et al., 2001).

Low oxygen concentration in bottom-water (defining hypoxia as $0 < O_2 < 1.4$ $ml \cdot l^{-1}$, Ekau et al., 2010), also influences bioturbation and the consequences of bioturbation, often by decreasing megafaunal or macrofaunal biodiversity (e.g., Smith et al., 2000; Levin, 2003; Belley et al., 2010). However, a lack of opportunities for repeat observations limits our knowledge of oxygen concentration effects on bioturbation along continental margins (Robert and Juniper, 2012). Mass sediment properties, especially grain size distributions and permeability to fluid flow, partly determine biogeochemical cycling properties which add to the complexity of understanding the rates and mechanisms of sediment mixing (reviewed by Shum and Sundby, 1996; Huettel and Webster, 2001), and thus to benthic ecosystem functions (Snelgrove et al., 2014).

Past studies have assessed bioturbation in different ways, based on habitat characteristics and organisms present, and considered the time scales of mixing. For example, researchers have used invasive techniques for direct collection of sediment and bioturbation features and structures. Those methods include creating castings by inserting resin into burrows, which harden over time and can be removed intact for further analysis (Cadee, 1976; Seike et al., 2012). Entrapment refers to volume measurements of reworked sediment ejected at the sediment-water interface by the organism and collected in a trap placed around the site of sediment rejection (Rhoads et al., 1963; Maire et al., 2008). Levelling consists of measuring changes in the height of the sediment-water interface over time, using the original sediment-water level as a reference. The accumulated sediment can be collected and then weighed to estimate sediment reworking (Cadee, 1976; Maire et al., 2008; Seike et al., 2012). The quantification of either natural (e.g., radionuclides) or added (e.g., luminophores) (Wheatcroft, 1991; Maire et al., 2008) tracers offers another mechanism to assess the vertical movement of particles within sediments. Surface image analysis, a non-destructive approach, offers an alternative method to assessing short-term temporal changes in

sediment reworking. For example, Robert and Juniper (2012) used a real-time camera to monitor bioturbation by flatfish, echinoderms, and gastropods, and to estimate the time required for organisms to turn over surface sediments. Belley et al. (2010) used video imagery to quantify bioturbation in the Gulf of Lawrence by quantifying surface relief of traces left by biological activity on the sediment surface. Solan and Kennedy (2002) and Solan et al. (2004) used a sediment-profile image camera (SPI) consisting of a camera, a prism-shaped box that penetrates the sediment, and a mirror located on the back side of the prism, to provide in-situ undisturbed cross-sectional images of the benthos (Rhoads and Cande, 1971). Coupling this technique with others, such as the addition of luminophores, enables visual identification of species and provides quantifiable information on infaunal activity.

Other than as a tool to quantify megafaunal composition over large spatial scales, relatively few studies have used the non-destructive technique of sonar imaging to quantify bioturbation activity (Roberts and Juniper, 2012). Sonar images, in tandem with continuous video, have been used to study trawling impacts on the seabed (De Leo et al., 2017), to analyze pit formation in relation to seafloor roughness (DuVal et al., 2021), and to study nearshore bedform development following a storm and in response to changes in wave direction (Hay and Wilson, 1994; Maier and Hay, 2009).

Bioturbation often leaves a variety of types of visible traces on seafloor known as ‘‘*lebensspuren*’’, a German term for life traces (Mauviel and Sibuet, 1985; Bell et al., 2013). Some of these traces, which include “pits” and “mounds” in an acoustic context, refer to seabed formations that originate from biological activity. Macrofauna form pits to either avoid predators, capture prey (Auster et al., 1995), or through feeding activities of deposit feeders (Nowell et al., 1984). Mounds refer to sediment defecated by macrofauna back to the surface, which can coil into

characteristic fecal mounds (Kukert and Smith, 1992). Traces also fall under two main groups according to their morphology: surface-traces and relief-traces (Mauviel and Sibuet, 1985). Surface traces refer to features created by mixing sediment in the upper few millimeters or centimeters of the sediment, in contrast to relief traces created by animals mixing deeper sediment layers and bio-irrigating (Belley et al., 2010). Furthermore, changes in pit size and shape can be indicative of enhanced sediment reworking or hydrodynamic activities (Hay and Wilson, 1994; DuVal et al., 2021). Changes in pit morphology may occur in environments with moderate currents and pit aspect ratios (depth/diameter) between 0.5 and 2, because particle fluxes and particle residence time increase (Yager et al., 1993). Consequently, the increased particle flux and vortex at pit walls can increase bio-irrigation, elevating labile organic matter content in the pit and attracting more organisms, further increasing sediment mixing. However, sonar images can identify pits as circular shadow zones. The way in which scanning sonar systems function and the geometry of their setup precludes direct observation of the target itself, but rather its acoustical "shadow". In contrast, rotary sonar and multibeam allow sea-floor habitat mapping, and extrapolation of benthic habitat characteristics across large areas of sea floor (Kostylev et al., 2008) Jones and Traykovski (2018) note that the (typically) higher mounting of the sonar instrument well above the bioturbated sediment transmits a pulse of acoustic waves that hits the sediment diagonally. The sonar then records the low intensity of the reflected return signal (backscatter). Biological (bioturbation) bedforms typically occur in sets where subsequently formed bedforms truncate the shadow cast from a given bedform (Jones and Traykovski, 2018).

Given the limited studies that compared video and sonar images to evaluate deep-sea reworked sediment and traces as proxies of bioturbation activity, assessing the advantages, limitations, and complementarity of video and sonar images can potentially enhance the toolbox

available for bioturbation studies. Therefore, our study aimed to combine and compare the two methodologies. Such non-destructive techniques augment the potential for long-term sustained observation aligned with monitoring of ecosystem biodiversity and function. Moreover, we also assessed reworked sediment traces and pit formation over small spatial scales (cm to 20s of m) in response to periods of contrasting bottom-water oxygen concentration levels on the upper continental slope in Barkley Canyon. Specifically, using video images, we examine density and diversity of benthic megafauna, sediment traces, and total bioturbated area over time. In parallel, we assessed bioturbated seafloor based on sonar images by examining the number of pits and the total area covered by pits during different times of the year. Finally, because we hypothesized that changes in pit features may result from biological or hydrodynamic (or both) factors in concert, our study also addresses changes in pit features, specifically in terms of circularity and diameter.

3.3 Materials and Methods

Barkley Canyon, a continental slope feature located 100 km off the coast of Vancouver Island, has a backbone fiber optic cable - part of the Ocean Networks Canada (ONC) cabled observatory (Barnes et al., 2007) - that sends real-time data to a shore station in Port Alberni, British Columbia, and onward to the University of Victoria (**Fig. 3.1. A**).

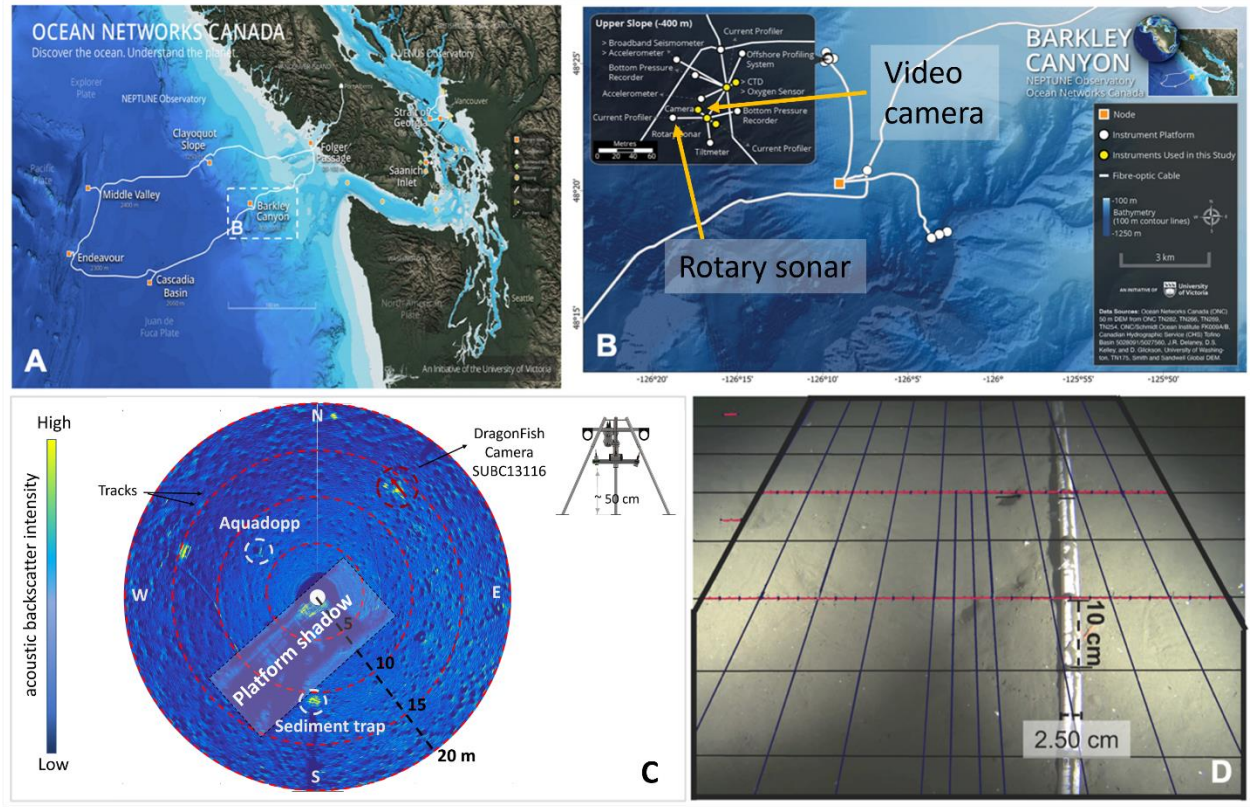

Fig. 3.1. A) Ocean Networks Canada cabled observatory off Vancouver Island, NE Pacific; B) Barkley Canyon Upper Slope location highlighting the positioning of all instruments used in the study; C) Example of a rotary sonar 360° sweep image covering a 20-m radius field of view (FOV), showing a few of the visible high acoustic backscatter targets, and indicating the relative positions of the video camera, Aquadopp, sediment trap, and instrument platform (IP) in the center of the image (the image is oriented with respect to true north); D) Dragonfish SUBC13116 video camera field of view with overlaid perspective grid for scaling, constructed based on reference geometry (i.e., camera height above the seabed, lens aperture angles, and the 10-cm graduated white PVC ruler).

At the Barkley Canyon Upper Slope sampling site, an instrument platform deployed at 396 m depth has been connected to the observatory network since May 2009 (**Fig. 3.1 B**). A SubC

DragonFish Camera was mounted on a galvanized steel tripod and placed approximately 10 m away from the main IP using a Remotely Operated Vehicle (ROV). We used only the inner ~ 0.5 m^2 of the images for our analysis, encompassed in a perspective grid created using the program GIMP (GIMP Development Team, 2019). The grid was created using geometry based on the height of the lens above the seafloor (45 cm), and the lens' aperture angles, $\alpha = 34.5$ (vertical) and $\beta = 53.3$ (horizontal), as described in Command et al. (2023). Video recording was triggered by turning on a pair of Remote Ocean Systems (ROS) 100W LED lights with 400 lumen output. A 1-m long white PVC pipe marked at 10-cm intervals was placed on the seafloor perpendicular to the long axis of the imaging platform, with one end directly below the camera on the seafloor (Nadir point) and the other extending away from the study area to act as a scaling ruler (Fig 1D). This marker helped to calibrate the perspective grid. All video recordings were stored in Ocean Network Canada's Oceans 3.0 data archiving system, which users can download from the ONC web portal (https://data.oceannetworks.ca/DataSearch).

The Kongsberg Mesotech Rotary Sonar (**Table 3.1**) mounted on the Barkley Canyon Upper Slope pod imaged both burrows and trawling tracks while collecting a single sonar sweep every 4 minutes. The 20-m sonar radius covered a total area of ~1268.3 m^2 of the seafloor oriented towards true north (Fig 1C).

Table 3.1. Characteristics of the sonar head

Sonar characteristics	
Rotary step size	0.225˚
Beam width	0.9˚
Range resolution*	1.95 cm
Frequency	675 KHz

* The resolution of a sonar image limits the size of the smallest detectable object. Therefore, the coarser the resolution (e.g. > 1 cm), the harder it is to detect small objects (Hay and Wilson, 1994).

We used ImageJ software 1.8.0 (freely available, https://imagej.nih.gov/ij, Rasband 2018) to estimate the total bioturbated area as well the as total number and shape of pits on sonar scan files. We estimated the bioturbated area and quantified burrows from their shadows, represented by black spots in the sonar images. The shadows represent lower acoustic backscatter intensity.

We analyzed data from May 18-31 and September 20 - October 5, 2013 (**Fig. 3.2**) because this time range spanned the period of lowest and highest bottom-water oxygen concentrations of 0.8 ml l^{-1} ± (SD) and 1.3 ml l^{-1} ± 0.18 (SD), respectively. However, for the pit shape analysis, we also included December 20-30 2013 to assess any changes in shape over time. Bottom-water oxygen concentration in December was ~ 1.09 ml l^{-1} ± 0.11 (SD). We measured bottom-water column characteristics and *in-situ* oxygen concentrations using a Conductivity-Temperature-Depth (CTD) profiler (Sea-Bird SeaCAT SBE16plus V2 7029) and a dissolved oxygen sensor (Sea-Bird SBE 63 Dissolved Oxygen Sensor 630110), respectively (see **Supplementary table 3.1**).

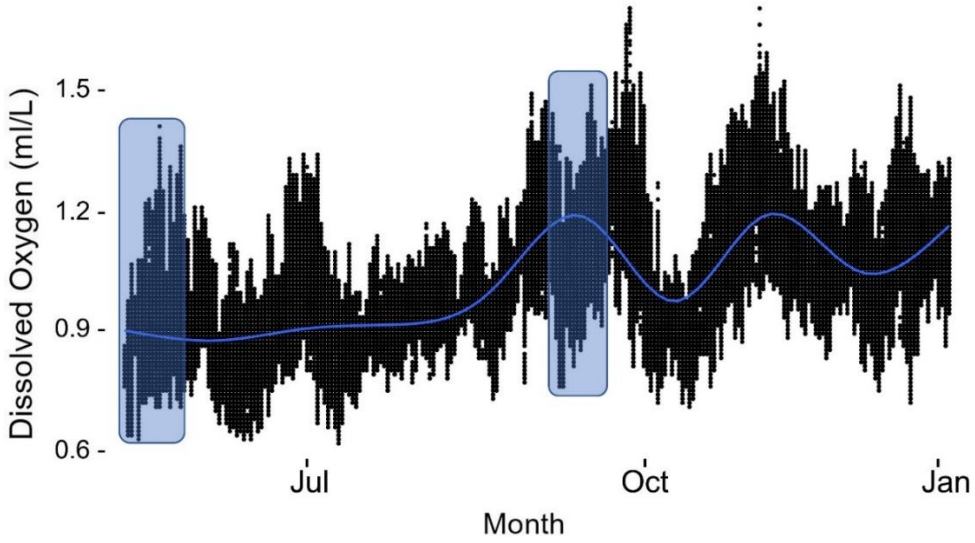

Fig. 3.2. Oxygen concentration data from May-December 2013 modified from Ocean Networks Canada's Oceans 3.0 data portal. Blue squares indicate the time windows analyzed for this study. Oxygen concentrations from January to May 9th were not available.

In 2012-2013 the platform at the canyon Upper Slope was equipped with two upward-looking Acoustic Doppler Current Profilers, one 300 kHz unit, and one 2 MHz Aquadopp profiler. The right-angle head of the 2 MHz system was mounted on the flat low profile secondary platform, in contrast to the 300 kHz unit mounted on the main platform approximately 2 m above the sea floor. An ROV deployed this secondary platform near (< 5 m) the main lander. The low-profile platform and right-angle head configuration of the profiler enabled near-bottom measurements from 10 cm height above the seabed to 150 cm height above bottom (HAB). We present data from the 2 MHz unit to investigate sediment resuspension and mobilization. The 2 MHz Aquadopp sampled at 10 s intervals, and we present data averaged over 15-min periods. In order to evaluate near-bottom flow, but away from any flow disturbance caused by the instrument platform, we selected data from the 10th bin (21 cm HAB) for the directional histogram shown in **Supplementary Fig. 3.1**. The windrose was drawn using m_windrose from the m_map toolbox (Pawlowicz, 2020).

3.3.1 Reworked sediment characterization using an underwater video camera

3.3.1.1 Benthic community and sediment traces

Five-minute video sequences were recorded every two hours with a color high-definition camera (all videos are available at https://data.oceannetworks.ca/SeaTube). For our study, we analyzed one minute (from ~2min 30s to ~3 min 30s) out of every 5 minutes of each video (Chauvet et al., 2018), for the two chosen time periods (May and September). Each of the daily 12 videos recorded the same area of seafloor; for our analysis, we therefore randomly selected one video frame per day to evaluate species and trace abundance as well as diversity to avoid pseudo-replication (Belley et al., 2017), and to avoid the period of time when the light was off.

We calculated alpha biodiversity (Shannon – Wiener diversity index (H'), Simpson's index, Pielou's evenness index (J'), and species richness (S)) based on non-transformed megafaunal densities. Within the video frames, we identified and enumerated benthic megafaunal organisms to the lowest feasible taxonomic level. We calculated densities by dividing abundance by the surface area of the analyzed field of view (~ 0.5 m^2). Consequently, we did not count any fauna outside the ~ 0.5 m^2. We calculated bioturbation activity by measuring the sizes of benthic organisms and traces using a perspective grid specifically created to analyze the oblique images using the PVC pipe, the GIMP program, and ImageJ software. ImageJ calculated the area covered by each object of interest, which we multiplied by the number of individual traces.

We followed Belley et al. (2010) in determining the number of images to analyze in our study. Specifically, by plotting species-traces accumulation curves and calculating the mean and variance of the accumulated species and traces, they concluded that analysis of 15 images sub-sampled randomly from 157 would be sufficient to allow them to evaluate species and trace distributions

without significantly affecting their conclusions. Accordingly, we analyzed 14 of 168 images per month.

We separated traces into surface and relief categories, which we then separated into sub-groups (Jones et al., 2007; Belley et al., 2010). The surface traces included organisms, organism imprints, ploughs, ridges, trails, and depressions, whereas the relief traces included small burrows (0.5-1 cm), medium burrows (1- 5 cm), and large burrows (> 5 cm) (Belley et al., 2010). We specifically measured surface, relief, and total trace (surface + relief traces) density and diversity. For each trace category, we measured density as the number of traces divided by the surface area of the analyzed field of view, and calculated trace diversity components as Shannon–Wiener diversity (H'), Simpson diversity, Pielou's evenness (J'), and species richness.

3.3.1.2 Estimating total reworked sediment area

We measured the bioturbated area as the total area covered by both surface and relief traces. To obtain an estimate of the total area of burrow openings, we averaged the area covered by small and medium burrows for each time period. To calculate the area covered by small burrows for periods with contrasting oxygen concentrations we multiplied the average small burrow area by the number of small burrows. We used the same approach for medium burrows. Similarly, we calculated the average area covered by surface traces during different bottom oxygen conditions as the seafloor area covered by benthic megafaunal imprints (including organisms present on the seafloor), trails, and ploughs.

In addition, we measured the time that small and medium burrows persisted by creating time-lapse videos from screenshots taken from every subsample video image using "Video editor".

3.3.2 Reworked sediment characterization using rotary sonar

3.3.2.1 Counting of pits

To count the number of pits, we analyzed daily averaged sonar images collected from May 20-30, and September 20-30, 2013, using Image J, eliminating the shadow from the frame supports, the sediment trap, and the camera frame, which appear in the same location in each image as yellow spots (high backscatter returns from the instrument itself). We also eliminated the acoustic shadow "behind" the instruments. We completed the following steps to enumerate the pits (**Fig. 3.3**): (1) image 'binarization', from color to grayscale (8-bit transform); (2) 'thresholding', generating a binary image from bi-chromatic grayscale image; (3) elimination of extra shadows such as the platform and sediment trap shadows; (4) analyze and count visual features selecting feature size (shadow zones) between 0.2 and infinity in m^2, without fitting any specific feature shape. The threshold and size limit steps were imposed to restrict the impact of noise (**Fig. 3.3 C**), acknowledging that this filtering may exclude some pits, while not eliminating all noise.

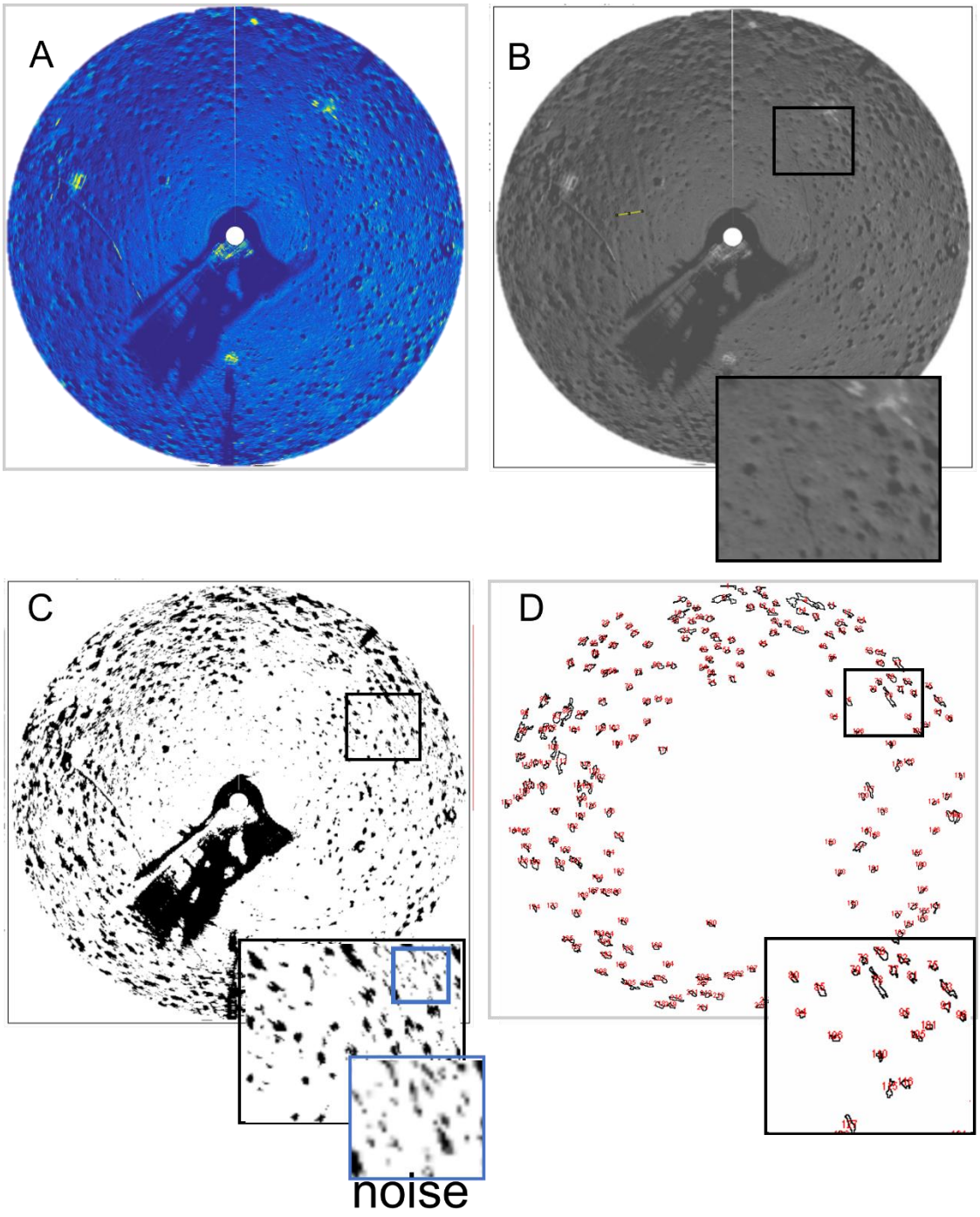

Fig. 3.3. Summary of steps performed by automated image analysis protocol: A) Original image; B) 8-bit grayscale image; C) Thresholding – zoomed-in blue box exemplifies area impacted by "noise" (particles < 0.2 at a set scale of 1 m^2); D) Count features based on chosen size and shape. Black boxes indicate a zoomed-in sub-section area.

3.3.2.2 Estimating total bioturbated area

We calculated the bioturbated area as the average area of pits measured by ImageJ using the algorithm described in 2.2.1 (**Fig. 3.3**), initially setting the scale according to known distances (3 m) between the two parallel tracks ("platform tracks") thought to have been created by fishing gear entangling and dragging the instrument platform in January 2011. These tracks were visible on the left side of each sonar image for both bottom-water oxygen concentration scenarios. This interpretation is consistent with a fishing trawl 'hit' event that took place in February of 2011. Based on archived rotary sonar images, these seafloor track marks only appeared after May 2011 (F. De Leo, pers. obs.). Thus, the long-term persistence and changes in the backscatter strength signals of these tracks provide an indicator of how the combined effects of bottom current hydrodynamics and bioturbation can mobilize sediments and refill irregular seafloor depression areas.

3.3.2.3 Measuring pit shape

To analyze the shape of the pits we focused on the circularity and diameter descriptors provided by ImageJ. Here, circularity refers to 4π*area/perimeter^2. A value of 1.0 indicates a perfect circle and a value approaching 0.0 indicates an increasingly elongated shape, noting that circularity values may be invalid for very small objects. Diameter refers to the longest distance between any two points along the selection boundary.

We looked at the bioturbation feature size descriptors over the 20-m radius sonar FOV images and in four selected subsections and compared the May, September, and December 10-d sampling periods. The reason we selected the sonar image FOV subsections was to identify whether bioturbation feature sizes changed uniformly across the entire area of the seafloor imaged by the sonar. These selected subsections contained a minimum area covered by instrument platforms,

instrument shadows, or sediment disturbances caused by platform tracks, thus avoiding underestimation of reworked sediment area measurements. For the four subsections, we set the threshold as described above (**Fig. 3.3**), and set the circularity range from 0.0 to 1 for subsections 1 and 4, and from 0.2 to 1 for subsections 2 and 3. The latter two showed different mean elevated backscatter (noise).

3.3.3 Estimating seafloor marks residence time

The presence of the two long and linear seafloor scar marks described above provided a proxy for both the persistence and transformation of bioturbation marks caused by benthic megafauna. The scars were clearly visible in the W sector of all analyzed rotary sonar images. In this specific case, we used the platform tracks as indicators of sediment refilling rates of megafaunal pits, which were challenging to detect through the sonar images that could not provide measures of bedform height/depth individually. In addition, deeper tracks accumulate more sediment along the track edge, narrowing the track width. The opposite effect occurs when sediment refills the platform track. Accordingly, we measured the width of each track by initially choosing six points at random along the track in the first images of May, subsequently reducing sampling to three points by the last images of December (**Supplementary Fig. 3.2**) because the visual distinctiveness of the points decreased over time. We selected points equidistant from one another (**Supplementary Fig. 3.2**).

3.3.4 Summary of features analyzed through video and sonar images, respectively

We summarize the two methodological approaches, highlighting which scales and factors we analyzed to address our main questions from video and sonar images, respectively (**Table 3.2**).

Table 3.2. Spatial scale, biological, and sedimentary variables analyzed through video and sonar images. “N.A.” indicates a specific variable not analyzed from the specific instrument.

	Video Images	Sonar Images
Spatial scale	~ 0.5 m^2	~1268 m^2
Biological variable	Megafaunal diversity and density	N.A.
Sedimentary variable	*"Lebensspuren"* or bioturbation traces (superficial and relief)	Pits
	Traces diversity and abundance	Number, circularity, and diameter
	Averaged reworked sediment area (from sediment traces)	Averaged reworked sediment area (from pits)
	N.A.	Platform traces refilling as indices of either hydrodynamic or biological or both activities

3.3.5 Statistical analysis

3.3.5.1 Video data analysis

We calculated univariate indices including Shannon - Wiener diversity index (H'), Simpson's index, Pielou's evenness index (J'), species richness (S), and density for benthic megafaunal communities for both bottom-water oxygen concentration scenarios, as well as sediment trace density (%), and diversity.

We used a stepwise general linear model (GLM) to determine which environmental factors (oxygen saturation (O_2), temperature (T), and salinity (S)) potentially exerted influence over the univariate diversity indices listed above. GLM is a class of regression models that supports non-normal distributions (Nelder and Wedderburn, 1972) and can be implemented through the R glm()

function. Thus, we treated Shannon diversity (H'), Simpson diversity, Pielou's evenness (J'), and species richness (S) for the megabenthic community, and total-traces density (%), surface-trace density (%), relief-trace density (%), total-trace diversity, surface-trace diversity, relief-trace diversity, or trace richness (T) as dependent variables. We used the "vif" function from the "car" package (Fox and Weisberg, 2011) to check for multicollinearity between the explanatory variables, and verified homogeneity and normality of residuals with Shapiro -Wilk and Levene tests, respectively. When data did not meet the assumptions, we performed either $\log_{10}$ or sqrt data transformations. If assumptions were still not met, we ran a non-parametric Kruskal-Wallis test.

To investigate variation in multivariate taxonomic community composition among oxygen levels (two levels: hypoxia 1, hypoxia 2) we ran a multivariate analysis of variance (PERMANOVA) performed with 999 random permutations of appropriate units (McArdle and Anderson, 2001). We calculated the resemblance matrices from Bray-Curtis distances of transformed benthic community data, verifying homogeneity of multivariate dispersion using the PERMDISP routine (Anderson et al., 2008).

3.3.5.2 Sonar data analysis

For the sonar analysis, we also ran stepwise GLM for each of the following dependent variables: number of pits, total bioturbated area, circularity, and diameter of pits. We used oxygen concentration (O_2) and temperature, and salinity as environmental predictor variables. Using the same techniques described above, we verified homogeneity and normality of residuals, and once again transformed data in cases that did not meet assumptions. If transformed data still did not meet assumptions, we performed a non-parametric Kruskal-Wallis test, and a post-hoc pairwiseWilcoxon test. When we observed significant differences in dependent variables among the three study periods, we performed post-hoc pairwise Tukey tests.

In order to evaluate hydrodynamic effects on the sediment surface, we ran a linear regression between the width of platform tracks and the time periods of this study. We verified homogeneity of residuals and normality with a Shapiro–Wilk test and a Levene test, respectively. When the data assumptions were not met, we applied a $\log_{10}$ transformation.

All statistical analyses were performed using the package "vegan" (Oksanen et al., 2013) in R software (R Core Team, 2016).

3.4 Results

The rarefaction curves of both the numbers of observed taxa and total traces showed that the number of videos analyzed in our study generally captured most of the taxa and traces present in the study area (**Fig. 3.4**). In contrast, the total trace curve in September did not plateau, indicating incomplete taxonomic sampling (**Fig. 3.4 B**).

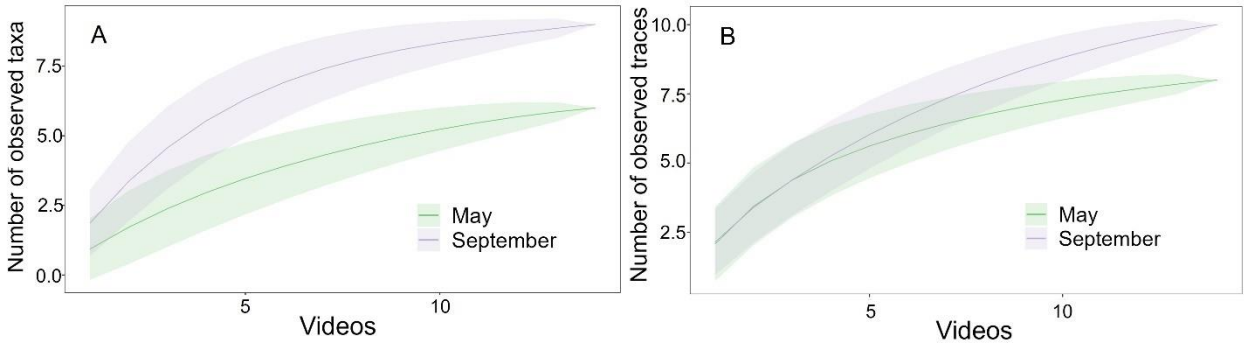

Fig. 3.4. Rarefaction curves for megafaunal communities (A) and sediment traces (B) in surface sediments per video collected each month (May and September).

3.4.1 Megafaunal community structure from the video camera

The GLM analysis showed multicollinearity between oxygen, temperature, and salinity in relation to megafaunal density and diversity; we therefore decided to use oxygen as the explanatory variable for further analysis in order to focus on the main research question for this study.

We observed 17 counts spanning eight different taxa in May, and 44 counts spanning nine different taxa in September, with significant differences (t-test, $p = 0.0001$) in population density between the two bottom-water oxygen conditions. The highest average value (6.3 count $m^{-2} \pm 4.1$ (SD)) occurred in relatively high oxygen concentrations, in contrast to 2.4 count $m^2 \pm 2.4$ (SD) in May under lower oxygen (**Fig. 3.5**).

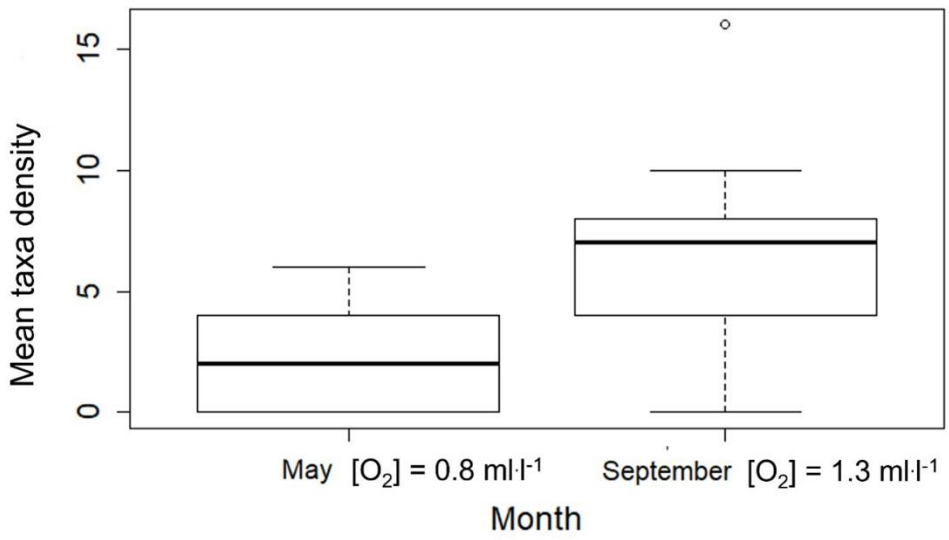

Fig. 3.5. Average megafaunal density (count m^{-2}) measured in May (n =17) and September (n = 44).

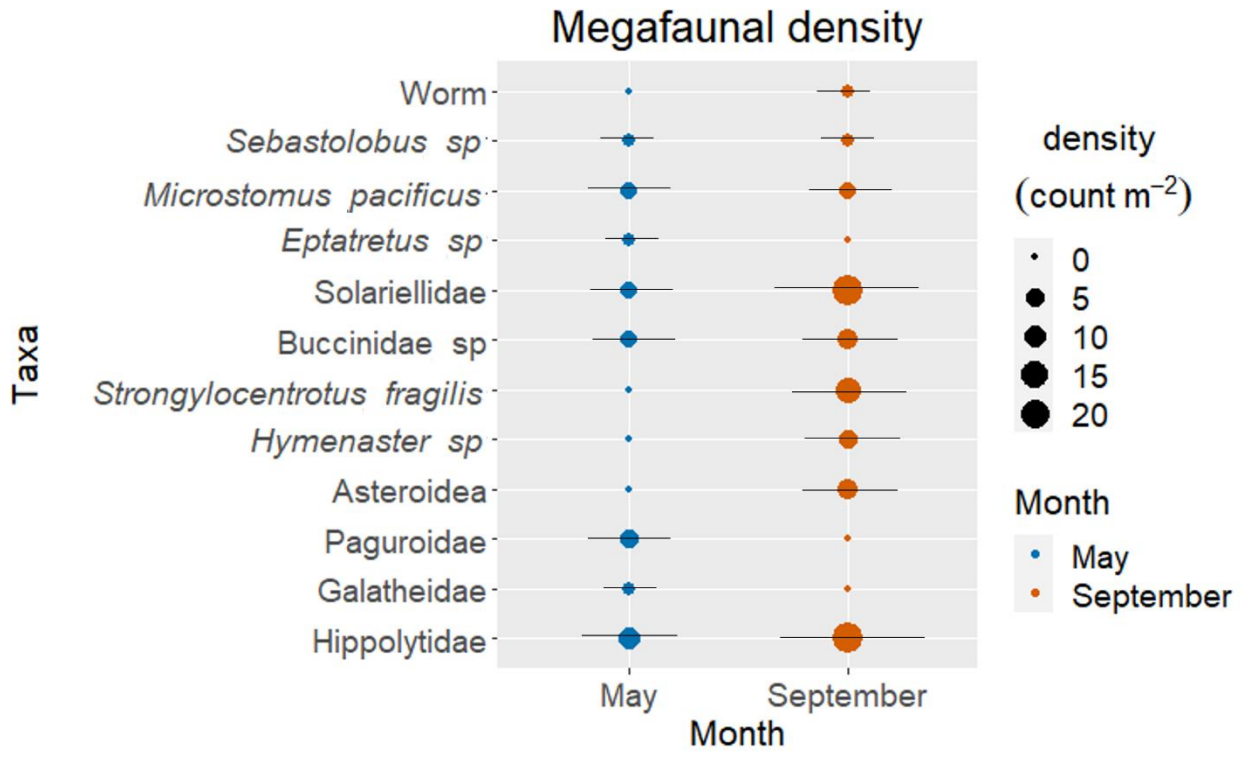

Fig. 3.6. Averaged density of the observed megafaunal groups in May and September, respectively, grouped by phylum. Error bars represent standard deviation.

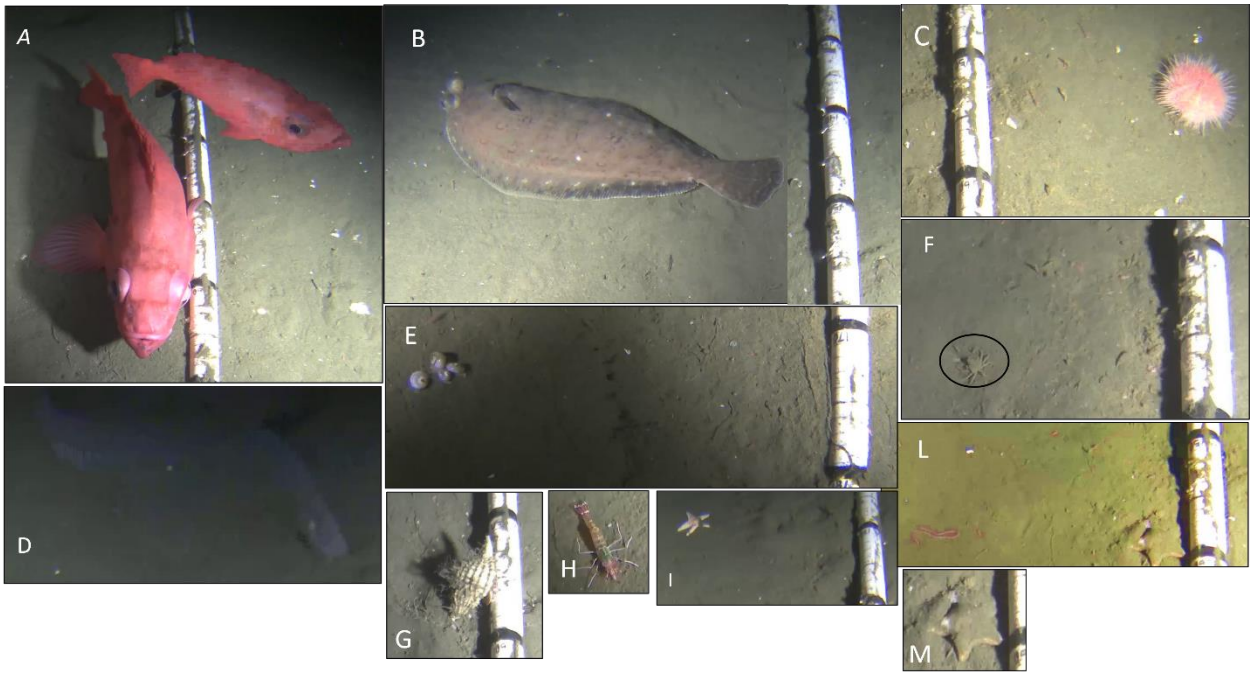

Fig. 3.7. Photographic examples of the most common taxa in Barkley Canyon Upper Slope observed in May 18-31, and September (20-30), October (1-5) 2023. A) *Sebastes* sp, B) *Microstomus pacificus*, C) *Strongylocentrotus fragilis*., D) *Eptatretus* sp.., E) Solariellidae sp., F) Galatheidae sp., G) Buccinidae sp., H) Hippolytidae sp., I) Asteroidea sp., L) unidentified worm, M) *Hymenaster* sp.

Decapod shrimp (Hippolytidae) were the most abundant taxon in both oxygen conditions, in addition to a gastropod, likely belonging to the family Solariellidae, and the pink sea urchin *Strongylocentrotus fragilis* in September. Interestingly, we did not observe *S. fragilis* in May, nor the two sea star taxa, Asteroidea sp., and *Hymenaster* sp. In contrast, we did not observe Paguroidea, Galatheidae crab, and *Eptatretus* sp. in September. (**Fig. 3.6, 3.7**). Moreover, we observed no significant difference in diversity indices between May and September, with diversity indices slightly greater in September than May, except for Simpson's indices (**Table 3.3**).

Table 3.3. Average diversity indices (Shannon-Wiener; Simpson; Species richness; Pielou's evenness) during each sampling month, with Kruskal-Wallis test and GLM results for each diversity index.

Month	Shannon-Wiener	Simpson	Species richness	Pielou's evenness
May $[O_2] = 0.8$ ml l^{-1}	0.35 ± 0.12	0.66 ± 0.10	1.14 ± 0.31	0.49 ± 0.14
September $[O_2] = 1.3$ ml l^{-1}	0.35 ± 0.13	0.49 ± 0.09	1.86 ± 0.33	0.77 ± 0.10
Kruskal-Wallis test	0.35	/	/	0.30
GLM (p values)	/	0.17	0.12	/

PERMANOVA did not reveal significant differences between community assemblages for the two bottom-water oxygen concentrations ($F = 1.03$ $p = 0.27$).

3.4.2 Reworked sediment trace patterns from the video camera

Regarding trace density and diversity analyses, GLM analysis with oxygen, temperature, and salinity as explanatory variables and sediment traces density and diversity as response variables showed multicollinearity between the three explanatory variables. Once again we used oxygen as the primary explanatory variable for further analyses, recognizing the difficulty in disentangling our correlated explanatory variables.

We observed a similar number of total sediment traces for the two oxygen levels, with 74 in May and 75 in September; we also observed that oxygen explained Pielou's evenness only for the total traces during the two time periods we analyzed, but not others given non-significant results (**Table 3.4**). Representative images of sediment traces in Barkley Canyon Upper Slope are shown in **Fig. 3.8**.

Table 3.4. Results of GLM and Kruskal-Wallis tests showing F-values and p values for each different analyzed variable. The columns show variables included in the analysis (*Variable (J' = Pielou's evenness))*; type of test run (GLM) (*Test*); and p-value (*P-value*).

Variable	*Test*	*F-value*	*P-value*
Total trace density	*GLM*	0.03	0.95
Surface trace density	*GLM*	3.13	0.08
Relief trace density (log_{10})	*GLM*	1.10	0.31
Total trace diversity	*GLM*	0.30	0.60
Surface trace diversity	*GLM*	1.85	0.18
Relief trace diversity*	/		/
J' total traces	***Kruskal-wallis***		**0.02**

*Limited number of observations precluded statistical analysis

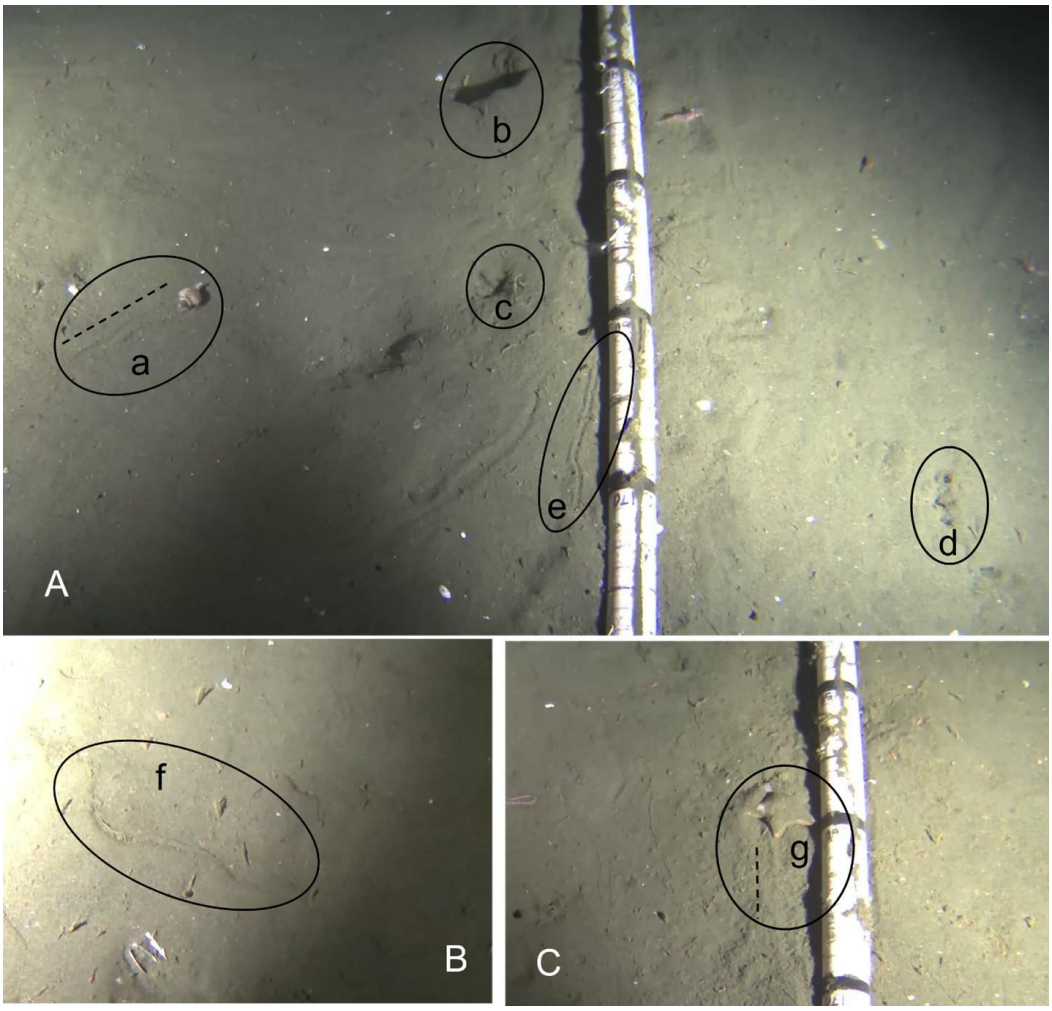

Fig. 3.8. Representative photographs of bioturbated surface and relief traces in Barkley Canyon Upper Slope from May and September 2013. A) a) Paguroidea trail, b) large burrow, c) medium burrow, d) small burrow, e) simple plough. B) f) single plough. C) g) *Hymenaster* sp. trail.

Although relief (n = 74) and surface traces (n = 76) contributed similarly to total traces in May, we observed more surface traces (n = 118) than relief traces (n = 30) in September, with organism imprints playing a major role in total traces (n = 44), followed by depressions (n = 3). Among surface traces, we observed *Eptatretus* sp., Galatheidae sp., and Paguroidea sp. imprints only in May. In contrast, we observed traces from *S. fragilis, Hymenaster* sp. and an unidentified

worm only in September. We also observed depressions and burrowing sea stars of both Asteroidea sp. and *Hymenaster* sp. only in September. Regarding relief trace diversity, we observed small and medium burrows at both oxygen levels. However, we observed a higher density of small and medium burrows in May (average 2.3 and 3.1 count m^{-2}) compared to September (1.4 and 0.6 count m^{-2}), when we also observed few large burrows (0.14 count m^{-2}).

The small burrows lasted for a maximum of 1 d under both oxygen conditions. In contrast, the medium burrows persisted for 3-7 d.

In addition, the average total bioturbated area between the two time periods did not differ significantly ($p = 0.8$), varying from ~ 0.6 m^2 in September to 0.2 m^2 in May. We observed similar values for relief traces of 0.00096 m^2 and 0.00089 m^2, for May and September, respectively. In addition, surface traces in September covered an area of 1.19 m^2, versus 0.42 m^2 in May.

3.4.3 Sediment trace patterns from rotary sonar

Our two GLMs showed that the total reworked sediment area differed significantly between the two periods of contrasting bottom-water oxygen concentrations ($p = 0.01$), as did the number of pits ($p < 0.001$), with the highest reworked sediment area and highest number of pits occurring in September (**Fig. 3.9**). On average, we counted 298.6 pits and a reworked sediment area of 138.8 m^2 in September, in contrast to 199.9 pits and 99.4 m^2 of the reworked sediment area in low oxygen conditions during May (**Fig. 3.9**). In addition, pit diameter averaged 55 cm during both time periods.

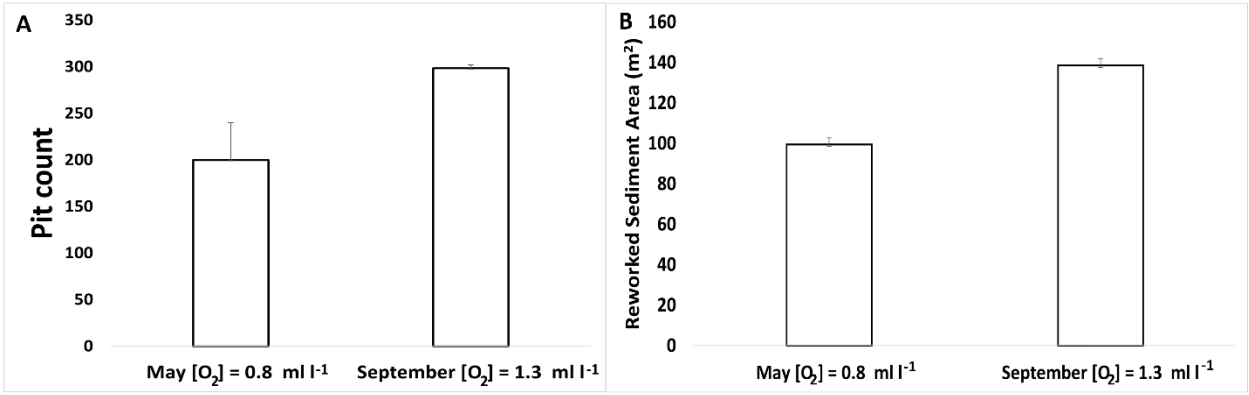

Fig. 3.9. Average number of pits A) and reworked sediment area B) in May and September (based on 11 images per month). Error bars indicate standard deviation.

We also observed changes in pit shapes concurrently between the two periods of contrasting bottom-water oxygen concentrations when focusing on the entire sonar FOV (**Table 3.5**). On average, the circularity descriptor was directly proportional to oxygen levels, specifically, 0.21 in May, 0.24 in September, and 0.25 in December (**Fig. 3.10**). However, the size of the pits did not always change significantly when we focused on a specific subsection of the FOV (**Fig. 3.10**; **Table 3.5**), such as in section 2. In sections 1, 3, and 4, circularity increased from ~ 0.24 to ~ 0.35, from May to December (**Fig. 3.10**). Diameter did not differ significantly (Kruskal-Wallis test $p = 0.35$) between different oxygen concentrations (**Table 3.5**).

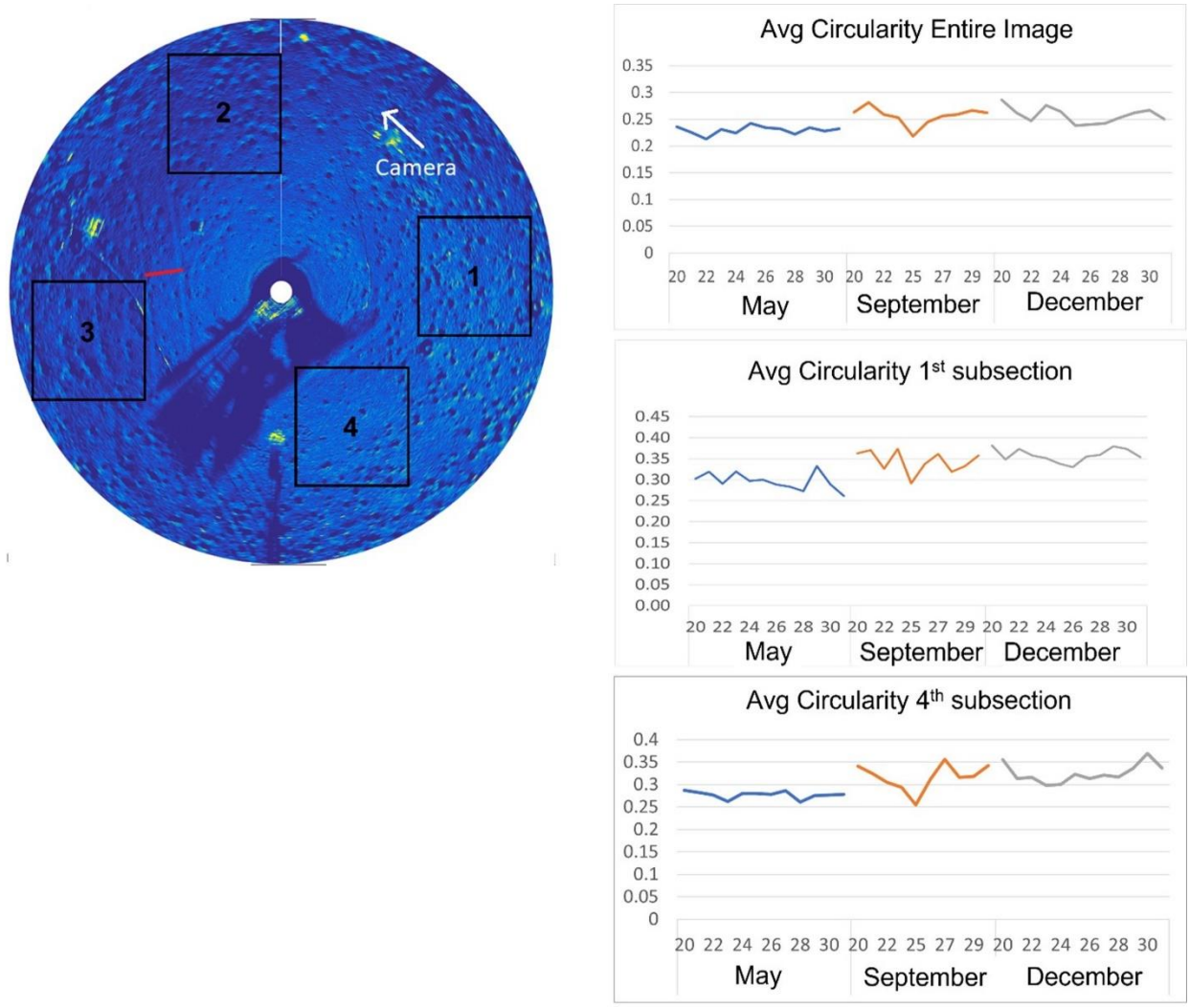

Fig. 3.10. Left: sonar image overlaid with subsections used in analyses. Right: change in pit circularity for the entire FOV, and for the first and fourth subsections. The x-axis of each "Avg Circularity" plot indicates the range of time used for our analysis from 20 to 30 d in May, September, and December, respectively. Different color lines in each "Avg Circularity" plot refer to: Blue = May; Orange = September; Gray = December.

Table 3.5. Generalized linear model (GLM), Kruskal-Wallis test (K-W), and Post-hoc tests (pairwise Wilcoxon test (P-W); Tukey HSD test (THSD)) performed on two pit size descriptors related to the entire FOV, and the fourth selected FOV subsections. *Log_{10} = logarithmic transformation data. Bolded terms indicate significant differences.

		GLM / Kruskal-Wallis test		**Post-hoc test**		
	Size descriptors	*Df*	P-value			
Entire FOV (1268.3 m²)	Circularity	2	**6.6e-15** *(K-W)*	*(P-W)*	December	May
				May	**5.5e-12**	-
				September	0.6	**4.2e-12**
	Diameter	2	0.35 *(K-W)*	NA		
1st section (~35 m²)	Circularity	2	**1.4e-08** *(K-W)*	*(P-W)*	December	May
				May	**5.5e-08**	-
				September	0.6	**9.6e-06**
	Diameter	2	0.13 *(K-W)*	NA		
2nd section (~35 m²?)	Circularity	2	0.62 *(K-W)*	NA		
	Diameter	2	0.28 *(K-W)*	NA		
3rd section (~35 m²)	Circularity (log_{10})*	2	**6.5e-08** *(glm)*	*(THSD)*	December	May
				May	**0.02**	-
				September	**0.002**	0.9
	Diameter	2	0.53 *(K-W)*	NA		
4th section (~35 m²	Circularity	2	**1.4e-07** *(K-W)*	*(P-W)*	December	May
				May	**1.9e-06**	-
				September	0.7	**3.5e-06**
	Diameter	2	0.38 *(K-W)*	NA		

Moreover, examination of sections 1 and 4 showed that the small circularity category (from 0.26 to 0.37) of pits was responsible for the significant differences among oxygen levels (see **Fig. 3.11 A, B, C**).

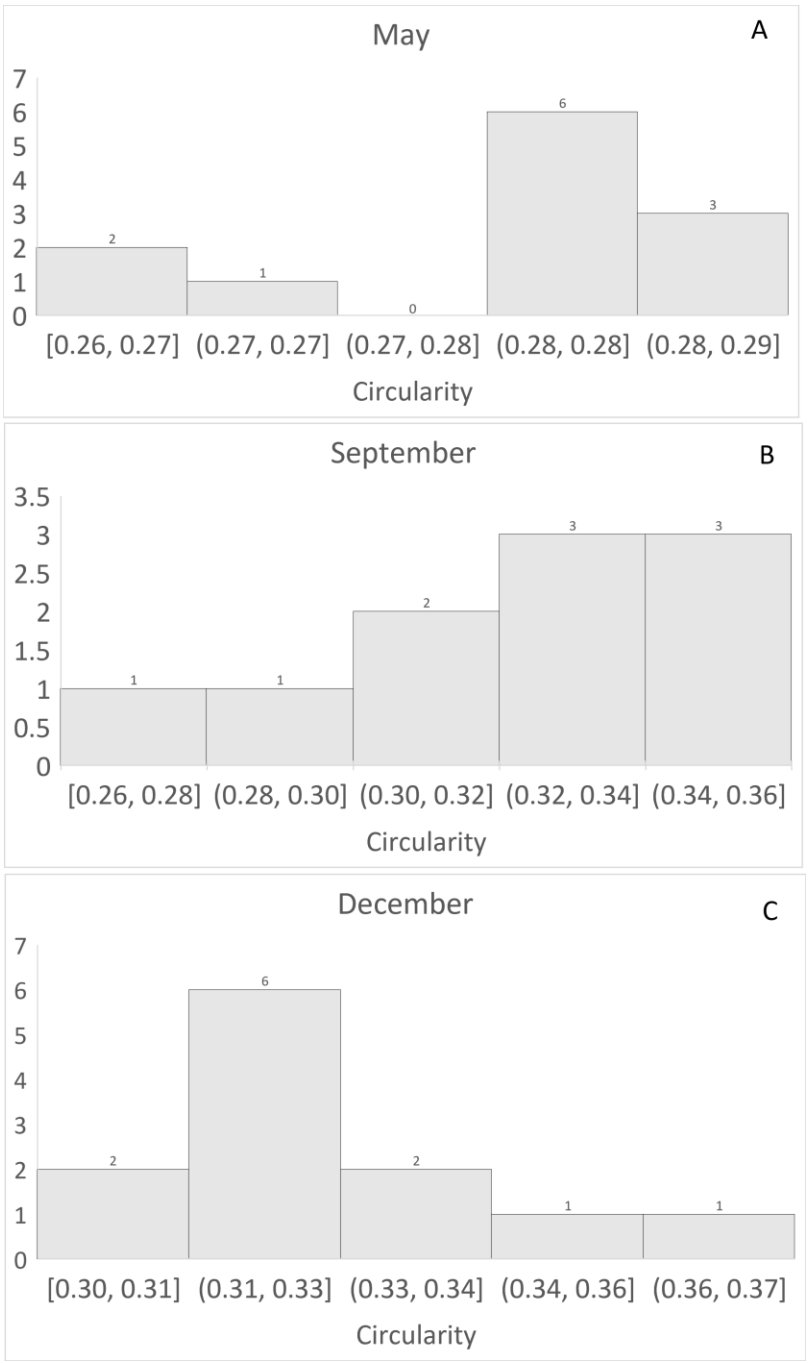

Fig. 3.11. Histogram showing the distribution of the circularity descriptor (x-axis) among the three different oxygen concentrations/months (A, B, C).

In addition, width size of sediment tracks on the sediment measured in May and September decreased significantly over time (**Supplementary table 3.2**).

3.5 Discussion

By combining two different imaging techniques, video with a small-scale field of view (~ 0.5 m^2) versus sonar with a much larger scale FOV (~1268 m^2), we were able to draw a complementary and more detailed interpretation of how oxygen concentrations differed between the two time periods of observation, May and September 2013, affect sediment reworking activity. Different environmental conditions may refer to different oxygen concentrations near the seafloor, which were difficult to disentangle from other biotic and abiotic variables. Whereas the bioturbation features captured by video imagery allowed us to evaluate the role of individual benthic taxa in producing bioturbation features, the sonar imagery allowed us to assess indirectly the overall levels of biological activity at Barkley Canyon Upper Slope. From the sonar imagery, we observed significantly larger areas affected by reworked sediment during the period of higher bottom-water oxygen concentrations. In contrast, at the small spatial scale monitored using the video camera, we detected no significant differences in reworked sediment between periods of contrasting oxygen concentrations.

The sonar images proved to be the only efficient method for quantifying large bioturbation traces (pits). The pits ranged 40 – 70 cm in diameter, with smaller pits increasing in number and size over time, indicating increased faunal activity and likely sediment mixing. In parallel, video analysis enabled the identification of similarities and dissimilarities in species composition, including dominant species, between the two periods of contrasting bottom-water oxygen concentrations. *Sebastes* sp., Pacific dover sole *Microstomus pacificus*, Buccinidae sp. gastropods, Solariellidae sp., and Hippolytid shrimps were all present during both sampling periods, but with significantly higher densities in September under higher bottom-water oxygen concentrations. Consequently, we could identify those species (e.g., shrimp, gastropods, flatfishes, etc.) in addition

to Asteroidea sp. *Hymenaster* sp. sea stars, and *S. fragilis* sea urchins responsible for producing the smaller bio-traces. We could also evaluate the average persistence time for each trace, and estimate small-scale reworked sediment area.

3.5.1 Benthic megafaunal composition

Acknowledging the major role of dissolved oxygen concentration in shaping megafaunal community structure, most marine benthic communities also depend heavily on organic matter supplied from the water column above (Smith et al., 2008). In our study, although megabenthic assemblages did not differ significantly in composition between May and September, periods of contrasting bottom-water oxygen concentrations, faunal densities were nonetheless three times higher in September, when dissolved oxygen concentration increased by 62%. However, we acknowledge the challenges of disentangling the influence of oxygen concentrations on benthic community structure relative to other environmental variables such as temperature, salinity and OM. Previous studies have established a direct relationship between low oxygen concentrations (hypoxic conditions) and reduced benthic macro- and megafaunal abundance and diversity in oxygen minimum zones (OMZs) (Levin et al., 1991; Levin et al., 2004; Ingole et al., 2010; De Leo et al., 2017). Moreover, Murty et al. (2009) attributed the absence of megafauna in the OMZ core (~400 m depth, $[O_2] = 0.1$ ml l^{-1}) of the Pakistan margin to a critical oxygen threshold ranging 0.15 - 0.3 ml l^{-1} that influenced the presence/absence of megafauna. However, oxygen thresholds vary among species according to their physiology (Pihl et al., 1991; Vaquer-Sunyer et al., 2008; Matabos et al., 2014). In addition, species migration could contribute to presences/absence of some species. Some organisms can migrate to avoid very low O_2 concentrations, or to avoid strong currents that may be challenging to relatively small-sized organisms such as shrimp (Matabos et al., 2014). Our study confirmed observations of higher megafaunal diversity under higher bottom-

water oxygen concentrations, but under these same conditions, megafaunal diversity and evenness were not statistically different compared to the low oxygen sampling period (May). Although we observed taxa in common between May and September (e.g., Solariellidae and Buccinidae gastropods, and Hippolytidae shrimps), we also observed unshared taxa such as Paguroidea, Galatheidae crabs, and *Eptatretus* sp. that typified May, whereas *S. fragilis* sea urchins, and the two *Hymenaster* sp., and Asteroidea sea star taxa typified September only. Once again, we were unable to establish a direct relationship between oxygen and megafaunal diversity. We infer that restricted FOV limited our observations of different species. Murty et al. (2009) observed a bimodal trend in megafaunal diversity along an oxygen and depth gradient and also could not specifically link patterns to oxygen concentrations. Belley et al. (2010) observed no significant difference in macrobenthic species richness between the hypoxic and normoxic stations (>300 m deep) in the St. Lawrence Estuary and the Gulf of St. Lawrence, Canada, respectively. They also reported increased numbers of small surface deposit feeders and increased abundance of polychaetes tolerant of low oxygen concentrations compared to macrofaunal communities in the 1980s. This pattern was reflected in decreasing species richness, Shannon diversity, and abundance of molluscs, crustaceans, and mobile omnivorous species in the hypoxic region in response to oxygen depletion. However, we infer that some of our taxa were more physiologically adapted to low dissolved oxygen concentration than others. Indeed, previous studies have established that physiological adaptations of species (Vetter et al., 1994) align with a range of environmental variables (Hunter et al., 1990; Rex and Etter, 1998). Presence/absence and quality of food (Campanyà-Llovet and Snelgrove, 2018) can control species diversity patterns, a key aspect of benthic community structure. Previously, Chauvet et al. (2018) reported abundant, though not dominant, hippolytid shrimp under both bottom-water oxygen conditions in the canyon axis,

indicative of a typical shrimp with some degree of adaptation to low oxygen concentration. A small-sized hippolytid shrimp size was also reported by Hendrickx and Hastings (2007) in a low-oxygen region of the Gulf of Maine, supporting the idea that hippolytid shrimp tolerate moderate (0.28-0.6 ml $\cdot$ l^{-1}) hypoxia. Moreover, Ruhl and Smith (2004) reported an increase in abundance of some holothurian species at Station M, 4000 m deep in the Northeast Pacific continental margin, with reduced organic matter supply, but a positive relationship with POC flux in other species. Dissolved oxygen concentrations in our two sampling periods differed by 0.5 ml l^{-1}, and the fauna observed in the video never experienced severe hypoxia, i.e., $[O_2] < 0.5$ ml l^{-1}, (Levin et al., 2001). This relatively small dissolved oxygen gradient, aligned with the low number of observations, may explain why we observed little difference between benthic assemblages in May and in September.

We observed numerous Buccinidae and Solariellidae gastropods, and although the Buccinidae were mostly responsible for surface traces, the Solariellidae were responsible for the numerous small burrows (based on video observation) that dominated the period with lower bottom-water oxygen; Solariellids can burrow rapidly into sediment (Williams et al., 2022). Gastropods such as Buccinidae, Solariellidae, and Cymatiidae can tolerate low oxygen concentrations (Theede, 1973) and commonly occur in hypoxic zones, as reported in Barkley Canyon (Chauvet et al., 2018; Command et al., 2023), for species such as *Fusitriton oregonensis* Cymatiidae (, De Leo et al., 2017; Domke et al., 2017), and along the Chilean coast (*Jerrybuccinum kantori* Buccinidae, Fraussen et al., 2014).

In contrast to previous work at the same location in years before and after our study (Robert and Juniper, 2012; De Leo et al., 2017; Command et al., 2023) we did not observe strong dominance by the sea urchin *S. fragilis* and rockfish *Sebastes* spp., which may also contribute to bioturbation activity through sediment resuspension. We observed only modest numbers (14 count

m^{-2}, noting limited number of observations) of *S. fragilis* during the highest bottom-water oxygen period (1.3 ml l^{-1}), but not with lower oxygen concentration in May. Our results align with De Leo et al. (2017), who reported *S. fragilis* densities up to 2 orders of magnitude higher outside the OMZ (DO ~ 1.4 ml l^{-1}) than inside the OMZ (DO < 0.5 ml l^{-1}) between 500 and 600 m at the edge of the OMZ near Vancouver Island. We cannot offer a definitive explanation for the decrease in this species relative to previous studies, but trawling impacts on the British Columbia upper continental slope in 2011 might have altered environmental and particularly biological conditions, changing benthic community composition (Puig et al., 2012; De Leo et al., 2017). Although *S. fragilis* can tolerate low oxygen, it nonetheless prefers well-oxygenated environments (Command et al., 2023). The low number of sea urchins in our study could also relate to the longer observation time (1 hr; 30 min; and 5 min every second hour) adapted by Robert and Juniper (2012) who used 99 sea urchins to back calculate the area of reworked sediment. Command et al. (2023) also analyzed more video sequences (~ 480 between September and December 2013) compared to the 246 one-minute video sequences we adapted. Moreover, although sea urchins were not the dominant taxon in our study, they likely influenced nutrient cycling at our study site through their locomotion and bioturbation activity in large aggregates (Campanyà-Llovet et al., 2018). For example, sea urchins can remix surface sediments at a rate between 15.1 and 21.0 $m^2\ y^{-1}$ (Robert and Juniper, 2012), thereby moving nutrients and oxygen in and out of the sediment.

Microstomus pacificus, a flatfish species known to tolerate different levels of hypoxia, depresses its metabolism to limit energy consumption in an environment with low food availability (Vetter et al., 1994). Flatfish, including *M. pacificus*, create depressions as they move around sediments to avoid predators and seek prey (Robert and Juniper, 2012). The ~ 55 cm diameter pit detected in our sonar images aligns with observations from A. Hay (pers. comm.) and might

represent a depression created by flatfish; however, unlike Yahel et al. (2008) and Robert and Juniper (2012), we did not observe burrowing flatfish in our visual analysis.

3.5.2 Reworked sediment traces at small scales (video camera)

Our study showed strong multicollinearity between bottom-water dissolved oxygen, temperature, and salinity as potential drivers of sediment traces in Barkley Canyon sediments. However, bottom-water oxygen saturation did not directly explain sediment trace variability in our video (smaller spatial scale) analysis. Our results mainly support the idea that the environment under OMZ (we were unable to definitively disentangle O_2, T, and S) directly affects faunal community structure (i.e., species composition and relative abundances) and indirectly shapes sediment mixing as well as oxygen and nutrient exchange with the sediment. We also suggest that, given higher relief traces created by mixing deeper sediment layers and bio-irrigation (Belly et al., 2010) in May than in September, the two observation periods differed, although not significantly, in mixing within deep sediment layers rather than on the sediment surface. However, the inherent difficulty in reconciling deep sediment mixing solely relying on video observations and relief traces points to a need for further study. Furthermore, the higher density of relief traces with low bottom-water oxygen conditions, as opposed to higher oxygen conditions, contrasts Belley et al. (2010), who reported higher density of surface-traces in the hypoxic region (>300 m deep) of the Lower St. Lawrence Estuary. They attributed this pattern to increased activity by the surface deposit feeder *Ophiura* sp. perhaps reflecting stress behavior in response to hypoxia. In our study, small burrows made by solariellid gastropods dominated relief traces; this species can likely tolerate reduced oxygen concentrations.

Unfortunately, our inability to identify typical Solariellidae burrowing behavior limits our capacity to infer its bioturbation potential. Nevertheless, based on shallow-water studies (Morton,

1990; Cheung et al., 2008), we infer that these gastropods spend most of their time burrowed beneath the sediment surface, emerging only when they detect food at the surface. Thus, we infer by association their active role in continuous sediment mixing at our Barkley Upper Slope site, with potential effects on dissolved oxygen penetration into sediments. Moreover, previous studies have suggested gastropods are especially capable and adapted to reworking coarse-grained sediments (Gibson et al., 2006), which characterizes Barkley Upper Slope (Campanyà-Lovet et al., 2018). Compared to mud, less cohesive sand sediment break apart more easily and offer less resistance to burrowing organisms (Gibson et al., 2006). The high degree of cohesiveness of fine muddy sediments can form a wall-like structure that requires organisms to expend more energy to move, therefore expending less on protecting themself, feeding, or reproducing (Gibson et al., 2006). The overlying sediment exerts an important but non-uniform force on an animal, whether stationary or mobile, facilitating burrowing, as with the solariellid gastropods in our study; Kanazawa (1992) showed that the dome shape of sea urchins living in sand can sustain the downward weight of the sand above them. Therefore, ease of burrowing by gastropods might also explain the rapid turnover (1-3 d) in small burrows compared to large burrows (~ 7 d) in our study. Although we were unable to measure the depth of small burrows, our results support the idea that sand facilitates gastropod movement as they move within and mix the upper few centimeters of sediment (Dashtgard et al., 2012).

We observed a similar proportion of reworked sediment areas between the two time periods of contrasting bottom-water oxygen, a finding that contrasts previous reports of reduced bioturbation with decreasing oxygen concentration (Diaz and Rosenberg, 1995, 2008; Levin et al., 2009; Middelburg and Levin, 2009). Several factors might explain the similar proportions in our study, including the low number of observations. Alternatively, the larger number of small and

medium burrows in May might cover a sediment area similar to the larger surface imprints observed in September. Gastropods can quickly burrow, and re-work varied features on the sediment to produce the small and medium burrows that dominated the total reworked sediment area in May. Moreover, we also infer that our video image methodology to evaluate average total reworked sediment area may have influenced our results. The video camera imaged the same field of view as different organisms reworked the same patch of sediment, likely re-working it more than once over the observation period. For example, we observed that a sea star and *S. fragilis* moved through the same patch of sediment repeatedly, however, our analysis counted that area as re-worked only once. Consequently, we potentially over- or under-estimated the bioturbated seafloor area in both study periods. Moreover, larger organisms appeared to be responsible for most surface traces in our study and contributed substantively to local community assemblages, as reported in previous studies (Robert and Juniper, 2012; Belley et al., 2017). Robert and Juniper (2012) indicated sediment reworking rates between 26.0 and 35.1 $cm^2\ y^{-1}$ by Dover sole, *M. pacificus*, Pacific halibut, *H. stenolepis,* and the fragile pink sea urchin *S. fragilis.*

In short, our small-spatial scale video analysis enabled coarser investigations of biological aspects of Barkley Canyon Upper Slope under low bottom-water oxygen conditions compared to previous studies that used a larger number of videos. Nonetheless, our analysis provided sufficient information regarding presence/absence of organisms to enable comparisons with concurrent sonar images. Despite the small area of sediment imaged by the video camera, we also demonstrated important contributions of small burrows to sediment mixing in low bottom-water oxygen conditions. Our results indirectly point to the importance of particle reworking in permeable sand, which acts as a biofilter by enhancing particulate organic matter filtration into the sediment and accelerating OM remineralization and nutrient recycling (see also D'Andrea et al., 2004).

3.5.3 Reworked sediment traces at large scales (sonar)

Previous studies attribute biological pit formation to flatfish as they avoid predators or seek prey (Auster et al., 1995). Although sonar images did not enable species identifications, we infer that the observed increase in the number of pits with increasing bottom-water oxygen concentrations might reflect increasing megafaunal density and differences in assemblage composition during the contrasting periods of bottom-water oxygen conditions, as suggested by video analysis. Indeed, although we rarely observed Dover sole, *M. pacificus*, Pacific halibut *H. stenolepis,* and rays such *as Raja rina*, and *Bathyraja* spp., Robert and Juniper (2012) observed them frequently, specifically noting halibut burrowing. Moreover, previous studies documented these two rays leaving oval imprints 6 to 10 cm deep in the sediment (Howard et al., 1977; Gregory et al., 1979; Thrush et al., 1991; Martinell et al., 2001). Sonar imaging provided valuable information about the extent of seafloor bioturbated area which increased in September when the averaged bottom-water oxygen concentrations and temperature values increased. However, we again note a need for caution in relating increasingly reworked sediment to a single environmental factor in our study given the challenges in disentangling O_2, temperature, and salinity and the strong influence that OM might have on bioturbators and organisms.

The species that create burrows also perform a function that benefits other species in that other bioturbators can utilize the burrows, including species that lack the behavioral plasticity or morphological attributes to make their own (Auster et al., 1995; Smith et al., 2000; Levin, 2003; Robert and Juniper, 2012; Thurber et al., 2014). Therefore, burrows play an important ecological function and enhance particle deposition in addition to oxygenating sediments (Yager et al., 1993). Moreover, currents of ~25 cm s^{-1} can affect burrow shape and/or size and consequently promote sediment re-working and organic matter remineralization. Kenyon et al. (2002) showed that

bottom currents of 25 cm s^{-1} can move fine-grained sand on the seafloor, the grain size reported by Campanyà-Llovet et al. (2018) for our study area. Indeed, we observed significant increasing circularity over time and across the entire FOV, noting a current of 0-25 cm s^{-1} measured from the Aquadopp profiler. The infilling track information provides evidence of hydrodynamic and bioturbation events that refill the tracks because those activities could also refill pits and influence circularity and shape changes. Moreover, although the data available for this study does not elucidate which factor(s) contributed most to refilling both tracks and pits, we infer that a hydrodynamic event contributed to refilling. Through visual examination, we observed changes in track width along the entire track rather than specifically at a site as might occur with bioturbation activity. Noting a dearth of previous studies on pit size and shape, we infer that reduced re-working occurs in low bottom-water oxygen conditions that limit most taxa.

In summary, our sonar imagery analysis documented sediment reworking activity over a relatively large scale that varied temporally and spatially, and under different oxygen concentrations that resulted in significant differences in bioturbated seabed features. In contrast, video analyses showed no significant effect of different oxygen concentrations on reworked seabed features, likely indicating that different spatial scales influence the evaluation of bioturbation activity. Moreover, our sonar analysis documented the importance of hydrodynamic and biological activity in remixing sediment. The limited FOV of the camera precluded this sort of analysis.

3.6 Conclusions

Our study provides the first analysis of deep-sea benthic bioturbation activity in the NE Pacific that combines video and sonar images. Using sonar images in particular, we showed that environmental conditions, such as different oxygen concentrations near the seabed, affect sediment reworking. Except for relief burrows, higher reworked sediment, generally coincided with higher

bottom-water oxygen concentrations, though not significant, this trend corroborates past OMZ studies that link faunal abundance, diversity, and activity to an oxygen gradient. Moreover, our study illustrates the complementarity of video and sonar imaging systems, noting that the absence of one would not have allowed us to study the full range of sediment features that the second instrument could not document. Despite the limited number of observations, video imagery allowed us to investigate megafaunal distributions and the role of small burrows in sediment remixing, whereas sonar documented bioturbation pit distribution and increases in pit size as oxygen levels increased. We also note the critical importance of selection of appropriate spatial scales when defining a sampling methodology to investigate bioturbation activity. We also recognize the need for improvements when combining video and sonar imaging. For example, future studies could mount a sonar and camera near the seafloor in such a way that their FOVs partially overlap, therefore simultaneously sampling and comparing benthic habitat and fauna directly. We conclude by suggesting that the combined use of both video and sonar images will enable future studies that enhance knowledge of benthic ecosystems at larger scales than possible with fixed-point video imagery alone.

3.7 Author contributions

AC conducted the literature review, empirical analysis, and wrote the manuscript. PS, DS, and FDL helped to formulate the ideas, content, and structure of the manuscript and provided editorial guidance. DS also helped with sonar analysis.

3.8 Acknowledgments

Ocean Networks Canada is funded through the Canada Foundation for Innovation-Major Science Initiative (CFI-MSI) fund 30199. We are thankful for the support from ONC's marine and digital operations staff for servicing and maintaining the NEPTUNE observatory and for the

curation and quality control of all oceanographic data streams used in this study. We thank Dr. Jacopo Aguzzi for providing suggestions on the oblique perspective grid, and Azeez Sarafadeen, for help with the video analysis. Drs. Amanda Bates and Suzanne Dufour, three examiners of the Ph.D. thesis, and three anonymous reviewers provided very helpful comments on an earlier draft of this manuscript. This research was sponsored by the Natural Sciences and Engineering Research Council of Canada (NSERC). We also thank the School of Graduate Studies at Memorial University for additional financial support.

3.9 Supplementary tables and figures

Supplementary table 3.1. Minimum (Min), maximum (Max), and average (Avg) values of bottom-water oxygen concentration for each studied month.

	Min $[O_2]$ level $ml \cdot l^{-1}$	Max $[O_2]$ level $ml \cdot l^{-1}$	Avg $[O_2]$ level $ml \cdot l^{-1}$
May	0.71	1.40	0.8
September	0.91	1.65	1.22
October	0.71	1.47	1.09

Supplementary table 3.2. Linear regression results between the platform track's length and the time periods of this study (May, September). Data were $\log_{(10)}$ transformed.

	Df	SumSq	MeanSq	F value	Pr(>F)
Month	1	1.087	1.087	11.81	0.0009***
Residuals	85	7.822	0.092		

Fig.s.

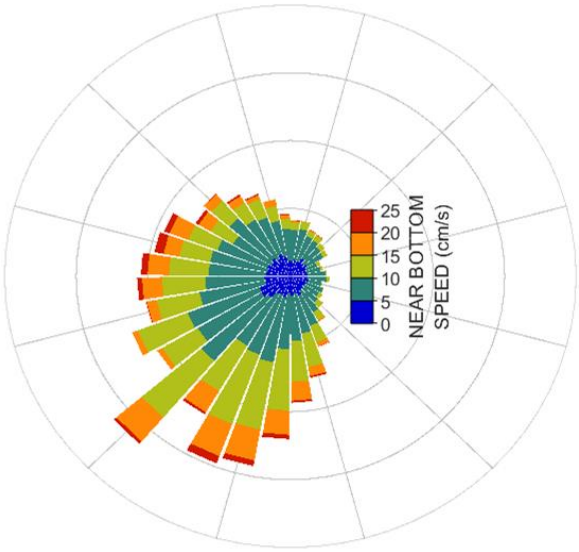

Supplementary Fig. 3.1. Angular histogram also called rose diagram. Each ring is 2%, ranging from 2-8%. The colour corresponds to the near bottom horizontal velocity. The direction is flow towards in oceanographic convention (direction toward which the current is flowing). Data collected from the Aquadopp sonar (also visible in sonar images) from May and December. Histogram made using m_map (Pawlowicz, 2020).

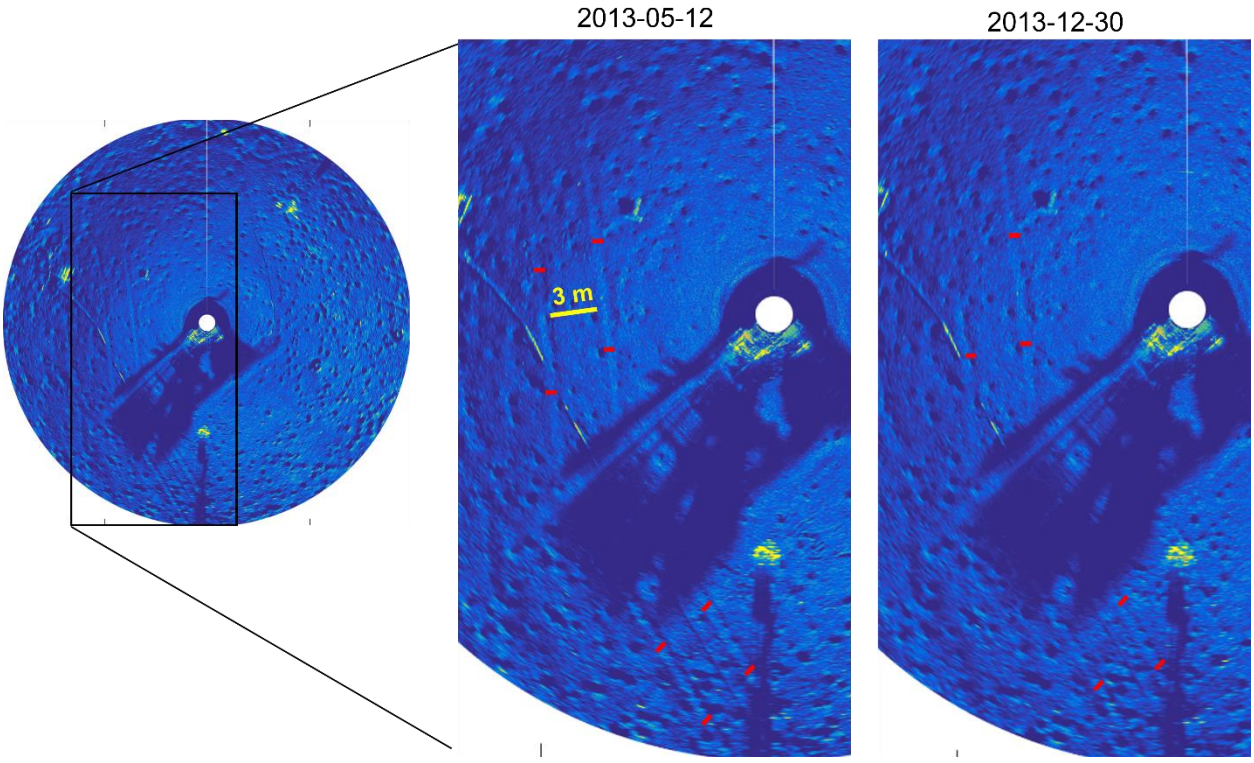

Supplementary Fig. 3.2. Platform tracks on the sediment - indicated from the black box - originated during a trawling impact in 2011. Red symbols in the zoomed-in figures (right side) indicate the points where we measured width of features.

3.10 References

Anderson, M., Gorley, R., Clarke, K. P. 2008. for PRIMER: guide to software and statistical methods. Primer-e, Plymouth, UK, 32.

Auster, P. J., Malatesta, R. J., LaRosa, S. C. 1995. Patterns of microhabitat utilization by mobile megafauna on the southern New England (USA) continental shelf and slope. Mar. Ecol. Prog. Ser., 127, 77-85.

Barnes, C. R., Best, M. M. R., Bornhold, B. D., Juniper, S. K., Pirenne, B., et al. 2007. The NEPTUNE Project-a cabled ocean observatory in the NE Pacific: Overview, challenges and

scientific objectives for the installation and operation of Stage I in Canadian waters. Symposium on Underwater Technology and Workshop on Scientific Use of Submarine Cables and Related Technologies. 308-313.

Bell, J. B., Jones, D. O., Alt, C. H. 2013. Lebensspuren of the bathyal mid-Atlantic ridge. Deep Sea Res. Part II:, 98, 341-351.

Belley, R., Archambault, P., Sundby, B., Gilbert, F., Gagnon, J. M. 2010. Effects of hypoxia on benthic macrofauna and bioturbation in the Estuary and Gulf of St. Lawrence, Canada. Cont. Shelf Res., 30 (12), 1302-1313.

Belley, R., Snelgrove, P. V. R. 2017. The role of infaunal functional and species diversity in short-term response of contrasting benthic communities to an experimental food pulse. J. Exp. Mar. Biol. Ecol., 491, 38-50.

Cadée, G. C. 1976. Sediment reworking by *Arenicola marina* on tidal flats in the Dutch Wadden Sea. Neth. J. Sea Res., (4).

Campanyà-Llovet, N., Snelgrove, P. V. R., Parrish, C. C. 2017. Rethinking the importance of food quality in marine benthic food webs. Prog Oceanogr., 156, 240-251.

Campanyà-Llovet, N., Snelgrove, P. V. R., De Leo, F. C. 2018. Food quantity and quality in Barkley Canyon (NE Pacific) and its influence on macroinfaunal community structure. Prog. Oceanogr, 169, 106-119.

Chauvet, P., Metaxas, A., Hay, A. E., Matabos, M. 2018. Annual and seasonal dynamics of deep-sea megafaunal epibenthic communities in Barkley Canyon (British Columbia, Canada): A response to climatology, surface productivity and benthic boundary layer variation. Prog. Oceanogr, 169, 89-105.

Cheung, S. G., Chan, H. Y., Liu, C. C., Shin, P. K. S. 2008. Effect of prolonged hypoxia on food consumption, respiration, growth and reproduction in marine scavenging gastropod *Nassarius festivus*. Mar. Pollut. Bull., 57 (6-12), 280-286.

Command, R., De Leo, F.C., Robert, K., 2023. Temporal dynamics of the deep-sea pink urchin *Strongylocentrotus fragilis* on the Northeast Pacific continental margin. Deep-Sea Research I 193, https://doi.org/10.1016/j.dsr.2022.103958.

D'Andrea, A. F., Lopez, G. R., Aller, R. C. 2004. Rapid physical and biological particle mixing on an intertidal sandflat. J. Mar. Res., 62 (1), 67-92.

Dashtgard, S. E., Gingras, M. K. 2012. Marine invertebrate neoichnology. Elsevier. Sedimentology. 64, 273-295.

De Leo, F. C., Gauthier, M., Nephin, J., Mihaly, S., Juniper, S. K. 2017. Bottom trawling and oxygen minimum zone influences on continental slope benthic community structure off Vancouver Island (NE Pacific). Deep Sea Res. Part II Top. Stud. Oceanogr., 137, 404-419.

De Leo, F. C., Ogata, B., Sastri, A. R., Heesemann, M., Mihály, S., et al. 2018. High-frequency observations from a deep-sea cabled observatory reveal seasonal overwintering of *Neocalanus* spp. in Barkley Canyon, NE Pacific: insights into particulate organic carbon flux. Prog. Oceanogr, 169, 120-137.

Diaz, R. J., Rosenberg, R. 1995. Marine benthic hypoxia: a review of its ecological effects and the behavioural responses of benthic macrofauna. Oceanogr. Mar. Biol., 33, 245-03.

Diaz, R. J., Rosenberg, R. 2008. Spreading dead zones and consequences for marine ecosystems. Science, 321 (5891), 926-929.**Domke**, L., Lacharité, M., Metaxas, A., Matabos, M. 2017. Influence of an oxygen minimum zone and macroalgal enrichment on benthic megafaunal community composition in a NE Pacific submarine canyon. Mar. Ecol. Prog. Ser., 38 (6), e12481.

DuVal, C. B., Trembanis, A. C., Miller, D. C. 2021. A regime-state framework for morphodynamic modeling of seabed roughness. J. Geophys. Res. Oceans, 126 (5), e2020JC016769.

Ekau, W., Auel, H., Pörtner, H. O., Gilbert, D. 2010. Impacts of hypoxia on the structure and processes in pelagic communities (zooplankton, macro-invertebrates and fish). Biogeosciences, 7(5), 1669-1699.

Fox J, Weisberg S. 2011. An {R} companion to applied regression, 2 Edition.

Fraussen, K., Sellanes, J., Stahlschmidt, P. 2014. The South American radiation of *Jerrybuccinum* (Gastropoda, Buccinidae), with a new deep-water species from Chile. ZooKeys, (409), 61.

Furukawa, Y., Bentley, S. J., Lavoie, D. L. 2001. Bioirrigation modeling in experimental benthic mesocosms. J. Mar. Res., 59 (3), 417-452.

Gibson, R. N., Atkinson, R. J. A., Gordon, J. D. M. 2006. Macrofaunal burrowing: the medium is the message. Oceanogr. Mar. Biol., 44, 85-121.

Gregory, M. R., Ballance, P. F., Gibson, G. W., Ayling, A. M. 1979. On how some rays (Elasmobranchia) excavate feeding depressions by jetting water. J. Sediment. Res., 49 (4), 1125-1129.

Hay, A. E., Wilson, D. J. 1994. Rotary sidescan images of nearshore bedform evolution during a storm. Mar. Geol., 119 (1-2), 57-65.

Hendrickx, M. E., Hastings, P. A. 2007. Ecological data for *Myxine circifrons* Garman, 1899 (Myxiniformes: Myxinidae) in the Gulf of California, Mexico. Hidrobiológica, 17 (3), 273-276.

Howard, J., Mayou, T., Heard, R. 1977. Biogenic sedimentary structures formed by rays. Jour. Sed. 47 (1), 339-346.

Huettel, M., Webster, I. T. 2001. Porewater flow in permeable sediments. in: Boudreau, B.P. et al. (eds.) The Benthic Boundary Layer: Transport Processes and Biogeochemistry., 144 - 177.

Hunter, J. R., Butler, J. L., Kimbrell, C., Lynn, E. A. 1990. Bathymetric patterns in size, age, sexual maturity, water content, and caloric density of Dover sole, *Microstomus pacificus*. CalCOFI Invest. Rep, 31, 132-144.

Ingole, B. S., Sautya, S., Sivadas, S., Singh, R., Nanajkar, M. 2010. Macrofaunal community structure in the western Indian continental margin including the oxygen minimum zone. Mar. Ecol. Prog. Ser., 31 (1), 148-166.

Jones, D. O., Bett, B. J., Tyler, P. A. 2007. Megabenthic ecology of the deep Faroe–Shetland channel: a photographic study. Deep Sea Res. Part I Oceanogr. Res. Pap., 54 (7), 1111-1128.

Jones, K. R.,Traykovski, P. 2018. A method to quantify bedform height and asymmetry from a low-mount ed sidescan sonar. J Atmos Ocean Technol, 35 (4), 893-910.

Kanazawa, K. I. 1992. Adaptation of test shape for burrowing and locomotion in spatangoid echinoids. Paleontology, 35 (4), 733-750.

Kenyon, N. H., Akhmetzhanov, A. M., Twichell, D. C. 2002. Sand wave fields beneath the Loop Current, Gulf of Mexico: reworking of fan sands. Mar. Geol., 192 (1-3), 297-307.

Kristensen, E. 2000. Organic matter diagenesis at the oxic/anoxic interface in coastal marine sediments, with emphasis on the role of burrowing animals. Life at interfaces and under extreme conditions, Hydrobiologia, 426 (1), 1-24.

Kristensen, E., Penha-Lopes, G., Delefosse, M., Valdemarsen, T., Quintana, C. O., et al. 2012. What is bioturbation? The need for a precise definition for fauna in aquatic sciences. Mar. Ecol. Prog. Ser., 446, 285-302.

Kostylev, V. E., Todd, B. J., Fader, G. B., Courtney, R. C., Cameron, G. D., et al. 2001. Benthic habitat mapping on the Scotian Shelf based on multibeam bathymetry, surficial geology and sea floor photographs. Mar. Ecol. Prog., 219, 121-137.

Kukert, H., Smith, C. R. 1992. Disturbance, colonization and succession in a deep-sea sediment community: artificial-mound experiments. Deep Sea Res. Part I Oceanogr. Res. Pap., 39 (7-8), 1349-1371.

Levin, L. A., Huggett, C. L., Wishner, K. F. 1991. Control of deep-sea benthic community structure by oxygen and organic-matter gradients in the eastern Pacific Ocean. J. Mar. Res., 49 (4), 763-800.

Levin, L. A. 2003. Oxygen minimum zone benthos: adaptation and community response to hypoxia. Oceanogr. Mar. Biol. 41, 1-45.

Levin, L. A., Ekau, W., Gooday, A. J., Jorissen, F., Middelburg, J. J., 2009. Effects of natural and human-induced hypoxia on coastal benthos. Biogeosciences, 6 (10), 2063-2098.

Levin, L. A., McGregor, A. L., Mendoza, G. F., Woulds, C., Cross, P., et al. 2013. Macrofaunal colonization across the Indian Margin oxygen minimum zone. Biogeosciences, 10 (11), 7161-7177.

Levin, L. A., Etter, R. J., Rex, M. A., Gooday, A. J., Smith, C. R., et al. 2001. Environmental influences on regional deep-sea species diversity. Ann. Rev. Ecol. Syst. 32, 51–93.

Maier, I., Hay, A. E. 2009. Occurrence and orientation of anorbital ripples in near-shore sands. J. Geophys. Res., 114 (F4).

Maire, O., Lecroart, P., Meysman, F., Rosenberg, R., Duchêne, J. C., et al. 2008. Quantification of sediment reworking rates in bioturbation research: a review. Aquat. Biol., 2 (3), 219-238.

Martinell, J., De Gibert, J. M., Domènech, R., Ekdale, A. A., Steen, P. P. 2001. Cretaceous ray traces? an alternative interpretation for the alleged dinosaur tracks of La Posa, Isona, NE Spain. Palaios, 16 (4), 409-416.

Matabos, M., Bui, A. O., Mihály, S., Aguzzi, J., Juniper, S. K., et al.. 2014. High-frequency study of epibenthic megafaunal community dynamics in Barkley Canyon: A multi-disciplinary approach using the NEPTUNE Canada network. J. Mar. Syst., 130, 56-68.

Mauviel, A., Sibuet, M. 1985. Répartition des traces animals et importance de la bioturbation. Peuplements profonds du Golfe de Gascogne: Campagnes BIOGAS. IFREMER, 157-173.

McArdle, B. H., Anderson, M. J. 2001. Fitting multivariate models to community data: a comment on distance-based redundancy analysis. Ecology., 82 (1), 290-297.

Miatta, M., Snelgrove, P. V. R. 2021. Benthic nutrient fluxes in deep-sea sediments within the Laurentian Channel MPA (eastern Canada): The relative roles of macrofauna, environment, and sea pen octocorals. Deep-Sea Res. I: Oceanogr. Res. Pap., 178, 103655.

Middelburg, J. J., Levin, L. A. 2009. Coastal hypoxia and sediment biogeochemistry. Biogeosciences, 6 (7), 1273-1293.

Morton, B. 1990. The physiology and feeding behaviour of two marine scavenging gastropods in Hong Kong: the subtidal *Babylonia lutosa* (Lamarck) and the intertidal *Nassarius festivus* (Powys). J. Molluscan Stud., 56 (2), 275-288.

Murty, S. J., Bett, B. J., Gooday, A. J. 2009. Megafaunal responses to strong oxygen gradients on the Pakistan margin of the Arabian Sea. Deep Sea Res. Part II Top. Stud. Oceanogr., 56 (6-7), 472-487.

Nelder, J. A., Wedderburn, R. W. 1972. Generalized linear models. J R Stat Soc Ser A Stat Soc, 135 (3), 370-384.

Nowell, A. R., Jumars, P. A., and Fauchald, K. 1984. The foraging strategy of a subtidal and deep-sea deposit feeder 1. Limnol. Oceanogr., 29 (3), 645-649.

Oksanen J., Blanchet, F. G., Kindt, R., Legendre, P. et al. 2013 vegan: community ecology package. R package version 2.0-10. http://CRAN.Rproject.org/package=vegan.

Pawlowicz, R., 2020. "M_Map: A mapping package for MATLAB", version 1.4m, [Computer software], www.eoas.ubc.ca/~rich/map.html.

Pihl, L., Baden, S. P., Diaz, R. J. 1991. Effects of periodic hypoxia on distribution of demersal fish and crustaceans. Mar. Biol., 108, 349-360.

Puig, P., Canals, M., Company, J. B., Martín, J., Amblas, D., et al. 2012. Ploughing the deep-sea floor. Nature, 489 (7415), 286-289.

R Core Team. 2016. R: A Language and Environment for Statistical Computing. Vienna, Austria. Retrieved from https://www.R-project.org/.

Rasband, W.S., 1997-2018. ImageJ, U. S. National Institutes of Health, Bethesda, Maryland, USA, https://imagej.nih.gov/ij/.

Rex, M. A., Etter, R. J. 1998. Bathymetric patterns of body size: implications for deep-sea biodiversity. Deep Sea Res. Part II Top. Stud. Oceanogr., 45 (1-3), 103-127.

Rhoads, D. C. 1963. Rates of sediment reworking by *Yoldia limatula* in Buzzards Bay, Massachusetts, and Long Island Sound. J. Sediment. Res., 33 (3), 723-727.

Rhoads, D. C., Cande, S. 1971. Sediment profile camera for in situ study of organism-sediment relations 1. Limn, Oceanogr., 16 (1), 110-114.

Robert, K., Juniper, S. K. 2012. Surface-sediment bioturbation quantified with cameras on the NEPTUNE Canada cabled observatory. Mar. Ecol. Prog. Ser., 453, 137-149.

Ruhl, H. A., Smith J. K. L. 2004. Shifts in deep-sea community structure linked to climate and food supply. Science, 305 (5683), 513-515.

Seike, K., Jenkins, R. G., Watanabe, H., Nomaki, H., Sato, K. 2012. Novel use of burrow casting as a research tool in deep-sea ecology. Biol. Lett., 8 (4), 648-651.

Shull, D. H. 2009. Bioturbation. Ocean Sci., 3, 671-676.

Shum, K. T., Sundby, B. 1996. Organic matter processing in continental shelf sediments—the subtidal pump revisited. Mar. Chem., 53 (1-2), 81-87.

Smith C.R., De Leo, F.C., Bernardino, A.F., Sweetman, A.K., Arbizu, P.M. 2008. Abyssal food limitation, ecosystem structure and climate change. Trends Ecol. Evol., 23 (9), 518-528.

Smith, C. R., Levin, L. A., Hoover, D. J., McMurtry, G., Gage, J. D. 2000. Variations in bioturbation across the oxygen minimum zone in the northwest Arabian Sea. Deep Sea Res. Part II Top. Stud. Oceanogr., 47 (1-2), 227-257.

Smith, L. M., Cimoli, L., LaScala-Gruenewald, D., Pachiadaki, M., Phillips, B., et al. 2022. The deep ocean observing strategy: addressing global challenges in the deep sea through collaboration. Mar. Technol. Soc. J., 56 (3), 50-66.

Snelgrove, P. V. R., Thrush, S. F., Wall, D. H., and Norkko, A. 2014. Real world biodiversity–ecosystem functioning: a seafloor perspective. Trends Ecol. Evol., 29 (7), 398-405.

Solan, M., Kennedy, R. 2002. Observation and quantification of in situ animal-sediment relations using time-lapse sediment profile imagery (t-SPI). Mar. Ecol. Prog. Ser., 228, 179-191.

Solan, M., Wigham, B. D., Hudson, I. R., Kennedy, R., Coulon, C. H., et al. 2004. In situ quantification of bioturbation using time lapse fluorescent sediment profile imaging (f SPI), luminophore tracers and model simulation. Mar. Ecol. Prog. Ser., 271, 1-12.

Sweetman, A. K., Witte, U. 2008. Response of an abyssal macrofaunal community to a phytodetrital pulse. Mar. Ecol. Progr. Seri., 355, 73-84.

The **GIMP** Development Team. 2019. GIMP. Retrieved from https://www.gimp.org.

Theede, H. 1973. Comparative studies on the influence of oxygen deficiency and hydrogen sulphide on marine bottom invertebrates. Neth. J. Sea Res., 7, 244-252.

Thomsen, L., Aguzzi, J., Costa, C., De Leo, F., Ogston, A., et al. 2017. The oceanic biological pump: rapid carbon transfer to depth at continental margins during winter. Sci. Rep., 7 (1), 1-10.

Thrush, S. F., Pridmore, R. D., Hewitt, J. E., Cummings, V. J. 1991. Impact of ray feeding disturbances on sandflat macrobenthos: Do communities dominated by polychaetes or shellfish respond differently? Mar. Ecol. Prog. Ser., 69 (3), 245-252.

Thurber, A. R., Sweetman, A. K., Narayanaswamy, B. E., Jones, D. O., Ingels, J., et al. 2014. Ecosystem function and services provided by the deep sea. Biogeosciences, 11 (14), 3941-3963.

Vaquer-Sunyer, R., Duarte, C. M. 2008. Thresholds of hypoxia for marine biodiversity. Proc. Natl. Acad. Sci. U. S. A., 105 (40), 15452-15457.

Vardaro, M. F., Bagley, P. M., Bailey, D. M., Bett, B. J., et al. 2013. A Southeast Atlantic deep-ocean observatory: first experiences and results. Limnol Oceanogr- Meth, 11 (6), 304-315.

Vetter, R. D., Lynn, E. A., Garza, M., Costa, A. S. 1994. Depth zonation and metabolic adaptation in Dover sole, *Microstomus pacificus*, and other deep-living flatfishes: factors that affect the sole. Mar. Biol., 120 (1), 145-159.

Yager, P. L., Nowell, A. R., Jumars, P. A. 1993. Enhanced deposition to pits: a local food source for benthos. J. Mar. Res., 51 (1), 209-236.

Yahel, G., Yahel, R., Katz, T., Lazar, B., Herut, B., et al. 2008. Fish activity: a major mechanism for sediment resuspension and organic matter remineralization in coastal marine sediments. Mar. Ecol. Prog. Ser. 372, 195-209.

Wheatcroft, R. A. 1991. Conservative tracer study of horizontal sediment mixing rates in a bathyal basin, California borderland. J. Mar. Res., 49 (3), 565-588.

Williams, S. T., Noone, E. S., Smith, L. M., Sumner-Rooney, L. 2022. Evolutionary loss of shell pigmentation, pattern, and eye structure in deep-sea snails in the dysphotic zone. Evolution, 76 (12), 3026-3040.

Witte, U., Aberle, N., Sand, M., and Wenzhöfer, F. 2003. Rapid response of a deep-sea benthic community to POM enrichment: an in situ experimental study. Mar. Ecol. Prog. Seri., 251, 27-36.

Chapter 4. - Contrasting Benthic Ecological Functions in Deep-Sea Canyon and Non-Canyon Habitats: Macrofaunal Diversity and Nutrient Cycling[4]

[4]Ciraolo, A. C., and Snelgrove, P. V. R. (2023). Contrasting benthic ecological functions in deep-sea canyon and non-canyon habitats: Macrofaunal diversity and nutrient cycling. *Deep Sea Res. Part I Oceanogr. Res*. 197, 104073.

4.1 Abstract

Understanding ecosystem functioning and stability of continental slope environments requires assessing the effects of habitat heterogeneity (canyon and non-canyon habitats) on benthic macrofaunal communities and ecosystem functioning. We evaluated the importance of habitat heterogeneity and phytodetrital enrichment in canyon, channel, and inter-canyon habitats of the Gulf of Maine, Northwest Atlantic. Using an ROV, we collected sediment cores at five seafloor sites in the Gulf of Maine (663-969 m depth). Over ~ 24 h, we incubated ~ 6 cores per site, three of which were enriched with the diatom *Chaetoceros muelleri.* For all core treatments, we measured macrofaunal composition, functional diversity indices (functional richness, evenness, and divergence), and benthic nutrient fluxes (ammonium, nitrate, phosphate, and silicate), as well as oxygen consumption. We also dedicated two non-incubated cores to quantifying sedimentary and chemical-physical characteristics. We found that benthic communities differed among the three habitats, but these differences and our phytodetrital additions did not translate to significant differences in rates of benthic fluxes among habitats., expect for nitrate and phosphate fluxes. Total organic carbon and chlorophyll-*a* explained most of the variation in oxygen consumption, which was similar in enriched and control cores. We conclude that large-scale habitat heterogeneity contributes to variation in benthic community composition, but with no consistent effect on nutrient fluxes. These results also suggest that phytodetrital deposition influences oxygen consumption but plays a lesser role in short-term

nutrient cycling in deep-sea heterogeneous habitats, perhaps masked by other environmental variables. Moreover, sediments with high functional richness and relatively high functional divergence may sometimes lack the specific trait types that rapidly enhance nutrient regeneration and thus contribute to ecosystem functioning of deep-sea sediments.

4.2 Introduction

The deep-sea, Earth's vastest ecosystem, provides vital ecosystem functions such as nutrient and carbon cycling essential to sustaining primary and secondary production (Danovaro et al., 2008; Sweetman et al., 2019; Jameson et al., 2021). Deep-sea communities typically share some common characteristics including low biomass, slow growth rates, slow reproduction and recruitment rates, and food-limited conditions largely dependent on sinking organic material produced in surface waters (Kelly et al., 2010). The bioavailability of organic matter in marine sediments ranges from labile and easily digestible material to refractory material that decomposes slowly and thus tends to accumulate in sediments (Mayer et al., 1995; Middelburg et al., 1999). Within the labile fraction, total organic carbon (TOC) includes protein, carbohydrates, and lipids (Fabiano et al., 1995). However, the use of TOC as a proxy of labile organic C depends on its origin and molecular composition. Furthermore, sediment organic matter also includes an autotrophic fraction often characterized by photosynthetic pigment concentrations (chlorophyll-*a*, and phaeopigments) (Montagna et al., 1983; MacIntyre et al., 1996) resulting from phytodetritus that sinks to deep-sea sediments. Numerous studies therefore use phytopigment concentration as a proxy for material reaching the seafloor from upper layers (Witte et al., 2003a,b).

Deep-sea environments encompass a heterogeneous mix of habitats, particularly on continental slopes that feature shelf breaks with elevated production, sediment-dominated and outcrop-dominated seafloor, and submarine canyons (Ramirez-Lodra et al., 2010; Zeppilli et al., 2016). Each of those habitats supports different types of biological communities and species, suggesting that the combination of habitat and community differences may lead to different effects on ecosystem functioning. Several studies link high biodiversity to increased efficiency in ecosystem function, such as with nutrient cycling (Cardinale et al., 2012; Gamfeldt et al., 2014;

Piot et al., 2014), and/or resilience (Oliver et al., 2015). However, beyond species richness, species-specific traits may represent a clearer link between biodiversity and ecosystem functions (BEF) (Norling et al., 2007). Consequently, the functional traits of each organism may respond to contrasting environments differently, thereby altering ecosystem processes and services (De Bello et al., 2010; Mouchet et al., 2010). Understanding the overall functioning of the global biosphere hinges upon understanding potential differences in ecosystem functioning of contrasting habitats and the role of biodiversity in those processes (Worm et al., 2006; Zeppilli et al., 2016).

Deep-sea ecosystem functions include habitat provisioning, secondary and primary production, transfer of organic matter (OM) to higher trophic levels, OM decomposition, and nutrient regeneration (Karl et al., 1994; Brunnegård et al., 2004). However, these processes link closely to the collective activities of animals, protists, and prokaryotes, particularly in exploiting and recycling inputs of material from the photic zone (Mermillod-Blondin, 2011).

Functional diversity, defined as the range and value of those species and organism traits that influence ecosystem functioning, offers a pathway to studying ecosystem functions (Tilman et al., 2001). The functional diversity concept complements species presence or absence by examining the function that each species (functional trait) plays and quantifying associated resource use in the ecosystem. Recent studies therefore emphasize functional diversity as an important driver of ecosystem functioning (Diaz and Cabido, 2001; Bremner et al., 2003; Hooper et al., 2005; Belley and Snelgrove, 2016). Most studies of functional diversity typically use three main indices: functional richness (FRich), functional evenness (FEve), and functional divergence (FDiv) (Mason et al., 2005; Villéger et al., 2008; Pla et al., 2012). FRich represents the amount of functional space filled by a community, namely whether the community uses available resources (Mason et al., 2005; Villéger et al., 2008). FEve describes whether functional traits are distributed evenly in the

community. Therefore, low FEve indicates incomplete use of all available resources (Mason et al., 2005; Villeger et al., 2008). Finally, FDiv indicates the degree of differenced traits; high FDiv corresponds to a high degree of differentiation and low resource competition (Mason et al., 2005).

The combination of different infaunal groups and associated functions characterize marine-soft-bottom environments. The latter plays a pivotal role in remineralizing OM that settles to the seafloor and can act as both a major source of nutrients and carbon to the overlying water column or/and as a significant sink (Link et al., 2013; Miatta and Snelgrove, 2021a). Typically, a large fraction of exported OM undergoes biologically mediated degradation and oxidation through a complex web of redox reactions, leaving behind a (typically) small fraction of material that may become permanently buried (Berner, 2020). Evaluating spatial variation and partitioning of fluxes into (influx) and out of (efflux) sediments can improve our understanding of regional biogeochemical cycles (Hensen et al., 2000; Koho et al., 2008; Link et al., 2013) and, hence, overall ecosystem functioning. Benthic communities play an important role in recycling OM and respond quickly to fresh OM deposition on the continental shelf and in the deep sea (Moodley et al., 2005), facilitated by both infaunal organisms and microbes.

Infaunal organisms directly ingest and excrete OM but also influence OM through their digestive processes that break down OM physically, and through bio-irrigation and bioturbation that oxygenates sediments. The latter pathway supports growth and spatial structuring of different functional microbial communities (Fenchel and Finlay, 2008), which consequently break down OM and deoxygenate sediments (Grossart et al., 2006). Among macrofaunal organisms, the Polychaeta that often dominate sediments (Ellingsen, 2001; Witte et al., 2003a) encompasses a high level of taxonomic and functional diversity, referring to different types of movement, feeding

modes, and sediment reworking that affect ecosystem functions (Hutchings, 1998; Queirós et al., 2013).

Continental slopes account for more than 20% of total marine productivity and receive a significant proportion of OM exported to the seafloor (Levin and Sibuet, 2012), thus representing an ideal environment in which to investigate benthic ecosystem functioning relationships across contrasting habitats. High spatial heterogeneity in seafloor biodiversity characterizes many slope environments (Menot et al., 2010; Baldrighi et al., 2017), typically driven by variables such as substrate heterogeneity, depth, water circulation, oxygen availability, and food resources (Levin et al., 1997; Campanyà-Llovet et al., 2018; Di Franco et al., 2021). We therefore selected study locations in the Northwest Atlantic that we expected would encompass different habitat conditions to test how contrasting environmental factors may influence benthic ecosystem function relationships.

Canyons and adjacent slope environments that characterize the Northwest Atlantic exemplify contrasting habitats in which we might anticipate differences in sedimentary characteristics as well as in biodiversity (Etter et al., 1992; Cosson et al., 1997; Belley and Snelgrove, 2016). Canyons funnel currents, driving sediments and particle-reactive substances toward the deep sea (Weaver, 2000; Oliveira, 2007; De Leo et al., 2014; Puig et al., 2014), and sometimes vice-versa (Klinck, 1996; Allen and De Madron, 2009). Canyons can enhance primary productivity through upward transport of iron, an important regulator of phytoplankton productivity, to the euphotic zone (Ryan et al., 2005). Canyons also represent hotspots of OM transport and benthic biomass (Bianchelli et al., 2008; Ingels et al., 2009; Tyler et al., 2009; De Leo et al., 2010). Despite their widespread distribution along ocean and island margins (De Leo et al., 2010; Harris and Baker, 2019), researchers have studied only a small proportion (< 0.5%) of the world's canyons in terms of

benthic community structure, standing stock, species richness, and diversity (e.g., De Leo et al., 2010; Vetter et al., 2010; Paterson et al., 2011; De Leo et al., 2012).

Although infaunal macrobenthos account for a large part of known metazoan species diversity on the seafloor, few macrofaunal studies have focused on submarine canyons (Cúrdia et al., 2004; Paterson et al., 2011). A few studies in frequently disturbed canyon soft-sediment environments, such as in Monterey Canyon, report reduced species richness, possibly influenced by increased sedimentation and/or bioturbation disturbance near canyon walls (McClain and Barry, 2010). Sites at shelf-depths and at the head of La Jolla canyon enriched with kelp and surf grass detritus showed reduced diversity relative to nearby slope sites, a pattern the researchers attributed to dominance by opportunistic species such as *Capitella capitata* (polychaete), *Orchomene limodes* (amphipod), and *Nebalia* sp. (leptostracan) (Vetter and Dayton, 1998). Enhanced abundances and biomass of macro-and megabenthos relative to open slope habitats appear to be a widespread canyon feature as a consequence of organic enrichment (e.g., De Leo et al., 2010; Leduc et al., 2014). However, previous studies document differences in community structure between canyon and non-canyon slope systems, largely relating to dominance by opportunistic species in organically-enriched settings (Paterson et al., 2011; De Leo et al., 2014).

In light of the rarity of comparative studies on ecological functioning (e.g., community respiration, productivity, nutrient cycling, OM supply, and remineralization rates) we focused on contrasting environments in the Gulf of Maine continental slope to develop a more comprehensive understanding of deep-sea biodiversity, ecosystem functioning, and habitats. Relatively complex bathymetry and geology characterize the Gulf of Maine deep-sea region, which covers ~ 25,000 km^2 (Kelly et al., 2010) and encompasses six distinct sub-regions: the continental shelf-slope break, continental slope, Northeast Channel, continental rise, submarine canyons, and Bear

Seamount (the western-most seamount of the New England Seamount chain). Submarine canyons interrupt the otherwise generally homogeneous slope relief. Outcrops of bedrock and clay on the steep canyon walls extend from the canyon heads at the continental shelf-slope break down to the base of the continental slope and rise. Three steep canyons comprise the Northeast Channel between Georges Bank and Browns Bank, dropping to depths of ~1000 m and bounded by flat sandy bottom, although a mixture of pebble, cobble, boulders, and rocky outcrops dominates much of the substrate. The topographic complexity and spatio-temporal variability within canyons tend to promote biodiversity but also make sampling difficult, particularly from surface ships. This region also represents one of the primary locations for the exchange of water between the Gulf of Maine and the North Atlantic Ocean (Kelly et al., 2010).

Here we evaluate the importance of habitat heterogeneity and other environmental variables over different spatial scales in driving benthic macrofauna community structure (including abundance and diversity) and associated OM recycling in submarine canyons and non-canyons of the Gulf of Maine. Specifically, we investigate whether:

1) Macrofaunal community structure density, taxonomic diversity, community composition, and functional diversity differ spatially, and whether environmental drivers such as detritus supply and seafloor habitat heterogeneity contribute to such differences;
2) Benthic nutrient fluxes vary spatially in any consistent pattern with respect to seabed topography, and what factors contribute to spatial variation;
3) Pulses of OM to the seafloor result in rapid increases in oxygen and nutrient flux rates.

4.3 Materials and Methods

Using the remotely operated vehicle (ROV) Remotely Operated Platform for Ocean Science, (ROPOS , www.ropos.com) deployed from the NOAA research vessel Henry B. Bigelow (June

14-27, 2019), we collected sediment push cores in the Gulf of Maine from Corsair Tributary Canyon, Powell-Munson Inter-canyon, Kinlan-Heezen Mid Inter-canyon, and Northeast Channel (**Table 4.1, Fig. 4.1**). **Table 4.2** describes general sedimentary and environmental features of canyon, inter-canyon, and channel habitats of the Gulf of Maine continental slope. ROPOS collected between 6 and 15 cores per site (i.d. = 6.7 cm, L = 35.6 cm). We used 1-2 cores per site to determine sediment properties, and the remaining cores for *ex-situ* incubations to measure nutrient fluxes and for subsequent macrofaunal identification. We also collected bottom-water samples using a Niskin bottle and recorded temperature and salinity with a Seabird 19 conductivity-temperature-depth (CTD) instrument, both mounted on the ROV. **Supplementary table 4.1** shows more details on core distributions at each station.

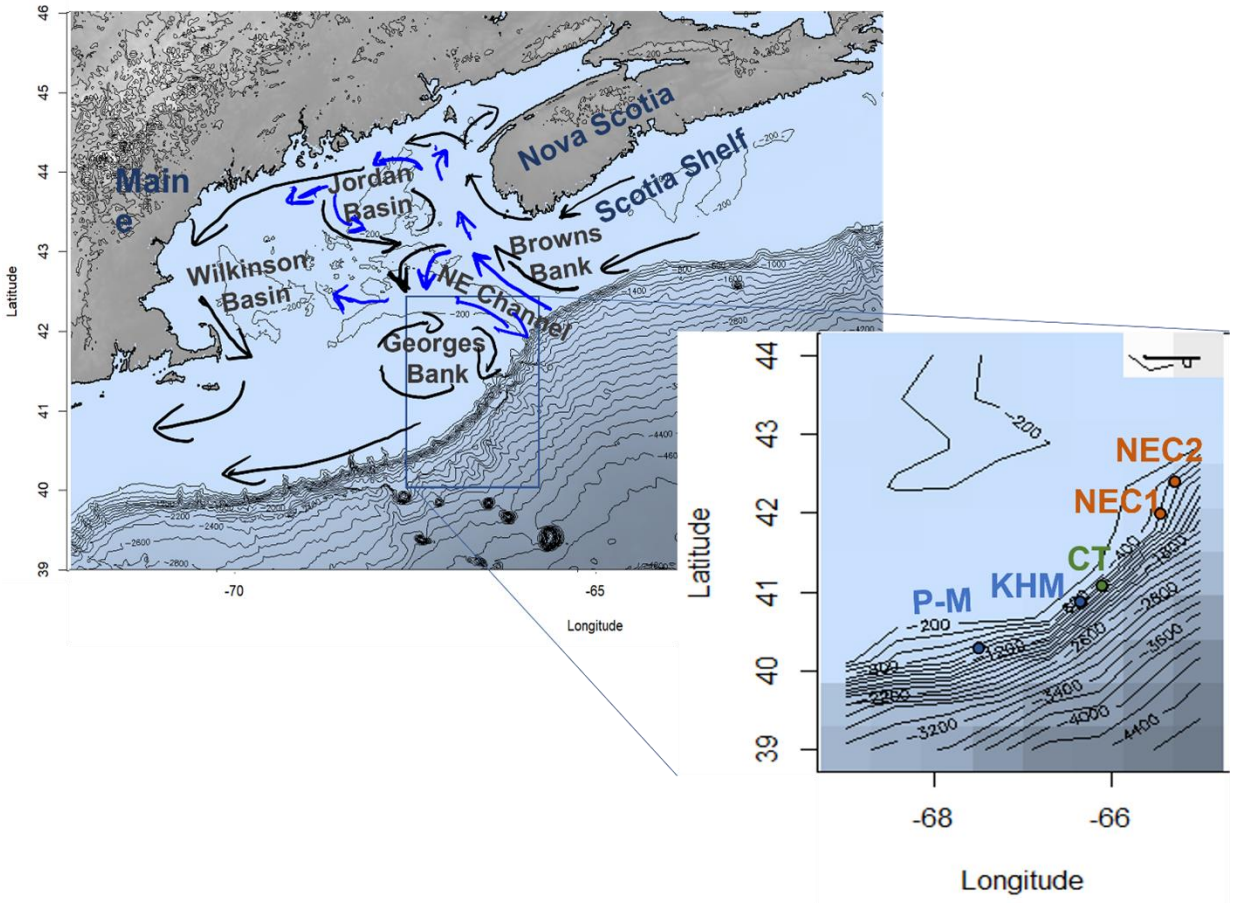

Fig. 4.1. Map of stations sampled in the Gulf of Maine in June 2019. Label symbols: 1) C-T: Corsair Tributary Canyon; KHM: Kinlan-Heezen Inter-canyon; P-M: Powell-Munson inter-canyon; NEC1: Northeast Channel 1; NEC2: Northeast Channel 2. Colors indicate three different habitats sampled: green = Canyon habitat; blue = Inter-canyon habitat; orange = NE Channel habitat. Black arrows represent Scotian shelf surface currents. Blue arrows represent deep bottom currents entering from NE Channel.

Table 4.1. Number, name, latitude, longitude, water depth, and sub-region of each sampling station in the Gulf of Maine.

Site number	Site Name	Site Lat	Site Long	Water Depth (m)	Sub Region
R 2117	NE Channel 2 (NEC2)	42.40	-65.28	663	NE Channel
R 2113	NE Channel 1 (NEC1)	42.00	-65.45	672	NE Channel
R 2110	Kinlan-Heezen Mid Inter-canyon (KHM)	40.85	-66.35	804	Inter-canyon
R 2108	Powell-Munson Inter-canyon (P-M)	40.30	-67.50	962	Inter-canyon
R 2112	Corsair Tributary Canyon (C-T)	41.80	-66.10	969	Canyon

Table 4.2. General characteristics of canyons, inter-canyons, NE Channel of the Gulf of Maine. Table modified from Kelly et al. (2010), including Quattrini et al. (2015), and Miatta and Snelgrove (2021b).

Sub-region	Depth	Gradient	Sediment composition	Linkages	Additional Characteristics
Canyons	Bisects the continental slope, largest are 400 m deep and 5 Km wide.	Highly variable, ranging from 3-70.°	Highly variable, ranging from mud/sit/clays to boulder fields and rocky outcroppings.	Areas of strong currents influenced by bottom topography and areas of sediment transport from the continental shelf Gulf of Maine to the deep Atlantic.	Majority located along the southern edge of Georges Bank.
Inter-canyons	Slope area between canyons. Similar in depth to canyons.	Unknown.	Various combinations of gravel, sandy sediments, and sandy silt.	Understudied region in which hydrodynamics inhibit OM deposition. Reduced macrofaunal density and diversity. Intermediate-high rates of benthic nutrient fluxes.	Unknown.
NE Channel	210-900 m.	Deep valley between Georges Bank and Browns Bank.	Poorly sorted mixture of pebble, cobble and boulder, with stretches of sand.	Main connection between the continental shelf Gulf of Maine and the Continental slope.	Major site of water mass exchange.

4.3.1 Incubations

Immediately upon recovery of the submersible, we sealed all incubation cores with water-tight lids equipped with magnetic stirrers and gas-tight sampling ports prior to moving them into a cold room set at the *in-situ* temperature (14-16 °C) for each station in order to simulate the deep-sea environment, acknowledging potential effects of pressure on species' behavior and physiology. In order to allow any sediment particles resuspended during transport to settle back to the sediment surface, we waited for ~12 h before beginning the 24-h incubations. We chose 24 h as the incubation time to avoid consumption of more that 15-30% of available oxygen (Hammond et al., 1985; Belley and Snelgrove, 2016), and because of logistical constraints.

At the end of the incubation period, we sectioned each core into three sediment layers (0-2, 2-5, 5-10 cm) which we transferred into 500- or 1000-ml plastic jars and fixed with a 4% buffered formaldehyde and seawater mix prior to storage in 70% ethanol until further analysis in lab. Some cores did not penetrate to a sufficient depth to capture the entirety of the deepest layer (5-10 cm), however, the low numbers of individuals in the 5-10 fraction and absence of the deep layer from some cores led us to focus on only the 0-2 and 2-5 cm sections for taxonomic analysis. In addition, in contrast to the water samples collected from incubated cores collected from our five sites (NEC1, NEC2, KHM, P-M, C-T), we used sediment cores from only four sites (NEC1, KHM, P-M, C-T) to investigate macrofaunal communities because we dedicated the samples from the Northeast Channel to a different experiment.

4.3.2 Laboratory analysis

4.3.2.1 Macrofauna analysis and taxonomic identification

In the laboratory, we carefully sieved macrofaunal organisms from sediments through a 300-µm sieve prior to subsequent storage in 70% ethanol. Following staining with Rose Bengal (0.5 $g \cdot L^{-1}$), we completed taxonomic analysis under a binocular dissection microscope and identified individuals to family, or order, depending on the taxon. We determined abundance (N) for each taxon and defined taxonomic richness (S) as the number of taxa at the lowest taxonomic level present in each sediment core. We also determined diversity indices including Simpson's index (Simp), Expected number of Taxa (ES[25] i.e., the expected number of taxa in a hypothetical random sample of 25 individuals combining the data from the entire 10 cm core per site), and Shannon-Wiener (H') as well as Pielou's evenness (J'), for each sediment core. All analyses were conducted in R (R Core Team 2016), using the package "vegan" (Oksanen et al., 2013).

4.3.2.2 Biological traits and functional diversity

We selected three biological traits (mobility, sediment reworking functional type, and feeding type) and 16 modalities from published sources (Queirós et al., 2013; WoRMS Editorial Board 2015), based on their presumed influence on benthic fluxes (**Table 4.3, Supplementary table 4.2**). Using a "fuzzy coding" approach, we allowed more than one functional trait for a given taxon and scored them from 0 to 1, where 0 reflected no affinity for the given trait, whereas 1 denoted exclusive affinity. When a taxon shared more than one trait that varied with environment, we scored each trait as 0.5 for two traits, and 0.3 for three traits. For example, the polychaete Glyceridae family may include both carnivores, surface and subsurface deposit feeders. We used trait category scores for each taxon and taxa abundance matrices to obtain functional diversity (FD) indices using the "FD" package (Laliberte and Legendre, 2010) in R. We then computed the following multidimensional FD indices for use in subsequent analyses: functional richness (FRich), functional evenness (FEve), and functional divergence (FDiv) (Villéger et al., 2008).

Table 4.3. Biological traits and modalities used in trait analysis.

Trait	Level
Movement	live in fixed tubes (FT)
	limited movement (LM)
	slow movement (SM)
	free movement in sediment matrix (FMSM)
	free movement in burrow system (FMBS)
Reworking types	epifauna (E)
	surficial modifiers (S)
	upward conveyors (UC)
	downward conveyors (DC)
	biodiffusors (B)
	regenerators (R)
Feeding type	carnivorous (predator or passive suspension) (C)
	surface deposit feeder (D)
	filter/Suspension feeder (F)
	omnivorous (scavenger) (O)
	parasite (P)
	subsurface deposit feeder (SB)

4.3.2.3 Benthic nutrient fluxes in the sediment-water interface

In order to evaluate benthic nutrient fluxes at the sediment-water interface we measured oxygen consumption at 4–6-h intervals using pre-fitted, non-invasive oxygen sensor spots and a Fibox Polymer Optical Fiber Oxygen System (PreSens, Regensburg, DE). At the onset of incubations, we collected initial water samples from each core for future nutrient analysis, as well as two replicate water samples at the middle and the end of each incubation. In each case, we replaced the removed water with bottom water collected with the CTD rosette. Nutrient samples were stored in an upright position in 50 ml pre-acid-washed plastic falcon tubes in a dark freezer at -20 °C until analysis. We determined concentrations of NH_4^+, NO_3^-, $Si(OH)_4$, PO_4^{3-} in the water using a SEAL AutoAnalyzer 3 HR nutrient water analyzer at Fisheries and Ocean Canada, St John's, NL, Canada.

4.3.2.4 Enrichment experiments

To evaluate macrofaunal response to fresh organic matter, at the beginning of the incubation we added 0.02 g of the diatom, *Chaetoceros muelleri* in three cores from each site; this addition corresponds to 25.5 mg · C · m^{-2} · yr^{-2}. We choose *C. muelleri* because diatoms are the dominant phytoplankton group during spring blooms in the Gulf of Maine (Townsend et al., 2005, 2006). An additional 2-3 cores received no algal additions and served as experimental controls to document ambient nutrient fluxes and respiration rates for the study sites.

The algae were grown at the Dr. Joe Brown Aquatic Research Building (http://www.mun.ca/osc/jbarb/index.php) and centrifuged following harvesting to produce an algal paste, which we froze at -20 °C until needed for the cruise.

4.3.2.5 Laboratory analysis of sediment organic matter

We collected sediments for analysis of organic matter and grain size from the upper 0-2 cm of the dedicated non-incubate core(s) (**Supplementary table 4.1**) at each site, homogenizing the sediment and then placing it in Whirl-Pak bags prior to storage in the dark at -20 °C until analyzed (except for samples for lipid analysis, which were stored in pre-combusted aluminium tin foil at -80 °C). We measured OM to summarize practical proxies of OM quantity and quality. Therefore, we used total organic carbon (TOC) to describe food quantity. To characterize quality we used chlorophyll-*a* (Chl*a*), phaeopigments (Phaeo), and the chlorophyll-*a*:phaeopigment ratio (Chl*a*:Phaeo) as indicators of short-term OM freshness and quality (Le Guitton et al., 2015); algae and photosynthetic pigments degrade faster than lipids and provide a measure of freshness of OM over time scales of days-weeks. We also used total lipid concentrations as an indicator of intermediate-term (weeks to months) OM lability/quality (Mayer et al., 1995) because lipids degrade at slower rates compared to pigments. Finally, we used the carbon:nitrogen (C:N) ratio as

an indicator of long-term (months to years) OM quality, with lower C:N indicating fresher and higher quality OM because of more rapid use of nitrogen than carbon (Le Guitton et al., 2015).

4.3.2.5.1 CHN analysis

Total organic carbon and total nitrogen were determined by drying a sediment subsample of 1-5 g (wet weight) at 60 °C for 24 h, grinding it to a fine powder, and then weighing and acidifying (with pure HCl fumes) for 24 h to eliminate inorganic carbon. Samples were dried again at 60 °C for 24 h before starting CHN analysis. We then weighed an aliquot of dried decarbonated sediments (15 mg) and folded it tightly into a tin capsule. A Carlo Erba NA1500 Series II elemental analyser (EA) determined concentrations of TOC and TN in sediments, expressed as carbon/nitrogen percent weight.

4.3.2.5.2 Phytopigment content

We measured chlorophyll-*a* and phaeopigments spectrophotometrically (Cary 300 BIO) (Danovaro 2009), noting that spectrophotometric assays are generally used for pigments in sediments with concentrations > 0.5 Chl*a* $\mu g \cdot g^{-1}$. For each sample, we placed 2 g of frozen sediment in a transparent falcon tube wrapped with aluminium foil to block out light. We extracted pigments from the sediment in 90% acetone, vortexed the solution for 30 s, and then treated them in an ultrasound bath in ice at 50-100 W for 3 min, with a 30 s interval between each minute of sonication prior to overnight storage at 4 °C in the dark. The following day we centrifuged the samples for 10 min at 800 x g (3800 rpm) and analyzed the supernatant in order to measure absorbance at wavelengths of 750 nm and 665 nm (against a blank of 90% acetone). At the same wavelengths, we determined phaeopigments by acidifying the acetone extract with 200 µL of 0.1 N HCl added directly to the cuvette. We dried the remaining sediment at 60 °C for 24 h prior to weighing.

4.3.2.5.3 Lipid content

We extracted frozen lipid samples according to Parrish (1999), a method that required repeating specific steps three times. We used a combination of chloroform:methanol:water (4:2:1.5) in order to create an upper inorganic and a lower organic layer. We were interested in removing and then analysing the bottom organic layer that contained lipids and therefore sonicated the sample for 4 min in an ice bath followed by two minutes of centrifuging. Without disturbing the top aqueous layer, we used a double pipetting technique that required 2 lipid-cleaned Pasteur pipettes, a long 1-ml pipette inside a short 1-ml pipette. We then added chloroform back to the extraction test tube. As a final step, we transferred all of the organic layer into a lipid-cleaned vial, concentrating samples under a flow of nitrogen gas.

4.3.2.5.4 Grain size

Sample analysis at the Bedford Institute of Oceanography, Marine Environmental Geoscience, Nova Scotia, used a Beckman Coulter LS 230 Laser Diffraction analyzer set at a 0.4 – 2000 μm range. Samples were subjected to 35% hydrogen peroxide digestion over several days to remove organic particles, then centrifuged and freeze-dried. After freeze drying, we immediately capped and weighed the vials. Grain size analysis then proceeded on individual samples by first removing the cap and then disaggregating the sample using a metal spoonula before pouring the contents over a 2-mm sieve. The >2 mm material was then weighed at ¼ phi intervals and values recorded. The <2 mm fraction was either used in its entirety or microsplit for analysis in the Beckman Coulter LS13-320 laser diffraction analyzer. Samples were then disaggregated completely in an ultrasound bath before they were introduced into the laser diffraction analyser; daily control samples ensured consistency. Samples were analyzed for a full 60 s and graphed based on size. Laser files were logged and processed using Femto Particle Sizing

Software (PSS) version 5.6. Laser diffraction data was then merged with the gravel fraction to normalize the distribution. PSS uses Folk and Ward graphic statistical parameters based on phi midpoints and a geometric mean. Sediments at each station were classified following the sediment classification scheme based on percentages of sand, silt, and clay (Wentworth, 1929).

4.3.3 Data analysis

All statistical analyses used R software.

We initially examined spatial variation in infaunal density per core among sites (NEC1 (Northeast Channel 1), KHM (Kinlan-Heezen Inter-canyon), P-M (Powell-Munson Inter-canyon), C-T (Corsair Tributary Canyon), and then compared the three different environments (Channel, Inter-canyon, and Canyon) using one-way ANOVA with all cores. However, homogeneity (Shapiro test) was not met in both cases, therefore we performed a non-parametric test (Kruskal-Wallis test), after trying log and sqrt transformations of our response variable.

In order to investigate variation in multivariate taxonomic community composition, indices (species richness, Shannon-Wiener, Simpson, Pielou's) and functional indices (functional richness, evenness, divergence) among our studied habitats (three levels: Canyon, Inter-canyon, Channel), we ran two separate (one for community composition and one for taxonomic and functional indices) Permutational Multivariate Analysis of Variances (PERMANOVA). This analysis used the "adonis2" function (McArdle and Anderson, 2001) with 9999 random permutations of appropriate units. We calculated resemblance matrices from Euclidean distances of standardized diversity indices and functional diversity indices, and based on Bray-Curtis dissimilarities of benthic community data. We verified homogeneity of multivariate dispersion using the PERMDISP routine (Anderson et al., 2008). We further analysed significant terms within the full models using appropriate pair-wise comparisons. Non-metric multidimensional scaling

(nMDS) ordinations of similarity matrices provided visualizations of multivariate patterns, and we determined taxa that contributed most to within site similarity and dissimilarity between sites using SIMPER (Similarity percentage analyses) (Clarke 1993). In addition, in order to provide a better understanding of which environmental variables could best explain benthic community variation among habitats, we performed a redundancy analysis (RDA – through the "rda" function) with a type II scaling that focuses on the explanatory variables rather than response variables. We transformed our data based on a Hellinger transformation prior to the RDA using the "decostand" function in R. We further analysed multi-collinearity of predictor variables from the full models with a variance inflation factor (VIF) test using the "vif" function from the "car" package (Fox et al., 2012). All predictor variables from the selected best model had a VIF < 10 (Zuur et al., 2009). We also calculated the significance (%) of each predictor variable for both benthic community and benthic flux variation with the "vartest" function (Borcard et al., 2018).

We investigated variation in benthic nutrient fluxes for each nutrient (ammonium, nitrate, silicate, and phosphate) focusing on control incubated cores from each habitat type and using one-way ANOVA with the fixed factor "Habitat". We first examined data normality visually with Q-Q plots and, noting that visual inspection can be unreliable, we also ran a Shapiro-Wilk's test (p-value > 0.05). Levene's tests evaluated homogeneity of variance of the residuals. When data failed to meet homogeneity of variances assumption, we conducted a non-parametric Kruskal-Wallis test.

To test for differences in single nutrient fluxes between enriched and control cores for Inter-canyon habitat, we used a t-test with the fixed factor "treatment" (2 levels). Exclusion of outliers did not change our results. Therefore, we retained outliers, noting the low number of observations

per nutrient. Due to the very small sample size for our Canyon habitat sites (enriched n = 3; control n = 2), we ran a non-parametric two-sample Wilcoxon test.

We also performed multiple linear regression models to understand better the relationship between each single nutrient and the environmental variables included in our study, and to determine the best combination of environmental drivers for each specific benthic flux.

To understand OM addition effect on benthic nutrient fluxes, we then compared variation in benthic nutrient fluxes for each nutrient among treatments (2 levels: enriched and control) separately for each of our study habitats (Canyon, Inter-canyon, Channel), using a Student's t-test. Once again, we retained all samples, including outliers, to avoid loss of observations. Moreover, we performed a multivariate analysis of variance (two-way crossed PERMANOVA) with 9999 random permutations to test for benthic flux spatial variation and treatment effect among habitat, with the factor "Habitat" (Three levels, fixed: Canyon, Inter-canyon, Channel, crossed with "Treatment" (two levels, fixed: control and enriched), and their interaction. We calculated the resemblance matrices from Euclidean distances of standardized benthic flux and diversity indices, and from Bray-Curtis distances of benthic community data. We verified homogeneity of multivariate dispersion using the PERMDISP routine (Anderson et al., 2008), and further analysed significant terms within the full models using appropriate pair-wise comparisons. Non-metric multidimensional scaling (nMDS) ordinations of similarity matrices visualized multivariate patterns and SIMPER analysis determined taxa that contributed most to within site similarity and dissimilarity between.

Once we established significant differences from PERMANOVA analysis, we also examined relationships between our response variables (benthic nutrient fluxes) and explanatory variables (environmental, biological) using two separate redundancy analyses with type II scaling.

Specifically, the RDA approach considered all benthic fluxes from both enriched and control cores within the same analysis to determine the best combination of environmental drivers for all benthic fluxes. For each RDA, we followed the same steps descripted above.

4.4 Results

4.4.1 Spatial patterns in Gulf of Maine benthic communities

We ran 23 incubations that spanned five different sites where we identified a total of 365 macrofaunal individuals. The most abundant class, the Polychaeta, typically accounted for 77.3% in Northeast Channel 1, 76.1% in Corsair Tributary Canyon, 74.1% in Powell-Munson Inter-canyon, and 73.4% in Kinlan-Heezen Inter-canyon (on average ~73.4% in Inter-canyon habitat), followed by smaller percentages of Crustacea and Bivalvia. Crustacea were slightly more abundant in Channel and Inter-canyon habitats, ~9.2% and ~6,2%, respectively, than Bivalvia in the same habitat, ~4.3% and ~5%, respectively. In contrast, in Canyon habitat Bivalvia represented a slightly higher percentage (10%), than Crustacea, (4%). Spionidae was the most abundant taxon in Corsair Tributary Canyon (33 individuals in all cores combined), whereas Cirratulidae was most abundant in Northeast Channel 1 (25 total individuals), family Paraonidae in Kinlan-Heezen Inter-canyon (58 individuals), and Powell-Munson Canyon (28 individuals). Crustacea was the second most diverse and abundant group with Isopoda as the most abundant taxon in Inter-canyon, and Amphipoda in Northeast Channel 1. The most abundant functional groups in all sampling sites were categorized as surface deposit feeders, surficial modifiers, and freely mobile within the sediment matrix.

Despite variation in abundance among the four sites, our comparisons of macrofaunal abundance in relation to either site (Northeast Channel 1, Kinlan-Heezen Inter-canyon, Powell-Munson Inter-canyon, Corsair Tributary Canyon) or among habitats (Channel, Inter-canyon, and

Canyon) did not differ significantly (Kruskal Test p = 0.45, 0.61, respectively). However, PERMANOVA indicated significant differences in benthic assemblages among the three- studied habitat types (Canyon, Inter-canyon, Channel) (**Supplementary table 4.3**). Pair-wise comparisons showed significant differences between Inter-canyon and Canyon community assemblages (p = 0.004), Inter-canyon and Channel assemblages (p = 0.006), and Canyon and Channel assemblages (p = 0.007) (**Fig. 4.2**). We observed that the families Sphaerodoridae and Flabelligeridae contributed most to Inter-canyon and Canyon differences (6%) (**Supplementary table 4.4**), with greater abundances of Sphaerodoridae in Canyon (13 ind) than in Inter-canyon habitats (2 ind), and simile numeric presence of Flabelligeridae in both habitats (Inter-canyon = 2 ind; Canyon = 3 ind). Furthermore, we observed greater abundances of polychaetes and crustaceans in the Inter-canyon assemblage than in the Channel assemblage. Indeed, dissimilarity between Inter-canyon and Channel macrofauna averaged 19% (**Supplementary table 4.4**), where the polychaete families Paraonidae, Opheliidae, and Scalibregmidae, and amphipod crustaceans contributed most to these differences. However, all of those taxa, except Paraonidae were more abundant in Channel than Inter-canyon cores. Finally, differences between Canyon and Channel assemblages (30%) (**Supplementary table 4.4**) related to greater dominance of some polychaetes and bivalves in Canyon than in Channel habitats, in contrast to crustaceans which dominated Channel habitat. Among polychaete families, Spionidae, Scalibregmidae, Flabelligeridae, Arenicolidae, and Sphaerodidae contributed to the differences, with higher abundance in Canyon than Channel habitat, except for Scalibregmidae. Bivalvia was more abundant in Canyon than Channel cores, while amphipods were more abundant in Channel cores.

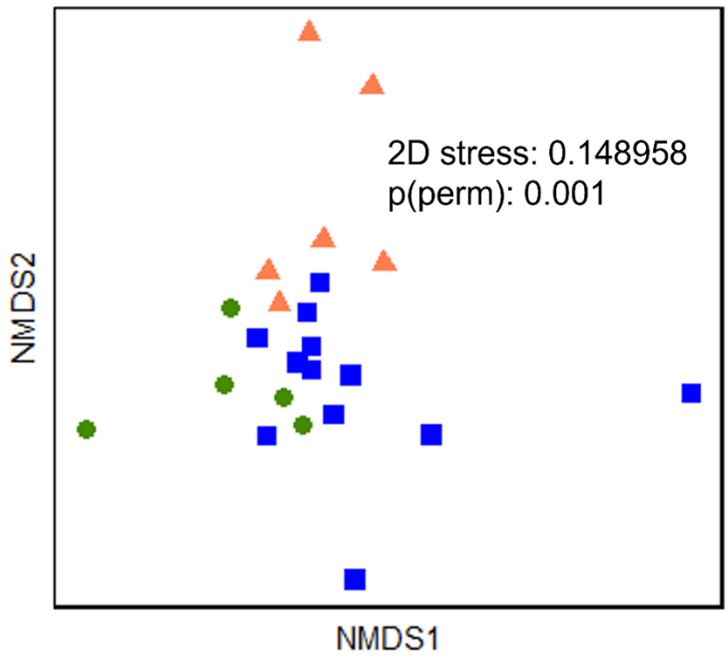

Fig. 4.2. Non-metric multi-dimensional scaling (nMDS) plot of benthic community assemblages sampled in each habitat type. Each dot/triangle/square indicates a single incubated core. Symbols and colours indicate different habitats. Green circles = Canyon (n = 5); orange triangles = Channel (n = 6); blue squares = Inter-canyon (n = 12).

Accordingly, functional diversity differed significantly among habitats (PERMANOVA p value = 0.02), especially between Canyon and Channel cores (pair-wise p value = 0.003). Specifically, SIMPER indicated significant differences in functional richness (p = 0.002) between Canyon (FRich = 0.41) and Channel (FRich = 28.34) cores, and between Canyon and Inter-canyon cores (FRich = 15.13), FEve (p = 0.03), and FDiv (p = 0.03). Similarly, infaunal taxonomic diversity also differed significantly among habitats, (PERMANOVA p value = 0.01), especially between Canyon and Channel (pair-wise p = 0.01), and Inter-canyon and Channel cores (p = 0.007). SIMPER showed significant differences among Canyon and Channel cores, and Inter-canyon and Channel cores in expected number of species (p = 0.005; 0.001, respectively).

4.4.2 Environmental drivers of benthic communities among sites

We aimed at understanding which environmental factors influence Gulf of Maine benthic assemblages. **Tables 4.4, 4.5, and 4.6** summarize the main sedimentary and chemical/physical variables considered and their variation across habitats. However, all the explanatory variables included in our model (ANOVA $p = 0.03$) showed strong multicollinearity (VIF > 10).

Table 4.4. Summary of sedimentary and OM properties measured from non-incubated cores from the three Gulf of Maine habitats, (average ± standard deviation, (Inter-canyon n = 3, Canyon n = 2, and Channel, n = 4)). C:N is carbon to nitrogen ratio, TOC is total organic carbon, TOM is total OM; Chl*a* is chlorophyll *a* concentration, Phaeo is phaeopigment concentration, Chl*a*: Phaeo is the chlorophyll-*a* to phaeopigment ratio, Tot lipids is total lipid concentration in control and enriched incubated cores.

Habitat	C:N	%TOC	Chl*a* ($\mu g \cdot g^{-1}$)	Phaeo ($\mu g \cdot g^{-1}$)	Chl*a*:Phaeo	Tot lipids ($mg \cdot g^{-1}$)
Inter-canyon	6.9 ± 0.7	0.8 ± 0.03	1.3 ± 1.3	20.1 ± 5.5	0.06 ± 0.0	0.5 ± 0.5
Canyon	8.8 ± 0.7	0.8 ± 0.2	2.8 ± 2.8	52.9 ± 56.1	0.05 ± 0.0	0.1 ± 0.0
Channel	20.4 ± 6.5	0.5 ± 0.3	2.4 ± 2.4	31.8 ± 36.4	0.06 ± 0.0	0.1 ± 0.1

Table 4.5. Summary of main sedimentary grain size properties in the three Gulf of Maine habitats (average ± standard deviation based on analysis of 3 sediment cores (Inter-canyon), 2 cores (Canyon), and 4 cores (Channel). % Gravel (>2 mm); % Sand ($0.0625 < x < 2$ mm); % Mud (<0.0625 mm and includes silt ($0.0625 < x < 0.004$), and clay ($0.004 < x < 0.001$)).

Habitat	% Gravel	% Sand	% Mud	% Silt	% Clay
Inter-canyon	1.1 ± 1.8	64.1 ± 7.3	34.8 ± 9.1	24.8 ± 6.6	10.1 ± 2.5
Canyon	1.4 ± 2.0	53.3 ± 17.9	45.3 ± 19.9	33.4 ± 11.3	11.9 ± 8.7
Channel	0.4 ± 0.8	85.0 ± 5.4	14.5 ± 5.2	9.5 ± 3.7	4.9 ± 1.5

Table 4.6. Summary of main chemical-physical properties in bottom water from the three Gulf of Maine habitats (average ± standard deviation). BWO_2 is bottom-water oxygen concentration.

Habitat	Depth (m)	Salinity (PSU)	Temperature (°C)	BWO_2 ($ml \cdot l^{-1}$)
Inter-canyon	965.1 ± 2.7	35.5 ± 0.2	14.3 ± 1.0	8.3 ± 0.3
Canyon	971.1 ± 2.4	35.6 ± 0.0	15.9 ± 0.0	7.58 ± 0.0
Channel	678.4 ± 24.8	35.6 ± 0.0	14.3 ± 0.4	7.8 ± 0.2

4.4.3 Individual benthic nutrient flux variation among habitats

In comparing single nutrient fluxes from incubated replicate cores without enrichment among habitats (ANOVA) we found no significant differences (**Supplementary table 4.5**), acknowledging the unbalanced data set and low statistical power. Average values for each nutrient at each habitat type indicated net influx rates for all five nutrients except for Inter-canyon phosphate (**Fig 4.3 A, B, C, D, E**). Multiple linear regression showed that only oxygen consumption across all habitat types was affected by the environmental drivers considered here.

Highest oxygen consumption occurred in Canyon habitat (-68.0 $mmol \cdot m^{-2} \cdot d^{-1}$ ± 13.8 (SE)), where we obtained data from only two cores (**Fig. 4.3 A**). Similar levels of oxygen consumption

characterized Inter-canyon and Channel habitats (-44.8 ± 23.0 (SE) and -49.0 mmol · m^{-2} · d^{-1} ± 4.7 (SE), respectively). However, we observed consistent oxygen consumption values within each habitat. %TOC and Chl*a* best explained oxygen consumption patterns, with the highest values in Canyon habitat (**Table 4.4**).

We observed net influxes of ammonium into the sediment for each habitat type (**Fig. 4.3 B**), with similar rates for Canyon and Channel habitats (-98.0 µmol · m^{-2} · d^{-1} ± 23.6 (SE) and -88.3 µmol · m^{-2} · d^{-1} ± 44.1 (SE), respectively), with a substantially lower rate, -31.7 ± 79.0 µmol · m^{-2} · d^{-1}, for Inter-canyon habitat which showed net effluxes in cores from the Kinlan-Heezen and Powell-Munson Inter-canyon sites.

We also observed net influx of nitrate into the sediment for each habitat type (**Fig. 4.3 C**). As with ammonium, we observed higher, but similar rates for Canyon and Channel habitats (-1272.5 ± 445.7 (SE) and -1082.7 µmol · m^{-2} · d^{-1} ± 504.8 (SE), respectively) than for the Inter-canyon habitat (-212.1 ± 389.6 (SE) µmol · m^{-2} · d^{-1}). Nitrate influx varied widely among cores from each habitat.

Net silicate influx occurred at all sites (**Fig. 4.3 D**), with similar values for Inter-canyon and Channel habitats, which were more than two times higher than for Canyon habitat (-443.5 ± 43507 (SE), -329.5 ± 168.6 (SE), and -150.1 ± 223.8 (SE) µmol · m^{-2} · d^{-1}, respectively). As with other nutrients, silicate fluxes varied widely among cores from each habitat.

Of the nutrients we examined, only phosphate showed both net influxes and effluxes (**Fig. 4.3 E).** Sediment uptake of phosphate in Canyon and Channel habitats (-87.8 ± 27.4 (SE) and -50.4 ± 12.6 (SE) µmol · m^{-2} · d^{-1}, respectively), contrasted a net release from Inter-canyon habitat (6.88 ± 109.6 (SE) µmol · m^{-2} · d^{-1}). Phosphate also varied widely among cores from each habitat.

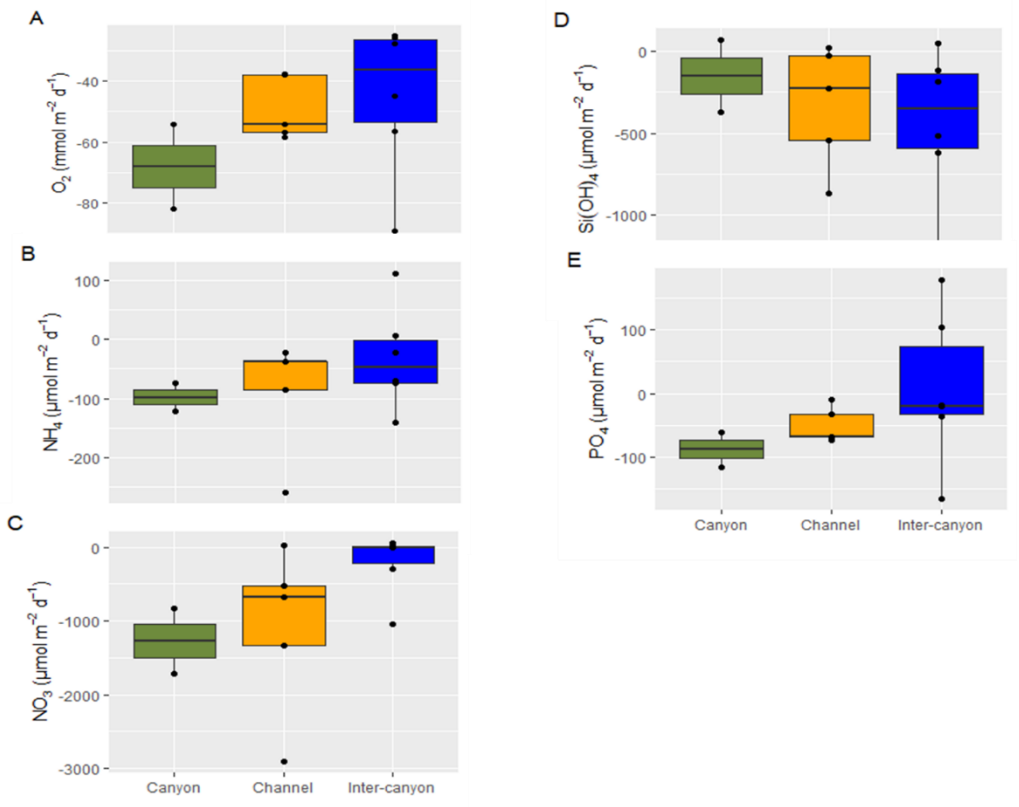

Fig. 4.3. Benthic fluxes of: A) oxygen, B) ammonium, C) nitrate, D) silicate, and E) phosphate from incubated control cores for Canyon (n = 2), Inter-canyon (n = 6), and Channel (n = 5) habitats. 0 along the y-axis indicates where fluxes change from net release from sediment (above 0) and influx into the sediment (below 0). Green box = Canyon; orange box = channel; blue box = Inter-canyon.

4.4.4 Do OM enrichment pulses to the seafloor result in rapid increases in oxygen and nutrient flux rates at each site?

We found significant differences between enriched and control incubations only for nitrate flux for Inter-canyon habitat and phosphate flux for Channel habitat. No significant differences were evident for other nutrients (Student's t-test analysis, **Supplementary table 4.6**).

Following the addition of OM, oxygen consumption rate was higher in enriched than control cores for all habitats (**Fig. 4.4 A**), although with the minimal highest values in Inter-canyon and Canyon habitats. Indeed, we observed average oxygen consumption rates for control and enriched cores of -68.0 mmol $\cdot$ m^{-2} $\cdot$ d^{-1} and -93.5 mmol $\cdot$ m^{-2} $\cdot$ d^{-1}, respectively, for Canyon habitat; -44.8 mmol $\cdot$ m^{-2} $\cdot$ d^{-1} and -47.9 mmol $\cdot$ m^{-2} $\cdot$ d^{-1} for Inter-canyon habitat; and -49.0 mmol $\cdot$ m^{-2} $\cdot$ d^{-1} and -52.45 mmol $\cdot$ m^{-2} $\cdot$ d^{-1} for Channel habitat.

Ammonium influxes were higher in enriched than control cores for all habitat types (**Fig. 4.4 B)**. For Canyon habitat we observed average values of ammonium influx -98.04 µmol $\cdot$ m^{-2} $\cdot$ d^{-1} in control incubations in comparison with -208 µmol $\cdot$ M^{-2} $\cdot$ d^{-1} in enriched incubations, an higher influxes values (-83.7 µmol $\cdot$ m^{-2} $\cdot$ d^{-1}) in enriched cores than control (-31.7 µmol $\cdot$ m^{-2} $\cdot$ d^{-1}) in the Inter-canyon habitat, and similarly, higher values in enriched (-162.0 µmol $\cdot$ m^{-2} $\cdot$ d^{-1}) than control cores (-88.3 µmol $\cdot$ m^{-2} $\cdot$ d^{-1}) in the Channel habitat. However, one Inter-canyon and Channel habitat enriched core showed net ammonium effluxes.

OM addition resulted in higher influxes of nitrate than control cores only for Inter-canyon habitat, where we observed average values (-443.5 µmol $\cdot$ m^{-2} $\cdot$ d^{-1}) in enriched cores in comparison to control cores (-212.1 µmol $\cdot$ m^{-2} $\cdot$ d^{-1}). Control cores also yielded the highest average values of nitrate influxes for all other habitats. For example, -1272.5 µmol $\cdot$ m^{-2} $\cdot$ d^{-} nitrate flux in the control treatment for Canyon habitat contrasted -776.3 µmol $\cdot$ m^{-2} $\cdot$ d^{-1} in the enriched treatment, and control treatments from Channel habitat of -1082.7 µmol $\cdot$ m^{-2} $\cdot$ d^{-1} contrasted -682.4 µmol $\cdot$ m^{-2} $\cdot$ d^{-1} in the enriched treatment (**Fig. 4.4 C**).

Silicate and phosphate were the only nutrients with higher effluxes in enriched treatments than control. Specifically, silicate effluxes for control and enriched treatments were -150.1 µmol $\cdot$ m^{-2} $\cdot$ d^{-1} and 20.4 µmol $\cdot$ m^{-2} $\cdot$ d^{-1}, respectively, for Canyon habitat and -329.5 µmol $\cdot$ m^{-2} $\cdot$ d^{-1} and 340.4

µmol · m^{-2} · d^{-1}, respectively, for Channel habitat. In contrast, we observed silicate influxes for Inter-canyon habitat both in control and enriched treatments, with -443.5 µmol · m^{-2} · d^{-1} and -723.1 µmol · m^{-2} · d^{-1} values, respectively (**Fig. 4.4 D**).

Phosphate efflux rates were higher after OM addition than control cores for all sampled habitats. The average efflux value of -87.8 µmol · m^{-2} · d^{-1} for the Canyon control treatment contrasted 54.5 µmol · m^{-2} · d^{-1} influx for the enriched treatment. We also observed high phosphate efflux in comparing control cores (6.8 µmol · m^{-2} · d^{-1}) and enriched cores (26.1 µmol · m^{-2} · d^{-1}). In contrast, phosphate influx in the control treatment for the Channel habitat (-50.3 µmol · m^{-2} · d^{-1}) switched to net efflux for the enriched treatment (194.8 µmol · m^{-2} · d^{-1}) (**Fig. 4.4 E**).

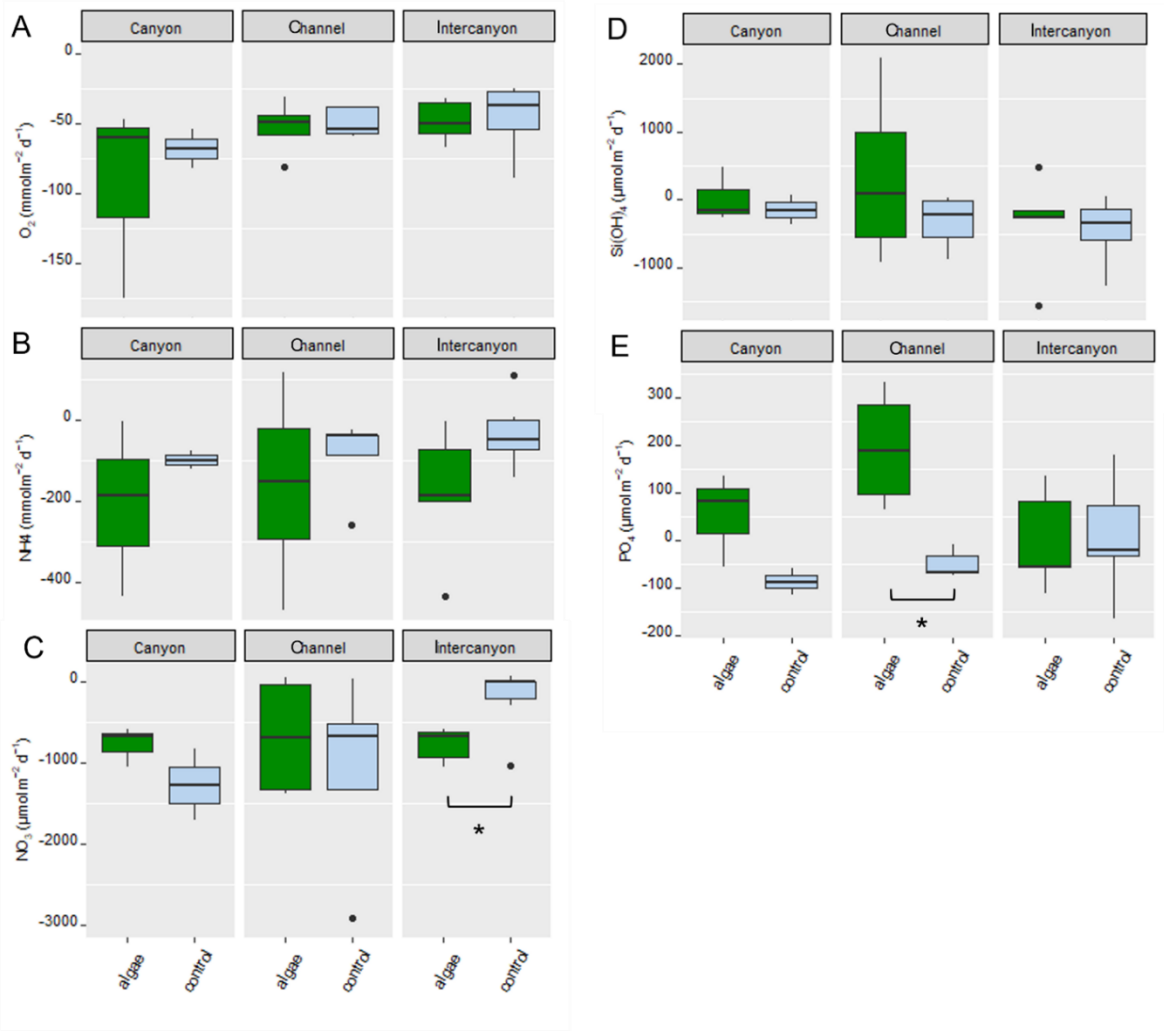

Fig. 4.4. Average values for: A) oxygen consumption, B) ammonium, C) nitrate, D) silicate, and E) phosphate fluxes ($\mu mol \cdot m^{-2} \cdot d^{-1}$), in enriched (green box) and control (light blue box) cores for each habitat (Canyon (enriched n = 3; control n = 2), Inter-canyon (enriched n = 5; control n = 6) and Channel (enriched n = 4; control n = 5)). Positive values indicate effluxes and negative values indicate influxes. Black dots indicate outliers. Asterisks indicate significant differences in Student t-test analysis between enriched and control cores in a given site.

4.4.5 Benthic nutrient fluxes among habitats and treatments

PERMANOVA indicated no significant differences in benthic fluxes among habitats in enrichment experiments (P (perm) = 0.38, treatments (P (perm) = 0.45) or their interaction (P (perm) = 0.40) (**Supplementary table 4.7, Fig. 4.5)**.

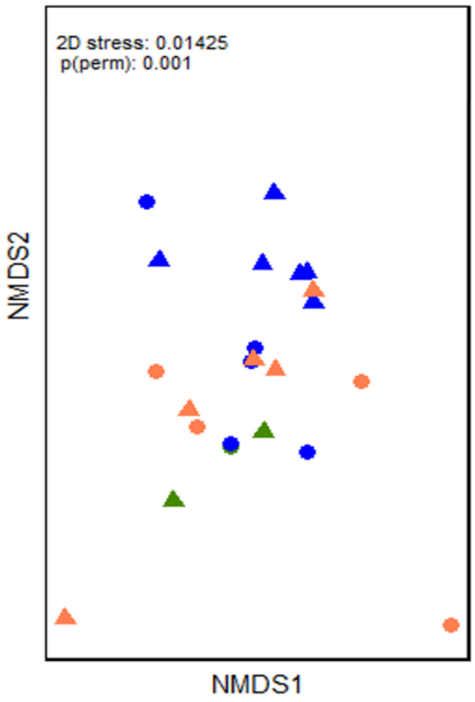

Fig. 4.5. nMDS plot of oxygen consumption and benthic fluxes (ammonium, nitrate, phosphate, and silicate) for each habitat type based on Euclidean similarity. Each dot indicates a single enriched core (Canyon n = 3; Inter-canyon n = 5; Channel n = 4), whereas each triangle

indicates a single (unenriched) control core (Canyon n = 2; Inter-canyon n = 6; Channel n =5). Colours indicate different habitats: green = Canyon; orange = Channel; blue = Inter-canyon.

4.4.6 Biological and environmental drivers of benthic nutrient fluxes

We performed two RDA models that included enriched and control cores in relation to environmental (C:N, %TOC, Chl*a*Phaeo, Tot_lipids, Depth, %Gravel, %Sand, %Mud, %Silt, %Clay, Salinity, Temperature, pH, O_2W), and biological factors (FRich, FEve, Fdiv, S, H, J, Simpson, ES[25]), respectively, because of the non-significant results from the PERMANOVA analysis. However, both RDA models were not significant (anova.cca p = 0.49; 0.51, respectively). We therefore did not examine contributions of axis and explanatory variables.

4.5 Discussion

The spatial heterogeneity of our sampling area influenced benthic community composition, and functional and taxonomic diversity, but not infaunal abundance, and benthic nutrient fluxes. Specifically, Canyon and Channel habitats differed in species composition, functional richness, and expected number of taxa, as did Inter-canyon and Channel assemblages, and Canyon and Inter-canyon communities in FRich. The limited explanatory power of the environmental variables included in our analysis in describing community structure and natural benthic nutrient fluxes points to the importance of variables not included in our study. However, nutrient influxes into sediments generally characterized our habitats, except for phosphate in Inter-canyon habitat. High functional richness (FRich) in Channel and Inter-canyon habitats, in contrast to the Canyon site, suggests some degree of niche differentiation among the two habitats, which limits food competition, but that the biota may lack specific trait types that differentially enhance nutrient regeneration. Furthermore, the OM enrichments in our incubations partially influenced benthic nutrient fluxes as a proxy of OM remineralization rates in our habitats. Gulf of Maine sedimentary

communities remineralized and regenerated silicate and phosphate, noting net effluxes in all habitats except for Inter-canyon habitat where we observed silicate influxes. Oxygen consumption in enriched cores differed little from control incubations and, of the environmental variables measured, oxygen consumption patterns related mostly to %TOC and Chl*a*.

4.5.1 Spatial variation in benthic community composition

Our analyses showed no significant differences in abundance among the three sampled habitats (Canyon, Inter-canyon, and Channel), but significant differences in benthic community composition, and functional and taxonomic diversity. A more distinct benthic assemblage characterized Canyon and Channel habitats given the higher average dissimilarities (30%) between those two habitats compared to others (Canyon, Inter-canyon dissimilarities = 6%; Inter-canyon, Channel dissimilarity = 19%). High abundance of surface deposit-feeders Spionidae in Canyon habitat may reflect their ability to switch feeding behavior between suspension and deposit feeding depending on environmental conditions, especially in environments with varying flow characteristics such as canyons (Taghon et al., 1980). These contrasting community assemblages parallel De Leo et al. (2014), who reported different macrofaunal composition between canyon and slope sites off the Hawaiian Islands, and higher abundance of spionid in canyon than slope sites. In addition, the family Ophelidae that contributed to Inter-canyon and Channel differences in our study includes opportunistic (Gunton et al., 2015) species that take advantage of "pioneer" niches and re-establish chemical-physical conditions in disturbed sediment. These species, which were more abundant in Channel than Inter-canyon assemblages, might increase efficiency of resource use and thus increase ecosystem function, potentially explaining higher functional richness in Channel habitat than the other two habitats, and thus a higher degree of niche differentiation and reduced competition (Mason et al., 2005). If true, this explanation would

suggest that biota in Channel habitats may utilize resources more efficiently than the Inter-canyon and Canyon habitats in our study. In other words, our data support the assertion that Channel sites represent heterogeneous habitats that support a high level of resources and high diversity (Vetter, 1998; De Leo et al., 2010). Moreover, those results may enhance the role that the NE Channel plays in funneling nutrients into the Gulf of Maine from cold-water masses (Christensen et al., 1996). Consequently, NE Channel presumably provide more nutrients to its community than the rest of the Gulf.

The lowest functional diversity indices (FRich, FEve, FDiv) that characterized our Canyon habitat might be interpreted as indicative of an environment with low differentiation of biological traits and low use of available resources. This result is interesting given general recognition of canyons as mostly heterogeneous, highly vulnerable, and high biodiversity environments (Tyler et al., 2009; De Leo et al., 2010; De Leo et al., 2014).

Surprisingly, the environmental variables included in our study did not explain much of the variation in community structure among the three habitats, despite inclusion of OM, grain size, temperature, and other variables. OM quantity and quality often strongly influence deep-sea benthic community structure (Baldrighi et al., 2013; Campanyà-Llovet et al., 2018; Miatta and Snelgrove, 2021b). The multicollinearity observed from our analysis, in combination with low sample size, complicate efforts to evaluate how individual environmental factors influence communities, but a substantial body of evidence shows that environmental gradients may alter geographic patterns of diversity by influencing local processes such as predation, resource partitioning, competitive exclusion, and facilitation that determine species coexistence (e.g., Valladares et al., 2015). Deep-sea species diversity remains a vital question in comparing geographic patterns and evaluating their potential causes. The macrofauna of the Northwestern

Atlantic region tends to follow unimodal patterns of diversity with depth (Levin et al., 2001), and factors not included in our study, such as current speed, surface ocean productivity, and seasonality could affect benthic community structure (Loubere, 1991, 1998). Moderate currents can enable settlement of organic material that can enhance larval supply, macrofaunal diversity, and abundance (Levin et al., 2001). Strong currents (~ 25 $cm \cdot s^{-1}$) often reduce diversity by reducing habitat heterogeneity (Levin et al., 2001).

4.5.2 The role of sediments for Gulf of Maine macrofauna

Of the response flux variables considered in our study no single nutrient related closely to our environmental predictors. Only oxygen uptake linked to our environmental variables, in this case %TOC and Chl*a*, confirming its use as a proxy of benthic OM remineralization rate and as a measure of benthic ecosystem function (Glud, 2008; Hensen et al., 2006; Wenzhöfer and Glud, 2002). In our study, oxygen consumption rates were high compared to previous studies conducted in different deep oceans, in that they reached a value of -10 $\mu mol \cdot m^{-2} \cdot d^{-1}$ (e.g., Belley and Snelgrove, 2017). Moreover, of the three habitats we examined, the highest consumption rates occurred in Canyon habitat, where we also observed the highest %TOC and Chl*a*. Thus, increased organic matter likely resulted in increased oxygen consumption capacity, closely aligning with Caffrey et al. (1993). Moreover, Epping et al. (2002), showed that re-oxidation of reduced compounds (e.g., Fe^{2+}, Mn^{2+}, HS^{-}/H_2S) is the dominant oxygen consuming process in canyons (Nazar Canyon in their case), accounting for 40–50% of total oxygen flux. However, the percentage tends to decrease with increasing depth. Glud and Blackburn, (2002) and Epping et al. (2002) both showed that disturbance of sediment structure during core recovery and improper establishment of *in-situ* conditions during onboard measurements might result in overestimates in

ex-situ O_2 measurements. Therefore, we interpret our data with caution, noting the importance of the methodology (*in-situ* vs. *ex situ*) used to measure oxygen and nutrient fluxes.

The marine nitrogen cycle represents one of the most complex biogeochemical cycles in the ocean (Gruber, 2008), with a critical role in pelagic-benthic coupling. Once OM reaches oxygenated sediment, nitrification results in the formation of nitrate and nitrite as proxies of OM remineralization. However, we observed the opposite pattern with influxes of both ammonium and nitrate into sediments indicative of consumption of both nitrogen forms in all our habitat types. The high level of phaeopigments and low concentrations of Chl*a* suggest that we sampled post-OM seasonal input. Accumulation of phytodetritus on sediments can lead to oxygen and nitrogen consumption and thus denitrification. Link et al. (2013) noted the tendency for sediment uptake of nitrate during periods of low dissolved oxygen in the overlying water and high nitrite concentration. We cannot comment on nitrite concentrations in bottom waters at the sites in general, but we do note nitrogen consumption was highest in our Canyon habitats where we recorded the highest oxygen consumption. In addition, nitrogen fluxes might also link to the exchange of cold, fresh, and low-nutrient deep-water masses from the Labrador Sea slope (Christensen et al., 1984, 1987) that characterizes the western Gulf of Maine. However, our sampling did not focus on the same locations as a previous study in the Gulf of Maine region, and in a different year, showing a contrasting role of sediments for nitrogen fluxes (Miatta and Snelgrove 2021b). Our results suggest that over a broad scale Gulf of Maine sediments may act as a nitrogen sink during the summer season, retaining nitrogen and contributing to a low C:N ratio in Canyon and Inter-Canyon habitats, some of which is buried. In contrast, terrigenous organic matter and lower retained nitrogen in sediments related to its high C:N ratio might influence Channel habitat (Meyers, 1994).

Silicic acid, a major ocean nutrient, largely forms in deep-sea sediment through the dissolution of opal-A that reaches the seafloor. We therefore expected to see silicate effluxes from deep-sea sediments but instead observed silica influxes into sediments in all three of our habitat types However, none of the environmental variables explained the observed silica influxes. Furthermore, Varkouhi and Wells, (2020) reported that local consumption of silicic acid trapped in sediments enhances the development of a diagenetic transition zone in which biogenic silica transformation into diagenetic opal (opal-CT) offers a potential energy resource. At a smaller scale of individual cores, we observed some instances of low silica efflux, supporting the idea of sediments as a source of silica that becomes a sink at the habitat-scale. In short, Gulf of Maine sediments apparently represent a silicate sink in summertime.

Increasing rates of OM consumption or the presence of recent OM settling on the sediment may enhance phosphate fluxes. In our study, we observed phosphate uptake by the sediment in Canyon and Channel habitats, in contrast to phosphate release by Inter-canyon sediments. Phosphate fluxes usually relate to ferric iron in the sediment and more effective sediment oxygenation. Greater oxygenation of sediment by bioturbation and bioirrigation results in greater phosphate absorption by ferric iron (Ingall and Janke, 1994; Hensen et al., 2006).

In conclusion, excess OM in sediments following post-phytodetritus input may have characterized our sampling habitats, given high values of phaeopigments and total organic carbon content. Effectively, Miatta and Snelgrove, (2021b) also showed similar sediment %TOC values when referring to sites with similar depths of ours, such as Corsair Canyon in the Gulf of Maine. Partial use of OM and its potential burial in sediment may have increased oxygen consumption and activated denitrification. Once again, our study points to sediments in these Gulf of Maine habitats as nutrient sinks at the habitat scale.

4.5.3 Do OM enrichment pulses to the seafloor result in rapid increases in oxygen and nutrient flux rates at each site?

OM supply partially influenced benthic nutrient fluxes as a proxy of OM remineralization rates. Gulf of Maine sediments remineralize and regenerate silicate and phosphate, given our observation of effluxes in all habitats, except Inter-canyon habitat where we observed net silicate influx. Oxygen consumption in algae-enriched cores was higher by 24.5 mmol O_2 $m^{-2}{\cdot}d^{-1}$ compared to control incubations, with net ammonium and nitrate influxes into sediments in control and enriched incubated cores. The difference in oxygen consumption rates between the two treatments parallel organic enrichment experiments by Caffrey et al. (1993), who reported higher oxygen consumption in enriched treatment (-70 mmol $m^{-2}{\cdot}d^{-1}$) than control (30 mmol $m^{-2}{\cdot}d^{-1}$), as well as denitrification, and reduced nitrification. However, we note they based their findings on long-term experiments. We therefore suggest that nitrification-denitrification coupling might characterized sediments in our habitats, partially explaining nitrogen influxes. Effectively, Ciraolo and Snelgrove (2023) focused on benthic microbial communities at this same location and documented high abundances of bacteria and archaea specifically involved in nitrogen cycling.

4.5.4 Biological and environmental drivers of Gulf of Maine nutrient flux

Benthic nutrient fluxes, whether single or overall nutrient fluxes, did not vary significantly among our Canyon, Inter-canyon, and Channel habitats, indicating little effect of spatial heterogeneity on OM remineralization. We generally observed nutrient uptake by sediments, except for low levels of phosphate efflux in our Inter-canyon habitat. However, the biological and environmental variables in our study did not yield predictive models that explained variation in benthic nutrient fluxes. The lack of other studies measuring benthic nutrient fluxes in canyon, inter-canyon, and channel habitats limits our capacity to contrast our findings with other regions,

and points to the need for more studies investigating benthic processes in these environments. Miatta and Snelgrove, (2021b) focused on benthic nutrient fluxes in canyon and inter-canyon habitats of the Gulf of Maine. Interestingly, their benthic nutrients fluxes did not show clear differences among their studied habitats, but they showed more effluxes than influxes compared to our study, except for ammonium and nitrate. We clearly cannot fully compare nutrient fluxes result between the two studies, but we can infer that C:N and %TOC may provide a clue. The C:N and %TOC values in Miatta and Snelgrove, (2021b) study were notably higher (more than twice as much) than ours in both habitat types. Other studies point to the importance of quantity and quality of OM as a driver of benthic oxygen and nutrient fluxes variation (Caffrey et al., 1993; Belley and Snelgrove, 2016). The small sample size in our study potentially affected our results, particularly given the complexity of biogeochemical processes in marine sediments (Hall et al., 1996).

In terms of biological variables, previous studies (e.g., Belley and Snelgrove, 2016 although focused on shallow water) highlighted the greater importance of functional diversity indices of a community than taxonomic diversity in determining ecosystem functioning (Goswami et al., 2017; Song et al., 2014), such as nutrient fluxes. However, our RDA results did not align with these findings, likely reflecting several aspects of our approach. Lack of data on trait expression for certain taxa, lack of information on potentially important traits (e.g., bioirrigation, biodeposition), and the use of literature trait data rather than direct observation may have influenced our results, as reported by Link et al. (2013) and Miatta and Snelgrove (2021a,b). However, given the clear dominance of sediment nutrient influxes in our study, the high FRich in Channel and Inter-canyon (P-M) sites, but low FRich at the other site, and relatively high FEve and FDiv values among all habitats, we suggested that the communities might lack the specific functional traits required to

enhance nutrient re-generation or that the functional traits present tend to enhance fluxes into rather than from the sediment. Indeed, high functional richness (FRich) value, indicates community use of resources available in the environment (Channel and Inter-canyon (P-M) sites), whereas high FDiv values suggest a high degree of niche differentiation and low resource competition across habitats compared to others (Villéger et al., 2008). This interpretation might explain why we mostly observed nutrient influxes at a broader scale than effluxes. The greater influence of functional indices on benthic flux variation than measures of species diversity (Belley and Snelgrove, 2016) points to great importance of functional traits of a community than taxonomic diversity in determining functions, and that communities with multiple niches, but with functional characteristics that cannot fully take advantage of local conditions, do not necessarily enhance or differentiate benthic nutrient effluxes across habitats. Moreover, because the biological drivers we included in our study did not explain much of the total variance in benthic nutrient fluxes, we suggest that different biological variables such as subtle differences in macrofaunal bioturbation could play a critical role in nutrient cycling at the sediment-water interface (Foshtomi et al., 2015).

The second multivariate RDA did not allow us to select some environmental factors among bottom water characteristics, quality of OM, and sediment characteristics that could explain our nutrient fluxes. The difficulty in identifying any explanatory variables points out the complexity of processes occurring in marine sediments, which also complicates understanding them and our ability to identify their patterns clearly (Hall et al., 1996). Moreover, our results contrasted Miatta and Snelgrove's (2021b) study, which identified grain size (especially, the percentage of gravel) and bottom water oxygen as explanatory variables of nutrient fluxes at canyon and inter-canyon of the Gulf of Maine. Interestingly sandy sediment that characterized our habitats did not explain nutrient fluxes as much as the percent gravel in Miatta and Snelgrove (2021b). Nevertheless, both

gravel and sand are permeable sediments that may affects solute transport (e.g., dominance of porewater advection in gravel and sand and dominance of molecular diffusion in muddy sediments (Janssen et al., 2005). Moreover, among our variables, temperature could also affect our nutrient fluxes. Temperature plays a dual role in nutrient fluxes, in influencing phytoplankton blooms in surface waters (Friedland et al., 2023) and promoting bacterial production (Cammen, 1991), and metabolic activities of most organisms (Lomas et al., 2002), which then influences benthic nutrient rates. Whereas warming may favour bacterial activity in the deep sea, warming of surface waters can increase stratification and thereby change the availability of nutrients to surface phytoplankton, or influence the surface mixed layer depth, and affect overall benthic-pelagic coupling. Friedland et al. (2023) observed a change in autumn bloom timing in the Georges Bank ecoregion, where bloom initiation has shifted from late September to late October between 1998 and 2020. Bloom duration in this ecoregion also shortened from ~7.5 to 5 weeks. Accordingly, although we cannot directly link surface warming to our deep nutrient fluxes, we might infer an influence of climate change on nutrient flux pattern. Moreover, Belley et al. (2016) identified bottom water temperature as the primary environmental driver of benthic fluxes in comparing the shallow Salish Sea and deeper sites of the Northeast Pacific. Alonso-Perez et al. (2014) also identified bottom temperature as a significant influence on benthic nutrient fluxes, although they focused on sediments from coastal upwelling regions with relatively limited seabed temperature ranges (12.4-15.1 °C), noting little temperature variation among our habitats (14.3-15.9 °C). Once again, we cannot fully assess how temperature influenced fluxes in our study, however, temperature could exert effects at the scale of sites, noting among-site differences in flux rates. Additionally, the diatoms that dominate the spring bloom in the Gulf of Maine (Townsend et al., 2005, 2006), may influence regional silicate fluxes as large number of diatom frustules reach the seafloor. Currents tend to transport

silica from the NE Channel to the central Gulf of Maine, which differ in nitrate fluxes from sediments (Zang et al., 2022). Switzer et al., (2020) also observed accumulation of silica in deep waters (below 200 m) at sampling sites below locations of high primary production and bottom depths sufficiently shallow that detritus from surface waters might reach the seafloor and deep enough that it accumulates. The same study also focused on the role that density stratification near the seafloor in Wilkinson Basin might play in nutrient cycling. They hypothesized that stratification might reduce mixing of particulate material into the water column, recycling, or export elsewhere, and could exert effects at the scale of sites, noting among-site differences in flux rates. Additional factors that we did not measure but could also contribute to benthic flux variation include sediment resuspension (Niemistö et al., 2018), bio-irrigation (Archer and Devol, 1992), bacteria activity (Jørgensen and Boetius, 2007; Fuerst and Sagulenko, 2011; Hoffman et al., 2020). In contrast, environmental variables emerged as good predictors of oxygen consumption, and a proxy of OM remineralization as well as benthic nutrient fluxes.

4.6 Conclusions

Our study showed that habitat heterogeneity plays a role in determining variation in benthic community assemblages, functional and taxonomic diversity, in canyon and non-canyon habitats of the Gulf of Maine, where deposit feeders, surficial modifiers, and freely mobile organisms within the sediment matrix dominated the macrofauna. Moreover, habitat heterogeneity apparently had little influence on benthic nutrient fluxes, although small sample size may have influenced our results. We observed no direct effect of functional and taxonomic diversity on nutrient fluxes, indicating the complexity in understanding marine sediment biogeochemical processes and identifying their patterns.

The sediments at our study area may function more as a nutrient sink than nutrient source. Indeed, the sediments actively removed bioavailable nutrients from the system through nutrient influx into the sediment, except for phosphate at the Inter-canyon habitat. This finding challenges the view of Gulf of Maine sediments as consistent nutrient providers through mineralization of OM.

4.7 Author contributions

Alessia Ciraolo conducted the literature review, the empirical analysis, and wrote the manuscript. Paul Snelgrove helped to formulate the ideas, content, and structure of the manuscript and provided editorial guidance.

4.8 Acknowledgments

We thank Chief Scientist Dr. Martha Nizinski, Dr. Anna Metaxas, and crewmembers of the NOAA ship Henry B. Bigelow for ship logistic and sampling opportunities. We also thank Jeanette Wells (Memorial University) who helped with lipids analysis; Dr. Barbara Neves (Fisheries and Oceans Canada (DFO)) for assistance with phytopigment analysis, Dr. Owen Brown (Natural Resources Canada) for help with grain size analysis, Dr. Gary Maillet and Gina Doyle (DFO) for help with benthic nutrient analysis, and one anonymous reviewer for providing helpful comments on an earlier draft of this manuscript. We also thank the School of Graduate Studies at Memorial University for additional financial support. The National Oceanic and Atmospheric Association (NOAA) and the Natural Sciences and Engineering Research Council of Canada (NSERC) sponsored this research.

4.9 Supplementary tables

Supplementary table 4.1. Coring strategy at each station. “Total cores” refers to total number of cores collected at each station. Subsequent four columns refer to numbers of incubated cores

processed for taxonomy (enriched and control), and for nutrient analysis (enriched and control). Finally, "Non-Incubated" refers to numbers of non-incubated cores dedicated to organic matter analysis.

		Incubated				**Non incubated**
Site Name	**Total cores**	**Taxonomic Identification**		**Nutrient fluxes**		**OM**
		Enriched	Control	Enriched	Control	
NE Channel 2 (NEC2)	6	/	/	1	3	2
NE Channel 1 (NEC1)	8	3	3	3	2	2
Kinlan-Heezen Mid Inter-canyon (KHM)	8	3	3	3	3	2
Powell-Munson Inter-canyon (P-M)	7	3	3	2	3	1
Corsair Tributary Canyon (C-T)	7	3	2	3	2	2

Supplementary table 4.2. Functional traits used for each taxon. Phylum: "C" = Crustacea; " M" = Mollusca; "E" = Echinoidea; "A" = Annelid; Class: "MA" = Malacostraca; " OC" = Oligocostra; "B" = Bivalvia; "G" = Gastropod; "S" = Scaphopoda; "OP" = Ophiuroidea; " OL" = Oligochaeta; "P" = Polychaeta. Functional trait: Movement (FT;LM;FMSM;FMBS), Reworking types (E;S;UC;DC;B;R); Feeding type (C;D;F;O;P;S).

Phylum	Class	Order	Family	FT	LM	FMSM	FMBS	E	S	UC	DC	B	R	C	D	F	O	P	S
C	MA	Amphipoda		1	0	0	0	0	1	0	0	0	0	0	0	0	1	0	0
C				0	0	0	0	0	0	0	0	0	0	0	0	0	1	0	0
C	MA	Cumacea		0	0	1	0	0	1	0	0	0	0	0	0.33	0.33	0	0	0.33
C	MA	Isopoda		0	0	1	0	0	1	0	0	0	0	0.33	0	0.33	0	0.33	0
C	OC	Ostracoda		0	0	1	0	0	1	0	0	0	0	0	0	1	0	0	0
M	B			0	1	0	0	0	1	0	0	0	0	0	0	1	0	0	0
M	G			0	0.5	0.5	0	0.5	0.5	0	0	0	0	0.33	0	0.33	0.33	0	0
M	S			0	1	0	0	0	0	0.5	0.5	0	0	1	0	0	0	0	0
E	OP			0	0	0	0	0	0	0	0	0	0	0	0	0	0	0	1
A	OL			0	0	1	0	0	0	0	0	1	0	0	0	0	0	0	1
A	P		Ampharetidae	0	1	0	0	0	0	0.5	0.5	0	0	0	1	0	0	0	0
A	P		Aphroditidae	0	0	1	0	0	0	0	0	1	0	1	0	0	0	0	0
A	P		Apistobranchidae	0	0	1	0	0	0	0	0	1	0	0	1	0	0	0	0
A	P		Arabellidae	0	0	1	0	0	0	0	0	1	0	0	1	0	0	0	0
A	P		Arenicolidae	0	1	0	0	0	0.5	0.5	0	0	0	0	0	0.5	0	0	0.5
A	P		Bogoeidae	0	1	0	0	0	1	0	0	0	0	0	0	1	0	0	0
A	P		Capitellidae	0	1	0	0	0	0	1	0	0	0	0	0	0	0	0	1
A	P		Cirratulidae	0	1	0	0	0	1	0	0	0	0	0	0.5	0	0	0	0.5
A	P		Cossuridae	0	0	1	0	0	1	0	0	0	0	0	0	0	0	0	1
A	P		Dorvilleidae	0	0	1	0	0	0	0	0	1	0	0	0	0	0	0	1
A	P		Echiuridae	0	1	0	0	0	0	0	1	0	0	0	0	1	0	0	0
A	P		Eunicidae	0	0	0	0	0	0	0	0	0	0	0.5	0	0.5	0	0	0
A	P		Flabelligeridae	0	1	0	0	0	0	1	0	0	0	0	0.5	0.5	0	0	0
A	P		Glyceridae	0	0	1	0	0	0	0	0	1	0	0.33	0.33	0	0	0	0.33
A	P		Hesionidae	0	0	1	0	0	0	0	0	1	0	0	0	0	1	0	0

A	**P**		**Lumbrineridae**	**0**	**0**	**1**	**0**	**0**	**0**	**0**	**0**	**1**	**0**	**0.5**	**0**	**0**	**0.5**	**0**	**0**
A	**P**		**Maldanidae**	**0**	**0**	**0**	**0**	**0.5**	**0**	**0.5**	**0**	**0**	**0**	**0**	**0**	**0**	**0**	**0**	**1**
A	**P**		**Nephtyidae**	**0**	**0**	**1**	**0**	**0**	**0**	**0**	**0**	**1**	**0**	**1**	**0**	**0**	**0**	**0**	**0**
A	**P**		**Nereidae**	**0**	**0**	**0**	**1**	**0**	**0**	**0**	**0**	**1**	**0**	**0.33**	**0.33**	**0.33**	**0**	**0**	**0**
A	**P**		**Opheliidae**	**0**	**0**	**1**	**0**	**0**	**0**	**0**	**0**	**1**	**0**	**0**	**0**	**0**	**0**	**0**	**1**
A	**P**		**Orbiniidae**	**0**	**0**	**1**	**0**	**0**	**0**	**0**	**0**	**1**	**0**	**0**	**0.5**	**0**	**0**	**0**	**0.5**
A	**P**		**Oweniidae**	**0**	**1**	**0**	**0**	**0**	**1**	**0**	**0**	**0**	**0**	**0**	**0**	**0.5**	**0**	**0**	**0.5**
A	**P**		**Paraonidae**	**0**	**0**	**1**	**0**	**0**	**1**	**0**	**0**	**0**	**0**	**0**	**0.5**	**0.5**	**0**	**0**	**0**
A	**P**		**Phyllodocidae**	**0**	**0**	**1**	**0**	**0**	**0**	**0**	**0**	**1**	**0**	**0.5**	**0**	**0**	**0.5**	**0**	**0**
A	**P**		**Pilargidae**	**0**	**0**	**1**	**0**	**0**	**0**	**0**	**0**	**1**	**0**	**1**	**0**	**0**	**0**	**0**	**0**
A	**P**		**Pisionidae**	**0**	**0**	**1**	**0**	**0**	**0**	**0**	**0**	**1**	**0**	**0**	**0**	**0**	**0**	**0**	**1**
A	**P**		**Polynoidae**	**0**	**0**	**1**	**0**	**0**	**0**	**0.33**	**0.33**	**0.33**	**0**	**1**	**0**	**0**	**0**	**0**	**0**
A	**P**		**Scalibregmidae**	**0**	**0**	**0**	**1**	**0**	**0**	**0**	**0**	**1**	**0**	**0**	**0.5**	**0**	**0**	**0**	**0.5**
A	**P**		**Serpulidae**	**0**	**0**	**0**	**0**	**0**	**0**	**0**	**0**	**0**	**0**	**0**	**0**	**1**	**0**	**0**	**0**
A	**P**		**Sipunculidae**	**0**	**0**	**1**	**0**	**0**	**0**	**0**	**0**	**1**	**0**	**0**	**1**	**0**	**0**	**0**	**0**
A	**P**		**Sphaerodoridae**	**0**	**0**	**1**	**0**	**0**	**0.5**	**0**	**0**	**0.5**	**0**	**0.5**	**0.5**	**0**	**0**	**0**	**0**
A	**P**		**Spionidae**	**0**	**1**	**0**	**0**	**0**	**0**	**0.5**	**0.5**	**0**	**0**	**0**	**1**	**0**	**0**	**0**	**0**
A	**P**		**Syllidae**	**0**	**0**	**1**	**0**	**0**	**0.5**	**0**	**0**	**0.5**	**0**	**1**	**0**	**0**	**0**	**0**	**0**
A	**P**		**Tanaidacea**	**0**	**1**	**0**	**0**	**0**	**1**	**0**	**0**	**0**	**0**	**0**	**1**	**0**	**0**	**0**	**0**
A	**P**		**Terebellidae**	**1**	**0**	**0**	**0**	**0**	**0**	**0**	**1**	**0**	**0**	**0**	**1**	**0**	**0**	**0**	**0**
A	**P**		**Trichobranchidae**	**1**	**0**	**0**	**0**	**0**	**0**	**0**	**1**	**0**	**0**	**0**	**1**	**0**	**0**	**0**	**0**

Supplementary table 4.3. Permutational analysis of variance (PERMANOVA) results testing the effect of contrasting habitat on benthic community assemblages based on Bray-Curtis similarity matrices performed on normalized data.

	Df	Sums Sq	Mean Sq	F Model	R^2	Pr(>F)
Habitat	2	1.1	0.7	2.8	0.2	0.001***
Residuals	20	4.1	0.2		0.7	
Total	22	5.3			1.0	

Signif. Codes : 0 '***' 0.001 '**' 0.01 '*' 0.05 '.' 0.1 ' ' 1

Supplementary table 4.4. Simper table. Average dissimilarity within all species included in Inter-canyon and Canyon habitats; Inter-canyon and Channel; Canyon and Channel. Table shows only species with significant p-values.

	Average	Sd	Ratio	Ava	avb	cumsum	p	
Contrast: Inter-canyon_Canyon								
Average dissimilarities 6%								
Flabelligeridae	0.01	0.01	1.1	0.1	0.6	0.8	0.028	*
Sphaerodoridae	0.05	0.03	1.9	0.7	3.8	0.3	0.005	**
Contrast: Inter-canyon_Channel								
Average dissimilarities 19%								
Paraonidae	0.12	0.07	1.5	6.5	1.0	0.1	0.002	**
Ophelidae	0.02	0.03	0.7	0.2	1.0	0.5	0.048	*
Scalibregmidae	0.03	0.04	0.8	0.3	1.8	0.3	0.005	**
Amphipoda	0.02	0.02	1.2	0.3	1.3	0.4	0.003	**
Contrast: Canyon_Channel								
Average dissimilarities 30%								
Spionidae	0.11	0.11	1.0	6.6	1.5	0.1	0.005	**
Scalibregmidae	0.03	0.04	0.9	0.0	1.8	0.5	0.044	*
Amphipoda	0.02	0.02	1.2	0.4	1.3	0.5	0.038	*
Flabelligeridae	0.01	0.01	1.1	0.6	0.0	0.8	0.031	*
Bivalvia	0.05	0.03	1.6	3.2	1.0	0.3	0.008	**
Arenicolidae	0.01	0.01	0.4	0.2	0.0	0.9	0.008	**
Sphaerodoridae	0.07	0.03	2.1	3.8	0.6	0.3	0.001	***

Supplementary table 4.5. Statistical results of parametric ANOVA for control (unenriched) inorganic nutrient fluxes considered in our study among sites (factor "Habitat", three levels). Asterisks indicate significant p-values (<0.05). Df: degrees of freedom; Sum Sq: Sum of squares; F: F-statistic; p: p-value.

	Df	Sum Sq	Mean Sq	F (ANOVA)	Pr(>F)
O_2					
Habitat	2	809	404.3	10.0	0.3
Residuals	10	3979	397.9		
NH_4^+					
Habitat	2	11529	5765	0.7	0.5
Residuals	10	77508	7751		
NO_3^-					
Habitat	2	2815234	1407617	2.2	0.1
Residuals	10	6404348	640435		
$Si(OH)_4^+$					
Habitat	2	134223	67112	0.4	0.6
Residuals	10	1807942	815547		
PO_4^{3-}					
Habitat	2	76769	7677	1.1	0.3
Residuals	10	76769	7677		

Supplementary table 4.6. Statistical results of Student's t-test for enriched inorganic nutrient fluxes considered in our study between treatments (factor "Treatment", two levels) at each site (Canyon (n = 3 enriched; n = 2 control), Inter-canyon (n = 5 enriched, n = 6 control), Channel (n = 4 enriched, n = 5 control)). Asterisks indicate significant p-values (<0.05). Df: degrees of freedom; p: p-value; t: t-statistic.

Habitat	Nutrient	t-test	Df	p-value
Canyon	**O_2**	-0.6	2.4	0.6
	NH_4^+	-.0.9	2.1	0.5
	NO_3^-	1.1	1.2	0.5
	$Si(OH)_4^+$	0.5	2.7	0.6
	PO_4^{3-}	2.3	2.7	0.1
Inter-canyon	**O_2**	-0.2	8.2	0.8
	NH_4^+	-1.8	5.8	0.1
	NO_3^-	-2.8	7.5	**0.02***
	$Si(OH)_4^+$	0.2	6.6	0.8
	PO_4^{3-}	-0.1	8.9	0.9
Channel	**O_2**	-0.3	4.1	0.7
	NH_4^+	-0.5	3.7	0.6
	NO_3^-	0.6	6.9	0.5
	$Si(OH)_4^+$	0.9	3.4	0.3
	PO_4^{3-}	3.7	3.2	**0.03***

Supplementary table 4.7. Permutational analysis of variance (PERMANOVA) results testing the effect of sampled habitats and treatments on benthic nutrient fluxes based on Euclidean similarity matrices performed on normalized data.

	Df	Sums Sq	Mean Sq	F Model	R^2	Pr(>F)
Habitat	2	2179523	1089761	1.1	0.09	0.4
Treatment	1	776098	776098	0.7	0.03	0.5
Habitat: Treat	2	2046493	1023246	1.0	0.08	0.4
Residuals	19	18822684	990668		0.79	
Total	24	23824797			1.0	

4.10 References

Allen, S. E., Durrieu de Madron, X. 2009. A review of the role of submarine canyons in deep-ocean exchange with the shelf. Ocean Sci., 5 (4), 607-620.

Alonso-Pérez, F., Castro, C. G. 2014. Benthic oxygen and nutrient fluxes in a coastal upwelling system (Ria de Vigo, NW Iberian Peninsula): seasonal trends and regulating factors. Mar. Ecol. Prog. Ser., 511, 17-32.

Anderson, M., Gorley, R., Clarke, K. P. 2008. For PRIMER: guide to software and statistical methods. Primer-e, Plymouth, UK, 32.

Archer, D., Devol, A. 1992. Benthic oxygen fluxes on the Washington shelf and slope: A comparison of in situ microelectrode and chamber flux measurements. Limnol. Oceanogr., 37 (3), 614-629.

Baldrighi, E., Aliani, S., Conversi, A., Lavaleye, M., Borghini, et al. 2013. From microbes to macrofauna: an integrated study of deep benthic communities and their response to environmental variables along the Malta Escarpment (Ionian Sea). Sci Mar, 77 (4), 625-639.

Baldrighi, E., Giovannelli, D., D'Errico, G., Lavaleye, M., Manini, E. 2017. Exploring the Relationship between Macrofaunal Biodiversity and Ecosystem Functioning in the Deep Sea. Front. Mar. Sci., 4. https://doi.org/10.3389/fmars.2017.00198.

Belley, R., Snelgrove, P. V. R. 2016. Relative contributions of biodiversity and environment to benthic ecosystem functioning. Front. Mar. Sci., 3, 242.

Belley, R., Snelgrove, P. V. R. 2017. The role of infaunal functional and species diversity in short-term response of contrasting benthic communities to an experimental food pulse. J. Exp. Mar. Biol. Ecol., 491, 38–50. https://doi.org/10.1016/j.jembe.2017.03.005.

Belley, R., Snelgrove, P. V. R., Archambault, P., Juniper, S. K. 2016. Environmental drivers of benthic flux variation and ecosystem functioning in Salish Sea and Northeast Pacific sediments. PloS one, 11 (3), e0151110.

Berner, R. A. 2020. Early Diagenesis: A Theoretical Approach. Princeton University Press.

Bianchelli, S., Gambi, C., Pusceddu, A., Danovaro, R. 2008. Trophic conditions and meiofaunal assemblages in the Bari Canyon and the adjacent open slope (Adriatic Sea). Chem Ecol 24 (1), 101–109. https://doi.org/10.1080/02757540801963386.

Borcard, D., Gillet, F., Legendre, P. 2018. Spatial analysis of ecological data. Numerical ecology with R, Springer, Cham. 299-367.

Bremner, J., Rogers, S. I., Frid, C. L. J. 2003. Assessing functional diversity in marine benthic ecosystems: a comparison of approaches. Mar. Ecol. Prog. Ser., 254, 11-25.

Brunnegård, J., Grandel, S., Ståhl, H., Tengberg, A., Hall, P. O. 2004. Nitrogen cycling in deep-sea sediments of the Porcupine Abyssal Plain, NE Atlantic. Prog. Oceanogr., 63 (4), 159-181.

Caffrey, J. M., Sloth, N. P., Kaspar, H. F., Blackburn, T. H. 1993. Effect of organic loading on nitrification and denitrification in a marine sediment microcosm. FEMS Microbiol. Ecol., 12 (3), 159-167.

Cammen, L. M. 1991. Annual bacterial production in relation to benthic microalgal production and sediment oxygen uptake in an intertidal sandflat and an intertidal mudflat. Mar. Ecol. Prog. Ser. Oldendorf, 71 (1), 13-25.

Campanyà-Llovet, N., Snelgrove, P. V. R., De Leo, F. C. 2018. Food quantity and quality in Barkley Canyon (NE Pacific) and its influence on macroinfaunal community structure. Prog. Oceanogr., 169, 106-119.

Cardinale B. J., Duffy, J.E., Gonzalez, A., Hooper, D.U., Perrings, C., et al. 2012. Biodiversity loss and its impact on humanity. Nature 489, 326–326.

Christensen, J. P., Rowe, G. T. 1984. Nitrification and oxygen consumption in northwest Atlantic deep-sea sediments. J. Mar. Res., 42(4), 1099-1116.

Christensen, J. P., Murray, J. W., Devol, A. H., Codispoti, L. A. 1987. Denitrification in continental shelf sediments has major impact on the oceanic nitrogen budget. Global Biogeochem Cy 1 (2), 97–116. https://doi.org/10.1029/gb001i002p00097.

Christensen, J. P., Townsend, D. W., Montoya, J. P. 1996. Water column nutrients and sedimentary denitrification in the Gulf of Maine. Cont. Shelf Res., 16 (4), 489-515.

Ciraolo, A., Snelgrove, P. V., and Algar, C. K. 2023. Habitat heterogeneity effects on microbial communities of the Gulf of Maine. Deep Sea Res. I: Oceanogr. Res. Pap., 104074.

Clarke, K. R. 1993. Non-parametric multivariate analyses of changes in community structure. Austral Ecol., 18 (1), 117-143.

Cosson, N., Sibuet, M., Galeron, J. 1997. Community structure and spatial heterogeneity of the deep-sea macrofauna at three contrasting stations in the tropical northeast Atlantic. Deep Sea Res. Part I Oceanogr. Res. Pap., 44 (2), 247-269.

Cúrdia, J., Carvalho, S., Ravara, A., Gage, J. D., Rodrigues, A. M., et al. 2004. Deep macrobenthic communities from Nazaré Submarine Canyon (NW Portugal). Sci. Mar. 68, (1), 171–180. https://doi.org/10.3989/scimar.2004.68s1171.

Danovaro, R., Gambi, C., Dell'Anno, A., Corinaldesi, C., Fraschetti, S., et al. 2008. Exponential decline of deep-sea ecosystem functioning linked to benthic biodiversity loss. Curr. Biol., 18 (1), 1–8.

Danovaro, R. 2009. Methods for the study of deep-sea sediments, their functioning and biodiversity. CRC press., 45-51.

De Bello, F., Lavorel, S., Díaz, S., Harrington, R., Cornelissen, et al. 2010. Towards an assessment of multiple ecosystem processes and services via functional traits. Biodivers. Conserv., 19 (10), 2873-2893.

De Leo, F. C., Drazen, J. C., Vetter, E. W., Rowden, A. A., Smith, C. R. 2012. The effects of submarine canyons and the oxygen minimum zone on deep-sea fish assemblages off Hawai'i. In Deep Sea Res. Part I Oceanogr. Res. Pap. 64, 54–70. https://doi.org/10.1016/j.dsr.2012.01.014.

De Leo, F. C., Smith, C. R., Rowden, A. A., Bowden, D. A., Clark, M. R. 2010. Submarine canyons: hotspots of benthic biomass and productivity in the deep sea. Proc. Royal Soc. B-Biol Sci, 277 (1695), 2783–2792.

De Leo, F. C., Vetter, E. W., Smith, C. R., Rowden, A. A., McGranaghan, M. 2014. Spatial scale-dependent habitat heterogeneity influences submarine canyon macrofaunal abundance and diversity off the Main and Northwest Hawaiian Islands. Deep Sea Res. Part II Top. Stud. Oceanogr., 104, 267-290.

Di Franco, D., Linse, K., Griffiths, H. J., Brandt, A. 2021. Drivers of abundance and spatial distribution in Southern Ocean peracarid crustacea. Ecol. Indic., 128, 107832.

Diaz, S., Cabido, M. 2001. Vive la différence: plant functional diversity matters to ecosystem processes. Trends Ecol. Evol. 16, 646–55.

Ellingsen, K. E. 2001. Biodiversity of a continental shelf soft-sediment macrobenthos community. Mar. Ecol. Prog. Ser., 218, 1-15.

Epping, E., van der Zee, C., Soetaert, K., Helder, W. 2002. On the oxidation and burial of organic carbon in sediments of the Iberian margin and Nazaré Canyon (NE Atlantic). Progr. Oceanogr., 52(2-4), 399-431.

Etter, R. J., Grassle, J. F. 1992. Patterns of species diversity in the deep sea as a function of sediment particle size diversity. Nature, 360 (6404), 576-578.

Fabiano, M., Danovaro, R., Fraschetti, S. 1995. A three-year time series of elemental and biochemical composition of organic matter in subtidal sandy sediments of the Ligurian Sea (northwestern Mediterranean). Cont. Shelf Res.,15 (11-12), 1453-1469.

Fenchel, T., Finlay, B. 2008. Oxygen and the spatial structure of microbial communities. Bio. Reviews, 83 (4), 553-569.

Foshtomi, Y. M., Braeckman, U., Derycke, S., Sapp, M., Van Gansbeke, D., et al. 2015. The link between microbial diversity and nitrogen cycling in marine sediments is modulated by macrofaunal bioturbation. PloS one, 10 (6), e0130116.

Fox, J., Weisberg, S., Adler, D., Bates, D., Baud-Bovy, et al. 2012. Package 'car'. Vienna: R Foundation for Statistical Computing, 16.

Friedland, K. D., Record, N. R., Pendleton, D. E., Balch, W. M., Stamieszkin, K., et al. 2023. Asymmetry in the rate of warming and the phenology of seasonal blooms in the Northeast US Shelf Ecosystem. ICES Mar. Sci. Symp., fsad007.

Fuerst, J. A., Sagulenko, E. 2011. Beyond the bacterium: planctomycetes challenge our concepts of microbial structure and function. Nat. Rev. Microbiol., 9 (6), 403-413.

Gamfeldt L., Lefcheck J.S., Byrnes, J. E. K., Cardinale, B. J., Duffy, J. E., et al. 2014. Marine biodiversity and ecosystem functioning: What's known and what's next? Oikos 124, 252-265.

Glud, R. N. 2008. Oxygen dynamics of marine sediments. Mar. Biol. Res., 4 (4), 243-289.

Glud, R. N., Blackburn, N. 2002. The effects of chamber size on benthic oxygen uptake measurements: a simulation study. Ophelia, 56 (1), 23-31.

Goswami, M., Bhattacharyya, P., Mukherjee, I., Tribedi, P. 2017. Functional diversity: an important measure of ecosystem functioning. Adv. Appl. Microbiol., 7 (01), 82.

Grossart, H. P., Czub, G., Simon, M. 2006. Algae–bacteria interactions and their effects on aggregation and OM flux in the sea. Environ. Microbiol., 8 (6), 1074-1084.

Gruber N. 2008. The marine nitrogen cycle: overview and challenges. Capone DG, Bronk DA, Mulholland MR, Carpenter EJ (eds) Nitrogen in the marine environment. Academic Press, San Diego, 1-50.

Gunton, L. M., Neal, L., Gooday, A. J., Bett, B. J., Glover, A. G. 2015. Benthic polychaete diversity patterns and community structure in the Whittard Canyon system and adjacent slope (NE Atlantic). Deep Sea Res. Part I Oceanogr. Res. Pap., 106, 42-54.

Hall P. O. J., Hulth, S., Hulthe, G., Landén, A., Tengberg, A. 1996. Benthic nutrient fluxes on a basin wide scale in the Skagerrak (North-Eastern North Sea). J. Sea Res., 35(1-3), 123-137.

Hammond, D. E., Fuller, C., Harmon, D., Hartman, B., Korosec, M., et al. 1985. Benthic fluxes in San Francisco Bay. Hydrobiologia 129, 69-90.

Harris, P. T., Baker, E. K. 2019. Seafloor Geomorphology as Benthic Habitat: GeoHab Atlas of Seafloor Geomorphic Features and Benthic Habitats. Elsevier.

Hensen, C., Zabel, M., Schulz, H. D. 2000. A comparison of benthic nutrient fluxes from deep-sea sediments off Namibia and Argentina. Deep Sea Res. Part II Top. Stud. Oceanogr., 47 (9-11), 2029-2050.

Hensen, C., Zabel, M., Schulz, H. N. 2006. Benthic cycling of oxygen, nitrogen and phosphorus. Mar Chem, Springer, Berlin, Heidelberg. 207-240.

Hoffmann, K., Bienhold, C., Buttigieg, P. L., Knittel, K., Laso-Pérez, R., et al. 2020. Diversity and metabolism of *Woeseiales* bacteria, global members of marine sediment communities. The ISME J., 14 (4), 1042-1056.

Hooper, D. U., Chapin, F. S., Ewel, J. J., Hector, A., Inchausti, P., et al. 2005. Effects of biodiversity on ecosystem functioning: a consensus of current knowledge. Ecol. Monogr. 75, 3–35.

Hutchings, P. 1998. Biodiversity and functioning of polychaetes in benthic sediments. Biodivers. Conserv., 7 (9), 1133-1145.

Ingall, E., Jahnke, R. 1994. Evidence for enhanced phosphorus regeneration from marine sediments overlain by oxygen depleted waters. Geochim. Cosmochim. Acta, 58 (11), 2571-2575.

Ingels, J., Kiriakoulakis, K., Wolff, G. A., Vanreusel, A. 2009. Nematode diversity and its relation to the quantity and quality of sedimentary OM in the deep Nazaré Canyon, Western Iberian Margin. Deep Sea Res. Part I Oceanogr. Res. Pap., 56 (9), 1521–1539. https://doi.org/10.1016/j.dsr.2009.04.010.

Jameson, B. D., Berg, P., Grundle, D. S., Stevens, C. J., Juniper, S. K. 2021. Continental margin sediments underlying the NE Pacific oxygen minimum zone are a source of nitrous oxide to the water column. Limnol. Oceanogr. Letters, 6 (2), 68-76.

Janssen, F., Huettel, M., Witte, U. 2005. Pore-water advection and solute fluxes in permeable marine sediments (II): benthic respiration at three sandy sites with different permeabilities (German Bight, North Sea). Limnol. Oceanogr. 50, 779–792. doi: 10.4319/lo.2005.50.3.0779.

Jørgensen, B. B., Boetius, A. 2007. Feast and famine—microbial life in the deep-sea bed. Nat. Rev. Microbiol., 5 (10), 770-781.

Karl, D. M., Tilbrook, B. D. 1994. Production and transport of methane in oceanic particulate OM. Nature, 368 (6473), 732-734.

Kelly, N. E., Shea, E. K., Metaxas, A., Haedrich, R. L., Auster, P. J. 2010. Biodiversity of the deep-sea continental margin bordering the Gulf of Maine (NW Atlantic): relationships among sub-regions and to shelf systems. PloS One, 5 (11), e13832.

Klinck, J. M. 1996. Circulation near submarine canyons: A modeling study. J. Geophys. Res. Oceans, 101 (C1), 1211-1223.

Koho, K. A., Langezaal, A. M., Van Lith, Y. A., Duijnstee, I. A. P., Van der Zwaan, G. J. 2008. The influence of a simulated diatom bloom on deep-sea benthic foraminifera and the activity of

bacteria: a mesocosm study. Deep Sea Res. Part I Oceanogr. Res. Pap., 55 (5), 696-719.

Laliberte E, Legendre P. 2010. A distance-based framework for measuring functional diversity from multiple traits. Ecol., 91, 299-305.

Le Guitton, M., Soetaert, K., Damsté, J. S., Middelburg, J. J. 2015. Biogeochemical consequences of vertical and lateral transport of particulate OM in the southern North Sea: a multiproxy approach. Estuar. Coast. Shelf Sci., 165, 117-127.

Leduc, D., Rowden, A. A., Nodder, S. D., Berkenbusch, K., Probert, P. K., et al. 2014. Unusually high food availability in Kaikoura Canyon linked to distinct deep-sea nematode community. Deep Sea Res. Part II Top. Stud. Oceanogr., 104, 310–318. https://doi.org/10.1016/j.dsr2.2013.06.003.

Levin, L. A., Etter, R. J., Rex, M. A., Gooday, A. J., Smith, C. R., et al. 2001. Environmental influences on regional deep-sea species diversity. Annu Rev Ecol Evol Syst, 32 (1), 51-93.

Levin, L. A., Gage, J., Lamont, P., Cammidge, L., Martin, C., et al. 1997. Infaunal community structure in a low-oxygen, organic rich habitat on the Oman continental slope, NW Arabian Sea. The responses of marine organisms to their environments: Proceedings of the 30th European Marine Biology Symposium, University of Southampton, Southampton, UK., 223230.

Levin, L. A., Sibuet, M. 2012. Understanding continental margin biodiversity: a new imperative. Ann Rev Mar Sci, 4, 79–112.

Link, H., Piepenburg, D., Archambault, P. 2013. Are hotspots always hotspots? The relationship between diversity, resource and ecosystem functions in the Arctic. PLoS ONE, 8 (9), 74077. https://doi.org/10.1371/journal.pone.0074077.

Lomas, M. W., Glibert, P. M., Shiah, F. K., Smith, E. M. 2002. Microbial processes and temperature in Chesapeake Bay: current relationships and potential impacts of regional warming. Glob. Change Biol. Bioenergy, 8 (1), 51-70.

Loubere, P. 1991. Deep-sea benthic foraminiferal assemblage response to a surface ocean productivity gradient: a test. Paleoceanography, 6 (2), 193-204.

Loubere, P. 1998. The impact of seasonality on the benthos as reflected in the assemblages of deep-sea foraminifera. Deep Sea Res. Part I Oceanogr. Res. Pap., 45 (2-3), 409-432.

MacIntyre, H. L., Geider, R. J., Miller, D. C. 1996. Microphytobenthos: the ecological role of the "secret garden" of unvegetated, shallow-water marine habitats. I. Distribution, abundance and primary production. Estuaries, 19 (2), 186-201.

Mason, N. W., Mouillot, D., Lee, W. G., Wilson, J. B. 2005. Functional richness, functional evenness and functional divergence: the primary components of functional diversity. Oikos, 111 (1), 112-118.

Mayer, L. M., Linda L, S., Sawyer, T., Plante, C. J., Jumars, P. A., et al. 1995. Bioavailable amino acids in sediments: A biomimetic, kinetics based approach. Limnol. Oceanogr., 40 (3), 511-520.

McArdle, B. H. and M. J. Anderson. 2001. Fitting multivariate models to community data: A comment on distance-based redundancy analysis. Ecol., 82, 290-297.

McClain, C. R., Barry, J. P. 2010. Habitat heterogeneity, disturbance, and productivity work in concert to regulate biodiversity in deep submarine canyons. Ecol., 91 (4), 964-976.

Menot, L., Sibuet, M., Carney, R. S., Levin, L. A., Rowe, G. T., et al. 2010. New perceptions of continental margin biodiversity. Life in the World's Oceans: Diversity, Distribution, and Abundance, edited by: McIntyre, AD, 79-103.

Mermillod-Blondin, F. 2011. The functional significance of bioturbation and biodeposition on biogeochemical processes at the water–sediment interface in freshwater and marine ecosystems. J. North Am. Benthol. Soc., 30 (3), 770-778.

Meyers, P. A. 1994. Preservation of elemental and isotopic source identification of sedimentary

organic matter. Chem. Geol., 114 (3-4), 289-302.

Miatta, M., Snelgrove, P. V. R. 2021a. Benthic nutrient fluxes in deep-sea sediments within the Laurentian Channel MPA (eastern Canada): The relative roles of macrofauna, environment, and sea pen octocorals. Deep Sea Res. Part I Oceanogr. Res. Pap., 178, 103655.

Miatta, M., Snelgrove, P. V. R. 2021b. Sedimentary OM shapes macrofaunal communities but not benthic nutrient fluxes in contrasting habitats along the Northwest Atlantic continental margin. Front. Mar. Sci., 1704.

Middelburg, J. J., Nieuwenhuize, J., van Breugel, P. 1999. Black carbon in marine sediments. Mar. Chem., 65 (3-4), 245-252.

Montagna, P. A., Coull, B. C., Herring, T. L., Dudley, B. W. 1983. The relationship between abundances of meiofauna and their suspected microbial food (diatoms and bacteria). Estuar. Coast. Shelf Sci., 17 (4), 381-394.

Moodley, L., Middelburg, J. J., Soetaert, K., Boschker, H. T. S., Herman, P. M. J., et al. Similar rapid response to phytodetritus deposition in shallow and deep-sea sediments. J. Mar. Res. 63 (2), 457–469. https://doi.org/10.1357/0022240053693662.

Mouchet, M. A., Villéger, S., Mason, N. W., Mouillot, D. 2010. Functional diversity measures: an overview of their redundancy and their ability to discriminate community assembly rules. Funct. Ecol., 24 (4), 867-876.

Niemistö, J., Kononets, M., Ekeroth, N., Tallberg, P., Tengberg, A., et al. 2018. Benthic fluxes of oxygen and inorganic nutrients in the archipelago of Gulf of Finland, Baltic Sea–Effects of sediment resuspension measured in situ. J. Sea Res., 135, 95-106.

Norling, K., Rosenberg, R., Hulth, S., Grémare, A., Bonsdorff, E. 2007. Importance of functional biodiversity and species-specific traits of benthic fauna for ecosystem functions in marine sediment. Mar. Ecol. Progr. Ser., 332, 11-23.

Oksanen, J., Blanchet, F. G., Kindt, R., Legendre, P., Minchin, P. R., et al. 2013. Package 'vegan'. Community ecology package, version, 2 (9), 1-295.

Oliveira, A., Santos, A. I., Rodrigues, A., Vitorino, J. 2007. Sedimentary particle distribution and dynamics on the Nazaré canyon system and adjacent shelf (Portugal). Mar. Geol., 246 (2), 105-122.

Oliver, T. H., Heard M. S., Isaac N. J. B., Roy, D.B., Procter D., et al. 2015 Biodiversity and resilience of ecosystem functions. Trends Ecol. Evol. 30 673-684.

Parrish, C. C. 1999. Determination of Total Lipid, Lipid Classes, and Fatty Acids in Aquatic Samples. In Lipids in Freshwater Ecosystems, 4-20. https://doi.org/10.1007/978-1-4612-0547-0_2.

Paterson, G. L. J., Glover, A. G., Cunha, M. R., Neal, L., de Stigter, H. C., et al. 2011. Disturbance, productivity and diversity in deep-sea canyons: A worm's eye view. Deep Sea Res. Part II Top. Stud. Oceanogr., 58 (23-24), 2448-2460. https://doi.org/10.1016/j.dsr2.2011.04.008.

Piot A., Nozais C., Archambault P. 2014. Meiofauna affect the macrobenthic biodiversity-ecosystem functioning relationship. Oikos 123 203-213.

Pla, L., Casanoves, F., Rienzo, J. D. 2012. Quantifying functional biodiversity. Functional diversity indices. Springer, 27-51.

Puig, P., Palanques, A., Martín, J. 2014. Contemporary sediment-transport processes in submarine canyons. Ann Rev Mar Sci, 6, 53-77.

Quattrini, A. M., Nizinski, M. S., Chaytor, J. D., Demopoulos, A. W. J., Roark, E. B., et al. 2015. Exploration of the canyon-incised continental margin of the northeastern united states reveals dynamic habitats and diverse communities. PLoS One 10:e0139904. doi: 10.1371/journal.pone.0139904.

Queirós, A. M., Birchenough, S. N., Bremner, J., Godbold, J. A., Parker, R. E., et al. 2013. A bioturbation classification of European marine infaunal invertebrates. Ecol. Evol., 3 (11), 3958-3985.

R Core Team. 2016. R: A Language and Environment for Statistical Computing. Vienna, Austria. Retrieved from https://www.R-project.org/.

Ramirez-Llodra, E., Brandt, A., Danovaro, R., De Mol, B., Escobar, E., et al. 2010. Deep, diverse and definitely different: unique attributes of the world's largest ecosystem. Biogeosciences, 7 (9), 2851-2899.

Ryan, J. P., Chavez, F. P., Bellingham, J. G. 2005. Physical-biological coupling in Monterey Bay, California: topographic influences on phytoplankton ecology. Mar. Ecol. Prog. Ser., 287, 23-32. https://doi.org/10.3354/meps287023.

Song, Y., Wang, P., Li, G., Zhou, D. 2014. Relationships between functional diversity and ecosystem functioning: A review. Acta Ecol. Sin., 34 (2), 85-91.

Sweetman, A. K., Smith, C. R., Shulse, C. N., Maillot, B., Lindh, M., et al. 2019. Key role of bacteria in the short-term cycling of carbon at the abyssal seafloor in a low particulate organic carbon flux region of the eastern Pacific Ocean. Limnol. Oceanogr., 64 (2), 694-713.

Switzer, M. E., Townsend, D. W., Pettigrew, N. R. 2020. The effects of source water masses and internal recycling on concentrations of dissolved inorganic nutrients in the Gulf of Maine. Cont. Shelf Res., 204, 104157.

Taghon, G. L., Nowell, A. R., Jumars, P. A. 1980. Induction of suspension feeding in spionid polychaetes by high particulate fluxes. Science, 210 (4469), 562-564.

Tilman, D. 2001. Functional diversity. Encyclopedia of biodiversity, 3 (1), 109-120.

Townsend, D. W., Thomas, A.C., Mayer, L. M., Thomas, M. A., Quinlan. J. A. 2006. Oceanography of the Northwest Atlantic continental shelf, p. 119-168. In A. R. Robinson and K. H. Brink [eds.], The Sea, v. 14. Cambridge MA: Harvard Univ. Press.

Townsend, D. W., Pettigrew, N.R., Thomas, A.C. 2005. On the nature of Alexandrium fundyense blooms in the Gulf of Maine. Deep. Res. Part II Top. Stud. Oceanogr. 52, 2603-2630. doi:10.1016/j.dsr2.2005.06.028.

Tyler, P., Amaro, T., Arzola, R., Cunha, M., de Stigter, H., et al. 2009. Europe's Grand Canyon: Nazaré Submarine Canyon. Oceanography, 22 (1), 46-57. https://doi.org/10.5670/oceanog.2009.05.

Valladares, F., Bastias, C. C., Godoy, O., Granda, E., Escudero, A. 2015. Species coexistence in a changing world. Front. Plant Sci., 6, 866.

Varkouhi, S., Wells, J. 2020. Bottom-water temperature controls on biogenic silica dissolution and recycling in surficial deep-sea sediments. Ocean Sci. Discussions, 1-55.

Vetter, E. W., Dayton, P. K. 1998. Macrofaunal communities within and adjacent to a detritus-rich submarine canyon system. Deep-Sea Res. Part II Top. Stud. Oceanogr., 45 (1-3), 25–54. https://doi.org/10.1016/s0967-0645(97)00048-9.

Vetter, E. W., Smith, C. R., De Leo, F. C. 2010. Hawaiian hotspots: enhanced megafaunal abundance and diversity in submarine canyons on the oceanic islands of Hawaii. Mar. Ecol., 31 (1), 183-199. https://doi.org/10.1111/j.1439-0485.2009.00351.x.

Villéger, S., Mason N. W. H., Mouillot, D. 2008. New multidimensional functional diversity indices for a multifaceted framework in functional ecology. Ecol. 89, 2290-2301.

Weaver, P. P., Wynn, R. B., Kenyon, N. H., Evans, J. 2000. Continental margin sedimentation, with special reference to the north-east Atlantic margin. Sedimentology, 47, 239-256.

Wentworth, C. K. 1929. Method of computing mechanical composition types in sediments. Geol. Soc. Am. Bull., 40 (4), 771-790.

Wenzhöfer, F., Glud, R. N. 2002. Benthic carbon mineralization in the Atlantic: a synthesis based on in situ data from the last decade. Deep Sea Res. Part I Oceanogr. Res. Pap., 49 (7), 1255-1279.

Witte, U., Aberle, N., Sand, M., Wenzhöfer, F. 2003a. Rapid response of a deep-sea benthic community to POM enrichment: an in situ experimental study. Mar. Ecol. Prog. Ser., 251, 27-36.

Witte, U., Wenzhöfer, F., Sommer, S., Boetius, A., Heinz, P., et al. 2003b. In situ experimental evidence of the fate of a phytodetritus pulse at the abyssal sea floor. Nature, 424, (6950), 763–766. https://doi.org/10.1038/nature01799.

Worm, B., Barbier, E. B., Beaumont, N., Duffy, J. E., Folke, C., et al. 2006. Impacts of biodiversity loss on ocean ecosystem services. Science, 314 (5800), 787-790.

WoRMS Editorial Board, 2015. World Register of Marine Species. http://www.marinespecies.org.

Zang, Z., Ji, R., Liu, Y., Chen, C., Li, Y., et al. 2022. Remote silicate supply regulates spring phytoplankton bloom magnitude in the Gulf of Maine. L&O Letters, 7(3), 277-285.

Zeppilli, D., Pusceddu, A., Trincardi, F., Danovaro, R., 2016. Seafloor heterogeneity influences the biodiversity–ecosystem functioning relationships in the deep sea. Sci. Rep., 6 (1), 1-12.

Zuur, A. F., Ieno E. N., Walker N. J., Saveliev A. A., Smith G. M. 2009. Mixed effects models and extensions in ecology with R. Springer, New York, NY, USA.

Chapter 5. - Habitat heterogeneity effects on microbial communities of the Gulf of Maine[5]

[5]Ciraolo, A. C., Snelgrove, P. V. R., Algar, C. K. (2023). Habitat heterogeneity effects on microbial communities of the Gulf of Maine. *Deep Sea Res. Part I: Oceanogr. Res*, 197, 104074.

5.1 Abstract

Many biological and physical variables influence microbes at the sediment-water interface, whose response to those variables affects the overall fate and residence time of organic matter (OM) in the marine environment. In addition to the many ecological roles microbes play in deep-sea sediments, further studies are needed to address microbial community diversity and its influence on seafloor organic matter remineralization rates. We explored microbial diversity, distribution, and associated organic matter remineralization among contrasting habitats and following 24-h experimental phytodetrital enrichment of sediments from Canyon, Inter-Canyon, and Channel habitats of the Gulf of Maine, Northwest Atlantic. Based on multivariate analyses of community composition we found that habitat heterogeneity influenced microbial community composition but not microbial diversity. Similarly, the phytodetrital addition did not translate to significant differences in microbial diversity but altered nitrate flux in Inter-canyon sediments and phosphate flux in Channel sediments. Bacteria were dominant over Archaea and, of the environmental variables we measured, quantity and quality of organic matter best explained overall microbial community variation. Proteobacteria, Bacteroidae, Acidobacteriota, Planctomycetota, and NB1-J Deltaproteobacteria dominated all habitats, but variation in the microbial community at our study sites explained only 7% of nutrient fluxes. Our exploratory study did not suggest a strong contribution of microbial community composition to OM remineralization variation both among contrasting habitats and in response to phytodetrital

addition, and thus to this aspect of deep-sea ecosystem functioning, at least over short-term incubations.

5.2 Introduction

Deep-sea sediments cover more of the Earth's surface area than any other seafloor habitat. The resident microbial communities in these habitats contribute significantly to global biogeochemical cycles of nutrients (e.g., nitrate and phosphate) and organic matter recycling and deep-sea food web structure. Indeed, microbes can rapidly degrade and utilize particulate organic matter (Li et al., 2009; Keuter et al., 2016) at the sediment-water interface, delivered either directly from the surface of the ocean or by lateral currents (Gooday and Turley, 1990; Bowman et al., 2003; Jørgensen and Boetius, 2007; Fuerst et al., 2011; Hoffman et al., 2020). Consequently, nutrient fluxes at the sediment-water interface (SWI) enhance benthic-pelagic coupling. Bacteria and archaea also drive fundamental processes in marine sediments including oxidation of organic matter, production of methane and other hydrocarbons, and removal of sulfate from the ocean (Jørgensen, 1982; D'Hondt et al., 2004; Hinrichs et al., 2006). Archaea for example, which include ammonia-oxidizers, are among the most abundant microbes on Earth and contribute significantly to global and nitrogen cycles (Pester et al., 2011). However, Atlantic Ocean studies indicate that Archaea are less abundant than bacteria. Proteobacteria represent the most abundant bacterial phylum in deep-sea surface sediments; Gammaproteobacteria in particular dominate South Atlantic deep-sea surface sediments, followed by Deltaproteobacteria, Acidobacteria, and Flavobacteria (Schauer et al., 2010; Varliero et al., 2019). A study in the Stellwagen Bank National Marine Sanctuary, NW Atlantic, for example, reported only nine Archaea phyla, with dominance by Thaumarchaeota, a taxon particularly sensitive to temperature changes (Polinski et al., 2019). However, given the estimated subseafloor sedimentary microbial abundance in oceanic and coastal sediments of $2.9 \cdot 10^{29}$ cells (Kallmeyer et al., 2012), the response of microbes to many biological and physical variables at the sediment-water interface likely affects the overall fate and residence

time of organic matter at the seafloor, and also provides an important nutrient source for sedimentary infaunal communities.

In addition to clear evidence regarding the major ecological roles that microbes play in deep-sea processes, further studies have documented microbial community composition and distribution on the seafloor. Many studies of microbial composition have focused on ecological hot spots such as canyons (Roman et al., 2019), cold seeps (Levin, 2005), hydrothermal vents (Namirimu et al., 2023), and sediment at 10,000 m depth and to sediments 1000 m below the seafloor (Jørgensen and Boetius, 2007; Sanchez-Soto et al., 2023; Walker et al., 2023). The number of species present, their numerical composition, and diversity characterize the bacterial community in a given niche (Kim et al., 2017). Biological diversity refers to their variability, generally defined as species richness and relative abundance in space and time (Schloss et al., 2009).

Studies of microbial distribution patterns that considered prokaryotic abundance, richness, and evenness, often emphasize the importance of environmental factors (Keuter et al., 2016; Corinaldesi et al., 2019; Roman et al., 2019). Roman et al. (2019) reported higher microbial diversity in dynamic submarine canyons in the NW Mediterranean than in adjacent open-slope sediments. In contrast, Corinaldesi et al. (2019) indicated similar prokaryotic richness values among canyon and non-canyon habitats, suggesting that environmental factors do not significantly affect α-diversity of prokaryotic assemblages. Other studies report specific environmental or geographic influences on microbial biogeography such as salinity (Crump et al., 2004), depth (Ovreas et al., 1997), and latitude (Schwalbach et al., 2004). Trophic resources and depth explained differences in prokaryotic abundances in Bisagno and Polcevere Canyons in the Mediterranean, respectively (Corinaldesi et al., 2019). In addition to environmental selection and spatial separation, advection of water masses shapes marine microbial community composition,

presumably reflecting similar environmental conditions and upstream to downstream colonization by microorganisms (Wilkins et al., 2013).

Eutrophic versus oligotrophic conditions also influence microbial distributions. For example, high abundance of prokaryotes characterized eutrophic, high organic carbon-rich sediments of the Black Sea and Peru margins (Schippers et al., 2005; Schippers et al., 2012), in contrast to low microbial abundances in the relatively carbon-poor sediments of the equatorial Pacific (D'Hondt et al., 2004). Furthermore, the proportion of Bacteria and Archaea in marine sediments apparently varies greatly among sediments and sediment layers (Schippers et al., 2012), potentially resulting from different methodological analyses (e.g., insufficient quantitative extraction protocols, or primer mismatches (Teske and Sørensen, 2008), or possibly reflecting actual eutrophic/oligotrophic differences. Archaea dominate the oligotrophic sediments of the Mediterranean Sea, and their relative abundance varies inversely with sedimentary organic content (e.g., total organic content (TOC) (Keuter, 2016)). Teske and Sørensen (2008) showed that the use of primers that match only part of the archaeal population directly affects results by under-representing or excluding archaeal groups that yield mismatched sequences.

Few studies have tested the relationship between bacterial and benthic invertebrate abundances and diversities (e.g., Albertelli et al., 1999). However, aggregation or dissociation of particles through invertebrate faunal activity, such as feeding or burrows, may influence the diversity, structure, and function of sediment bacteria (Solan et al., 2005). Grazing pressure might also exert a control on their abundance (Albertelli et al., 1999). Consequently, interactions between these two groups strongly influence ecosystem processes.

Given evidence that contrasting habitats may influence microbial distribution, in this study we focus on deep-sea surface sediments in the NW Gulf of Maine from four different locations

that encompass Canyon, Inter-Canyon, and Channel habitats. Given documented differences among these habitats in terms of depth and nutrient supply (Christensen et al., 1996), we predicted that microbial patterns would differ among habitats, and we specifically considered microbial responses to organic matter in terms of diversity and organic matter remineralization, and the potential relationship between microbes and nutrient fluxes. We predicted that higher relative microbial abundance and stronger nutrient regeneration would characterize the Northeastern Channel and Canyon compared to Inter-Canyon sediments. Whereas the NE Channel funnels high nutrient, cold-water masses into the Gulf of Maine, turbidity currents disturb the seafloor within canyon habitats. This complexity led us to hypothesize that microbial diversity, remineralization, and nutrient fluxes would vary among habitats, with cascading effects on infaunal community composition and abundance (e.g., increased diversity and abundance with increased microbial diversity) linked to the interactive relationship between benthic microbes and infauna in organic matter remineralization (e.g., increased remineralization with increased macrofaunal functional diversity (Belley and Snelgrove, 2017)). Building on this background, we aimed to explore benthic microbial diversity and composition among canyon and non-canyon habitats, and to relate microbial composition to sediment nutrient fluxes (NH_4^+, NO_3^-, $Si(OH)_4^+$, PO_4^{3-}), and to the infaunal diversity patterns presented in Ciraolo and Snelgrove (2023). Specifically, we use 16s rRNA to quantify microbial diversity in terms of richness, and Shannon-Wiener (H') indices, and distributions in relation to habitat heterogeneity and phytodetrital addition. For each habitat we characterized habitat heterogeneity based on environmental variables such as depth, temperature, and organic matter properties (Chl*a*, Phaeo, Chl*a*:Phaeo, lipids, C:N, TOC%).

5.3 Materials and Methods

5.3.1 Sampling locations

We collected sediment cores from four sites in the Gulf of Maine, Corsair Tributary Canyon, Kinlan-Heezen Mid Inter-canyon, Northeast Channel 1, and Northeast Channel 2 (**Fig. 5.1, Table 5.1**), representing three different habitat types (Canyon, Inter-canyon, and Channel). The three habitat depths varied by around 300 m from the shallower Channel site to the deeper Canyon site (**Table 5.1**). We used the ROV Remotely Operated Platform for Ocean Science (ROPOS, www.ropos.com) deployed from the NOAA research vessel *Henry B. Bigelow* during a two-week oceanographic cruise in June 2019. We collected 2 non-incubated cores per site to determine sediment properties and prokaryotic community composition. We dedicated the remaining cores and respective overlying water to *ex-situ* incubations to measure nutrient fluxes and prokaryotic community composition patterns among contrasting habitats (**Supplementary table 5.1**). Cores at a given location were collected at distances of several m to 100s of m apart. We also collected bottom-water samples using a Niskin bottle and recorded temperature and salinity with a Seabird 19 conductivity – temperature - depth (CTD) instrument, both mounted on the ROV. We also tested whether temperature, salinity, and depth would affect microbial distribution among habitats.

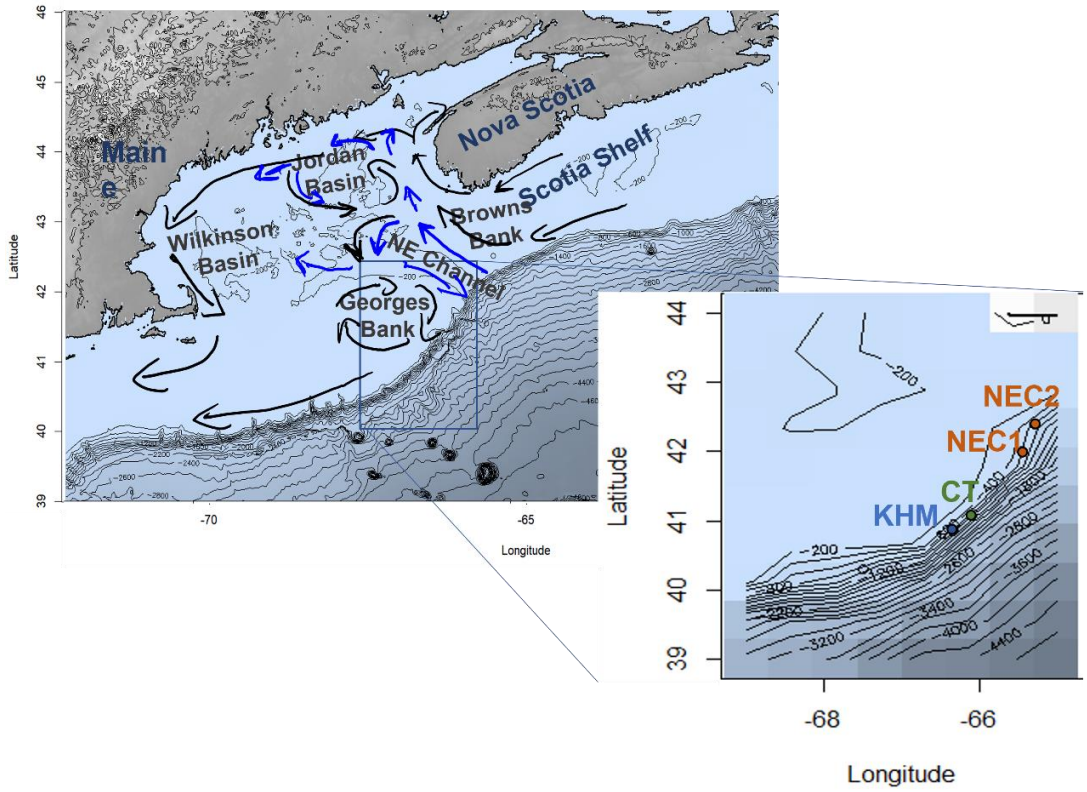

Fig. 5.1. Map of sites sampled in the Gulf of Maine in June 2019. Label symbols: CT: Corsair Tributary Canyon; KHM: Kinlan-Heezen Inter-canyon; NEC1: Northeast Channel 1; NEC2: Northeast Channel 2. Black arrows represent Scotian shelf surface currents. Blue arrows represent deep bottom currents entering from NE Channel.

Table 5.1. Site number, name, latitude, longitude, water depth, and sub-region of each sampling habitat in Gulf of Maine.

Dive number	Site Name	Site Lat	Site Long	Water Depth (m)	Habitat type
R 2117	NE Channel 2 (NEC2)	42.50	-65.28	~ 663	Channel
R 2113	NE Channel 1 (NEC1)	42.00	-65.45	~ 672	Channel
R 2110	Kinlan-Heezen Mid Inter-canyon (KHM)	40.58	-66.35	~ 804	Inter-canyon
R 2112	Corsair Tributary Canyon (CT)	41.80	-66.10	~ 969	Canyon

5.3.2 Incubations

Immediately upon recovery of the submersible, we sealed all of the incubation cores with water-tight lids equipped with magnetic stirrers and gas-tight sampling ports and moved them into a cold room set at the *in-situ* temperature (~14–16 °C) for each station in order to simulate the deep-sea environment, acknowledging potential effects of pressure on species' behavior and physiology. To allow any sediment particles resuspended during transport to settle back to the sediment surface, we waited for ~12 h before beginning the 24-h incubations. We chose 24 h as an incubation time both to avoid consumption of more than 15–30% of available oxygen (Hammond et al., 1985; Belley and Snelgrove 2016), and because of logistical constraints.

To evaluate microbial response to fresh organic matter, we added 0.02 g (wet weight of concentrated paste) of the diatom *Chaetoceros muelleri* in three of the cores (enriched cores) from each site, at the beginning of the incubation. This addition corresponded to 25.5 mg $\cdot$ C $\cdot$ m^{-2} $\cdot$ y^{-1} . We choose *C. muelleri* because diatoms are the dominant phytoplankton during the Gulf of Maine spring bloom (Townsend et al., 2005, 2006). An additional 2-3 cores received no algal additions and served as experimental controls to document ambient flux and respiration rates for the study sites in the absence of enrichment. Algae were grown at the Dr. Joe Brown Aquatic Research Building (http://www.mun.ca/osc/jbarb/index.php) and centrifuged following harvesting to produce an algal paste, which we froze at -20 °C until needed for the cruise. In order to evaluate benthic nutrient fluxes at the sediment-water interface we measured oxygen consumption at 4-6 h intervals using pre-fitted, non-invasive oxygen sensor spots and the Fibox Polymer Optical Fiber Oxygen System (PreSens, Regensburg, DE).

At the onset of incubations, we collected initial water samples from the overlying water of each core for nutrient analysis (NH_4^+, NO_3^-, $Si(OH)_4^+$, PO_4^{3-}), as well as two replicate water

samples at the middle and the end of each incubation, in each case replacing the removed water with bottom water collected with the CTD rosette. Nutrient samples were stored in an upright position in 50 ml pre-acid-washed plastic falcon tubes in a dark freezer at -20 °C until analyzed. We determined concentrations of NH_4^+, NO_3^-, $Si(OH)_4$, and PO_4^{3-} in the water samples using a SEAL AutoAnalyzer 3 HR nutrient water analyzer at Fisheries and Ocean Canada, St. John's, NL.

At the end of the incubations, we sectioned each core into three sediment layers (0-2, 2-5, 5-10 cm). Some cores did not penetrate to a sufficient sediment depth to capture the entirety of the deepest layer (5-10 cm), however, low numbers of individuals in the 5-10 fraction and the absence of a deep layer for some cores led us to focus on only the 0-2 and 2-5 cm sections for taxonomic analysis.

5.3.3 DNA extraction and sequencing

At the end of the incubations, we collected a small subset of the top 0-2 cm of the sediment from each incubated (enriched and control) and non-incubated core, and stored it at -80 °C, prior to subsequent DNA extraction at the Integrated Microbiome Resource (IMR; Dalhousie University, Nova Scotia, Halifax). Extraction of the DNA contained in ~ 0.25 g of sediment from each of 18 samples used the QIAGEN PowerFecal Pro HT kit on the QIAcube robot and a TissueLyser II for the Initial bead-beating step, following the manufacturer's instructions.

We used a dual-indexing, one-step PCR run to amplify the V4-V5 regions of the 16s rRNA of our samples with the Universal V4V5 Parada/Walters bacterial/archaeal primers pair (Comeau et al., 2017; https://imr.bio/protocols.html#libAmp) on the Illumina MiSeq using 2 x 300 bp pair-end. A dual-indexing, one-step PCR uses complete "fusion primers" that include Illumina Nextera adaptors, indices, and region-specific targeting (Comeau et al., 2017; https://www.protocols.io/workspaces/integrated-microbiome-resource-imr/publications). All

amplicon products were then pooled to create one library which was then quantified using the Invitrogen Qubit double-stranded DNA high-sensitivity (dsDNA HS) fluorescence-based method before sequencing. The data were then processed using an analysis pipeline called Microbiome Helper. FastQC was used to evaluate the quality of raw PE reads, followed by processing to create amplicon sequence variants (ASVs) in Deblur, as described in Comeau et al. (2017), using a custom SOP developed at the IMR as part of the Microbiome Helper. The exact version of the analysis pipeline used is available at https://github.com/LangilleLab/microbiome_helper/wiki/Amplicon-SOP-v2-(qiime2-2019.7). In summary, we used custom scripts and the QIIME2 program (Bolyen et al., 2019) to perform read quality-control, denoising data into ASVs using Deblur, and assignment of taxonomy against the SILVA 138 reference taxonomy (Quast et al., 2013). Subsequently, we applied those analyses to evaluate relative abundance (%) of each ASV, and diversity of different bacteria and archaea. In order to calculate relative abundances, we summed up all counts and divided each count by the overall sum. To evaluate diversity, we calculated the number of ASVs present in each sediment sample, and Shannon-Wiener (H').

5.3.4 Laboratory analysis of sedimentary organic matter

We collected sediments for analysis of organic matter and grain size from the upper 0-2 cm of the dedicated non-incubated core(s) at each site, homogenizing the sediment and then placing it in Whirl-Pak bags prior to storage in the dark at -20 °C until analyzed (except for samples for lipid analysis, which were stored in pre-combusted aluminum tin foil at -80 °C). We measured OM to summarize practical proxies of OM quantity and quality. Therefore, we used total organic carbon (TOC) to describe food quantity. To characterize quality we used chlorophyll a (Chl*a*), phaeopigments (Phaeo), and the chlorophyll *a*:phaeopigment ratio (Chl*a*:Phaeo) as indicators of

short-term OM freshness and quality (Guitton et al., 2015); algae and photosynthetic pigments degrade faster than lipids and provide a measure of freshness of OM over time scales of days-weeks. We also used total lipid concentrations as an indicator of intermediate-term (weeks to months) OM lability/quality (Mayer et al., 1995) because lipids degrade at slower rates compared to pigments. Finally, we used the carbon:nitrogen (C:N) ratio as an indicator of long-term (months to years) OM quality, with lower C:N indicating fresher and higher quality OM because of more rapid use of nitrogen than C (Guitton et al., 2015).

5.3.4.1 CHN analysis

Total organic carbon and total nitrogen (TN) were determined by drying a sediment subsample of 1-5 g (wet weight) at 60 °C for 24 h, grinding it to a fine powder, and then weighing and acidifying (with pure HCl fumes) for 24 h to eliminate inorganic carbon. Samples were dried again at 60 °C for 24 h before starting CHN analysis. We then weighed an aliquot of dried decarbonated sediments (15 mg) and folded it tightly into a tin capsule. A Carlo Erba NA1500 Series II elemental analyser (EA) determined the sediment concentration of TOC and TN, expressed as carbon/nitrogen percent weight.

5.3.4.2 Phytopigment content

We measured chlorophyll a and phaeopigments spectrophotometrically (Cary 300 BIO) (Danovaro, 2009), noting that spectrophotometric assays are generally used for pigments in sediments with concentrations > 0.5 Chl*a* $\mu g \cdot g^{-1}$. For each sample, we placed 2 g of frozen sediment in a transparent falcon tube wrapped with aluminum foil to block out light. We extracted pigments from the sediment in 90% acetone, vortexed the solution for 30 s, and then treated the sample in an ultrasound bath in ice at 50 - 100 W for 3 min, with a 30 s interval between each minute of sonication prior to overnight storage at 4 °C in the dark. The following day we

centrifuged them for 10 min at 800 x g (3800 rpm) and analyzed the supernatant in order to measure absorbance at wavelengths of 750 nm and 665 nm (against a blank of 90% acetone). At the same wavelengths, we determined phaeopigments by acidifying the acetone extract with 200 µL of 0.1 N HCl added directly to the cuvette. We dried the remaining sediment at 60 °C for 24 h prior to weighing.

5.3.4.3 Lipid content

We extracted frozen lipid samples according to Parrish (1999), a method that required repeating specific steps three times. We used a combination of chloroform:methanol:water (4:2:1.5) in order to create an upper inorganic and a lower organic layer. We were interested in removing and then analyzing the bottom organic layer that contained lipids and therefore sonicated the sample for 4 min in an ice bath followed by two minutes of centrifuging. Without disturbing the top aqueous layer, we used a double pipetting technique that required 2 lipid-cleaned Pasteur pipettes, a long 1-ml pipette inside a short 1-ml pipette. We then added chloroform back to the extraction test tube. As a final step, we transferred all the organic layers into a lipid-cleaned vial, concentrating samples under a flow of nitrogen gas.

Lipid class composition was determined at the Aquatic Research Cluster (ARC) at the Ocean Science Center of Memorial University, using an Iatroscan Mark VI TLC-FID (thin-layer chromatography-flame ionization detector system; Mitsubishi Kagaku Iatron, Inc., Tokyo, Japan), silica-coated Chromarods, and a three-step development method (Parrish, 1987). The lipid extracts were applied to the Chromarods and focused on a narrow band using 100% acetone. The first development system was hexane: diethyl ether: formic acid (99.95:1:00.05). The rods were developed for 25 min, removed from the system for 5 minutes, and then replaced for 20 min. The second development in hexane: diethyl ether: formic acid (79:20:1) lasted for 40 min. The final

development system required two steps, the first involving immersion in 100% acetone for two 15-minute periods, followed by two 10-min periods in chloroform:methanol:chloroform-extracted water (5:4:1). Before each solvent system was run, we dried the rods in a constant humidity chamber. After each development system, we scanned the rods in the Iatroscan and collected data using Peak Simple software (ver 3.67, SRI Inc). Chromarods calibration used standards from Sigma Chemicals (Sigma Chemicals, St. Louis, Mo., USA).

5.3.4.4 Grain size

Sample analysis at the Bedford Institute of Oceanography, Marine Environmental Geoscience, Nova Scotia, used a Beckman Coulter LS 230 Laser Diffraction analyzer set at a 0.4–2000 μm range. Samples were subjected to 35% hydrogen peroxide digestion over several days to remove organic particles, then centrifuged and freeze-dried. After freeze-drying, we immediately capped and weighed the vials. Grain size analysis then proceeded on individual samples by first removing the cap and then disaggregating the sample using a metal spoonula before pouring the contents over a 2-mm sieve. The >2 mm material was then weighed at ¼ phi intervals and values recorded. The <2 mm fraction was either used in its entirety or microsplit for analysis in the Beckman Coulter LS13-320 laser diffraction analyzer. Samples were then disaggregated completely in an ultrasound bath before they were introduced into the laser diffraction analyzer for analysis; a daily control sample ensured consistency. Samples were analyzed for a full 60 s and graphed based on size. The logged files were processed using Femto Particle Sizing Software (PSS) version 5.6. Laser diffraction data were then merged with the gravel fraction to normalize the distribution. PSS uses Folk and Ward graphic statistical parameters based on phi midpoints and a geometric mean.

5.3.5 Statistical analysis

In order to evaluate whether alpha diversity varied among habitats we used the "estimate" function in the R "vegan" package (Oksanen et al., 2005) to compare richness and Shannon diversity from 18 samples collected from Canyon, Inter-canyon, and Channel habitats. We also calculated accumulation curves using the vegan package and the "specaccum" function.

In order to investigate variation in multivariate taxonomic community composition, we performed three multivariate analyses of variances (PERMANOVAs) separately, with the factor "Sites" (four levels: C-T; KHM; NEC1; NEC2); "Habitat" (three levels: Canyon, Inter-Canyon, Channel), and "Treatments" (three levels: enriched incubated; control incubated; non-incubated cores) performed with 999 random permutations of appropriate units (Anderson and Walsh, 2013). We used the function "adonis2" to analyze and partition sums of squares using dissimilarities (McArdle and Anderson, 2001). We calculated the resemblance matrices based on Bray-Curtis dissimilarities of benthic community data and verified homogeneity of multivariate dispersion using the "betadisper" function (Anderson et al., 2006). We further analyzed significant terms within the full models using appropriate pair-wise comparisons. Non-metric multidimensional scaling (nMDS) ordinations of similarity matrices visualized multivariate patterns, and we determined taxa that contributed most to within-site similarity and dissimilarity between sites using SIMPER (Similarity percentage analyses) (Clarke, 1993).

To evaluate any possible differences in OM variables based on the three different habitats, we performed ANOVA analysis for each variable (C:N, %TOC, Chl*a*, Phaeo). When data failed to meet either normality (Shapiro test) or homogeneity (Levene test) assumptions, even after trying log and sqrt transformations of our response variable, we performed a non-parametric test (Kruskal.test),. In addition, redundancy analysis (RDA) provided a better understanding of which

environmental and sedimentary variables (C:N, %TOC, Chl*a*:Phaeo, Tot_lipids, Depth, %Gravel, %Sand, %Mud, %Silt, %Clay, Salinity, Temperature, pH, O_2W) best explained benthic microbial community composition variation among habitats, using a type II scaling that focuses on the explanatory variables rather than response variables. This analysis focused on dominant bacterial and archaeal genera, defined here as the most common ASVs. We transformed our data based on a Hellinger transformation prior to the RDA using the "decostand" function in R We further analyzed multi-collinearity of the predictor variables from the full models with a variance inflation factor (VIF) test using the "vif" function from the "car" package (Fox and Weisberg, 2011). All predictor variables from the selected best model had a VIF < 10 (Zuur et al., 2009). We also calculated the significance (%) of each predictor variable for both benthic community and benthic flux variation with the "vartest" function (Borcard et al., 2018). Finally, a second RDA evaluated the most abundant genera as drivers of benthic nutrient fluxes, following the steps mentioned above. In this second RDA, we used benthic nutrient fluxes from both incubated enriched and control cores, acknowledging the low number of observations for each treatment.

We investigated variation in benthic nutrient fluxes for each nutrient (ammonium, nitrate, silicate, and phosphate) focusing only on incubated control cores from each habitat type (Canyon, Inter-canyon, Channel), and using linear regression model (lm()) with the fixed factor "Habitat". We first examined data normality visually with Q-Q plots and, noting reliability concerns with visual inspections, we also ran a Shapiro-Wilk's test (p-value > 0.05 indicated normality). Levene's tests evaluated homogeneity of variance of the residuals. When the data did not meet homogeneity of variances, we conducted a non-parametric Kruskal-Wallis test.

To test for differences in single nutrient fluxes between enriched and control cores for each type of habitat, we performed a linear regression model with the "lm()" function. We confirmed

homogeneity and normality assumptions with Shapiro-Wilk's test (p-value > 0.05) and Levene's tests (p-value > 0.05), respectively.

We also performed linear regressions with the "lm()" function in order to investigate the potential roles of microbial diversity and composition in determining seafloor processes and infaunal patterns. We used microbial diversity (ASV richness and Shannon-Wiener indices) as explanatory variables, and macrofaunal diversity indices (Shannon-Wiener, Simpson, species richness, and Pielou's evenness) as response variables. Both the explanatory and response variables referred to data collected from the top 0–2 cm sediment layer of all the habitat types. We also verified the assumptions using the "check model" function, and when assumptions were not met we applied either log or sqrt transformation to our data.

5.4 Results

5.4.1 Microbial community and diversity comparisons among habitats

Our analysis documented a total of 4143 ASVs, including 74 Archaea ASVs (of which 68 were phylum Crenarchaeota, 7 phylum Nanonarchaeota) and 4069 Bacteria (spanning 37 families, 296 genera). Archaea comprised a small portion of the microbial community in each habitat, namely 2.3%, 3.8%, and 4.1%, in Canyon, Inter-canyon, and Channel habitats, respectively. In contrast, Bacteria represented 97.68%, 96.15%, and 95.92% of the microbial community in Canyon, Inter-canyon, and Channel, respectively, sharing the most abundant phyla. Among those, the dominant phylum Proteobacteria (~44%) (**Fig. 5.2**) included Gamma- (~34%) and Alpha- (~10%) proteobacteria. The order Alteromonadales (within the Gammaproteobacteria) and the Archaea Nitrososphaeria were more abundant in some Channel habitat cores than others, suggesting some patchiness in distribution. Other abundant phyla were Bacteroida (~16%), Acidobacteroida (~12%), Planctomyceta (~10%), and NB1-j (~7%) (**Fig. 5.2**; **Supplementary**

table 5.2). In total, we observed 28 phyla of Bacteria in the Inter-Canyon site, 30 in the Channel sites, and 32 in the Canyon site. Flavobacteriales, the most abundant bacterial order in all habitats, consisted almost exclusively of members of the family Flavobacteriacea (~7%). Other most abundant families shared among habitats were NB1-J (~4%), Woeseiaceae (~6%), and Pirellulaceae (~5%). Furthermore, all our samples included several microbial taxa involved in the nitrogen cycle, including the ammonia-oxidizing archaea *Nitrosopumilacea* (~4%), the nitrite oxidizers bacteria *Nitrospira* and *Nitrospina* (~1.8 and 1.2 %), the particulate organic nitrogen (PON) degrader *Pseudoalteromonas* (~10%), and the anammox *Pirellulacea* (~5%).

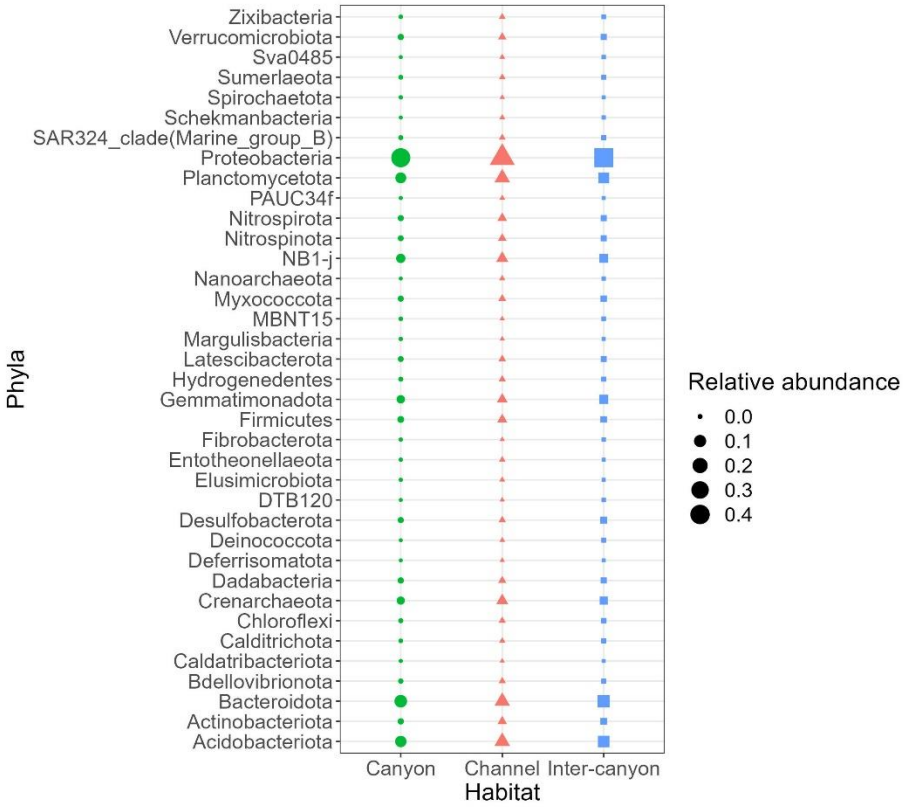

Fig. 5.2. Microbial phyla (n = 37) that characterized Canyon, Inter-canyon, and Channel habitats, identified by colour: Red = Canyon; Green = Channel; Blue = Inter-canyon. Dot size indicates the relative abundance calculated as the sum of all counts of a specific phylum in each habitat divided

by the overall sum in each habitat. Results were derived by pooling cores from all treatments at each habitat (enriched, control, non-incubated cores), noting that treatments did not differ.

Microbial community structure based on relative-ASV Bray-Curtis dissimilarities differed among habitats (Canyon; Inter-canyon; Channel (**Supplementary table 5.4**)), but did not differ among treatments both within sites (C-T; KHM, NEC1; NEC2 (**Supplementary table 5.3**) and among habitats (**Supplementary table 5.4**)). We ran PERMANOVAs to compare these habitats and treatments at all taxonomic levels combining incubated enriched and control cores, as well as non-incubated cores. We observed significant differences at class and genus levels among habitats (**Supplementary table 5.4**), but we focused on genus level to provide a more detailed view of microbial community structure. PERMANOVA at genus level showed that Channel and Canyon habitats differed significantly from one another (pairwise.adonis $R^2 = 0.15$; $p = 0.04$), but not from Inter-canyon habitats. Ten microbial genera contributed primarily to the dissimilarity (SIMPER) between Channel and Canyon habitats, with a total dissimilarity of 40% (**Fig. 5.3 A, B**). We did not observe significant differences among treatments at all taxonomic levels (**Supplementary table 5.3**).

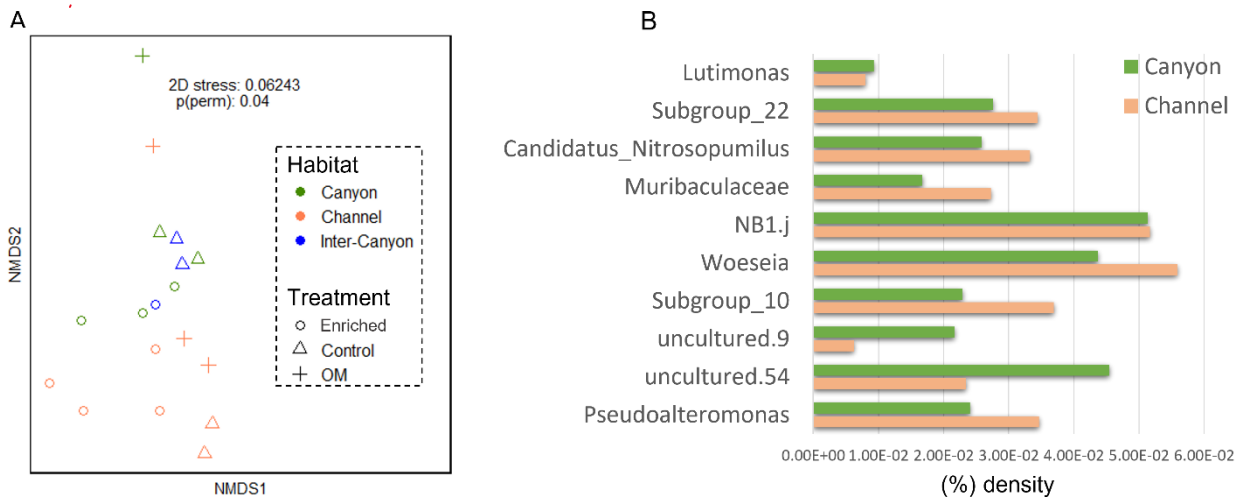

Fig. 5.3. A) Non-metric multi-dimensional scaling (nMDS) plot of genus level microbial community assemblages for each habitat type. Colors indicate different habitats: green = Canyon; orange = Channel; blue = Inter-canyon. Symbols indicate different treatments: circle = enriched incubated cores; triangle = control incubated cores; plus = unincubated cores from samples we collected to assess sedimentary OM. Each dot/triangle/square indicates a single incubated/unincubated core per habitat. Number of incubated enriched cores, control cores, non-incubated cores (OM) per habitat: 3,2,1 Canyon; 4,2,3 Channel; 1,2,0 Inter-canyon. B) Microbial genera that contributed most to Canyon and Channel dissimilarities based on SIMPER analysis.

The plateauing in all rarefaction curves for Canyon and Channel habitats indicates that we captured >90% of bacterial and archaeal diversity (**Supplementary Fig. 5.1**) and that the sequencing sufficiently captured most of the ASVs in the communities. In contrast, the Inter-Canyon curve did not plateau, indicating incomplete sampling (**Supplementary Fig. 5.1**).

Microbial diversity indices based on ASV values were similar across the three habitats (Canyon, Channel, and Inter-Canyon) (**Supplementary table 5.5**). Shannon index values (H') ranged from 4.7–4.8, and ANOVA indicated no significant differences among habitats and treatments (**Supplementary table 5.6**). Richness–was higher, though not significantly, in the Canyon site than in the Channel and Inter-canyon sites, and lower, but not significantly, in the Channel sites compared to the other habitats (**Supplementary Fig. 5.2, Supplementary table 5.6**). We did not detect significant differences in microbial diversity among treatments (**Supplementary table 5.6**), and thus we pooled both enriched and control cores, as well as non-incubated cores for each of the three-habitat types in the subsequent analyses in this study.

We observed substantially lower diversity in archaeal communities (Crenarchaeota and Nanoarchaeota) than in bacterial communities for all habitats, and therefore combined them with bacteria to produce estimates for microbes.

5.4.2 Sediment feature variation among habitats

The C:N ratio, in contrast to the total organic carbon in surface sediments, differed among habitats (C:N Kruskal Test, $p = 0.04$; % TOC $p = 0.2$), with the highest C:N ratio for the Channel sites (**Table 5.2**). The pairwise-tests showed that C:N from the Channel sites differed significantly from Canyon and Inter-canyon sites (Channel - Canyon $p = 0.03$, Channel - Inter-canyon $p = 0.04$). In addition, both Chl*a* and Phaeo in the top 2 cm of sediments were generally high and varied both within and among habitats (**Table 5.2**).

Table 5.2. Summary of the sedimentary and OM properties measured from non-incubated cores in the three Gulf of Maine habitats, (average ± standard deviation, (Inter-canyon n = 3, Canyon n = 2, and Channel, n = 4)). C:N is carbon to nitrogen ratio; TOC is total organic carbon; TOM is total OM; Chl*a* is chlorophyll-*a* concentration; Phaeo is phaeopigment concentration; Chl*a*: Phaeo is the chlorophyll *a* to phaeopigment ratio; Total lipids is total lipid concentration in control and enriched incubated cores.

Habitat	C:N	%TOC	Chl*a* ($\mu g \cdot g^{-1}$)	Phaeo ($\mu g \cdot g^{-1}$)	Chl*a*:Phaeo	Total lipids ($mg \cdot g^{-1}$)
Inter-canyon	7.2 ± 0.8	0.8 ± 0.03	1.6 ± 0.1	22.8 ± 5.5	0.06 ± 0.01	0.4 ± 0.4
Canyon	8.9 ± 0.7	0.9 ± 0.2	2.8 ± 2.8	53.0 ± 56.1	0.05 ± 0.01	0.4 ± 0.03
Channel	20.4 ± 6.5	0.5 ± 0.2	2.4 ± 2.4	31.8 ± 36.4	0.06 ± 0.02	0.1 ± 0.1

5.4.3 Environmental variables as drivers of microbial community structure

Based on our redundancy analysis using environmental variables (**Table 5.2** and **Supplementary table 5.7**) and microbial community structure at the genus level combining the three different core treatments (enriched incubated, control incubated, and non-incubated cores), environmental variables offered significant, though weak explanatory power for the Canyon and Channel sites, explaining 16% of total community variation (R^2 = 0.16, Adj. R^2 = 0.05, p = 0.009**) (**Fig. 5.4**). C:N and %TOC, the best explanatory variables, accounted for 10.0% and 9.6% of total variance, respectively. High C:N (20.4) and low %TOC (0.50%)) for the Channel sites contrasted C:N of 8.9 and %TOC of 0.9% for the Canyon site.

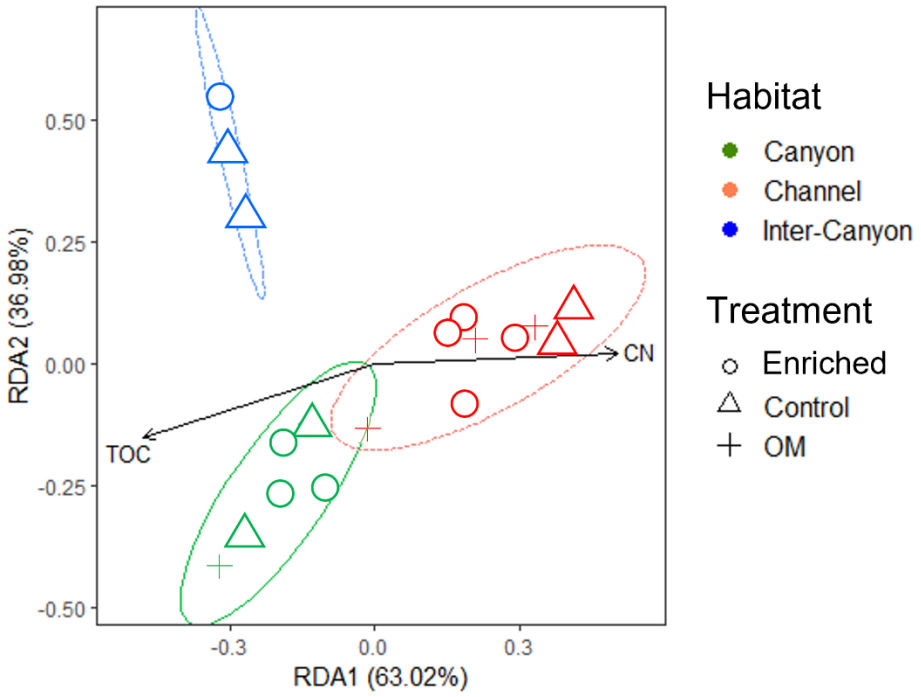

Fig. 5.4. Redundancy analysis model plot (scaling 2) of environmental factors best explaining variation in microbial community structure in Gulf of Maine sediments. C:N = Carbon to nitrogen ratio; TOC = % total organic carbon. Symbols and colours indicate individual cores for each site:

green open circle = enriched cores in Canyon; green triangle = control cores in Canyon; green cross = non-incubated cores in Canyon; red open circle = enriched cores in Channel; red triangle = control cores in Channel; red cross = non-incubated cores in Channel; blue open circle = enriched cores in Inter-canyon; blue triangle = control cores in Inter-canyon. Longer arrows indicate variables that contribute strongly to variation in the community matrix. Arrows pointing in the same direction as a given variable indicate a positive relationship, in contrast to negative relationships for arrows pointing in opposite directions of a given variable.

5.4.4 Benthic nutrient flux variation among habitats

In comparing replicate cores without enrichment among habitats, we found no significant differences in individual nutrient fluxes (**Supplementary table 5.8**), acknowledging the unbalanced design and low statistical power. Average values for each nutrient at each habitat type indicated net influx rates for all five nutrients except for nitrate and phosphate in the Inter-canyon site (Fig 5), where negative values indicate influxes (fluxes into the sediment), in contrast to positive values that indicate effluxes.

The highest oxygen consumption occurred in the Canyon site (-68.0 mmol $\cdot$ m^{-2} $\cdot$ d^{-1} $\pm$ 13.8 (SE)) where we obtained data from only two cores (**Fig. 5.5 A**), which was similar to the Inter-canyon site (-63.6 mmol $\cdot$ m^{-2} $\cdot$ d^{-1} $\pm$ 13.3 (SE)), but different from the Channel sites (-49.0 mmol $\cdot$ m^{-2} $\cdot$ d^{-1} $\pm$ 4.7 (SE)). However, within each of the three habitats, we observed consistent oxygen consumption values.

Nutrient fluxes across the three habitat types varied. We observed net influxes of ammonium into the sediment for each habitat type (**Fig. 5.5 B**), with similar rates for Canyon and Channel habitats (-98.0 µmol $\cdot$ m^{-2} $\cdot$ d^{-1} $\pm$ 23.6 (SE) and -88.3 µmol $\cdot$ m^{-2} $\cdot$ d^{-1} $\pm$ 44.1 (SE), respectively), with a substantially lower rate–of -34.3 µmol $\cdot$ m^{-2} $\cdot$ d^{-1} $\pm$ 75.7 (SE) for the Inter-canyon habitat,

noting we observed net efflux in one core from the Kinlan-Heezen Inter-canyon site. We also observed net influx of nitrate into the sediment in the Canyon and Channel habitats (-1272.54 µmol $\cdot m^{-2} \cdot d^{-1} \pm$ 445.7 (SE), and -1082.7 µmol $\cdot m^{-2} \cdot d^{-1} \pm$ 504.8 (SE), respectively) (**Fig. 5.5 C**), in contrast to low nitrate effluxes for the Inter-canyon habitat (1.4 µmol $\cdot m^{-2} \cdot d^{-1} \pm$ 1.26 (SE)). Nitrate influx varied widely among cores from each habitat. Net silicate influx occurred at all habitats (**Fig. 5.5 D**), with similar values for Inter-canyon and Channel habitats, which were more than two times higher than for the Canyon habitat (-252.2 µmol $\cdot m^{-2} \cdot d^{-1} \pm$ 197.1 (SE), -329.5 µmol $\cdot m^{-2} \cdot d^{-1} \pm$ 168.6 (SE), and -150.1 µmol $\cdot m^{-2} \cdot d^{-1} \pm$ 223.8 (SE), respectively). As with other nutrients, silicate fluxes varied widely among cores from each habitat.

Of the nutrients we examined, only phosphate showed both net influxes and effluxes (**Fig. 5.5 E**). Sediment uptake of phosphate in Canyon and Channel habitats (-87.8 µmol $\cdot m^{-2} \cdot d^{-1} \pm$ 27.4 (SE), and -50.4 µmol $\cdot m^{-2} \cdot d^{-1} \pm$ 12.6 (SE), respectively), contrasted a net release from Inter-canyon habitat (40.80 µmol $\cdot m^{-2} \cdot d^{-1} \pm$ 69.2 (SE)). Phosphate also varied widely among cores from each habitat.

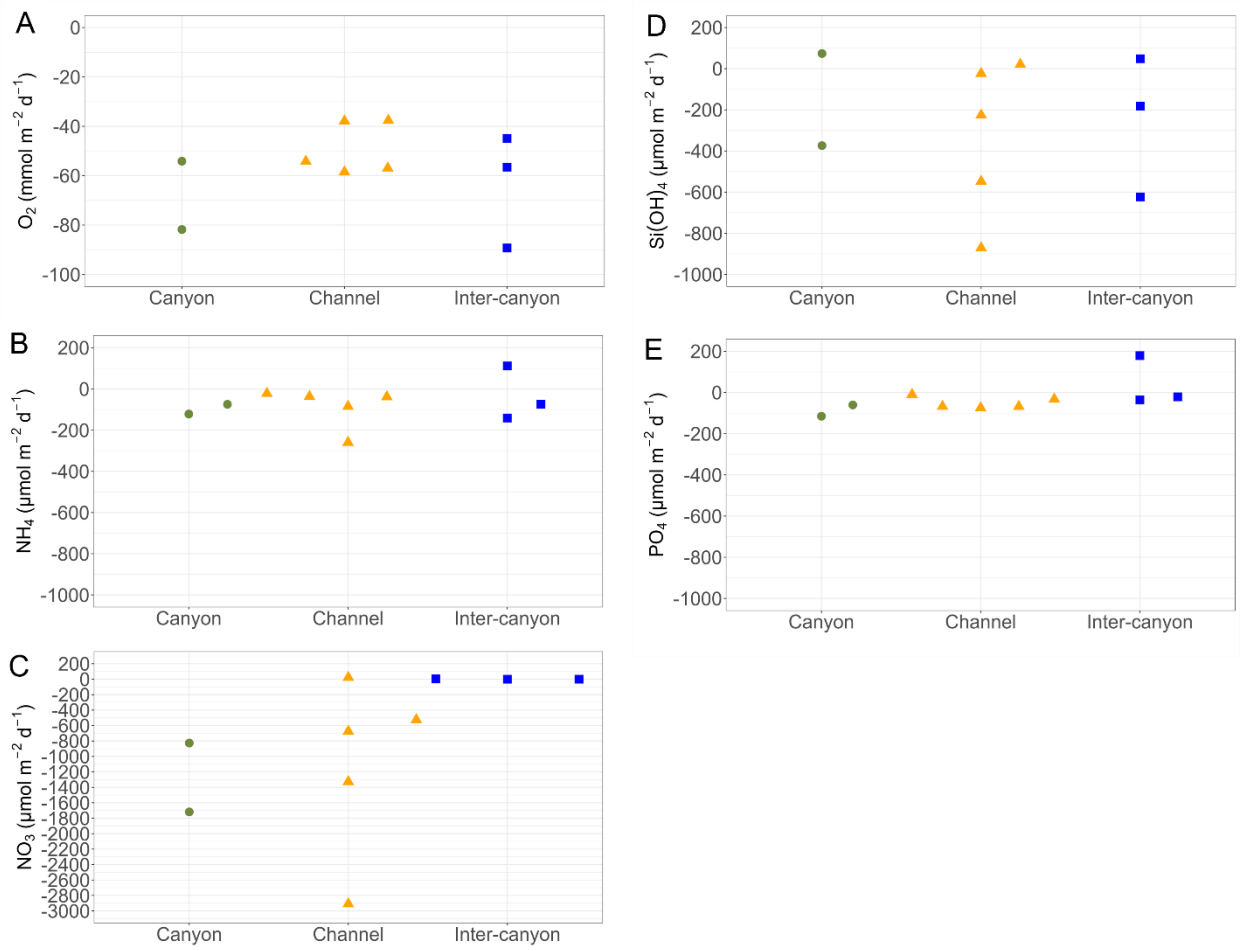

Fig. 5.5. Benthic fluxes of: A) oxygen, B) ammonia, C) nitrate, D) silicate, and E) phosphate from control cores for Canyon (n = 2), Inter-canyon (n = 3), and Channel (n = 5) sites. 0 along the y-axis indicates where fluxes change from net release from sediment above 0 and influx into the sediment below 0.

5.4.5 Benthic nutrient flux differences among treatments

We found significant differences in flux rates between enriched and control incubations only for nitrate and phosphate at the Inter-canyon and Channel habitats, respectively. No significant differences were evident for other nutrients (LM analysis, **Supplementary table 5.9**).

Following the addition of OM, the oxygen consumption rate increased in the Canyon habitat (**Fig. 5.6 A**), although with minimal increases in the Channel habitat, but maintained an average

value similar to the control cores in the Inter-canyon habitat. Indeed, we observed average oxygen consumption rates for control and enriched cores of -68.0 mmol $\cdot$ $m^{-2} \cdot d^{-1}$ and -93.5 mmol $\cdot$ $m^{-2} \cdot d^{-1} \cdot$ respectively, for Canyon habitat; -63.6 mmol $\cdot$ $m^{-2} \cdot d^{-1}$ and –57.7 mmol $\cdot$ $m^{-2} \cdot d^{-1}$ for Inter-canyon habitat; and -49.0 mmol $\cdot$ $m^{-2} \cdot d^{-1}$ and -52.4 mmol $\cdot$ $m^{-2} \cdot d^{-1}$ for Channel habitat.

Ammonium influxes increased after OM addition for all habitat types (**Fig. 5.6 B**). For Canyon habitat, we observed average values of ammonium influx of -98.0 µmol $\cdot$ $m^{-2} \cdot d^{-1}$ in control incubations in comparison with -208 µmol $\cdot$ $m^{-2} \cdot d^{-1}$ in enriched incubations, an increase from -34.3 µmol $\cdot$ $m^{-2} \cdot d^{-1}$ to -208.8 µmol $\cdot$ $m^{-2} \cdot d^{-1}$ influxes for Inter-canyon habitat, and an increase from -88.3 µmol $\cdot$ $m^{-2} \cdot d^{-1}$ to -162.0 µmol $\cdot$ $m^{-2} \cdot d^{-1}$ influxes for Channel habitat. However, one Inter-canyon and one Channel habitat enriched core showed net ammonium effluxes.

OM addition resulted in a significantly higher nitrate influx only for the Inter-canyon habitat, where we observed higher average values (-776.3 µmol $\cdot$ $m^{-2} \cdot d^{-1}$) in enriched cores compared to control cores (1.4 µmol $\cdot$ $m^{-2} \cdot d^{-1}$). Control cores also yielded the highest average values of nitrate influxes for all other habitats. For example, -1272.5 µmol $\cdot$ $m^{-2} \cdot d^{-1}$ nitrate flux in the control treatment for Canyon habitat contrasted -776.3 µmol $\cdot$ $m^{-2} \cdot d^{-1}$ in the enriched treatment, and control treatments from Channel habitat of -1082.7 µmol $\cdot$ $m^{-2} \cdot d^{-1}$ contrasted -682.4 µmol $\cdot$ $m^{-2} \cdot d^{-1}$ in the enriched treatment (**Fig. 5.6 C**).

The only nutrients for which enrichment resulted in an efflux rather than an influx were silicate and phosphate. Specifically, silicate fluxes for control and enriched treatments were -150.1 µmol $\cdot$ $m^{-2} \cdot d^{-1}$ and 20.4 µmol $\cdot$ $m^{-2} \cdot d^{-1}$, respectively, for Canyon habitat and -329.5 µmol $\cdot$ $m^{-2} \cdot d^{-1}$ and 340.4 µmol $\cdot$ $m^{-2} \cdot d^{-1}$, respectively, for Channel habitat. In addition, we observed an average silicate influx value of -252.8 µmol $\cdot$ $m^{-2} \cdot d^{-1}$ in control cores, and 20.4 µmol $\cdot$ $m^{-2} \cdot d^{-1}$ in enriched cores for Inter-canyon habitat (**Fig. 5.6 D**).

Phosphate efflux rates increased after OM addition for all sampled habitats. The average influx value of -87.8 µmol · m^{-2} · d^{-1} for the Canyon control treatment contrasted 54.5 µmol · m^{-2} · d^{-1} efflux for the enriched treatment. We also observed increasing phosphate efflux in comparing control cores (40.8 µmol · m^{-2} · d^{-1}) and enriched cores (54.4 µmol · m^{-2} · d^{-1}) in Inter-canyon habitat. In contrast, phosphate influx in the control treatment for the Channel habitat (-50.3 µmol · m^{-2} · d^{-1}) switched significantly to net efflux for the enriched treatment (194.8 µmol · m^{-2} · d^{-1}) (**Fig. 5.6 E**).

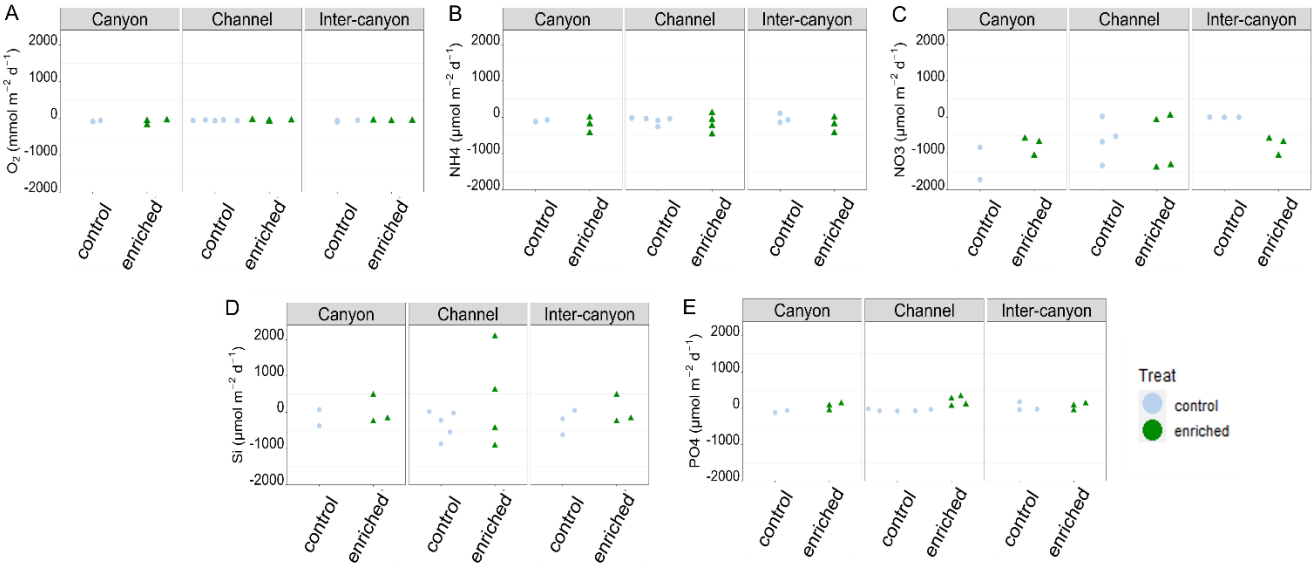

Fig. 5.6. Average values for: A) oxygen consumption, B) ammonium, C) nitrate, D) silicate, and E) phosphate fluxes, in enriched (green dot) and control (light blue dot) cores for each habitat (Canyon (n = 5), Inter-canyon (n = 6) and Channel (n = 9)). Positive values indicate effluxes and negative values indicate influxes. Asterisks indicate significant differences in GLM analysis between enriched and control cores in a given habitat.

5.4.6 Relationships between microbes and nutrient fluxes

The redundancy analysis comparing benthic nutrient fluxes in relation to the microbial genera that most contributed to microbial differences among habitats, explained only 7% of the total variance ($R^2 = 0.27$, $AdjR^2 = 0.07$). The first axis (RDA1) contributed more than RDA2 to the total explained variation (69% and 19%, respectively). Moreover, although all four genera chosen for our model (based on SIMPER analysis in section 3.2) contributed to the variation (NB1-J = 13.88%, Subgroup22 = 10.7%, *Pseudoalteromonas* spp. = 9.1%, and *Woeseia* spp. = 3.8%), only *Pseudoalteromonas* spp. and *Woeseia* spp. were not negatively related to nutrient fluxes.

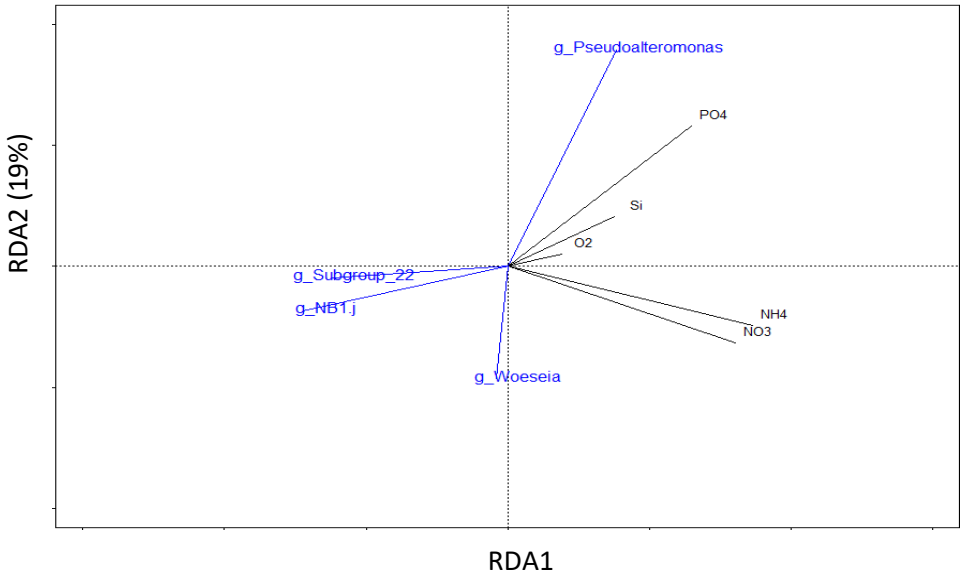

Fig. 5.7. Redundancy analysis model plot (scaling 2) of the four microbial genera best explaining variation in benthic fluxes measured in Gulf of Maine incubations. Longer arrows indicate a stronger driver of variation in the community matrix. Arrows pointing in opposite directions indicate a negative relationship. Arrows pointing in the same direction indicate a

positive relationship. Canyon n = 5; Inter-canyon n = 3; Channel n = 6. We excluded non-incubated cores given the absence of nutrient flux data.

5.4.7 Can prokaryotic diversity predict macrofaunal diversity of contrasting habitats?

Infaunal taxonomic diversity differed significantly among habitats, (PERMANOVA p value = 0.01), in comparing Canyon and Channel (p = 0.24), and Inter-canyon and Channel (p = 0.24) habitats. SIMPER showed significant differences among Canyon and Channel habitats, and Inter-canyon and Channel habitats in terms of expected number of species (p = 0.005; 0.001, respectively).

Linear regression between microbial diversity and macrofaunal diversity (**Table 5.3**) showed no significant relationship between the two (**Supplementary table 5.10**). For this analysis, we only considered incubated enriched and control cores for each habitat type, excluding the non-incubated cores, for which we lacked macrofaunal data.

Table 5.3. Macrofaunal and microbial diversity indices measured for each habitat from the 0-2 cm fraction of incubated enriched and control cores. H' = Shannon-Wiener; S = Species richness; J = Pielou's evenness indices.

				Macrofauna				Microbes	
Habitat	**Location**	**Core**	**Treatment**	**H'**	**Simpson**	**S**	**J**	**H'**	**S**
Canyon	Corsair Canyon Tributary	1	Enriched	2.0	0.8	9	0.9	4.6	254
Canyon	Corsair Canyon Tributary	2	Enriched	2.2	0.8	10	0.9	4.7	167
Canyon	Corsair Canyon Tributary	6	Enriched	2.4	0.9	13	0.9	4.9	348
Canyon	Corsair Canyon Tributary	3	Control	2.0	0.8	9	0.9	4.6	184

Canyon	Corsair Canyon Tributary	8	Control	2.2	0.8	12	0.9	5.0	403
Channel	Northeast Channel 1	1	Enriched	2.3	0.8	12	0.9	4.8	238
Channel	Northeast Channel 1	5	Enriched	1.9	0.7	9	0.8	5.1	247
Channel	Northeast Channel 1	10	Control	2.1	0.8	10	0.9	4.6	219
Channel	Northeast Channel 2	4	Enriched	2.5	0.9	15	0.9	5.0	191
Channel	Northeast Channel 2	8	Control	1.3	0.7	4	0.9	4.5	180
Channel	Northeast Channel 2	9	Control	2.3	0.8	11	0.9	4.8	212
Inter-canyon	Kinlan-Heezen Inter-canyon	3	Enriched	2.0	0.8	8	0.9	4.8	430
Inter-canyon	Kinlan-Heezen Inter-canyon	7	Control	2.2	0.8	13	0.8	4.6	181
Inter-canyon	Kinlan-Heezen Inter-canyon	5	Control	2.2	0.8	13	0.8	4.6	213

5.5 Discussion

The three different Gulf of Maine habitats clearly differed in microbial community structure. Channel and Canyon habitats differed in microbial composition. The Inter-canyon microbial community was difficult to contrast with our other study sites because of incomplete sampling, as indicated by the non-asymptote rarefaction curve. Specifically, among the 10 genera that contributed to the dissimilarity between the Canyon and Channel habitats, *Candidatus* Nitrosopumilus*, Woeseia* spp.*, Pseudoalteromonas* spp.*,* and *Muribaculacea* spp. occurred more frequently in Channel than Canyon habitat. By contrast, *Lutimonas* spp. and two uncultured groups typified the Canyon site. Moreover, microbial distributions in Canyon and Channel habitats were driven primarily by differences in quantity and quality of organic matter measured as %TOC and C:N. However, whereas habitat spatial heterogeneity often enhances biodiversity, we did not observe a spatial heterogeneity effect in our microbial diversity assessment. We found that our

three study habitats shared most of the same microbial taxa, such as phylotypes affiliated with Proteobacteria, Bacteroida, Acidobacteriota, Planctomyceta, and NB1-J Deltaproteobacteria. Furthermore, differences in microbial community composition in Canyon and Channel habitats explained only 7% of nutrient flux variation, noting microbes related to nitrogen and phosphate fluxes by highlighting the contribution of *Pseudoalteromonas* spp. and *Woeseia* spp. The latter, indeed, might primarily contribute to both nitrogen regeneration and consumption in sediment, however, they might also contribute to phosphate cycling in environments with limited nitrogen availability. Finally, the low number of replicates in our study likely limited our capacity to identify and predict those variables that shape benthic community composition of microbes and macrofauna. Indeed, we noted no relationship between microbial and infaunal communities in this study, although organic matter remineralization by microbes potentially affects macrofaunal community composition. Ciraolo and Snelgrove (2023) reported significant differences in infaunal diversity and assemblages among the three-habitat types. Polychaetes dominated the three habitats, although some polychaete families dominated one habitat over another. For example, the families Spionidae, Scalibregmidae, Flabelligeridae, Arenicolidae, and Sphaerodidae contributed most to Canyon and Channel differences (30%), with greater abundances of these taxa (except Scalibregmidae), in Canyon than in Channel habitats.

5.5.1 Microbial differences between Canyon and Non-Canyon habitats

We expected that environmental differences between Canyon and Non-Canyon habitats would contribute to differences in microbial communities. Indeed, we observed clear differences in sedimentary microbial communities, but not diversity between Canyon and Channel habitats. The genera that contributed most to Canyon and Channel dissimilarities generally represented a greater portion of the community in Channel than in Canyon sites. Previous studies linked the

higher dynamism in canyons to greater abundance (both for bacteria and archaea) and community heterogeneity (Polymenakou et al., 2008; Corinaldesi et al., 2019). Accordingly, the complex topography and strong, variable currents that characterize submarine canyons enhance marine landscape diversity by creating habitat heterogeneity for diverse fauna and prokaryotes (Huvenne and Davies, 2014; Fernandez-Arcaya et al., 2017; Ismail et al., 2018). For example, Roman et al. (2019) reported more heterogeneous microbial assemblages and a stronger influence of phytodetritus and organic matter in canyon sediments than on open slopes. A previous study of bacterial communities hosted by cold water coral in Corsair Canyon differed from the surrounding water (Weiler et al., 2018), but they did not document sediment microbial communities. However, although previous studies showed that canyon habitat can support a great microbial abundance, which was mostly explained by availability of trophic sources (Corinaldesi et al., 2019), we infer that Channel habitat in our study likely provided a more suitable environment for microbial growth than Canyon habitat. For example, the deep, cold and rich-nutrient water masses of NE Channel (Christensen et al., 1996) might favor higher benthic microbial abundance than in Canyon habitat.

Among microbes that may play a prevalent role in our sedimentary habitats, we note that *Woeseia* spp.*, Candidatus ,* Nitrosopumilus*,* and *Pseudoalteromonas* spp.*,* led to significant microbial differences between Canyon and Channel sites based on SIMPER analysis, but also dominated the Channel sites. *Woeseia* spp.*,* a type of Gammaproteobacteria, contributes to cycling of detrital proteins in marine benthic environments and particularly nitrogen; it is also a potential facultative chemolithoautotroph (Hoffman et al., 2020). The functioning of *Candidatus* Nitrosopumilus *,* an ammonium-oxidizing archaeon (Mosier et al., 2012), couples with the nitrite-oxidizing bacterium *Nitrospina* spp.*; C.* Nitrosopumilus. transforms ammonia to nitrite and subsequently *Nitrospina* converts nitrite to nitrate (Park et al., 2010; Lücker and Daims, 2014).

Nitrospina spp. was present in all our cores, though not as the most abundant taxon. *Pseudoalteromonas* spp., a Gammaproteobacteria, strongly dominated some cores from the Channel sites. *Pseudoalteromonas* spp. typically co-occurs with eukaryotic cells and produces extracellular enzymes that contribute to the decomposition of particulate organic matter in deep-sea sediments (Qin et al., 2011). Despite the common occurrence of *Pseudoalteromonas* spp. in sediments, little information exists on how they thrive in marine sedimentary environments. For example, in Okinawa, this genus produces abundant proteases and exopolysaccharides indicative of degradation of sedimentary PON (Qin et al., 2011).

Moreover, in contrast to inferences regarding *Woeseia* spp., *Candidatus* Nitrosopumilus , and *Pseudoalteromonas* spp., we lack ecological knowledge regarding functions of abundant *Muribaculacea* spp., or *Lutimonas* spp., which dominated our Channel and Canyon sites, respectively.

Except for Alphaproteobacteria, the dominance of Gammaproteobacteria in all our habitats, followed by Bacteroidetes, Acidobacteria, and Planctomycetes aligns with previous studies off the coast of California (Harrison et al., 2018). Li et al. (2009) suggested that the high sediment dominance and high versatility of Gammaproteobacteria in most sedimentary habitats indicate they can potentially grow rapidly on diverse carbon sources in different concentrations. Indeed, past studies describe Gammaproteobacteria as r-strategists, given their ability to withstand long periods of starvation and then becoming competitive when nutrient availability increases (Pinhassi and Berman 2003). Moreover, Gammaproteobacteria can degrade chitin and derivatives to obtain carbon and nitrogen, thereby expanding their distribution in sediments (Gärtner et al., 2011). Gammaproteobacteria also frequently occur both in oxygenated and low-oxygenated surface and subsurface sediments as chemolithoautotrophs, most likely as sulfur-oxidizers, potentially

trapping carbon in sediments and by tapping still-unknown energy sources (Dyksma et al., 2016). Chemolithoautotrophic sulfur-oxidizer Gammaproteobacteria may also encode an enzyme that oxidizes hydrogen sulfide to polysulfide (Bartsch and Kamen, 1960) which contributes to incorporation of sulfur into organic matter in reducing sediments (Vairavamurthy et al., 1992). Overall, accumulation of sulfide in sediment resulting from reduction of sulfate (Hargrave et al., 2008) inhibits mitochondrial cytochrome oxidase, therefore arresting aerobic metabolism and resulting in high toxicity for benthic organisms (Grieshaber and Völkel, 1998).

The high abundance of Alphaproteobacteria in our habitats may relate to availability of organic matter as indicated by high Chl*a,* and suggested by Polymenakou et al. (2009) in their study of three deep basins and two shallow upper-slope stations. Indeed, all three habitats in our study showed evidence of food availability and the presence of Alphaproteobacteria.

The NB1-j Deltaproteobacteria group, one of the microbial groups that typified our habitats, occurs widely in deep-sea sediments (Dell'Anno et al., 2021). However, its function and metabolic features remain unknown (Zhang et al., 2021).

5.5.2 Environmental drivers of microbial community composition

Of the three habitat types, two of the environmental variables included in our study, C:N and %TOC, played a role in structuring the microbial communities of Canyon and Channel habitats. The absence of any strong Inter-canyon microbial community predictor suggests that variables not included in our study, along with the small number of replicates, also played a significant role. We also observed contrasting environmental drivers in comparing Canyon and Channel habitats, noting higher C:N and lower %TOC in Channel than in Canyon habitat. Refractory compounds characterized organic matter in Channel habitat, indicative of accumulation of old organic matter. The C:N ratio of 20 suggests a potential terrestrial origin of some of the organic material (Meyers,

1994), which tends to be more refractory than marine sources (e.g., Hedges et al., 2000). Our results also align with Townsend et al. (2010) who emphasized the influence of the Penobscot and St John's Rivers that drain significant organic matter into the Gulf of Maine. The low amount of organic matter in Channel habitat may reflect the coarser sediment, in contrast to the higher organic content in Canyon habitat. In addition, the high total organic carbon and fresh quality in Canyon habitat, followed by Inter-Canyon and Channel habitat, was relatively consistent with other slope environments, such as Monterey Canyon (~0.1 %TOC, Paull et al., 2006). The fresh and abundant organic matter in Canyon habitat might support a high relative abundance of microbes able to use fresh organic matter. Indeed, fresh organic matter generally includes smaller molecules that can break down faster (Henrichs, 1992) compared to older organic matter, which may consist of macromolecules of uncertain composition that either resists decomposition or takes more time to degrade. Therefore, the contrasting environmental drivers we observed between Channel and Canyon habitats align with the hypothesis of a high degree of specificity in many deep-sea microbial communities in terms of taxa and ecological specializations in response to characteristic nutrients, particle fluxes, and pulses of organic carbon (Goffredi and Orphan, 2010; Jacob et al., 2013; Sevastou et al., 2013). In contrast, other factors that we did not quantify but that may influence the Inter-canyon community, might include nematode density and diversity. Specifically, previous studies report nematodes feeding on bacteria (Moens and Vincx, 1997), and other studies document microbial commensalism (Moens et al., 2005). Roman et al. (2019) reported a positive relationship between nematode density and bacterial diversity in slope sediments.

5.5.3 Microbial influences on nutrient fluxes

Microbial communities influence global biochemical cycles (Orsi et al., 2018) and our study provides further evidence of the complexity of sedimentary biogeochemical processes. Indeed, our nutrient flux measurements suggest limited nitrogen regeneration on a broader habitat scale and decoupling of nitrification and denitrification (Ciraolo and Snelgrove, 2023). Our sampling of organic matter after peak seasonal input (given the high level of phaeopigments and low concentrations of Chl*a*), and Gulf of Maine characteristic circulation might both contribute to the low rate of nitrogen regeneration. Christens et al. (1996) showed that the western Gulf of Maine receives low-nutrient deep-water masses from the Northeast Channel because of high nutrient uptake in the eastern Gulf, which links directly to the Northeast Channel. Moreover, some bacteria involved in nitrogen cycling, such as *Woeseia* spp. (Hoffman et al., 2020), and *Pseudoalteromonas* spp. (Qin et al., 2011) – linked to nutrient fluxes based on our RDA analysis - might provide some support for nitrification-denitrification. We also suggest a potential role for *Pseudoalteromonas* spp. in phosphate fluxes. We noted earlier the potential role of this genus in the nitrogen cycle, but we also infer that during periods of nitrogen limitation and environmental stress, it assimilates nitrogen and uses dissolved organic phosphate for building membrane lipids. Not all, but some *Pseudoalteromonas* spp. can adapt to environmental stress and build required membrane lipids. For example, P. *lypitica* biosynthesized phosphorous lipids when exposed to high phosphate concentration, and vice-versa (Carriot et al., 2022). Similarly*, P. haloplanktis* TAC 125 increases membrane phosphate content with increasing growth temperature (>20 ˚C) (Corsaro et al., 2004). Petrie and Yeats (2000) reported annual and spatial variation in nitrogen (and silicate) water column concentrations, but not in phosphate in the Gulf of Maine. Nitrogen cycling in surface waters increases in fall and early winter and decreases in late winter and summer; Petrie and Yeats

(2000) also observed a decrease in near-surface nitrogen concentration during winter in the Gulf of Maine in contrast to the Scotian shelf. Furthermore, they did not observe a pronounced seasonal cycle in phosphate, which instead decreased slowly over 6 mo. Therefore, we infer that some microbes might use more phosphate during periods of environmental stress, potentially representing a "new" limiting nutrient beyond nitrogen. Moreover, in anaerobic conditions, which might occur in some of our sediments given the high probability of nitrification-denitrification, bacterial organisms might use stored polyphosphate (polyP) as a source of energy to synthesize an organic electron acceptor. The resulting P release to the aqueous medium (Soudry, 2000), would thereby explain phosphate release from sediments in our Inter-canyon habitat. PolyP compounds are linear polymers that contain tens to hundreds of phosphate residues linked by energy-rich phosphoanhydride bonds (Kulaev, 1975; Achbergerová and Nahálka, 2011). PolyP compounds likely arise from a biological origin such as exoskeletons of dead plankton sinking to deep-sea sediments (Diaz et al., 2008; Achbergerová and Nahálka, 2011).

Although microbial communities exert an important role in OM remineralization, mineralization involves multiple processes influenced not only by microbial presence or absence of microbes, but by biological, chemical, and physical processes that presumably account for the 93% of nutrient flux variation our study could not account for. For example, noting different physiological pathways that compete for organic matter, thermodynamic and/or kinetic conditions under which microbes operate influence organic matter remineralization (Arndt et al., 2013). Temperature strongly influences microbial metabolisms and their enzymatic reactions that indirectly control rates of biogeochemical processes (Arndt et al., 2013). Organic matter origin (terrestrial and/or marine) and its composition also influence its degradability (Keil, 2011; Middelburg, 2011). Bioturbation (Ingall and Janke, 1994; Foshtomi et al., 2015), bio-irrigation

(Archer and Devol, 1992; Hensen et al., 2006), and grain size surface area (Mayer et al., 1994; Ransom et al., 1998) also control organic matter remineralization. The "rare biosphere", referring to the many rare and unexplored microbial forms reported in sediments (Sogin et al., 2006), add further complication; because we know little about their distribution and activity, we cannot assess their potential contributions to nutrient fluxes in our habitats. Low-abundance populations presumably experience less predation and direct competition with dominant community members (Sogin et al., 2006). The extreme phylogenetic diversity of the rare biosphere suggests these minor populations have persisted over geological time scales and that they may episodically reshape planetary processes (Sogin et al., 2006). Despite the poor relationship between microbial community composition and benthic nutrient fluxes in our study, the lack of differences in nutrient fluxes among habitats and between treatments might also potentially link to the absence of clear differences in microbial diversity.

The general pattern of net nutrient influxes in all habitats, especially nitrogen, and the documented presence of archaea and bacteria involved in the nitrogen cycle, led us to expect a clear relationship between them. However, our analysis showed no clear relationship between microbes and nutrient fluxes, suggesting that additional factors may be more important in driving benthic nutrient fluxes in our sampling region.

5.5.4 Prokaryotic diversity effects on macrofaunal diversity

Bacteria and archaea catalyze organic matter degradation on the sediment surface (Jørgensen 2006), likely shaping infaunal communities. Moreover, the sediment infaunal community strongly affects microbial communities through bioturbation and grazing (Albertelli et al., 1999; Solan et al., 2005, Kristensen et al., 2005). However, our analyses showed no significant relationship between micro- and macrofaunal sedimentary diversities. Once more, we infer complicated drivers

of infaunal patterns in the three habitats of our study. We therefore propose that variables not included in this study such as current speed, surface ocean productivity, and seasonality may influence infaunal communities (Loubere 1991, 1998; Ciraolo and Snelgrove, 2023). Furthermore, macrofauna and prokaryotes may potentially compete for the same organic matter substrate, especially during initial organic matter sedimentation, resulting in the dominance of one class over another in a different phase of the sedimentation process. For example, experiments that added organic matter to the sediment surface (Moodley et al., 2002; Witte et al., 2003b) identified uptake into the macrofaunal pool as the most important initial response to an organic carbon pulse, with bacterial uptake and respiration becoming more important over time.

Therefore, predicting and differentiating the factors that determine benthic community composition remains challenging, though a complex interplay of factors such as the nature and timing of food supply (Witte et al., 2003a, b), environmental stressors (Woulds et al., 2007), feeding strategies, and competition (Hunter et al., 2012) appear to be important.

5.6 Conclusions

Our results demonstrate the importance of spatial heterogeneity for relative microbial community abundance, but not for microbial diversity, especially Canyon and Channel habitats. Canyon and Channel habitats shared most of the same microbial genera but differed in relative abundance. Whereas *Woeseia* spp.*, Candidatus Nitrosopumilus* sp., *and Pseudoalteromonas* spp. dominated Channel sites, *Lutimonas* spp. and two uncultured groups typified Canyon habitat. These findings illustrate the challenge of explaining the complex variables that influence benthic nutrient cycling. Our sedimentary results also suggest a closer connection between the deep-sea seafloor of the Gulf of Maine to coastal areas through Northeast Channel more than Canyon and Inter-Canyon habitats. Furthermore, other than C:N and %TOC, we observed similar

environmental conditions in Canyon and Channel sediments, which might lead those habitats to harbor similar microbial genera but potentially in different proportions. Moreover, the addition of organic matter revealed no significant difference in microbial diversity, perhaps reflecting the relatively short incubation period, but it did indicate changes in nitrate and phosphate fluxes, though only in the Inter-canyon and Channel habitats, respectively. In addition, and noting similar microbial diversity among habitats in our short-term experiments, we only observed a modest influence of microbes on benthic nutrient fluxes, especially in terms of nitrogen and phosphate. However, key gaps remain in understanding relationships between nutrient fluxes and microbes, suggesting potentially interacting effects of other variables. Moreover, although different benthic group sizes share the same sediment environment, likely with similar organic matter availability, we found no relationship between microbial and macrofaunal community composition. This result highlights the challenge of identifying the factors that determine benthic community composition, and that enhance overall benthic ecosystem functioning. Future studies might include either wider spatial or temporal scales, and microbial functional analysis might provide a pathway to predict deep-sea remineralization processes more accurately. Moreover, future studies should also increase sample replication. For example, low sample size in Inter-canyon habitat limited our statistical power in drawing strong conclusions regarding Inter-canyon microbial assemblages. Similarly, increased number of both sedimentary and nutrient flux measurements might alter our conclusions.

5.7 Author contributions

Alessia Ciraolo conducted the literature review, the empirical analysis, and wrote the manuscript. Paul Snelgrove and Christopher Algar helped to formulate the ideas and content of

the manuscript. Paul Snelgrove also helped to formulate the structure of the manuscript and provided editorial guidance.

5.8 Acknowledgments

We thank Chief Scientist Dr. M. Nizinski, Dr. Anna Metaxas, and crewmembers of the NOAA ship *Henry B. Bigelow* for ship logistic and sampling opportunities. We also thank Jeanette Wells (Memorial University) who helped with lipids analysis, Dr. Bárbara Neves (Fisheries and Oceans Canada (DFO)) for assistance with chlorophyll analysis, Dr. Owen Brown (Natural Resources Canada) for help with grain size analysis, Dr Gary Maillet and Ms. Gina Doyle (DFO) for help with nutrient analysis, and Dr. Andrew Comeau (Dalhousie University) for help with microbial analysis. Dr. Amanda Bates, Dr. Suzanne Dufour, and two anonymous reviewers provided helpful comments on an earlier draft of this manuscript. We also thank the School of Graduate Studies at Memorial University for additional financial support. This research was sponsored by the Natural Sciences and Engineering Research Council of Canada (NSERC) Canadian Healthy Oceans Network, and the National Oceanic and Atmospheric Association (NOAA).

5.9 Supplementary tables and figures

Supplementary table 5.1. Number of cores used at each station. “Total cores” refer to the total number of cores at each station. The following four columns refer to the number of incubated cores used for “microbial analysis” (enriched and control), and “Nutrient flux analysis” (enriched and control). Finally, “Non-Incubated” refers to the number of non-incubated cores dedicated to organic matter analysis.

		Incubated				Non-incubated
Station Name	**Total cores**	**Microbial analysis (*)**		**Nutrient fluxes**		**OM**
		Enriched	Control	Enriched	Control	
NE Channel 2 (NEC2)	6	2	2	1	3	2
NE Channel 1 (NEC1)	7	2	0	3	2	2
Kinlan-Heezen Mid Inter-canyon (KHM)	7	1	2	3	2	2
Corsair Tributary Canyon (CT)	7	3	2	3	2	2

*Microbial analysis also included 2;1;1 non-incubated cores for NEC2; NEC1; CT, respectively.

Supplementary table 5.2. Relative abundance of each bacterial phylum for each habitat (Canyon, Channel, Inter-canyon).

Phyla	**%Abu_Canyon**	**%Abu_Channel**	**%Abu_Inter-canyon**
Acidobacteriota	0.1048	0.1128	0.1084
Actinobacteriota	0.0103	0.0176	0.0145
Bacteroidota	0.1415	0.1062	0.1339
Bdellovibrionota	0.0035	0.0040	0.0019
Caldatribacteriota	0.0001	0	0
Calditrichota	0.0008	0.0010	0.0025
Chloroflexi	0.0021	0.0036	0.0045
Crenarchaeota	0.0331	0.0470	0.03165
Dadabacteria	0.0101	0.0076	0.0087
Deferrisomatota	0	0	0
Deinococcota	0	0.0001	0.0016
Desulfobacterota	0.0089	0.0044	0.0178
DTB120	0	0	0.0004
Elusimicrobiota	0.0001	0.0003	0
Entotheonellaeota	0.0002	0.0014	0
Fibrobacterota	0.0002	0	0.0003
Firmicutes	0.0154	0.0226	0.0116
Gemmatimonadota	0.0375	0.0305	0.0507
Hydrogenedentes	0.0020	0.0029	0.0020
Latescibacterota	0.0070	0.0052	0.0073
Margulisbacteria	0.0003	0	0
MBNT15	0.0007	0	0.0009
Myxococcota	0.0083	0.0070	0.0103
Nanoarchaeota	0	0.0009	0.0001
NB1-j	0.0541	0.0512	0.0439

Nitrospinota	0.0072	0.0116	0.00816
Nitrospirota	0.0088	0.0198	0.0082
PAUC34f	7.23E-05	0.0002	0
Planctomycetota	0.0901	0.1110	0.09157
Proteobacteria	0.4375	0.4144	0.42429
SAR324clade (Marine_group_B)	0.0020	0.0023	0.00226
Schekmanbacteria	0	0.0002	0.00013
Spirochaetota	0.0002	0	0
Sumerlaeota	0.0013	0.0015	0.00165
Sva0485	0	0.0002	0.00032
Verrucomicrobiota	0.0101	0.0094	0.00841
Zixibacteria	0.0006	0.0020	0.00096

Supplementary table 5.3. Permutational analysis of variance (PERMANOVA) results from testing treatments (incubated enriched core, incubated control core, non-incubated core) on benthic microbial community assemblages within sites (C-T = Corsair Tributary Canyon; KHM = Kinlan-Heezen Mid Inter-canyon; NEC1 = Northeast Channel 1; NEC2 = and Northeast Channel 2) based on Bray-Curtis similarity matrices performed on relative abundance data. Df: degrees of freedom; SumOfSq: sum of squares; R^2:R^2 statistic; F value: F-statistic; p: p-value.

	Df	**SumOfSqs**	**R^2**	**F**	**Pr(>F)**
C-T					
Treatment	2	0.16	0.1	1.3	0.2
Residual	15	0.95	0.8		
Total	17	1.12	1		
KHM					
Treatment	2	0.17	0.1	1.3	0.2
Residual	15	0.97	0.8		
Total	17	1.14	1		
NEC1					
Treatment	2	0.16	0.1	1.3	0.2
Residual	15	0.94	0.8		
Total	17	1.11	1		
NEC2					
Treatment	2	0.16	0.1	1.3	0.2
Residual	15	0.94	0.8		
Total	17	1.11	1		

Supplementary table 5.4. Permutational analysis of variance (PERMANOVA) results testing the effect of habitat (Canyon, Channel, Inter-canyon), and Treatments (incubated enriched core, incubated control core, non-incubated core) on benthic microbial community assemblages at different taxonomic level (genera, order, family, class) based on Bray-Curtis's similarity matrices performed on relative abundance data. Df: degrees of freedom; SumOfSqs = sum of squares; R^2 = Statistic R^2; F value: F-statistic; p: p-value. Signif. codes: 0 '***' 0.001 '**' 0.01 '*' 0.05 '.' 0.1 ' ' 1.

Habitat						**Treatment**					
Genera level						**Genera level**					
	Df	SumOfSqs	R^2	F	Pr(>F)		Df	SumOfSqs	R^2	F	Pr(>F)
Habitat	2	0.2	0.1	1.7	**0.045***	Treatment	2	0.2	0.1	1.3	0.168
Residual	15	0.9	0.8			Residual	15	0.9	0.8		
Total	17	1.1	1			Total	17	1.1	1		
Order level						**Order level**					
Habitat	2	0.2	0.1	1.8	0.067	Treatment	2	0.1	0.2	1.3	0.205
Residual	15	0.7	0.8			Residual	15	0.7	0.8		
Total	17	0.8	1			Total	17	0.8	1		
Family level						**Family level**					
Habitat	2	0.2	0.1	1.7	0.058	Treatment	2	0.1	0.2	1.3	0.168
Residual	15	0.7	0.8			Residual	15	0.8	0.8		
Total	17	0.9	1			Total	17	0.9	1		
Class level						**Class level**					
Habitat	2	1.0	0.2	2.0	**0.002***	Treatment	2	0.5	0.1	0.9	0.657
Residual	16	3.9	0.7			Residual	16	4.4	0.8		
Total	18	4.9	1			Total	18	4.9	1		

Supplementary table 5.5. Shannon-Wiener and species richness values calculated per each sample (core) for each site. Avg per Habitat shows the average of Shannon-Wiener and species richness (S.obs) indices for each habitat (Canyon, Channel, Inter-canyon).

						Avg per Habitat	
Core	**Treatment**	**Site**	**Habitat**	**Shannon**	**S.obs**	**Shannon**	**S.obs**
R2112-C1	Incubated enriched core	CT	Canyon	4.6	238	4.7	237
R2112-C6	Incubated enriched core	CT	Canyon	4.9	254		
R2112-C4	OM	CT	Canyon	4.6	212		
R2112-C2	Incubated enriched core	CT	Canyon	4.7	181		
R2112-C8	Incubated control core	CT	Canyon	5.0	348		
R2112-C3	Incubated control core	CT	Canyon	4.6	191		
R2113-C1	Incubated enriched core	NEC1	Channel	4.8	403	4.8	295
R2113-C4	Incubated enriched core	NEC1	Channel	5.0	359		
R2113-C3	OM	NEC1	Channel	4.8	213		
R2113-C7	OM	NEC1	Channel	4.7	291		
R2113-C5	Incubated enriched core	NEC1	Channel	5.1	403		
R2117-C6	Incubated control core	NEC2	Channel	4.8	219		
R2117-C10	Incubated enriched core	NEC2	Channel	4.6	169		
R2117-C7	OM	NEC2	Channel	5.2	430		
R2117-C5	Incubated control core	NEC2	Channel	4.5	1.67E+02		
R2110-C7	Incubated control core	KHM	Inter-canyon	4.6	180	4.7	204
R2110-C5	Incubated control core	KHM	Inter-canyon	4.6	184		
R2110-C3	Incubated enriched core	KHM	Inter-canyon	4.8	247		

Supplementary table 5.6. Statistical results of parametric ANOVA for Shannon-Wiener and Richness indices among Habitats (Canyon; Inter-canyon; Channel), and Treatment (incubated enriched core; incubated control core; non incubate core). Df: degrees of freedom; F value: F-statistic; Pr (>F): p-value.

	Df	F value	Pr(>F)
Shannon-Habitat			
Habitat	2	0.64	0.53
Residuals	15		
Shannon-Treatment			
Treatment	2	0.13	0.87
Residuals	15		
Richness-Habitat			
Habitat	2	1.49	0.25
Residuals	15		
Richness-Treatment			
Treatment	2	0.21	0.81
Residuals	15		

Supplementary table 5.7. Summary of the main chemical-physical and sedimentary grain size properties of the bottom water in the three Gulf of Maine habitats (average ± standard deviation) based on analysis of 3 sediment non-incubated cores (Inter-canyon) , 2 cores (Canyon), and 4 cores (Channel). BWO_2 is bottom-water oxygen concentration' % Gravel (> 2 mm); % Sand (0.0625 < x < 2 mm); % Mud (< 0.0625 mm; it includes silt (0.0625<x< 0.004), and clay (0.004<x<0.001).

	Depth (m)	**Salinity (PSU)**	**Temperature (°C)**	**BWO_2 ($ml \cdot l^{-1}$)**	**% Gravel**	**% Sand**	**% Mud**	**% Silt**	**% Clay**
Inter-canyon	965.1 ± 0.0	35.4 ± 0.0	13.6 ± 0.0	8.5 ± 0.0	1.6 ± 2.3	65.2 ± 9.8	33.2 ± 12.2	23.6 ±8.9	9.5 ±3.2
Canyon	971.1 ± 0.0	35.6 ± 0.0	15.9 ± 0.0	7.5 ± 0.0	1.4 ± 2.0	53.2 ±17.9	45.3 ± 19.9	33.3 ±11.3	11.9 ± 8.7
Channel	678.4 ± 24.8	35.5 ± 0.02	14.3 ± 0.3	7.8 ± 0.2	0.4 ± 0.8	85.0 ± 5.48	14.5 ± 5.2	9.5 ±3.7	4.9 ± 1.4

Supplementary table 5.8. Statistical results of linear regression lm() for control inorganic nutrient fluxes considered in our study among sites (factor "Habitat", level "three"). Df: degrees of freedom; SumOfSqs = sum of squares; R^2 = Statistic R^2 ;F value: F-statistic; p: p-value.

	Df	Sum Sq	Mean Sq	F value	P value
O_2					
Habitat	2	689	404344	1.3	0.3
Residuals	7	1876	268		
NH_4^+					
Habitat	2	6904	3452	0.3	0.7
Residuals	7	74432	10633		
NO_3^-					
Habitat	2	2772887	1386444	1.7	0.2
Residuals	7	5493455	784779		
Si					
Habitat	2	47430	23715	0.2	0.8
Residuals	7	901632	128805		
PO_4^{3-}					
Habitat	2	23798	11899	2.5	0.2
Residuals	7	33415	4774		

Supplementary table 5.9. Statistical results of linear regression model (lm) for inorganic nutrient fluxes measure in enriched and control incubated cores at each habitat type. Asterisks indicates significant p-values (< 0.05). F value: F-statistic; p: p-value.

Habitat	Nutrient	F value	P
Canyon	**O_2**	0.23	0.6
	NH_4^+	0.5	0.5
	NO_3^-	1.7	0.3
	Si	0.2	0.6
	PO_4^{3-}	3.5	0.1
Inter-canyon	**O_2**	0.2	0.6
	NH_4^+	0.2	0.6
	NO_3^-	29.29	**0.005****
	Si	0.2	0.7
	PO_4^{3-}	0.2	0.7
Channel	**O_2**	0.1	0.8
	NH_4^+	0.1	0.8
	NO_3^-	0.4	0.6
	Si	1.2	0.3
	PO_4^{3-}	17.97	**0.004****

Supplementary table 5.10. Relationship between microbial diversity and macrofaunal diversity based on linear regression. Df: degrees of freedom; SumOfSqs = sum of squares; R^2 = Statistic R^2; F value: F-statistic; p: p-value.

	Independent variables	Df	SumOfSq	Mean Sq	F value	Pr(>F)
log1p(H) – macrofauna						
	log1p(S.obs_microbes)	1	0.0037	0.0037	0.4	0.5
	log1p(Shannon microbes)	1	0.0165	0.0165	1.6	0.2
	Residuals	11	0.1092	0.0099		
Log1p(Simpson) – macrofauna						
	log1p(S.obs_microbes)	1	0.0004	0.0004	0.5	0.5
	log1p(Shannon microbes)	1	0.0005	0.0005	0.7	0.4
	Residuals	11	0.0081	0.0007		
Log1p(S) – macrofauna						
	log1p(S.obs_microbes)	1	0.01046	0.010462	0.1	0.7
	log1p(Shannon microbes)	1	0.17021	0.170208	2.1	0.2
	Residuals	11	0.88251	0.080228		
sqrt(J) – macrofauna						
	sqrt(S.obs_microbes)	1	0.0001	0.0001	0.2	0.74
	sqrt(S.obs_microbes)	11	0.0002	0.0002	0.5	0.5
	Residuals	11	0.0044	0.00		

Fig.s.

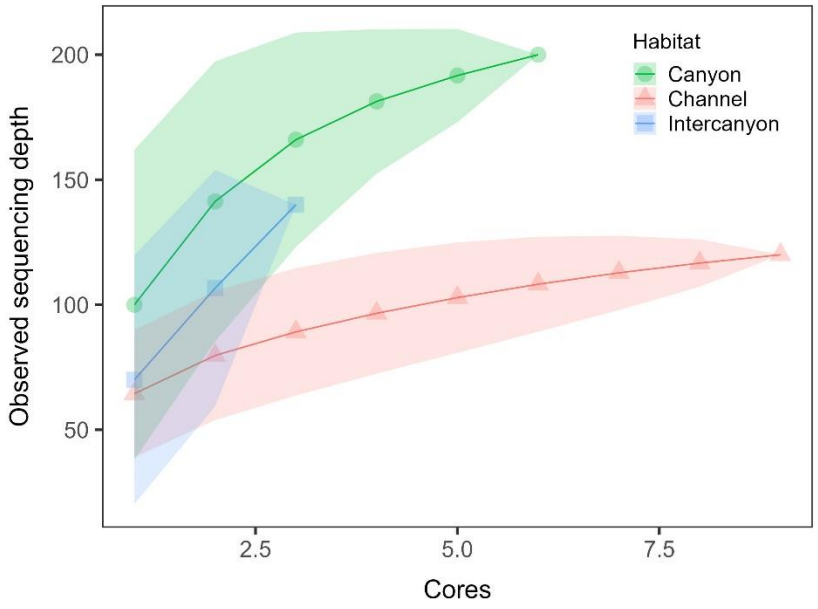

Supplementary Fig. 5.1. Accumulation curves for bacterial and archaea communities in surface (0-2 cm) sediments per cores (incubated enriched + incubated control + non-incubated) collected at each site. Light red, green and blue boxes indicate the three main sampling habitats. Canyon samples n = 6; Channel n = 9; Inter-channel n = 3.

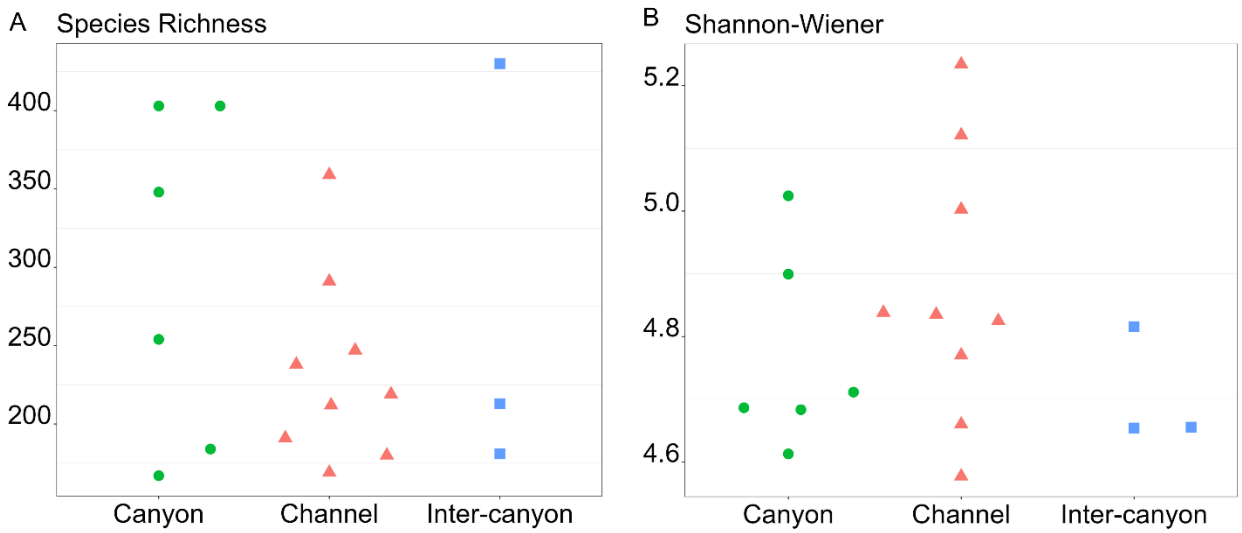

Supplementary Fig. 5.2. Average values of number of ASVs (Richness) and Shannon index sampled in each habitat. All three different treated cores were lumped together. Canyon samples n = 6; Channel n = 9; Inter-channel n = 3.

5.10 References

Achbergerová, L., Nahálka, J. Polyphosphate, 2011. An ancient energy source and active metabolic regulator. Microb Cell Fact 10, 63. https://doi.org/10.1186/1475-2859-10-63.

Albertelli, G., Covazzi-Harriague, A., Danovaro, R., Fabiano, M., Fraschetti, S.,et al. 1999. Differential responses of bacteria, meiofauna and macrofauna in a shelf area (Ligurian Sea, NW Mediterranean): role of food availability. J. Sea Res., 42 (1), 11-26.

Anderson, M. J. 2006. Distance-based tests for homogeneity of multivariate dispersions. Biometrics, 62 (1), 245-253.

Anderson, M. J., Walsh, D. C. 2013. PERMANOVA, ANOSIM, and the Mantel test in the face of heterogeneous dispersions: what null hypothesis are you testing?. Ecol. Monogr., 83 (4), 557-574.

Archer, D., Devol, A. 1992. Benthic oxygen fluxes on the Washington shelf and slope: A comparison of in situ microelectrode and chamber flux measurements. Limnol. Oceanogr., 37 (3), 614–629. https://doi.org/10.4319/lo.1992.37.3.0614.

Arndt, S., Jørgensen, B. B., LaRowe, D. E., Middelburg, J. J., Pancost, R. D., et al. 2013. Quantifying the degradation of organic matter in marine sediments: a review and synthesis. Earth-Sci. Rev., 123, 53-86.

Bartsch, R. G., and Kamen, M. D. 1960. Isolation and properties of two soluble heme proteins in extracts of the photoanaerobe Chromatium. JBC, 235(3), 825-831.

Belley, R., and Snelgrove, P.V.R. 2016. Relative contributions of biodiversity and environment to benthic ecosystem functioning. Front. Mar. Sci. 3(242)

Belley, R., and Snelgrove, P.V.R., 2017. The role of infaunal functional groups in short-term response of contrasting benthic communities to an experimental food pulse. J. Exp. Mar. Biol. Ecol. 491: 38-50.

Bolyen, E., Rideout, J. R., Dillon, M. R., Bokulich, N. A., Abnet, C. C., et al. 2019. Reproducible, interactive, scalable and extensible microbiome data science using QIIME 2. Nat. biotechnol, 37 (8), 852-857.

Borcard, D., Gillet, F., Legendre, P. 2018. Spatial analysis of ecological data. Numerical ecology with R, 299-367. Springer, Cham.

Bowman, J. P., McCuaig, R. D. 2003. Biodiversity, community structural shifts, and biogeography of prokaryotes within Antarctic continental shelf sediment. Appl. Environ. Microbiol, 69 (5), 2463-2483.

Carriot, N., Barry-Martinet, R., Briand, J. F., Ortalo-Magné, A., Culioli, G. 2022. Impact of phosphate concentration on the metabolome of biofilms of the marine bacterium Pseudoalteromonas lipolytica. Metabolomics, 18 (3), 1-16.

Christensen, J. P., Townsend, D. W., Montoya, J. P. 1996. Water column nutrients and sedimentary denitrification in the Gulf of Maine. Cont. Shelf Res., 16(4), 489-515.

Ciraolo, A. C., and Snelgrove, P. V. 2023. Contrasting benthic ecological functions in deep-sea canyon and non-canyon habitats: Macrofaunal diversity and nutrient cycling. Deep Sea Res. I: Oceanogr. Res. Pap., 104073.

Clarke K. R. 1993 Non-parametric multivariate analyses of changes in community structure. Aust J Ecol 18, 117-143.

Comeau, A. M., Douglas, G. M., Langille, M. G. 2017. Microbiome helper: a custom and streamlined workflow for microbiome research. MSystems, 2 (1), e00127-16.

Corinaldesi, C., Tangherlini, M., Rastelli, E., Buschi, E., et al. 2019. High diversity of benthic bacterial and archaeal assemblages in deep-Mediterranean canyons and adjacent slopes. Progr. Oceanogr., 171, 154-161.

Corsaro, M. M., Lanzetta, R., Parrilli, E., Parrilli, M., Tutino, M. L., et al. 2004. Influence of growth temperature on lipid and phosphate contents of surface polysaccharides from the Antarctic bacterium *Pseudoalteromonas haloplanktis* TAC 125. J. Bacterial., 186 (1), 29-34.

Crump, B. C., Hopkinson, C. S., Sogin, M. L. Hobbie, J. E. 2004. Microbial biogeography along an estuarine salinity gradient: combined influences of bacterial growth and residence time. Appl. Environ. Microbiol. 70, 1494–1505.

Danovaro, R. 2009. Methods for the study of deep-sea sediments, their functioning and biodiversity. CRC press., 45-51.

Dell'Anno, F., Rastelli, E., Tangherlini, M., Corinaldesi, C., Sansone, C., et al. 2021. Highly contaminated marine sediments can host rare bacterial taxa potentially useful for bioremediation. Front. Microb., 12, 584850.

D'Hondt, S., Jørgensen, B. B., Miller, D. J., Batzke, A., Blake, R., et al. 2004. Distributions of microbial activities in deep subseafloor sediments. Science, 306 (5705), 2216-2221.

Diaz J., Ingall E., Benitez-Nelson C., Paterson D., de Jonge M.D., et al., 2008. Marine polyphosphate: a key player in geologic phosphorus sequestration. Science, 320: 652-655. 10.1126/science.1151751.

Dyksma, S., Bischof, K., Fuchs, B. M., Hoffmann, K., Meier, D., et al. 2016. Ubiquitous Gammaproteobacteria dominate dark carbon fixation in coastal sediments. The ISME journal, 10 (8), 1939-1953.

Fernandez-Arcaya, U., Ramirez-Llodra, E., Aguzzi, J., Allcock, A. L., Davies, J. S., et al. 2017. Ecological role of submarine canyons and need for canyon conservation: a review. Front. Mar. Sci., 5.

Foshtomi, Y. M., Braeckman, U., Derycke, S., Sapp, M., Van Gansbeke, D., et al. 2015. The link between microbial diversity and nitrogen cycling in marine sediments is modulated by macrofaunal bioturbation. PloS one, 10 (6), e0130116.

Fox, J., Weisberg, S., Adler, D., Bates, D., Baud-Bovy, G., et al. 2011. Package "car": Companion to applied regression. Vienna: www. Cran. R-project. Org.

Fuerst, J. A., and Sagulenko, E. 2011. Beyond the bacterium: planctomycetes challenge our concepts of microbial structure and function. Nat. Rev. Microbiol., 9 (6), 403-413.

Gärtner, A., Blümel, M., Wiese, J. et al. 2011. Isolation and characterisation of bacteria from the Eastern Mediterranean deep sea. Antonie van Leeuwenhoek 100, 421–435. https://doi.org/10.1007/s10482-011-9599-5.

Grieshaber, M. K., and Völkel, S. 1998. Animal adaptations for tolerance and exploitation of poisonous sulfide. Annu. Rev. Physiol., 60(1), 33-53.

Gooday, A. J., and Turley, C. M. 1990. Responses by benthic organisms to inputs of organic material to the ocean floor: a review. Philos. Trans. Royal Soc. A, 331 (1616), 119-138.

Goffredi, S. K., and Orphan, V. J. 2010. Bacterial community shifts in taxa and diversity in response to localized organic loading in the deep sea. Environ. Microbiol., 12 (2), 344-363.

Guitton, M. L., Le Guitton, M., Soetaert, K., Sinninghe Damsté, J. S., Middelburg, J. J. 2015. Biogeochemical consequences of vertical and lateral transport of particulate organic matter in the southern North Sea: A multiproxy approach. Estuar. Coast. Shelf Sci., 165, 117–127. https://doi.org/10.1016/j.ecss.2015.09.010.

Hammond, D. E., Fuller, C., Harmon, D., Hartman, B., Korosec, M., et al. 1985. Benthic fluxes in San Francisco Bay. Hydrobiologia 129, 69-90.

Hargrave, B. T., Holmer, M., and Newcombe, C. P. 2008. Towards a classification of organic enrichment in marine sediments based on biogeochemical indicators. Mar. Pollut. Bull., 56(5), 810-824.

Harrison, B. K., Myrbo, A., Flood, B. E., Bailey, J. V. 2018. Abrupt burial imparts persistent changes to the bacterial diversity of turbidite-associated sediment profiles. Geobiology, 16 (2), 190-202.

Hedges, J. I., Mayorga, E., Tsamakis, E., McClain, M. E., Aufdenkampe, A., et al. 2000. Organic matter in Bolivian tributaries of the Amazon River: A comparison to the lower mainstream. Limnol. Oceanogr., 45 (7), 1449-1466.

Hensen, C., Zabel, M., Schulz, H. N. 2006. Benthic cycling of oxygen, nitrogen and phosphorus. Mar. Geochem., Springer, Berlin, Heidelberg, 207-240.

Henrichs, S. M. 1992. Early diagenesis of organic matter in marine sediments: progress and perplexity. Mar. Chem., 39 (1-3), 119-149.

Hinrichs, K. U., Hayes, J. M., Bach, W., Spivack, A. J., Hmelo, L. R., et al. 2006. Biological formation of ethane and propane in the deep marine subsurface. Proc. Natl. Acad. Sci. U.S.A., 103(40), 14684-14689.

Hoffmann, K., Bienhold, C., Buttigieg, P. L., Knittel, K., Laso-Pérez, R., et al. 2020. Diversity and metabolism of *Woeseiales* bacteria, global members of marine sediment communities. ISME J., 14 (4), 1042-1056.

Hunter, W. R., Levin, L. A., Kitazato, H., Witte, U. 2012: Macrobenthic assemblage structure and organismal stoichiometry control faunal processing of particulate organic carbon and nitrogen in oxygen minimum zone sediments, Biogeosciences, 9, 993–1006.

Huvenne, V. A., and Davies, J. S. 2014. Towards a new and integrated approach to submarine canyon research. Introduction. Deep Sea Res. Part II Top. Stud. Oceanogr., 104, 1-5.

Ingall, E., and Jahnke, R. 1994. Evidence for enhanced phosphorus regeneration from marine sediments overlain by oxygen depleted waters. Geochim. Cosmochim. Acta, 58 (11), 2571-2575.

Ismail, K., Huvenne, V., Robert, K. 2018. Quantifying spatial heterogeneity in submarine canyons. Prog. Oceanogr., 169, 181-198.

Jacob, M., Soltwedel, T., Boetius, A., Ramette, A. 2013. Biogeography of deep-sea benthic bacteria at regional scale (LTER HAUSGARTEN, Fram Strait, Arctic). PloS one, 8 (9), e72779.

Jørgensen, B. B. 1982. Mineralization of organic matter in the sea bed—the role of sulphate reduction. Nature, 296 (5858), 643-645.

Jørgensen, B. B., Boetius, A. 2007. Feast and famine—microbial life in the deep-sea bed. Nat. Rev. Microbiol., 5 (10), 770-781.

Kallmeyer, J., Pockalny, R., Adhikari, R. R., Smith, D. C., D'Hondt, S. 2012. Global distribution of microbial abundance and biomass in subseafloor sediment. PNAS, 109 (40), 16213-16216.

Keil, R. G. 2011. Terrestrial influences on carbon burial at sea. Proc. Natl. Acad. Sci. U.S.A., 108 (24), 9729-9730.

Keuter, S., and Rinkevich, B. 2016. Spatial homogeneity of bacterial and archaeal communities in the deep eastern Mediterranean Sea surface sediments. Int. Microbiol., 19 (2), 109-119.

Kim, B. R., Shin, J., Guevarra, R. B., Lee, J. H., Kim, D. W., et al. 2017. Deciphering diversity indices for a better understanding of microbial communities. J. Microbiol. Biotechnol. 27(12), 2089-2093.

Kristensen, E., and Kostka, J. E. 2005. Macrofaunal burrows and irrigation in marine sediment: microbiological and biogeochemical interactions. Interactions between macro-and microorganisms in marine sediments. American Geophysical Union, Washington, DC, 125-157.

Kulaev IS: Biochemistry of inorganic polyphosphates. Rev Physiol Biochem Pharmacol. 1975, 73: 131-158. 10.1007/BFb0034661.

Levin, L. A. 2005. Ecology of cold seep sediments: interactions of fauna with flow, chemistry and microbes. Oceanogr. Mar. Biol. 11-56. CRC Press.

Li, H., Yu, Y., Luo, W., Zeng, Y., Chen, B. 2009. Bacterial diversity in surface sediments from the Pacific Arctic Ocean. Extremophiles, 13 (2), 233-246.

Loubere, P. 1991. Deep-sea benthic foraminiferal assemblage response to a surface ocean productivity gradient: a test. Paleoceanography, 6 (2), 193-204.

Loubere, P. 1998. The impact of seasonality on the benthos as reflected in the assemblages of deep-sea foraminifera. Deep Sea Res. Part I Oceanogr. Res. Pap., 45 (2-3), 409-432.

Lücker S., Daims H. 2014 The Family *Nitrospinaceae*. In: Rosenberg E., DeLong E.F., Lory S., Stackebrandt E., Thompson F. (eds) The Prokaryotes. Springer, Berlin, Heidelberg. https://doi.org/10.1007/978-3-642-39044-9_402.

Mayer, L. M. 1994. Surface area control of organic carbon accumulation in continental shelf sediments. Geochim. Cosmochim. Acta, 58 (4), 1271-1284.

Mayer, L. M., Schick, L. L., Sawyer, T., Plante, C. J., Jumars, P. A., et al. 1995. Bioavailable amino acids in sediments: a biomimetic, kinetics-based approach. Limnol. Oceanogr., 40 (3), 511-520.

McArdle, B. H., Anderson, M. J. 2001. Fitting multivariate models to community data: a comment on distance-based redundancy analysis. Ecol., 82 1, 290-297.

Meyers, P. A. 1994. Preservation of elemental and isotopic source identification of sedimentary organic matter. Chem. Geol., 114 (3-4), 289-302.

Middelburg, J. J. 2011. Chemoautotrophy in the ocean. Geophys. Res. Lett., 38 (24).

Moodley, L., Middelburg, J. J., Boschker, H. T. S., Duineveld, G.C. A., Pel, R., et al. 2002. Bacteria and foraminifera: Key players in a short-term deep-sea benthic response to phytodetritus, Mar. Ecol. Prog. Ser., 236, 23–29.

Mosier, A. C., Allen, E. E., Kim, M., Ferriera, S., Francis, C. A. 2012. Genome sequence of "Candidatus Nitrosopumilus salaria" BD31, an ammonia-oxidizing archaeon from the San Francisco Bay estuary. J. Bacteriol. Res., 2121-2122.

Moens, T., Vincx, M. 1997. Observations on the feeding ecology of estuarine nematodes. J. Mar. Biolog. Assoc. U.K., 77 (1), 211-227.

Moens, T., Bouillon, S., Gallucci, F. 2005. Dual stable isotope abundances unravel trophic position of estuarine nematodes. J. Mar. Biolog. Assoc. U.K., 85 (6), 1401-1407.

Namirimu, T., Park, M. J., Kim, Y. J., Lim, D., Lee, J. H., et al. 2023. Microbial Diversity of Deep-sea Sediments from Three Newly Discovered Hydrothermal Vent Fields in the Central Indian Ridge. Ocean Sci. J., 58 (2), 11.

Oksanen J, Kindt R, Legendre P, O'Hara RB. 2005. Vegan: community ecology package version 1.7-82.

Orsi, W. D. 2018. Ecology and evolution of seafloor and subseafloor microbial communities. Nat. Rev. Microbiol., 16 (11), 671-683.

Øvreås, L., Forney, L., Daae, R. L., Torsvik, V. 1997. Distribution of bacterioplankton in meromictic Lake Sælenvannet, as determined by denaturing gradient gel electrophoresis of PCR-amplified gene fragments coding for 16S rRNA. Appl. Environ. Microbiol. 63, 3367–3373.

Park, B. J., Park, S. J., Yoon, D. N., Schouten, S., Sinninghe Damsté, J. S., et al. 2010. Cultivation of autotrophic ammonia-oxidizing archaea from marine sediments in coculture with sulfur-oxidizing bacteria. Appl. Environ. Microbiol.76 (22), 7575-7587.

Parrish, C. C. 1987. Separation of aquatic lipid classes by chromarod thin-layer chromatography with measurement by iatroscan flame ionization detection. Can. J. Fish. Aquat. Sci Aquat. Sci., 44 (4), 722–731. https://doi.org/10.1139/f87-087.

Parrish, C. C. 1999. Determination of Total Lipid, Lipid Classes, and Fatty Acids in Aquatic Samples. Arts, M.T., Wainman, B. C. (eds) Lipids in Freshwater Ecosystems. Springer, New York, NY., 4-20. https://doi.org/10.1007/978-1-4612-0547-0_2.

Paull, C. K., Ussler III, W., Mitts, P. J., Caress, D. W., West, G. J. 2006. Discordant 14C-stratigraphies in upper Monterey Canyon: A signal of anthropogenic disturbance. Mar. Geol, 233 (1-4), 21-36.

Pester, M., Schleper, C., Wagner, M. 2011. The Thaumarchaeota: an emerging view of their phylogeny and ecophysiology. Curr. Opin. Microbiol., 14 (3), 300-306.

Petrie, B., Yeats, P. 2000. Annual and interannual variability of nutrients and their estimated fluxes in the Scotian Shelf-Gulf of Maine region. Can. J. Fish. Aquat. Sci., 57 (12), 2536-2546.

Pinhassi J, Berman T. 2003. Differential growth response of colony-forming alpha- and gamma-proteobacteria in dilution culture and nutrient addition experiments from Lake Kinneret (Israel), the Eastern Mediterranean Sea, and the Gulf of Eilat. Appl Environ Microbiol 69:199–211

Polinski, J. M., Bucci, J. P., Gasser, M., Bodnar, A. G. 2019. Metabarcoding assessment of prokaryotic and eukaryotic taxa in sediments from Stellwagen Bank National Marine Sanctuary. Sci. Rep., 9 (1), 1-8.

Polymenakou, P. N., Lampadariou, N., Tselepides, A. 2008. Exo-enzymatic activities and organic matter properties in deep-sea canyon and slope systems off the southern Cretan margin. Deep Sea Res. Part I Oceanogr. Res. Pap., 55 (10), 1318-1329.

Polymenakou, P. N., Lampadariou, N., Mandalakis, M., Tselepides, A. 2009. Phylogenetic diversity of sediment bacteria from the southern Cretan margin, Eastern Mediterranean Sea. Syst. Appl. Microbiol., 32 (1), 17-26.

Quast C, Pruesse E, Yilmaz P, Gerken J, Schweer T, et al. 2013 The SILVA ribosomal RNA gene database project: improved data processing and web-based tools. Opens external link in new window Nucl. Acids Res. 41 (D1): D590-D596.

Qin, QL., Li, Y., Zhang, YJ. et al., 2011. Comparative genomics reveals a deep-sea sediment-adapted lifestyle of Pseudoalteromonas sp. SM9913. ISME J, 5, 274–284. https://doi.org/10.1038/ismej.2010.103.

Ransom, B., Kim, D., Kastner, M., Wainwright, S. 1998. Organic matter preservation on continental slopes: importance of mineralogy and surface area. Geochim. Cosmochim. Acta, 62 (8), 1329-1345.

Roman, S., Ortiz-Álvarez, R., Romano, C., Casamayor, E. O., Martin, D. 2019. Microbial community structure and functionality in the deep-sea floor: evaluating the causes of spatial heterogeneity in a submarine canyon system (NW Mediterranean, Spain). Front. Mar. Sci., 6, 108.

Sánchez-Soto, M. F., Cerqueda-García, D., Aguirre-Macedo, M. L., García-Maldonado, J. Q. 2023. Spatiotemporal dynamics of benthic bacterial communities in the Perdido Fold Belt, Northwestern Gulf of Mexico. Front. Mar. Sci.

Schauer, R., Bienhold, C., Ramette, A., Harder, J. 2010. Bacterial diversity and biogeography in deep-sea surface sediments of the South Atlantic Ocean. The ISME journal, 4 (2), 159-170.

Schloss, P. D., Westcott, S. L., Ryabin, T., Hall, J. R., Hartmann, M., et al. 2009. Introducing mothur: open-source, platform-independent, community-supported software for describing and comparing microbial communities. Appl. Environ. Microbiol. 75 (23), 7537-7541.

Schippers, A., Neretin, L. N., Kallmeyer, J., Ferdelman, T. G., Cragg, B. A., et al. 2005. Prokaryotic cells of the deep sub-seafloor biosphere identified as living bacteria. Nature, 433 (7028), 861-864.

Schippers, A., Kock, D., Höft, C., Köweker, G., Siegert, M. 2012. Quantification of microbial communities in subsurface marine sediments of the Black Sea and off Namibia. Front. Microbiol., 3, 16.

Schwalbach, M. S., Hewson, I., Fuhrman, J. A. 2004. Viral effects on bacterial community composition in marine plankton microcosms. Aquat. Microb. Ecol. 34, 117–127.

Sevastou, K., Lampadariou, N., Polymenakou, P. N., Tselepides, A. 2013. Benthic communities in the deep Mediterranean Sea: exploring microbial and meiofaunal patterns in slope and basin ecosystems. Biogeosciences, 10 (7), 4861-4878.

Sogin, M. L., Morrison, H. G., Huber, J. A., Welch, D. M., Huse, S. M., et al. 2006. Microbial diversity in the deep sea and the underexplored "rare biosphere" Proc. Natl. Acad. Sci. U.S.A., 103 (32), 12115-12120.

Solan, M., and Wigham, B. D. 2005. Biogenic particle reworking and bacterial-invertebrate interactions in marine sediments. Interactions between macro-and microorganisms in marine sediments. American Geophysical Union, Washington, DC, 105-124.

Soudry, D. 2000. Microbial Phosphate Sediment. In: Riding, R.E., Awramik, S.M. (eds) Microbial Sediments. Springer, Berlin, Heidelberg. https://doi.org/10.1007/978-3-662-04036-2_15.

Teske, A. P., Sørensen, K. B. 2008. Uncultured archaea in deep marine subsurface sediments: have we caught them all? ISME J. 2, (3), 18.

Townsend, D. W., Pettigrew N. R., Thomas A. C.. 2005. On the nature of Alexandrium fundyense blooms in the Gulf of Maine. Deep. Res. Part II Top. Stud. Oceanogr. 52: 2603–2630. doi: 10.1016/j.dsr2.2005.06.028.

Townsend, D. W., Thomas A. C., Mayer L. M., Thomas M. A., Quinlan J. A. 2006. Oceanography of the Northwest Atlantic continental shelf, p. 119–168. In A. R. Robinson and K. H. Brink [eds.], The Sea, v. 14. Cambridge MA: Harvard Univ. Press.

Townsend, D. W., Rebuck, N. D., Thomas, M. A., Karp-Boss, L., Gettings, R. M. 2010. A changing nutrient regime in the Gulf of Maine. Cont. Shelf Res., 30 (7), 820-832.

Vairavamurthy, A., Mopper, K., Taylor, B. F. 1992. Occurrence of particle-bound polysulfides and significance of their reaction with organic matters in marine sediments. Geophys. Res. Lett., 19(20), 2043-2046.

Varliero, G., Bienhold, C., Schmid, F., Boetius, A., Molari, M. 2019. Microbial diversity and connectivity in deep-sea sediments of the South Atlantic polar front. Front. Microbiol., 10, 665.

Walker, A. M., Leigh, M. B., Mincks, S. L. 2023. Benthic bacteria and archaea in the North American Arctic reflect food supply regimes and impacts of coastal and riverine inputs. Deep Sea Res. Part II Top. Stud. Oceanogr., 207, 105224.

Weiler, B. A., Verhoeven, J. T., Dufour, S. C. 2018. Bacterial communities in tissues and surficial mucus of the cold-water coral *Paragorgia arborea*. Front. Mar. Sci., 5, 378.

Wilkins, D., Van Sebille, E., Rintoul, S. R., Lauro, F. M., Cavicchioli, R. 2013. Advection shapes Southern Ocean microbial assemblages independent of distance and environment effects. Nat. Commun., 4 (1), 1-7.

Witte, U., Aberle, N., Sand, M., Wenzhofer, F. 2003a: Rapid response of a deep-sea benthic community to POM enrichment: an in situ experimental study, Mar. Ecol. Prog. Ser., 251, 27–36.

Witte, U., Wenzhofer, F., Sommer, S., Boetius, A., Heinz, P., et al. 2003b: In situ experimental evidence of the fate of a phytodetritus pulse at the abyssal sea floor, Nature, 424, 763– 766.

Woulds, C., Cowie, G. L., Levin, L. A., Andersson, J. H., Middelburg, J. J., et al. 2007: Oxygen as a control on seafloor biological communities and their roles in sedimentary carbon cycling, Limnol. Oceanogr., 52, 1698–1709.

Zhang, Y., Yao, P., Sun, C., Li, S., Shi, X., et al. 2021. Vertical diversity and association pattern of total, abundant and rare microbial communities in deep-sea sediments. Mol Ecol., 30 (12), 2800-2816.

Zuur A. F., Ieno E. N., Walker N. J., Saveliev A. A., Smith G. M. 2009. Mixed effects models and extensions in ecology with R. Springer, New York, NY, USA, 574.

Chapter 6. - Conclusions, summary, and future directions

Understanding the causal drivers that shape benthic patterns and critical ecological processes requires knowledge at different spatial scales. I therefore considered four different spatial scales in this study, working at large scales (contrasting habitats over 100s of km), medium scales (bottom water oxygen gradient, over 10s of km), medium-small scales (comparison of two underwater instruments over cm to m) and small scales (organic matter supply) (**Fig. 6.1 A**). In considering these different scales, I evaluated the patterns and drivers of benthic community structure, diversity and abundance, benthic nutrient fluxes, carbon uptake, and bioturbation in the Pacific and Atlantic Oceans (**Fig. 6.1 A**).

Fig. 6.1. A) Analysis of spatial heterogeneity at different spatial scales: "Large-; Medium-; Medium-Small-; and Small-scale" that correspond broadly to chapters dealing with "Contrasting habitats; Oxygen Minimum Zone; two different underwater Instruments; and Organic matter addition", respectively. We quanitfied benthic communities and organic matter remineralization using incubated sediment cores, and video and sonar images. B) The results section shows which response variable (indicated in the dark blue boxes on the top of the diagram) revealed significant variation at one or more spatial scales.

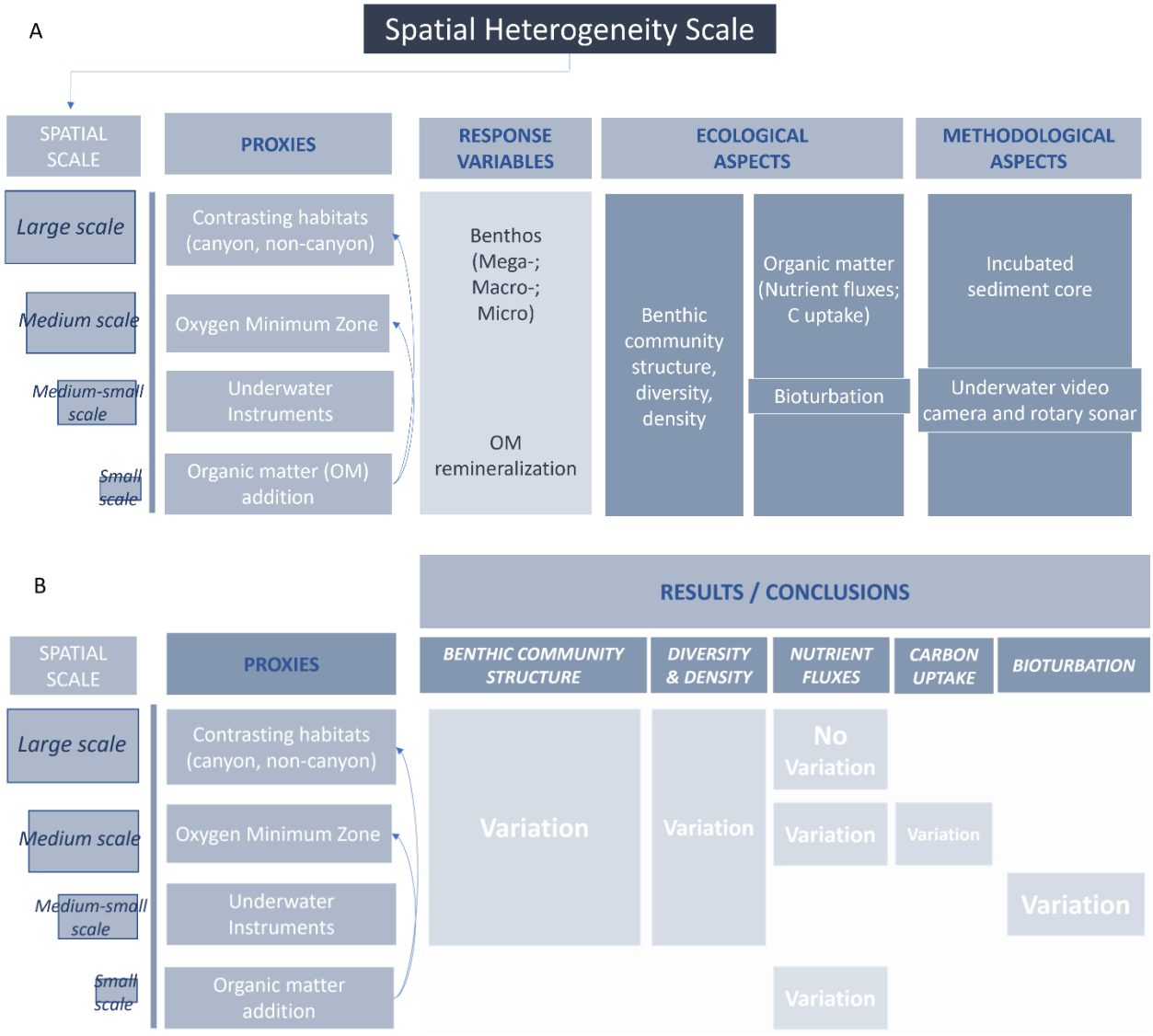

Based on univariate and multivariate analysis, and recognizing the limited power associated with some of my analyses, I documented the potential for different spatial heterogeneity scales to shape patterns and drive deep-sea benthic biodiversity and ecosystem functioning. Structural, diversity, and functional differences in benthic communities, as well as associated benthic functions (carbon cycling) and processes (reworked sediment), differed spatially and in their drivers across multiple spatial scales (**Fig. 6.1 B**). In contrast, large-scale differences in taxonomic diversity of microbes, and large- (benthic nutrient fluxes) and small- (OM addition) spatial scales

did not differ (**Fig. 6.1 B**). Benthic communities differed significantly across the multiple spatial scales of this study; however, food quality and quantity play an important role in structuring communities across medium and large scales, respectively.

Based on my study, I further conclude that the evaluation of spatial heterogeneity effects on benthic ecosystems depends strongly on the types of instruments used to collect data, noting the different but complementary roles that video and sonar images played in my preliminary evaluation of bioturbation activity.

6.1 Macrofaunal and megafaunal response to the Oxygen Minimum Zone in the NE Pacific Ocean

The NE Pacific Oxygen Minimum Zone influences biodiversity patterns that affect ecosystem functions at multiple spatial scales (Chapters 2 and 3). Specifically, I examined benthic ecosystem response to the oxygen minimum zone that impinges upon the Northeast Pacific continental slope off Vancouver Island (Chapter 2 and 3). I considered this question at different spatial scales, initially focusing on a transect spanning tens of kilometers across oxygen and depth gradients on the Clayoquot slope (Chapter 2), and then focusing on a single location on the Barkley Canyon upper slope that experiences strong annual variation in bottom-water oxygen (Chapter 3). In Barkley Canyon, I also considered temporal variation by comparing May, September, and December OMZ effects on the benthic ecosystem. Within Barkley Canyon, I considered two different small spatial scales using two underwater non-destructive methodologies, a fixed video camera (scale of centimeters), and a rotary sonar (scales of meters) as part of the Ocean Networks Canada Cabled Observatory. I, therefore, evaluated the megafaunal community and associated bioturbation activity at two spatial and seasonal scales. I then highlighted the advantages and disadvantages of the two underwater tools as inputs for future studies.

I observed clear effects of the quantity and quality of OM on benthic ecosystems, with shifts in community structure, species abundance, and species richness that collectively affected benthic ecosystem functions (Chapter 2). However, I was unable to fully disentangle the effects of different oxygen concentrations from various environmental variables identified in my study, such as temperature, and grain size, and particularly depth. Nonetheless, I inferred that oxygen concentrations played a role in these ecosystem shifts, noting that oxygen concentrations alone did not determine changes in ecosystem functions and patterns. Specifically, I observed decreased species abundance and richness at the hypoxic (850 m) Clayoquot slope site, and that surface deposit-feeding polychaetes dominated the macrofauna at all sites. In parallel with these biological changes, benthic ecosystem functions (carbon and benthic nutrient cycling) and processes (reworked sediment) shifted. Nutrient influxes mainly occurred under hypoxia, although I was unable to compare the two low oxygenated sites statistically. Moreover, quantity and quality of organic matter, measured as %TOC and CN, influenced Clayoquot slope benthic community structure for those macrofaunal taxa able to cope with permanent low oxygen concentrations. In contrast, my experiments did not strongly link nutrient fluxes with any of the biological or environmental variables considered, resulting in weak predictive models. I therefore infer that additional factors not measured in our study, such as sediment resuspension (Niemistö et al., 2018), bio-irrigation (Archer and Devol, 1992), and bacterial activity (Jørgensen and Boetius, 2007; Fuerst and Sagulenko., 2011; Hoffman et al., 2020) may also contribute to benthic flux variation.

The OMZ played a substantive role in structuring megafauna, and the analyses that focused on smaller spatial scales (cm to m) revealed strong effects on bioturbation activity (Chapter 3). Whereas megafaunal density and diversity and pits decreased with decreasing bottom-water oxygen concentrations, aligning with other multilinear environmental factors, patterns in

bioturbation traces varied with scales and instruments used in this study. Indeed, analysis of video imagery did not demonstrate a link between oxygen concentrations and bioturbation trace area and numbers, whereas analysis of sonar images indicated decreasing average total bioturbated area and number of pits with decreasing bottom-water oxygen concentrations. Nevertheless, video analysis demonstrated a central role for an unidentified gastropod in sediment mixing under hypoxia. Once again, although oxygen concentrations may have affected community structure and ecosystem functions and processes, oxygen concentrations alone could not fully explain ecosystem changes, and other (unmeasured) variables presumably also played a role. Collinearity between oxygen and temperature also complicated the interpretation of megafaunal and reworked sediment and traces.

In conclusion, evaluation of biodiversity-ecosystem functioning (BEF) in my benthic ecosystem study processes shifted in moving from small (cm-m) to larger spatial scales (m -km), highlighting the role of spatial heterogeneity scales in relation to BEF as also supported by previous studies (e.g., Gamfeldt et al., 2023, Romoth et al., 2023); the complexity of the OMZ environment with its multicollinear environmental factors complicates understanding the primary drivers that structure benthic biodiversity and functions.

6.2 Macrofaunal and microbial community response to habitat heterogeneity

My research (Chapters 4 and 5) is the first study to identify key explanatory environmental influences on differing sedimentary macrofaunal and microbial communities among Canyon and Channel habitats of the NW Atlantic Ocean. I evaluated how different habitats (Canyon, Inter-canyon, and Channel) with contrasting environmental conditions might affect both infaunal (Chapter 4) and benthic microbial (Chapter 5) communities. Specifically, I showed that habitat heterogeneity affected community structure of both macrofauna and microbes, as well as taxonomic and functional diversity of infauna. In contrast, heterogeneity did not clearly affect

infaunal abundance and microbial taxonomical diversity. Moreover, although %TOC and CN helped to explain variation in the microbial community, collinearity in environmental variables may have contributed to the difficulty in identifying strong predictors of macrofaunal patterns.

These results reinforce knowledge gained from previous studies that reported on the contributions of multiple environmental variables in structuring benthic communities, and the challenge of identifying strong environmental predictors at a large spatial scale.

6.3 The role of infauna and benthic microbes in carbon and nutrient cycling under natural disturbances and seafloor heterogeneity

My studies showed a central role for infauna (Chapters 2, 4) in the processing of freshly deposited OM in deep, low-oxygen sites in the NE Pacific and in contrasting habitats in the NW Atlantic ocean, but less of a role for microbes (Chapter 5).

I simulated phytodetritus pulses akin to seasonal food-pulses (albeit supplied in a single pulse) under hypoxia (Chapter 2), and to assess the role of habitat heterogeneity (Chapters 4, 5) and associated benthic macrofauna and microbes in the short-term processing and infaunal uptake of OM in soft-sediment habitats.

In both studies, I enriched sediment cores collected from two locations differing in bottom-water oxygen (Chapter 2) and from three different habitats - Canyon, Inter-canyon, and Channel- (Chapters 4, 5). I used ^{13}C labeled algal detritus in contrasting hypoxic sites described in Chapter 2, and unlabeled phytodetritus in Chapters 4 and 5, focusing on contrasting habitats. My studies (Chapter 2 and 4) showed that infauna play a relevant role in both carbon uptake and nutrient cycling. Specifically, my study from hypoxic sites emphasized the role of polychaetes in the uptake and control of C cycling, irrespective of bottom-water oxygen concentrations, the importance of different polychaete feeding behaviors, and the predominant role of polychaetes in the upper 0-2

cm of the sediment in C uptake. Furthermore, the limited explanatory power of both biological and environmental variables included in my analysis in describing natural benthic nutrient fluxes points to the importance of variables not included in the study. However, nutrient influxes into sediments generally characterized habitats, except for phosphate in Inter-canyon habitat. Moreover, the high functional diversity in my Atlantic region study suggests some degree of niche differentiation among species in Channel and Inter-canyon habitats, limiting competition for food, however, the biota may lack specific trait types that differentially enhance nutrient regeneration.

Further results (Chapter 5) did not suggest a strong, rapid contribution by the microbial community to organic matter remineralization following phytodetrital addition, and thus to this deep-sea ecosystem function. One explanation for this result likely relates to the short-term incubation time of my experiments, which did not allow microbes sufficient time to contribute to organic matter remineralization and demonstrate plasticity in their response. Specifically, I showed that the phytodetrital addition did not translate to significant differences in microbial diversity, but the addition had some effect on benthic nutrient fluxes, especially nitrate fluxes in the Inter-canyon, and phosphate in the Channel habitat. Overall, benthic microbial community composition explained only 7% of the benthic nutrient fluxes in this study, primarily contributing to nitrogen and phosphate fluxes, indicating a limited microbial contribution to short-term organic matter remineralization.

6.4 Methodological novelties for assessing BEF

Chapter 3 aimed to clarify the advantages and limitations of video and sonar instruments in collecting data to quantify deep-sea bioturbation activity under hypoxic conditions. My analyses showed that video images collected by a fixed camera enable identification of organisms, and observations of relatively small features (cm) that sonar images cannot resolve as a result of the

image resolution specific to this study. However, video images might affect animal behaviors by emitting light or through the presence of the white PVC ruler placed on the sediment for scale. In addition, sonar offers the important benefit of recording a larger FOV than video and thus image larger bioturbation traces more effectively. These attributes enable larger-scale assessment of distributions and size changes in bioturbation traces than possible with a video camera. Unfortunately, sonar images alone do not allow identification of organisms and small features given insufficient resolution, unless combined with video imaging of an overlapping FOV. In short, this methodological assessment illustrates the utility of the complementary use of both instruments to enhance knowledge of benthic ecosystem functions such as bioturbation activity at larger scales than possible with video imagery alone. I noted some methodological steps to improve the efficacy of future studies. These improvements include adopting an embedded sampling schedule that collects sonar imagery only over the FOV of the camera, reducing the acquisition time of single sonar images, and ensuring a sonar radius shorter than 20 m to improve spatial resolution of images.

6.5 Research and methodological limitations

My study highlights the challenges of specific techniques under the logistically challenging conditions encountered by deep-sea researchers, such as in a remote, hypoxic environment, and particularly the need to monitor and consider low oxygen concentrations, in tandem with the challenge of simulating deep seafloor conditions and limited replication of experimental treatments. Nonetheless, replicate cores in my shipboard incubations allowed me to assess biological patterns and some aspects of environmental variability. Previous studies documented altered activity levels, cell lysis, and death of microbes as a result of decompression (e.g., Park and Clark, 2002), raising concern that biological OM processing in shipboard incubations might differ

substantially from in situ rates. Amano et al. (2022) documented deep-sea (from ~1000 m depth) heterotrophic bacterial metabolic activity under in situ hydrostatic pressure about one-third of that measured in the same community at sea level atmospheric pressure. They also indicated a largely balanced POC supply to prokaryotic carbon demand ratio, inferring that the mismatch between organic carbon supply and prokaryotic carbon demand in the bathypelagic realm likely results from an overestimation of heterotrophic prokaryotic activity when measured in sea level incubations. Importantly my samples were collected from shallower depths, than Amano et al. (2022), but the lack of information on depressurization effects on deep-sea heterotrophic prokaryotic communities raises concerns. However, Woulds et al. (2007) compared shipboard and lander-derived data, and found that although shipboard incubations may create some artifacts, they did not appear sufficiently large to match other sources of error (e.g., patchiness), to adversely affect interpretation, or to outweigh the benefit of increased duration and replication of experiments.

The preservation of enriched macrofaunal samples could potentially influence isotope analysis because it can affect the C isotope ratio (e.g., Bosley and Wainright, 1999). However, Kelly et al. (2006) and Lau et al. (2012) reported a small or null influence of formalin-ethanol on C:N and ^{13}C compared to formalin, which yielded values generally consistent with ethanol-preserved samples. Kelly et al. (2006) also suggested that appropriate use of archived samples to reconstruct historical food webs will require species-specific experiments to determine the nature of preservation-induced shifts in tissue isotopic signatures. Therefore, numerous uncertainties associated with different preservation methods for isotope analysis persist.

6.6 Summary and future directions

In conclusion, my thesis showed that habitat heterogeneity of natural ecosystems largely defines biodiversity patterns and contributes to ecosystem functioning. Therefore, studies of benthic ecosystems must consider complex environmental and biological drivers. Excluding potential drivers may result in an ambiguous or inaccurate understanding of ecosystem processes. Given that deep-sea ecosystems may be sites of nutrient regeneration, understanding the role of microorganisms and macrofauna in these processes requires knowledge of the diverse nature of sedimentary organisms and their potential biotic and abiotic interactions within the ecosystem. Because microorganisms reproduce quickly and with strong seasonality (Findlay and Watling., 1998), and environmental factors also often vary seasonally, future studies might assess seasonality in microbial community structure and investigate microbial functions to clarify and predict OM remineralization in the NW Atlantic. Furthermore, we must recognize that relatively homogeneous parameters measured at one scale may appear heterogeneous at different observational scales (Levin 1992). Therefore, future studies might also need to explore both infaunal and microbial sedimentary communities on a smaller scale (e.g., more samples across the depth gradient) than that used in my study. Indeed, there is no single "correct" scale on which to describe species, populations, or ecosystems (Levin 1992), but the description of the system depends upon the window through which the system is viewed. Further studies performed under different spatial and temporal scales can only improve our knowledge because the observed variability of the system often depends on the scale of description (Lecours et al., 2015). We must think of the environment as a "cake", of which we only study and analyze a small dimensional slice accordingly to our perceptual capabilities, or constraints in technology or logistics.

We must also recognize that natural disturbances – OMZ in our case – can contribute to biodiversity change and associated shifts in BEF. We now recognize the deep sea as a vulnerable and heterogenous environment, in which biota can respond quickly when resource availability changes, as shown by the hypoxia study (Chapter 2). Therefore, while acknowledging the cost and logistical challenges of deep-sea research, significant knowledge gaps remain in understanding deep-sea environments and how to protect them. Experiments, lab-work, field-work, and new approaches such as those suggested in Chapter 3 illustrate how to enhance knowledge of deep-sea benthic ecosystem functions. Future research should also determine whether deep-sea infaunal response, nutrient fluxes, bioturbating organisms, or bioturbation activity vary seasonally under similar low-oxygenated conditions. Moreover, future studies could examine benthic community response to different food resources, such as diatoms and coccolithophorids, and whether environmental conditions, such as hypoxia, alter that response.

6.7 References

Amano, C., Zhao, Z., Sintes, E. et al. 2022 Limited carbon cycling due to high-pressure effects on the deep-sea microbiome. Nat. Geosci. 15, 1041–1047. https://doi.org/10.1038/s41561-022-01081-3.

Archer, D., Devol, A. 1992. Benthic oxygen fluxes on the Washington shelf and slope: A comparison of *in-situ* microelectrode and chamber flux measurements. Limnol. Oceanogr., 37 (3), 614–629.

Bosley, K. L., Wainright, S. C. 1999. Effects of preservatives and acidification on the stable isotope ratios (15N:14N, 13C:12C) of two species of marine animals. Can. J. Fish. Aquat. Sci., 56 (11), 2181–2185. https://doi.org/10.1139/f99-153.

Findlay, R. H., and Watling, L. 1998. Seasonal variation in the structure of a marine benthic microbial community. Microb. Ecol., 36(1), 23-30.

Fuerst, J. A., and Sagulenko, E. 2011. Beyond the bacterium: planctomycetes challenge our concepts of microbial structure and function. Nat. Rev. Microbiol., 9 (6), 403-413.

Gamfeldt, L., Hagan, J. G., Farewell, A., Palm, M., Warringer, J., et al. 2023. Scaling-up the biodiversity–ecosystem functioning relationship: the effect of environmental heterogeneity on transgressive overyielding. Oikos, 2023(3), e09652.

Hoffmann, K., Bienhold, C., Buttigieg, P. L., Knittel, K., Laso-Pérez, R., et al. 2020. Diversity and metabolism of *Woeseiales* bacteria, global members of marine sediment communities. The ISME Journal, 14(4), 1042-1056.

Jørgensen, B. B., and Boetius, A. 2007. Feast and famine—microbial life in the deep-sea bed. Nat. Rev. Microbiol., 5 (10), 770-781.

Kelly, B., Dempson, J. B., Power, M. 2006. The effects of preservation on fish tissue stable isotope signatures. J. Fish Biol., 69 (6), 1595–1611.

Lau, D. C. P., Leung, K. M. Y., Dudgeon, D. 2012. Preservation effects on C/N ratios and stable isotope signatures of freshwater fishes and benthic macroinvertebrates. Limnol. Oceanogr-Meth., 10 (2), 75–89.

Lecours, V., Devillers, R., Schneider, D. C., Lucieer, V. L., Brown, C. J., et al. 2015. Spatial scale and geographic context in benthic habitat mapping: review and future directions. Mar. Ecol. Prog. Ser., 535, 259-284.

Levin S.A. 1992 The problem of pattern and scale in ecology. Ecology, 73, 1943–1967.

Niemistö, J., Kononets, M., Ekeroth, N., Tallberg, P., Tengberg, A., et al. 2018. Benthic fluxes of oxygen and inorganic nutrients in the archipelago of Gulf of Finland, Baltic Sea–Effects of sediment resuspension measured in situ. J. Sea Res., 135, 95-106.

Park, C., and D. S. Clark. 2002. Rupture of the cell envelope by decompression of the deep-sea methanogen *Methanococcus jannaschii*. Appl. Environ. Microbiol. 68: 1458–1463.

Romoth, K., Darr, A., Papenmeier, S., Zettler, M. L., and Gogina, M. 2023. Substrate heterogeneity as a trigger for species diversity in marine benthic assemblages. Biol., 12 (6), 825.

Woulds, C., Cowie, G. L., Levin, L. A., Andersson, J. H., Middelburg, J. J., et al. 2007. Oxygen as a control on sea floor biological communities and their roles in sedimentary carbon cycling. Limnol. Oceanogr., 52 (4), 1698–1709.